

**Exploiting Intramolecularity:
Exploring Aldehyde-Catalyzed Intermolecular
Hydroaminations and Mixed Aminal Chemistry**

By

Didier Alexandre Bilodeau

Thesis submitted to the
Faculty of Graduate and Postdoctoral Studies
University of Ottawa
In partial fulfillment of the requirements for the
M.Sc. degree in the

Ottawa-Carleton Chemistry Institute
University of Ottawa

Candidate

Supervisor

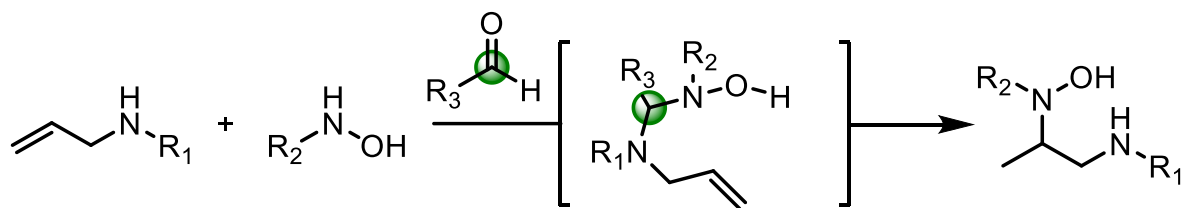
Didier Alexandre Bilodeau

Dr. André M. Beauchemin

Abstract

Hydroamination reactions are very attractive to form new C-N bonds, though broadly applicable synthetic methods do not exist. The hydroamination of unactivated alkenes is especially difficult to accomplish given its negative reaction entropy, as well as potentially being a thermodynamically unfavourable transformation with some substrates. Thus, previously reported systems have often consisted of biased intramolecular systems or metal-catalyzed intermolecular variations operating at low temperatures. Recently, our group discovered that intermolecular Cope-type hydroamination of unactivated alkenes is achievable through the use of aldehydes as catalysts. These organocatalysts act solely through promoting the pre-association of reacting partners, hydroxylamines and allyl amines, in order to induce temporary intramolecularity; thus allowing for very mild reaction conditions and access to important 1,2-Diamine motifs.

Aldehyde Catalyzed Intermolecular Cope-Type Hydroamination



Catalysis through Temporary Intramolecularity

This thesis presents studies expanding upon initial reports of aldehyde-catalyzed Cope-type intermolecular hydroamination. In the scope of these studies standard conditions were developed to compare aldehyde catalytic activity. These evaluations led to further strengthening our understanding of hypothesized trends in aldehydes' catalytic efficiencies,

notably the impact of electronic, steric and solvent effects. Furthermore, the possibility of using a catalytic precursor species for hydroamination was evaluated. While this symmetrical hydroxylamine dimer precursor did not result in increased hydroamination yields, it did allow for easier manipulations as well as allow preliminary kinetic isotope effect studies to study formaldehyde as a precatalyst. These KIE studies allowed to reconfirm that hydroamination was highly likely the rate determining step of our proposed catalytic cycle. Derivatization of hydroamination products was also accomplished to access important 1,2-Diamine motifs from simple starting materials, also allowing to access difficult hydroamination products through the application of quantitative amounts of aldehyde, followed by hydrolysis of the formed heterocycles. Additional studies into nitron reactivity led us to access a novel synthesis of enantiomerically enriched chiral cyclic nitrones through a sequence of nucleophilic addition, Cope-type hydroamination and Cope elimination. However, this sequence proved unpractical and of very narrow applicability, while affording only modest enantioselectivities (up to 78% *ee*), therefore further exploration was not warranted.

A collaborative study was also undertaken in collaboration with the Wennemers group from ETH Zurich. This exploratory study had the goal of examining the potential for combining small peptide catalysis with aldehyde catalysis inducing temporary intramolecularity. It was hypothesized that the combination of both catalytic systems could improve upon the conjugate addition of nucleophiles to certain electrophiles, such as nitroolefins; in a potentially stereoselective manner. Although initial trials did not yield productive reactions, evidence for potential new mixed aminals with formaldehyde and

various nucleophiles was found. Furthermore, the background reactivity of various nucleophile and electrophile pairings was assessed, allowing for better calibration of future efforts in studying such systems.

Table of Contents

Abstract.....	ii
List of Figures.....	vii
List of Schemes.....	x
List of Tables.....	xii
List of Abbreviations.....	xiii
Annex I.....	77
Annex II - Experimental Section	78
Annex III - NMR Spectra and HPLC Data	93
Chapter 1 – Aldehyde Catalyzed Cope-Type Hydroamination of Unactivated Alkenes.....	1
1.1 Introduction.....	1
1.2 Carbonyl Catalysis	5
1.3 Cope-Type Hydroamination	15
Chapter 2 – Further Studies of Cope-Type Hydroamination Reactions of Unactivated Alkenes.....	31
2.1 Comprehensive Aldehyde Scan	31
2.2 Derivatization of Hydroamination Products.....	35
2.3 Preliminary Kinetic Isotope Effect with Formaldehyde.....	39
2.4 Hydroxylamine Dimer as a Precursor to Cope-type Hydroamination.....	43
2.5 Synthesis of Enantiomerically Enriched Chiral Nitrones.....	46
Chapter 3 – Small Peptide Catalysis and Mixed Aminals	59

3.1 Introduction to Small Peptide Catalysis	59
3.2 Small Peptide Catalysis with Mixed Aminals	63
Chapter 4 - Conclusions	72
4.1 Conclusions and Potential Future Studies	72

List of Figures

Figure 1.1 Various amination methods of alkenes.....	2
Figure 1.2 Targeted stepwise approach to tethering for challenging intermolecular reactions and catalytic alternative.....	5
Figure 1.3 Reported examples of amide hydrolysis via carbonyl catalysis.....	7
Figure 1.4 Reported examples of ester hydrolysis via carbonyl catalysis.....	8
Figure 1.5 Transesterification of α -hydroxy esters via carbonyl catalysis.....	9
Figure 1.6 Strategies for directed C-H bond activation.....	10
Figure 1.7 C(sp ³)-H arylation using an amino acid as a transient directing group.....	11
Figure 1.8 C(sp ³)-H arylation of aliphatic aldehydes and amines via transient directing groups.....	12
Figure 1.9 Palladium catalyzed synthesis of amino alcohols via in situ tether formation with trifluoroacetaldehyde.....	13
Figure 1.10 Desymmetrization of <i>syn</i> 1,2-diols through the application of a scaffolding catalyst.....	14
Figure 1.11 Summary of reactivity trends for the Reverse Cope Cyclization.....	17
Figure 1.12 Organocatalytic tethering strategy to promote difficult intermolecular reactions through temporary intramolecularity.....	19

Figure 1.13 Proposed catalytic cycle for the catalytic variant of the Cope-type intramolecular hydroamination.....	23
Figure 1.14 Initial examples of intermolecular Cope-type hydroamination of alkenes with aqueous hydroxylamine and <i>N</i> -alkylhydroxylamines.....	24
Figure 1.15 Revised catalytic cycle for the catalytic variant of the Cope-type intramolecular hydroamination.....	27
Figure 1.16 Enantioselective intramolecular thiourea-catalyzed Cope-type hydroamination.....	28
Figure 1.17 Basis for enantioselective aldehyde catalyzed Cope-type hydroamination.....	29
Figure 2.1 Asymmetric intramolecular hydroaminations controlled by chiral nucleophilic addition.....	47
Figure 2.2 Synthesis of chiral cyclic nitron through application of nucleophiles.....	49
Figure 2.3 Sterically hindered aldehydes for cyclic chiral nitron synthesis.....	56
Figure 3.1 General Structure of Tripeptide Catalysts.....	59
Figure 3.2 Overview of tripeptide catalyzed reactions by the Wennemers group.....	59
Figure 3.3 Mechanisms of proline organocatalyzed reactions.....	61
Figure 3.4 Comparison between proline catalysis and small peptide catalysis.....	62
Figure 3.5 Suggested catalytic cycle for nucleophilic addition via peptide and aminal catalysis.....	64

Figure 3.6 Mixed aminor formation with pyrrolidine as a model for tripeptide catalyst.....	65
Figure 3.7 Preliminary study of background reactivity with β -nitrostyrene.....	67
Figure 3.8 Evaluation of background with β,β -disubstituted nitroolefins for tripeptide catalysis.....	67
Figure 3.9 Evaluation of background reactivity between aniline and N-benzylhydroxylamine and various potential electrophiles for tripeptide catalysis.....	68
Figure 3.10 Investigations into aldehyde and small peptide dual-catalysis.....	70

List of Schemes

Scheme 1.1 Intermolecular and intramolecular hydroamination of alkenes and selectivity.....	3
Scheme 1.2 Cope elimination of trialkylamine-N-oxides.....	16
Scheme 1.3 Oppolzer's cyclic Cope-type hydroamination.....	16
Scheme 1.4 General overview of hydroamination through temporary intramolecularity....	20
Scheme 1.5 Heterocyclic product formation through transient hydroxylamine formation.....	20
Scheme 1.6 Knight's initial nitron as a precursor to intramolecular hydroamination.....	21
Scheme 1.7 Knight's comparison of nitron reactivity.....	21
Scheme 1.8 Intermolecular Cope-type hydroamination of unbiased allylic amines promoted via hydrogen bonding.....	25
Scheme 2.1 Derivatization of diamine motifs.....	36
Scheme 2.2 Unexpected imidazolidine synthesis.....	38
Scheme 2.3 Hydrolysis of cyclic adducts.....	38
Scheme 2.4 Deuterium kinetic isotope effect experiment for α -benzyloxyacetaldehyde....	40
Scheme 2.5 Synthesis of benzylhydroxylamine homodimer.....	41
Scheme 2.6 Deuterium kinetic isotope effect experiment using a formaldehyde-hydroxylamine dimer as formaldehyde source.....	41

Scheme 2.7 Formaldehyde hydroxylamine dimer as a precursor to active catalytic species.....	42
Scheme 2.8 Formaldehyde catalyzed hydroamination of secondary allylamines.....	45
Scheme 2.9 Asymmetric hydroaminations using chiral aldehydes.....	46
Scheme 2.10 Optimized reaction conditions for chiral cyclic nitron synthesis.....	55
Scheme 2.11 Napthalene nitron for synthesis of cyclic chiral nitron.....	56

List of Tables

Table 1.1 Scope of asymmetric hydroaminations catalyzed by chiral aldehydes.....	30
Table 2.1 Comprehensive aldehyde scan in CHCl ₃ and <i>t</i> -BuOH.....	32
Table 2.2 Cope-type Hydroamination with Low Formaldehyde Loadings.....	34
Table 2.3 Hydroamination of Allylic Amines Using a Formaldehyde Precursor Dimer.....	43
Table 2.4 Intramolecular hydroamination of nitrones promoted by nucleophilic addition.....	48
Table 2.5 Nucleophilic scan for chiral cyclic nitron synthesis.....	51
Table 2.6 Solvent scan for chiral cyclic nitron synthesis.....	53
Table 2.7 Additive and reaction conditions scan for chiral cyclic nitron synthesis.....	54
Table 2.8 Secondary nucleophile scan for chiral cyclic nitron synthesis.....	55

List of Abbreviations

Å	angstrom (10 ⁻¹⁰ metres)
Ac	acetyl
<i>anti</i>	against, opposite
aq	aqueous
Ar	aryl
Bn	benzyl
Boc	<i>tert</i> -butoxycarbonyl
bp	boiling point
Bu	butyl
BuOH	butyl alcohol
cat.	catalytic
Cbz	benzyloxycarbonyl
°C	degree Celsius
<i>cis</i>	on the same side
conc.	concentrated
δ	chemical shift in parts per million
<i>d</i>	deuterium (in NMR solvents)
DCM	dichloromethane
DMF	dimethylformamide
DMSO	dimethyl sulfoxide
<i>ee</i>	enantiomeric excess
EI	electron impact
Equiv.	equivalent
Et	ethyl
EtOAc	ethyl acetate
FT	Fourier transform
g	gram
h	hour
Hex	hexanes
<i>hν</i>	light; electromagnetic radiation

HRMS	high-resolution mass spectrometry
Hz	Hertz
<i>i</i>	iso
IR	infrared
<i>J</i>	coupling constant
L	litre; ligand
LAH	lithium aluminum hydride
μL	microlitre
<i>m</i>	meta
M	molar; metal
Me	methyl
mg	milligram
min	minute
mL	millilitre
mmol	millimole
Nu	nucleophile
NMR	nuclear magnetic resonance
<i>p</i>	para
Ph	phenyl
ppm	parts per million
Pr	propyl
Prep.	preparatory
R	carbon-based substituent
rt	room temperature
<i>s</i>	secondary
s	second
sat.	saturated
<i>syn</i>	together, same side
<i>t</i>	tertiary
THF	tetrahydrofuran
TLC	thin layer chromatography
UV	ultra-violet
wt	weight

Chapter 1 – Aldehyde Catalyzed Cope-Type Hydroamination of Unactivated Alkenes

1.1 Introduction

Nitrogen-containing molecules are a highly valuable class of chemicals with widespread applications as pharmaceutical agents, specialty chemicals and industrially relevant compounds. Due to their wide applicability there exists several classical methods to achieve their synthesis. However, many classical routes to carbon-nitrogen bond formation involve the use of specialized starting materials, which more often than not contain pre-activated functional groups; common methods include reductive amination and nucleophilic substitution. When forming new carbon-nitrogen bonds, chemists often consider using alkenes as substrates, due to their wide availability, variety of substitution patterns and ease of transformation. Transformations creating new carbon-nitrogen bonds from alkenes include hydroamination, aziridation, aminocarbonylation and diamination (Fig 1.1). This chapter will focus on the hydroamination of unactivated alkenes, as this strategy promises to be an efficient and atom economical way of forming new carbon-nitrogen bonds. This will also present the appropriate background for the research presented in this thesis.

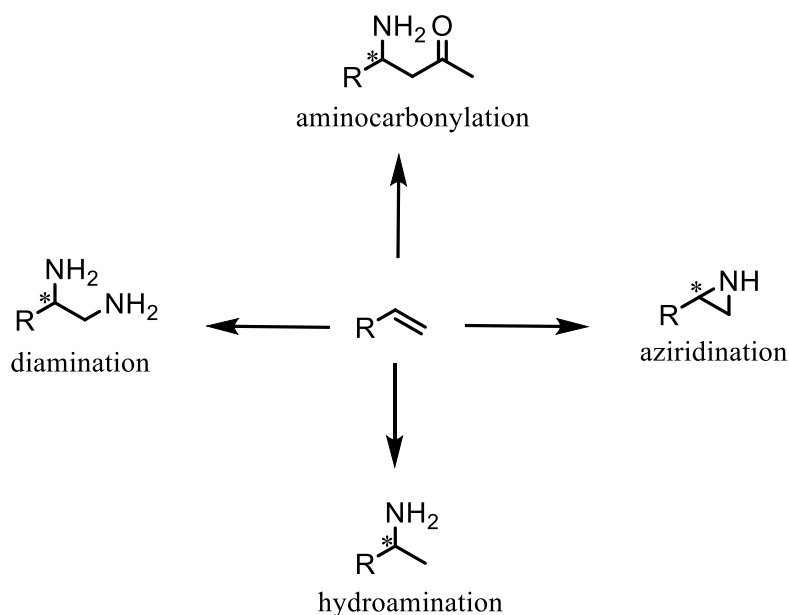


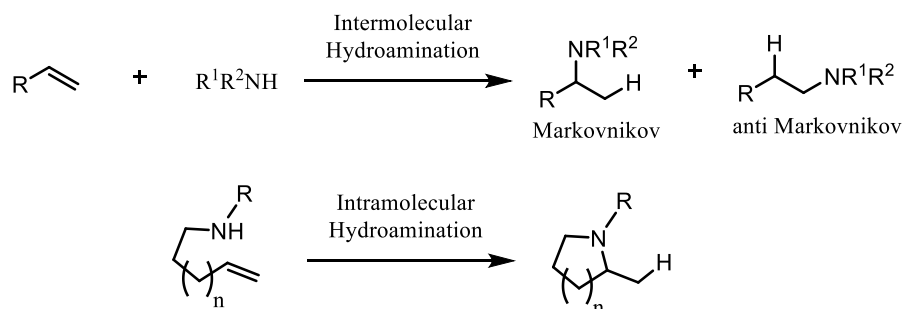
Figure 1.1 Various amination methods of alkenes

Hydroamination consists of the direct addition of an amine across an unsaturated C-C bond. The reaction is theoretically completely atom-efficient, however an excess of either the alkene or amine coupling partner is very often required in intermolecular systems. Nonetheless, hydroamination remains a very attractive solution to C-N bond formation, even though a generalized solution does not exist.¹ Many barriers need to be overcome in order for the intermolecular hydroamination of unactivated alkenes to be possible. Firstly, intermolecular alkene hydroamination is only slightly exothermic or even thermoneutral, thus leading to a potentially unfavorable reaction thermodynamically. Secondly, there exists electrostatic repulsion between the electron rich alkene and the lone pair of the nitrogen. Lastly, the reaction presents high negative entropy, which can make new C-N bond formation more unfavorable as the temperature is elevated. To overcome some of these issues,

¹ (a) Muller, T. E.; Hultsch, K. C.; Yus, M.; Foubelo, F.; Tada, M. *Chem. Rev.* **2008**, *108*, 3795. (b) Hultsch, K. C. *Adv. Synth. Catal.* **2005**, *347*, 367. (c) Muller, T. E.; Beller, M. *Chem. Rev.* **1998**, *98*, 675.

catalysts are employed, but unfortunately this remains often accompanied by the use of elevated temperatures.

Hydroamination can occur in intermolecular or intramolecular systems (Scheme 1.1). The lower entropic penalty of the intramolecular version of this reaction makes it a much more attractive strategy to employ. In addition to facilitating the desired transformation, preference for specific cyclization pathways typically dictates product distribution, whereas in intermolecular reactions the formation of both Markovnikov and anti-Markovnikov products can occur.



Scheme 1.1 Intermolecular and intramolecular hydroamination of alkenes and selectivity

The use of tethered or directed reactions to perform difficult intermolecular reactions has emerged as powerful strategy.² The use of temporary tethers allows for increased reaction rates by lowering the entropic term (ΔS^\ddagger) in Gibbs free energy of activation ($\Delta G^\ddagger = \Delta H^\ddagger - T\Delta S^\ddagger$) through temporary intramolecularity.³ The use of this strategy mimics nature,

² Rousseau, G.; Breit, B. *Angew. Chem., Int. Ed.* **2011**, *50*, 2450–2494.

³ For an overview of tethering chemistry: F. Diederich, P. J. Stang, *Templated Organic Synthesis*, Wiley-VCH, Chichester, UK, 2000. For selected examples in which the catalytic systems operate via preassociation and substrate activation: (a) Sammakia, T.; Hurley, T. B. *J. Am. Chem. Soc.* **1996**, *118*, 8967–8968. (b) Sammakia, T.; Hurley, T. B. *J. Org. Chem.* **1999**, *64*, 5652–5653. (c) Sammakia, T.; Hurley, T. B. *J. Org. Chem.* **2000**, *65*, 974–978. (d) Bedford, R. B.; Coles, S. J.; Hursthouse, M. B.; Limmert, M. E. *Angew. Chem. Int. Ed.* **2003**, *42*, 112–114. (e) Lightburn, T. E.; Dombrowski, M. T.; Tan, K. L. *J. Am. Chem. Soc.* **2008**, *130*, 9210–9211. (f) Grünanger, C. U.; Breit, B. *Angew. Chem., Int. Ed.* **2008**, *47*, 7346–7349. (g) Fuchs, D.; Rousseau, G.; Diab, L.; Gellrich, U.; Breit, B.

in which enzymes are used to facilitate difficult intermolecular reactions. Synthetic chemists have tried to develop catalysts to emulate the efficiency of enzymes in catalyzing challenging bimolecular reactions (with rate accelerations as high as 10^{17}).⁴

Enzymes employ a strategy of pre-organization of substrates through covalent and non-covalent interactions to facilitate these reactions, thus resulting in preassociation of substrates which reduces the entropic barrier of the reaction. In such a manner, rate accelerations of up to 10^4 - 10^8 for 1M reactants at room temperature can be achieved solely through the application of temporary intramolecularity.⁵ Chemists are therefore very motivated to attempt to duplicate enzymes' remarkable efficiency.

Even with significant advances in the field of temporary tethers, there still remains many critical limitations to this strategy. Most tethered reactions suffer from the drawbacks of auxiliary-type approaches and require additional steps in order to form and cleave the "temporary" tether (Figure 1.2).⁶ This results in lengthier syntheses and an overall wasteful process that usually generate by-products. Therefore, catalytic methods by which the formation of tether, the desired reaction and the cleavage of the tether occur in one-pot, are very attractive. Furthermore, catalytic versions of tethered reactions are rare in the literature, but would constitute a superior strategy, as it would generate less by-products

Angew. Chem., Int. Ed. **2012**, *51*, 2178-2182. (h) Worthy, A. D.; Joe, C. L.; Lightburn, T. E.; Tan, K. L. *J. Am. Chem. Soc.* **2010**, *132*, 14757-14759. (i) Sun, X.; Worthy, A. D.; Tan, K. L. *Angew. Chem., Int. Ed.* **2011**, *50*, 8167-8171. (j) Murphy, S. K.; Coulter, M. M.; Dong, V. *Chem. Sci.* **2012**, *3*, 355-358. (k) Worthy, A. D.; Sun, X.; Tan, K. L. *J. Am. Chem. Soc.* **2012**, *134*, 7321-7324.

⁴ Radzicka, A.; Wolfenden, R. *Science* **1995**, *267*, 90-93.

⁵ Jencks, W. P. *Adv. Enzymol. Relat. Areas Mol. Biol.* **1975**, *43*, 219-410.

⁶ (a) Diederich, F.; Stang, P. J. *Templated Organic Synthesis*; Wiley-VCH: Chichester, U.K., **2000**. (b) Bols, M.; Skrydstrup, T. *Chem. Rev.* **1995**, *95*, 1253-1277. (c) Fensterbank, L.; Malacria, M.; Sieburt, S. *Synthesis* **1997**, 813-854. (d) Gauthier, D. R., Jr.; Zandi, K. S.; Shea, K. J. *Tetrahedron* **1998**, *54*, 2289-2338.

and allow for product formation in a single operation. In recent years, the Beauchemin group has shown interest in the use of aldehyde catalysis as a means to reversibly form a tether between two reagents and thusly induce temporary intramolecularity. It was hypothesized that this strategy could be employed to improve the rates and scope of intermolecular hydroamination reactions.

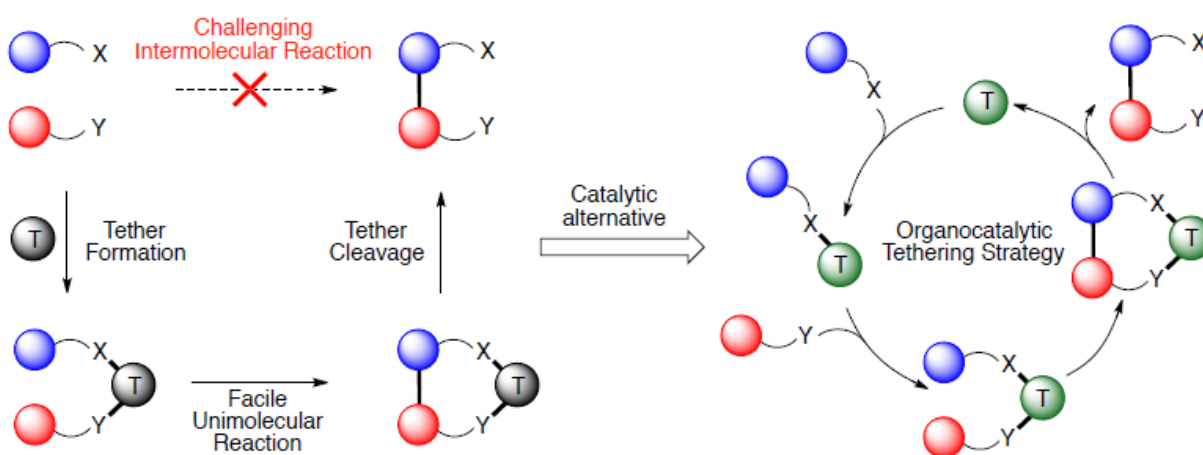


Figure 1.2 Targeted stepwise approach to tethering for challenging intermolecular reactions and catalytic alternative

1.2 Carbonyl Catalysis

As previously stated, catalysis consists of a robust solution to promoting difficult intermolecular reactions, often times by reducing the high activation energy costs. Traditionally this is accomplished by activating the reagents involved in the reaction, however it is also possible to achieve catalysis solely by preassociating reagents. This idea has led chemists to emulate enzymes' mode of action through the application of small organic molecules. The hypothesis being that through the formation of temporary covalent

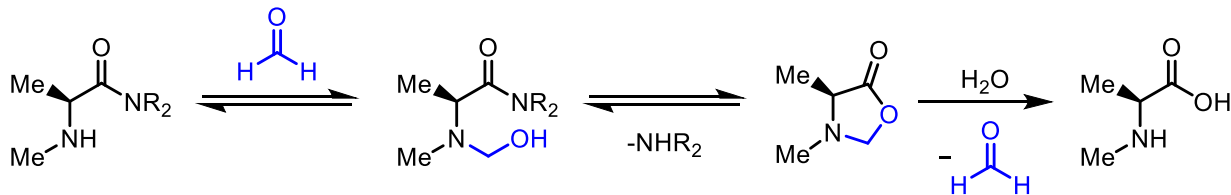
interactions, a difficult intermolecular reaction can be achieved through a temporary intramolecular pathway, thusly controlling regioselectivity and potentially stereoselectivity.

However, catalysts that operate solely through this concept of temporary intramolecularity are quite rare and often suffer from the disadvantages of stoichiometric loadings. Other strategies may also require longer syntheses, for example by requiring steps to install and cleave directing groups. Despite these initial hurdles, carbonyl catalysis shows promise for application in the field of temporary intramolecularity. Carbonyl catalysis was primarily used as a tool to promote hydrolysis and hydration reactions. Using water as a reactant and stoichiometric amounts of a ketone or aldehyde, Commeyras and coworkers were able to accomplish the hydrolysis of α -aminoamides into amino acids (See Figure 1.3).⁷ The reaction is initiated by the reaction of the carbonyl (formaldehyde) with the amine moiety. This is followed by an intramolecular attack on the amide moiety by the oxygen of the newly formed hemiaminal. The hydrolysis of the heterocycle affords an amino acid and the regeneration of the carbonyl. Expanding upon this initial concept, Seto *et al.* employed ketones to achieve the hydrolysis of α -mercaptoamides. They were able to report a rate acceleration of 15,000 times when compared to the background (catalyst-free reaction) (see Figure 1.3).⁸

⁷ Pascal, R.; Lasperas, M.; Taillades, J.; Commeyras, A. *New. J. Chem.* **1987**, *11*, 235-244.

⁸ Ghosh, M.; Conroy, J. L.; Seto, C. T. *Angew. Chem., Int. Ed.* **1999**, *38*, 514-516.

Commeyras *et al.*



Seto *et al.*

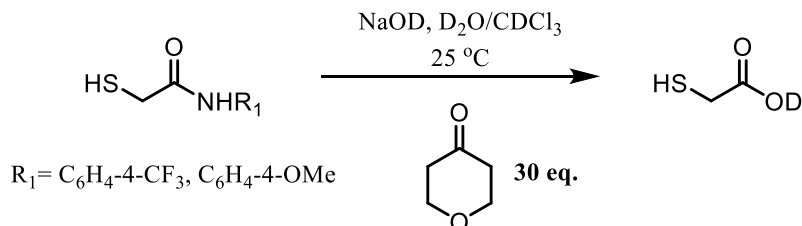


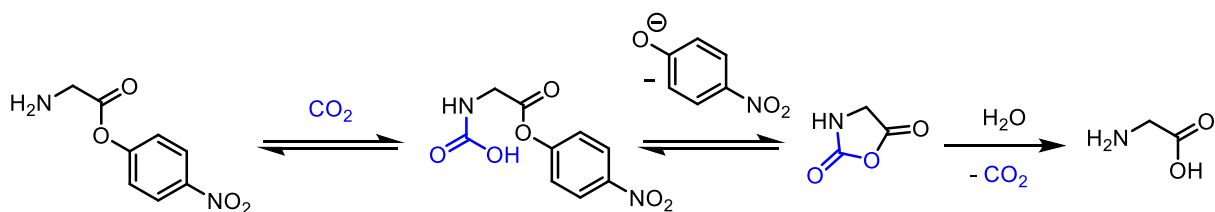
Figure 1.3 Reported examples of amide hydrolysis via carbonyl catalysis

Ester hydrolysis also represents another reaction to which carbonyl catalysis has been applied. In 1956, Wieland and his group reported on the hydrolysis of *p*-nitrophenyl esters, catalyzed by carbon dioxide from bicarbonate. The proposed mechanism is similar to the previously mentioned hydrolysis reaction, namely through initial condensation of the carbonyl, followed by formation of a cyclic intermediate (anhydride). The cycle is terminated by the hydrolysis event and the release of an equivalent of carbon dioxide. Following these initial findings, other groups reported the use of aromatic aldehydes as effective catalysts for this transformation. (see Figure 1.4).⁹ It should be noted that one main limitation of these approaches consists of the need for *p*-nitrophenyl esters for hydrolysis to take place.

⁹ (a) Wieland, V. T.; Lambert, R.; Lang, H. U.; Schramm, G. *Justus Liebigs Ann. Chem.* **1956**, 597, 181.

(b) Wieland, V. T.; Jaenicke, F. *Justus Liebigs Ann. Chem.* **1956**, 599, 125. (c) Capon, B.; Capon, R. J. *Chem. Soc., Chem. Commun.* **1965**, 20, 502-503. (d) Hay, R. W.; Main, L. *Aust. J. Chem.* **1968**, 21, 155-169.

Wieland



Other reported examples

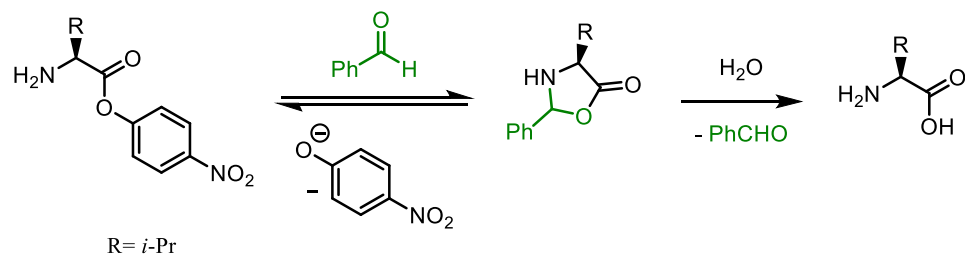


Figure 1.4 Reported examples of ester hydrolysis via carbonyl catalysis

Another example of carbonyl catalysis through temporary intramolecularity consists of the transesterification of α -hydroxy esters developed by Samakia and coworkers.¹⁰ This reaction follows a mechanism similar to previously presented examples. The initial condensation is followed by the formation of a cyclic 5-membered acetal intermediate, which is followed by the transesterification of the initial ester. It should be noted that under these conditions the transesterification is limited to the formation of methyl esters from *p*-nitrophenyl esters. The use of electron-withdrawing ketones is postulated to promote the initial addition/condensation (see Figure 1.5). The cyclic acetal was observed via NMR monitoring of the reaction, which supports the theory of carbonyl catalysis through temporary intramolecularity. This work is also one of the rare examples in which sub-

¹⁰ (a) Samakia, T.; Hurley, T. B. *J. Am. Chem. Soc.* **1996**, *118*, 8967-8968. (b) Samakia, T.; Hurley, T. B. *J. Org. Chem.* **1999**, *64*, 5652-5653. (c) Samakia, T.; Hurley, T. B. *J. Org. Chem.* **2000**, *65*, 974-978.

stoichiometric amounts of catalyst are used, supporting the idea that temporary intramolecularity catalysis does not necessitate stoichiometric conditions.

Sammakia

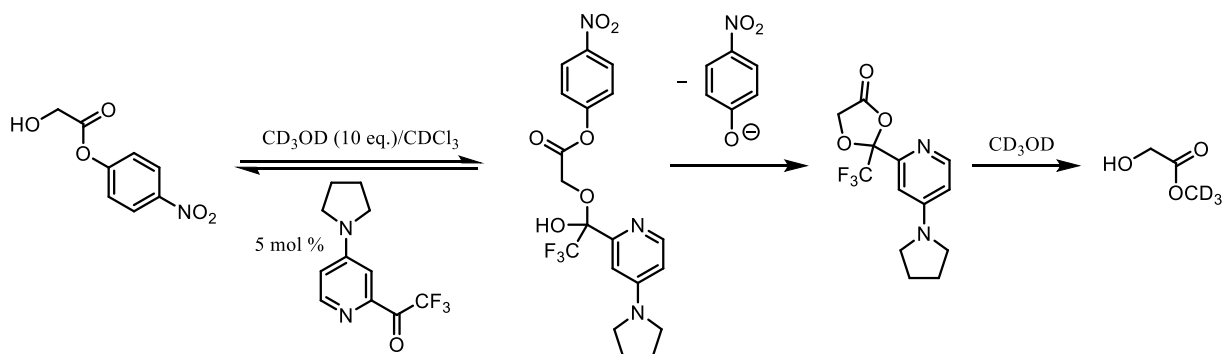


Figure 1.5 Transesterification of α -hydroxy esters via carbonyl catalysis

In more recent developments, aldehydes and ketones have been used as transient directing groups to promote difficult reactions.¹¹ In these types of approaches, the ability of carbonyls to reversibly form imines and enaminals/acetals is once again exploited. Aldehydes or ketones are appended with various directing groups, which in turn allows for the temporary attachment of the directing group to a desired reagent with appropriate functionality (free amine or hydroxyl group). The directing group then promotes the recruitment of another reagent or metal catalyst, which allows for catalysis through temporary intramolecularity. Transient directing groups have been used in the field of C-H activation to allow for some previously difficult transformations. Figure 1.6 illustrates the general principle behind this strategy.

¹¹ For a review of directed reactions of organocopper reagents: Schmidt, Y.; Breit, B. *Chem. Rev.* **2008**, *108*, 2928–2951.

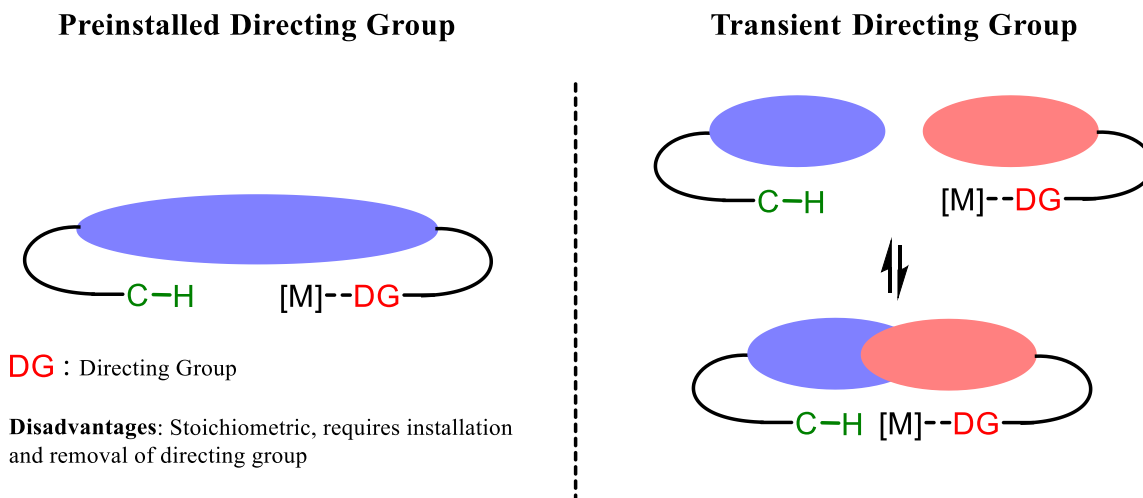


Figure 1.6 Strategies for directed C-H bond activation

Yu and coworkers utilized this concept to achieve proximity-driven metalation. They reported the use of amino acids as transient directing groups via in situ reversible formation of imines with ketones and aldehydes. After imine formation, palladium catalysts can be directed to the desired reagent via the free carboxylate group, which allows for C(sp³)-H bond activation in the β or γ position. As opposed to most previously presented examples, this methodology only requires catalytic amounts of both the amino acid (40-50 mol%) and metal catalyst (5-10 mol%) to achieve arylation of a wide scope of both aromatic aldehydes and aliphatic ketones. They were also able to demonstrate the potential of achieving enantioselective arylation reactions via the use of chiral amino acids (see Figure 1.7). Although the scope of the reactivity is impressive, it is important to note that arylation of aliphatic aldehydes could not be achieved due to the competing reaction pathways leading to the decomposition of starting materials.¹² This example displays the advantages of

¹² Zhang, F.-L.; Hong, K.; Li, T.-J.; Park, H.; Yu, J.-Q. *Science* **2016**, *351*, 252-256.

exploiting the reversible formation of imines in order to promote temporary intramolecularity.

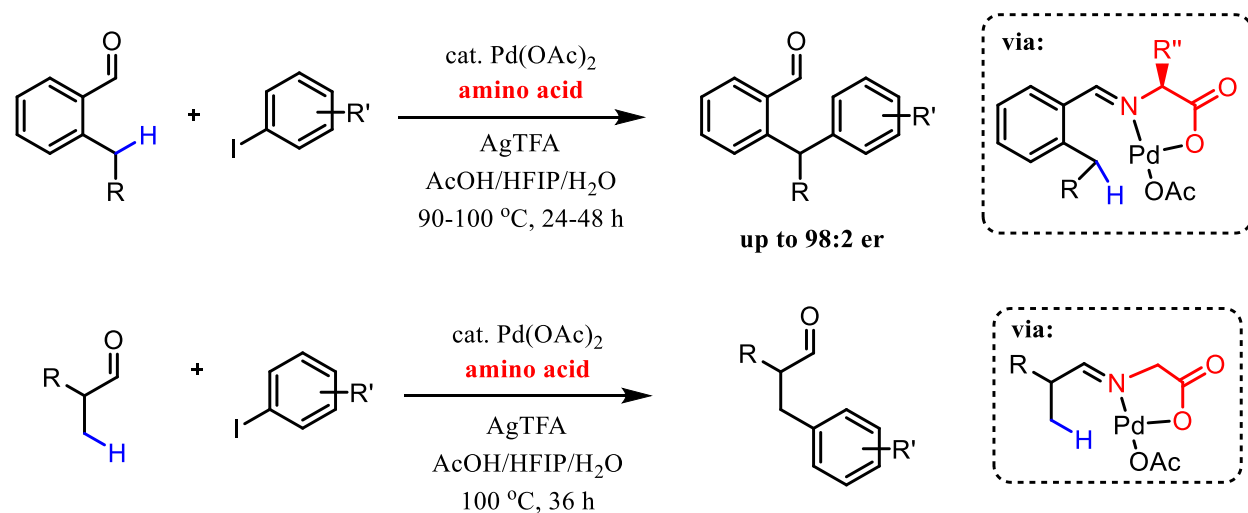


Figure 1.7 C(sp³)-H arylation using an amino acid as a transient directing group

Ge and coworkers were also able to utilize transient directing groups to achieve difficult arylation reactions. Once again, by exploiting the propensity for aldehydes to reversibly form imines, metalation directing groups can be temporarily appended to substrates for transformation. In a first example, the group achieves the direct arylation of aliphatic aldehydes via Pd-catalyzed sp³ C-H bond functionalization by using 3-aminopropanoic acids as the transient directing groups. The reaction shows excellent chemoselectivity in which the preference is for the functionalization of unactivated β-C-H bonds of methyl groups (see Figure 1.8).¹³ In this case, the aldehydes serve as substrates for the 3-aminopropanoic acid directing groups, however the reversal of roles can also be achieved. In another study, Ge's group were able to achieve the C-H bond functionalization of aliphatic amines, while using glyoxylic acid to form the transient directing group. Once

¹³ Ge, H.; Li, G.; Li, Q.; Liu, Y.; Yang, K. *J. Am. Chem. Soc.* **2016**, *138*, 12775–12778.

again, high site selectivity was achieved for γ -C-H bonds of unactivated sp^3 carbons (see Figure 1.8).¹⁴ Both of these examples highlight the advantages of transient directing groups and the use of carbonyl catalysis, namely achieving temporary intramolecularity, thus avoiding stoichiometric conditions, additional synthetic steps (addition and removal of directing groups) and expensive catalysts. The high importance and prevalence of aliphatic aldehydes and amines in the fields of organic synthesis and medicinal chemistry displays the need to further develop new efficient strategies for their functionalization.

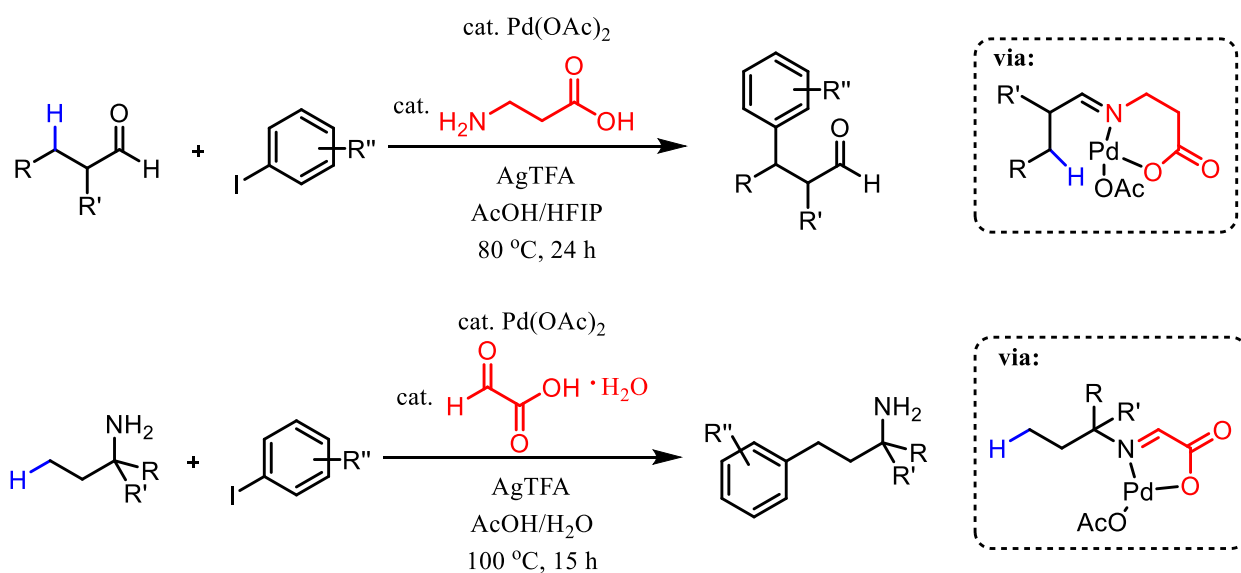


Figure 1.8 C(sp³)-H arylation of aliphatic aldehydes and amines via transient directing groups

Another recent example which highlights the potential of carbonyls to act as tethers facilitating difficult intermolecular reactions, is the work in olefin oxy- and aminoalkynylation by Waser and coworkers.¹⁵ Although the work does not represent a catalytic example of carbonyls acting as temporary tethers, it is still an important

¹⁴ Liu, Y.; Ge, H. *Nat. Chem.* **2017**, *9*, 26-32.

¹⁵ Orcel, U.; Waser, J. *Angew. Chem. Int. Ed.* **2015**, *54*, 5250-5254.

development demonstrating induced intramolecularity. The use of fluoroacetaldehyde (used in its hemiacetal form) allows for the palladium-catalyzed carbo-oxygenation of allylamines through tether formation. This tethering process allows for both the formation of amino alcohols, and the concomitant incorporation of alkynyl, vinyl or aryl moieties (see Figure 1.9). While this tethering strategy requires stoichiometric application of the aldehyde and subsequent hydrolysis, it does improve on traditional strategies which require the stepwise introduction of the tether, followed by the desired reaction and subsequent removal of the tether. This approach combines the advantages of intramolecular and intermolecular reactions, allowing for high regioselectivity as well as stereoselectivity, while greatly accelerating reaction rates and also further highlights the strength of carbonyls as potential tethering reagents.

Waser

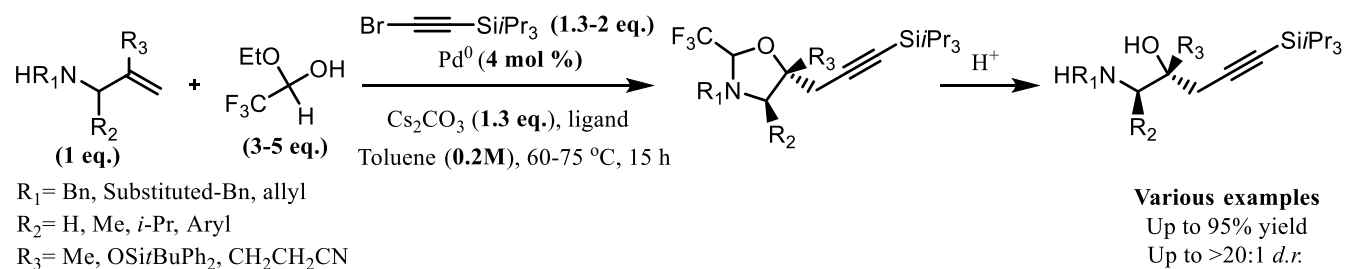


Figure 1.9 Palladium catalyzed synthesis of amino alcohols via in situ tether formation with trifluoroacetaldehyde

Recently, the strategy of catalysis through temporary intramolecularity has been employed by Tan and coworkers in order to accomplish the desymmetrization of *syn* 1,2-diols through silylation in a highly enantioselective fashion. The use of a scaffolding catalyst allows for the coordination of the 1,2-diol, which in turn allows for the acceleration of the silylation reaction as well as affording excellent enantioselectivities under very mild

conditions (See Figure 1.10).¹⁶ Once again, this rate acceleration is not achieved through substrate activation, but rather through temporary intramolecularity. The substrate scope was also shown to be quite broad with good to excellent yields being observed for a variety of cyclic diols as well as some acyclic examples. The relatively low catalyst loading utilized as well as the mild conditions used, further reinforce the hypothesis that organocatalysis through temporary intramolecularity is a highly viable strategy.

Tan

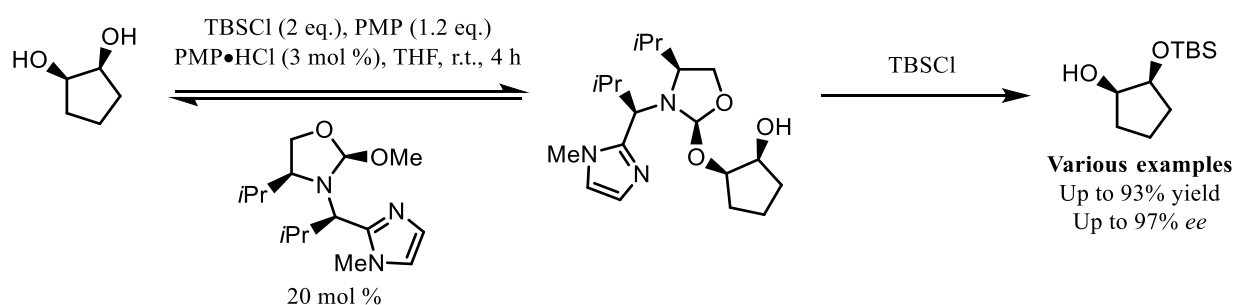


Figure 1.10 Desymmetrization of *syn* 1,2-diols through the application of a scaffolding catalyst

Presented examples highlight the potential of carbonyl catalysis to promote difficult intramolecular reactions through intramolecularity. Initial forays into achieving these transformations consisted mostly of hydrolysis and other simple transformations, therefore the scope and applicability of these strategies were somewhat limited. Furthermore, mostly stoichiometric amounts of catalyst were used in most reactions, the use of lower concentrations and thus the achievement of true catalysis should be possible. These initial strategies attempting to harness temporary intramolecularity through carbonyl catalysis highlight the potential for further development and the potential application of such strategies to more complex intramolecular reactions. The goal being to be able to control

¹⁶ Sun, X.; Worthy, A.D.; Tan, K.L. *Angew. Chem. Int. Ed.* **2011**, *50*, 8167-8171.

regioselectivity and stereoselectivity through the application of simple organic molecules serving only as temporary tethers, thus promoting temporary intramolecularity. More recent examples, such as the work by Ge, Beauchemin and Tan show that true catalysis that harnesses temporary intramolecularity is possible. Further development of such strategies will allow for more efficient reactions which display great chemoselectivity, regioselectivity, as well as enantioselectivity.

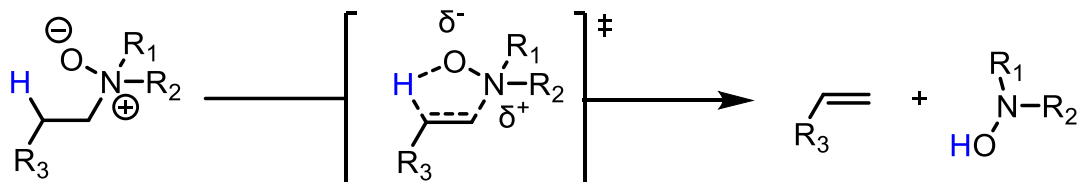
1.3 Cope-Type Hydroamination

The Cope-type hydroamination represents an interesting candidate for the application of aldehyde catalysis. This reaction represents the microscopic reverse of the Cope elimination. The Cope elimination was discovered by Cope and co-workers in 1949. In these studies, it was demonstrated that by heating trialkylamine-*N*-oxides possessing a β -hydrogen, one could obtain an olefin and a *N,N*-dialkylhydroxylamine, through a *syn* elimination (See Scheme 1.2).¹⁷ The microscopic reverse of this process was first reported by House in 1976, when his group discovered that the reverse of the Cope elimination could yield cyclic hydroxylamines through an intramolecular "hydroamination" reaction.¹⁸ Labelled the "reverse Cope cyclization", this process occurred under mild conditions and at room temperature. For many years, the exact mechanism remained debated until 1994, when Oppolzer provided strong evidence that the reaction proceeded through a suprafacial

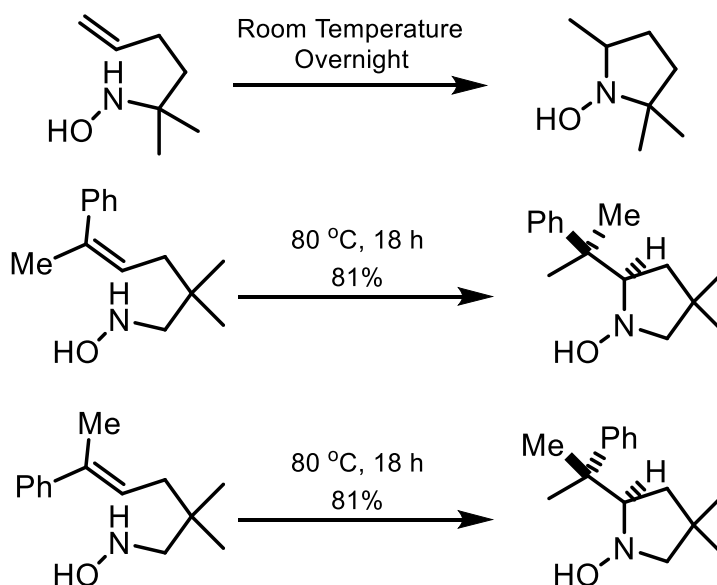
¹⁷ Cope, A. C.; Foster, T. T.; Towle, P. H. *J. Am. Chem. Soc.* **1949**, *71*, 3929.

¹⁸ (a) House, H. O.; Manning, D. T.; Melillo, D. G.; Lee, L. F.; Haynes, O. R.; Wilkes, B. E. *J. Org. Chem.* **1976**, *41*, 855-863. (b) House, H. O.; Lee, L. F. *J. Org. Chem.* **1976**, *41*, 863-869.

and stereospecific five-membered transition state (Scheme 1.3).^{19,20} These findings allowed for the expansion of the scope of Cope-type hydroamination to methodologies involving alkynes²¹ and towards the synthesis of saturated heterocycles.²²



Scheme 1.2 Cope elimination of trialkylamine-*N*-oxides



Scheme 1.3 Oppolzer's cyclic Cope-type hydroamination

¹⁹(a) Black, D. St. C.; Doyle, J. E.; *Aust. J. Chem.* **1978**, *31*, 2317. (b) Ciganek, E. *J. Org. Chem.* **1990**, *55*, 3007-3009. (c) Ciganek, E.; Read, J. M. Jr.; Calabrese, J. C. *J. Org. Chem.* **1995**, *60*, 5795-5802. (d) Ciganek, E. *J. Org. Chem.* **1995**, *60*, 5803-5807.

²⁰ Oppolzer, W.; Spivey, A. C.; Bochet, C. G. *J. Am. Chem. Soc.* **1994**, *116*, 3139-3140.

²¹ (a) Pradhan, S. K.; Akamanchi, K. G.; Divakaran, P. P.; Pradhan, P. M. *Heterocycles* **1989**, *28*, 813-816. (b) Holmes, A. B.; Smith, A. L.; Williams, S. F.; Hughes, L. R.; Lidert, Z.; Swithenbank, C. *J. Org. Chem.* **1991**, *56*, 1393-1405. (c) Fox, M. E.; Holmes, A. B.; Forbes, I. T.; Thompson, M. *Tetrahedron Lett.* **1992**, *33*, 7421-7424.

²² (a) Bagley, M. C.; Tovey, J. *Tetrahedron Lett.* **2001**, *42*, 351-353. (b) Knight, D. W.; Leese, M. P.; De Kimpe, N. *Tetrahedron Lett.* **2001**, *42*, 2597-2600. (c) Knight, D. W.; Leese, M. P. *Tetrahedron Lett.* **2001**, *42*, 2593-2597.

Figure 1.11 summarizes the key findings about the reactivity and scope of this reverse Cope cyclization.²³ Most reported intramolecular cases are activated via the Thorpe-Ingold effect, which greatly increases the cyclization rate. Due to the bicyclic nature of the transition state, 5-membered ring formation is favored, while larger ring sizes are more difficult to synthesize. Alkene substitution also stabilizes the asynchronous concerted transition state via electron density donation to the partial positive charge formed, thus resulting in slower cyclization.

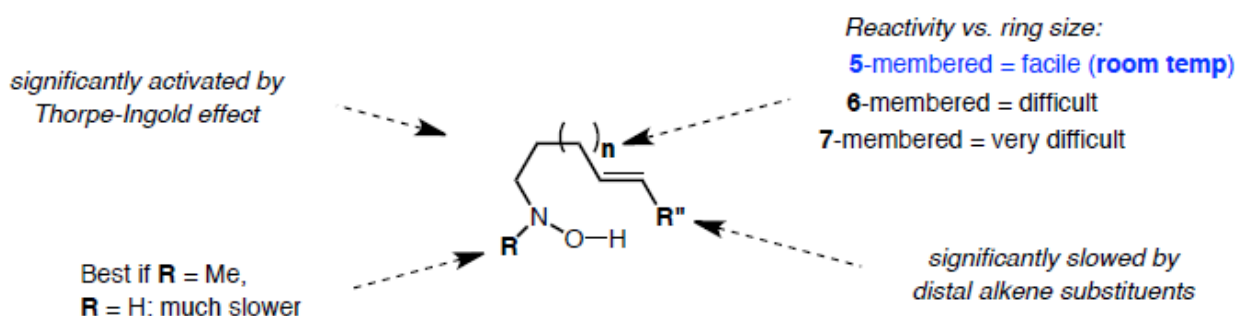


Figure 1.11 Summary of reactivity trends for the Reverse Cope Cyclization

The intermolecular variant of this reaction, defined as the Cope-type hydroamination is much more difficult and remains underdeveloped. Therefore, in 2008, our research group decided to tackle the issue of developing the intermolecular variant of the reaction. Focus was put on the development of methods for the hydroamination of unbiased alkenes and alkynes, while also exploring the possibility of enantioselective methods, which are still quite rare in the literature.²⁴ Initial successful reactions were limited by the use of biased alkenes

²³ Cooper, N. J.; Knight, D. W. *Tetrahedron* **2004**, 243-269.

²⁴ Reviews of enantioselective hydroaminations: (a) Müller, Beller, Yus, Foubelo, Tada *Chem. Rev.* **2008**, 108, 3795-3892. (b) Hesp, K. D.; *Angew. Chem. Int. Ed.* **2014**, 53, 2034-2036.

and harsh conditions (high temperature and microwave irradiation)²⁵. Our group wanted to overcome these limitations and allow for the use of much milder reaction conditions, while improving the substrate scope. The hypothesis of using aldehyde catalysis to facilitate the intermolecular Cope-type hydroamination through temporary intramolecularity was thus put forward.

Due to their ability to reversibly form acetals and amins, aldehydes consist of a good target for application to tethering catalysis. However, a few problems had to be overcome in order for this strategy to be successful. For catalysis of hydroamination to be possible, the chosen aldehyde catalyst must have the propensity to preassociate both substrates, as opposed to solely forming homodimers. Furthermore, a temporary tethering catalysis system would have a driving force to allow for catalyst regeneration and turnover. Figure 1.12 illustrates these basic challenges.

²⁵ (a) Beauchemin, A. M.; Moran, J.; Lebrun, M. E.; Séguin, C.; Dimitrijevic, E.; Zhang, L.; Gorelsky, S. I. *Angew. Chem. Int. Ed.* **2008**, *47*, 1410-1413. (b) Moran, J.; Gorelsky, S. I.; Dimitrijevic, E.; Lebrun, M. E.; Bédard, A. C.; Seguin, C.; Beauchemin, A. M. *J. Am. Chem. Soc.* **2008**, *130*, 17893-17906. (c) Bourgeois, J.; Dion, I.; Cebrowski, P. H.; Loiseau, F.; Bédard, A. C.; Beauchemin, A. M. *J. Am. Chem. Soc.* **2009**, *131*, 874-875.

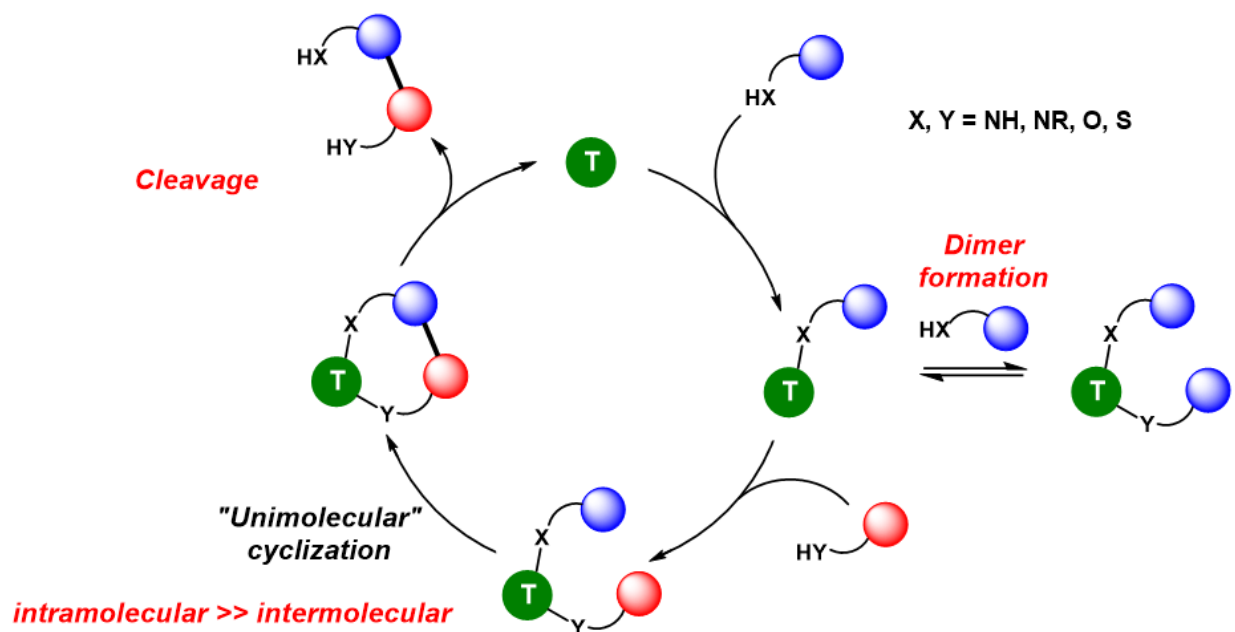
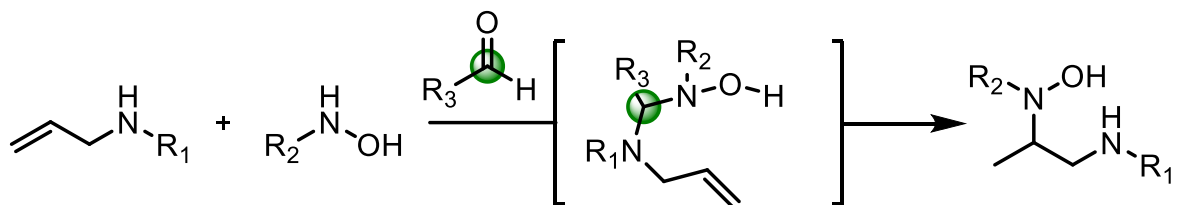


Figure 1.12 Organocatalytic tethering strategy to promote difficult intermolecular reactions through temporary intramolecularity

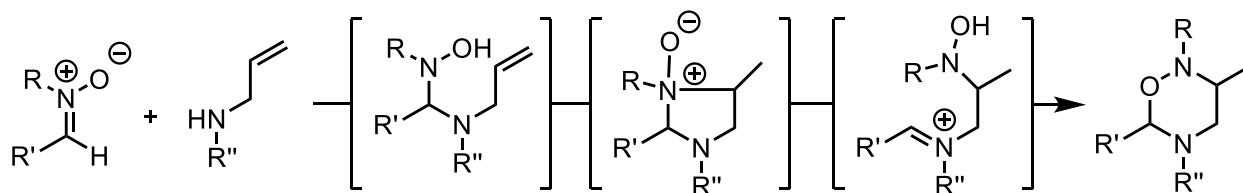
As previously discussed, intermolecular hydroamination represents a challenging reaction due to many factors such as requiring metal catalysts, harsher conditions and often times biased substrates. Furthermore, this reaction has negative entropy and typically had to overcome a high activation energy.²⁶ However, by applying aldehydes to form temporary tethers between hydroxylamines and allylamines, a system is created which mirrors the intramolecular hydroaminations, which can occur at room temperature. Formation of this mixed aminal would lead to the aldehyde forming a one-carbon tether and would allow for the facile five-membered transition state (Scheme 1.4).

²⁶ Johns, A. M.; Sakai, N.; Ridder, A.; Hartwig, J. F. *J. Am. Chem. Soc.* **2006**, *128*, 9306-9307.



Scheme 1.4 General overview of hydroamination through temporary intramolecularity

Previous work done by Knight and coworkers led us to believe that the application of aldehyde catalysis could be fruitful, due to their findings of successful reactions between nitrones and allylamines under stoichiometric conditions.²⁷ This work shows that nitrones can act as precursors to induce an intramolecular hydroamination reaction. Through a sequence of amination formation, followed by hydroamination, then ring-opening and finally ring-closing, the nitrones can be incorporated into heterocyclic products (see Scheme 1.5).

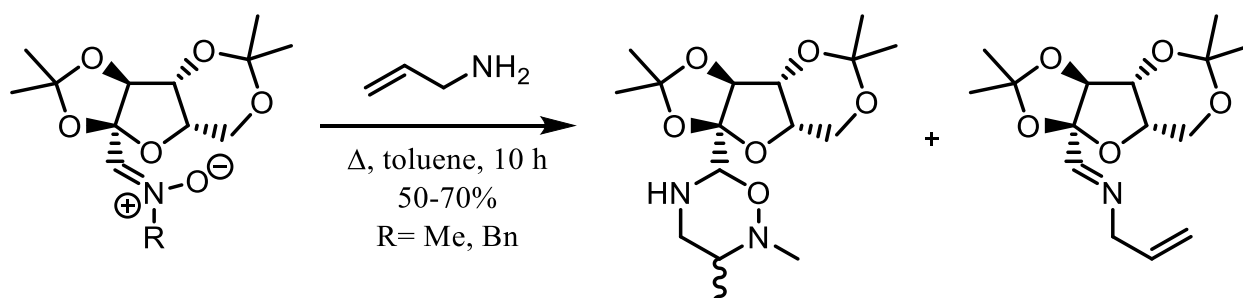


Scheme 1.5 Heterocyclic product formation through transient hydroxylamine formation (Knight and coworkers)

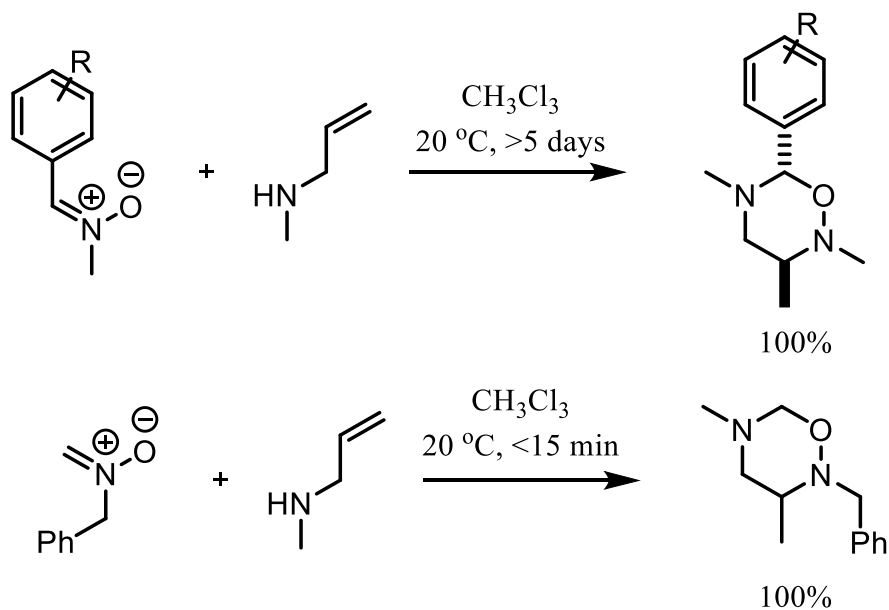
Knight's initial involvement in the area of the reverse Cope cyclisation began with efforts to improve the stereoselectivity of [1,3]-dipolar cycloaddition between nitrones (derived from hexafluoranosonic acid) and allylic amines (see Scheme 1.6).²³ It was initially thought that the unprotected allylamine would add to the nitronium (through the free amine),

²⁷ (a) Gravestock, M. B.; Knight, D. W.; Thornton, S. R. *J. Chem. Soc., Chem. Commun.* **1993**, 169-171. (b) Bell, K. E.; Coogan, M. P.; Gravestock, M. B.; Knight, D. W.; Thornton, S. R. *Tetrahedron Lett.* **1997**, 49, 8545-8548. (c) Gravestock, M. B.; Knight, D. W.; Abdul Malik, K. M.; Thornton, S. R. *J. Chem. Soc., Perkin Trans. 1* **2000**, 3292-3305.

but that this process would not hinder the cycloaddition, due to the reversible nature of this addition. However, the isolated products consisted mostly of the isomeric oxadiazinanes (with a *trans/cis* ratio of 3:1), with traces of imine product. This initial result pointed to the possibility of the nitrones acting as precursors of intramolecular hydroamination, through the initial formation of a mixed aminal with the allylamine. To further explore this possibility, a much more easily handled benzaldehyde-derived nitrone was treated with allylamine, giving almost quantitative yield of *trans*-oxadiazinane.



Scheme 1.6 Knight's initial nitrone as a precursor to intramolecular hydroamination



Scheme 1.7 Knight's comparison of nitrone reactivity

Thus, Knight's research suggested that a catalytic variation of this reaction could be possible if aldehydes that promoted preassociation, but avoided the final ring-closing step and therefore heterocyclic product formation, were discovered. Some other results obtained by Knight provided insight into the fact that more electron-withdrawing aldehydes might improve the reaction by forming destabilized nitrones. In his work, Knight showed that benzaldehyde derived nitrones reacted much more slowly (5 days) with *N*-methylallylamine, when compared to formaldehyde derived nitrones (15 minutes) (see Scheme 1.7). As previously outlined, the proposed catalytic (see Figure 1.13) cycle of the reaction would proceed with initial condensation between the aldehyde and the hydroxylamine, thus forming the nitron. Nitron formation would then be followed by a 1,2-addition of the allylamine to form a mixed aminal. With the aminal formed, the intramolecular Cope-type hydroamination should readily occur at room temperature. The cycle would be complete with aminal cleavage, followed by the regeneration of the nitron. Therefore, at the inception of this project aldehydes, that favored preassociation and avoided 6-membered heterocyclic products, needed to be discovered.

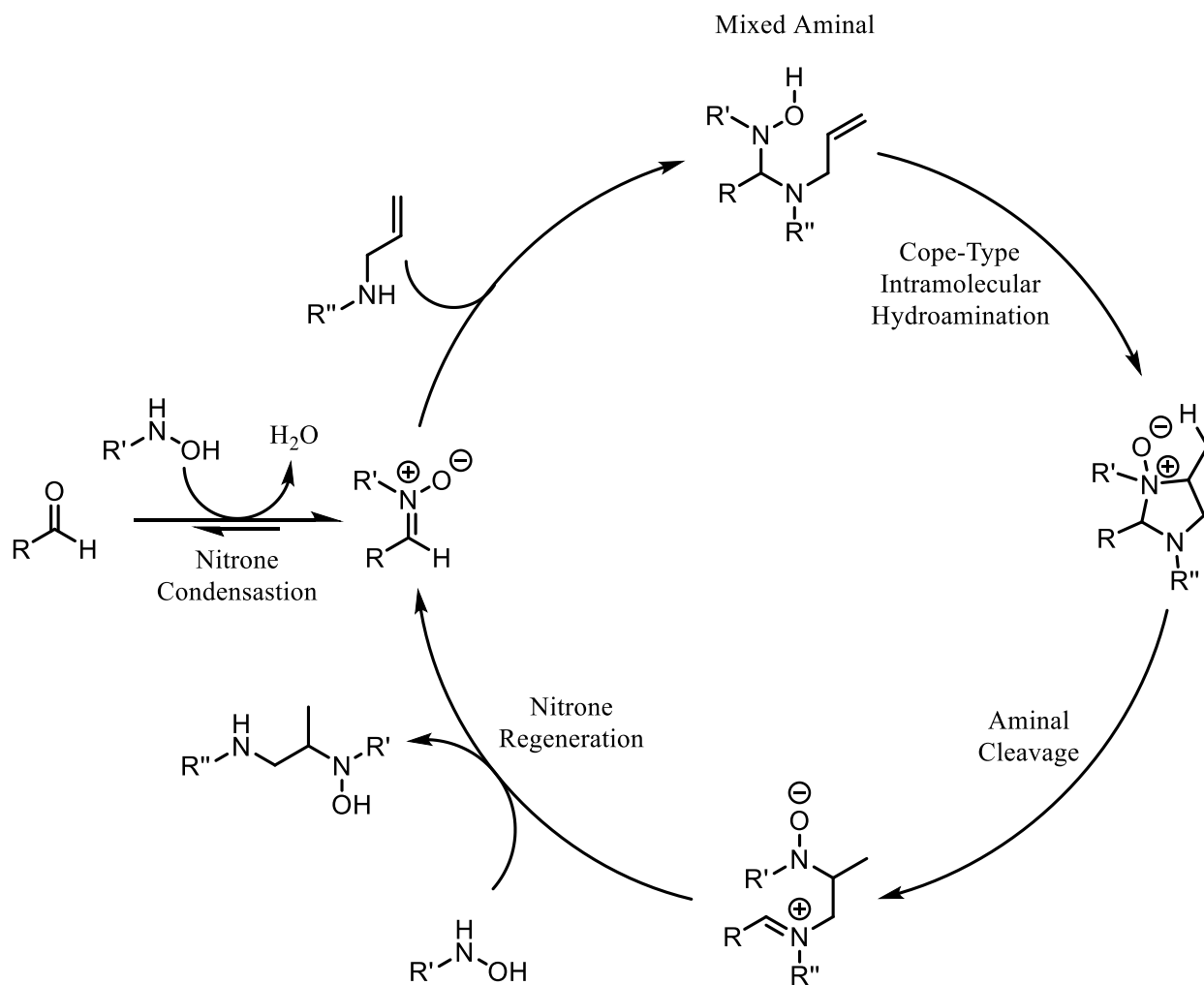


Figure 1.13 Proposed catalytic cycle for the catalytic variant of the Cope-type intramolecular hydroamination

In 2008, our group reported the intermolecular Cope-type hydroamination of alkenes with aqueous hydroxylamine and *N*-alkylhydroxylamines.²⁸ Norbornene and other such strained alkenes showed good reactivity with the aforementioned hydroxylamines.

²⁸ Moran, J.; Gorelsky, S. I.; Dimitrijevic, E.; Lebrun, M-E.; Bédard, A-C.; Séguin, C.; Beauchemin, A. M. *J. Am. Chem. Soc.* **2008**, *130*, 17893.

However, unbiased (unstrained or electron deficient) alkenes only displayed poor to moderate reactivity, even at higher temperatures (Figure 1.14).

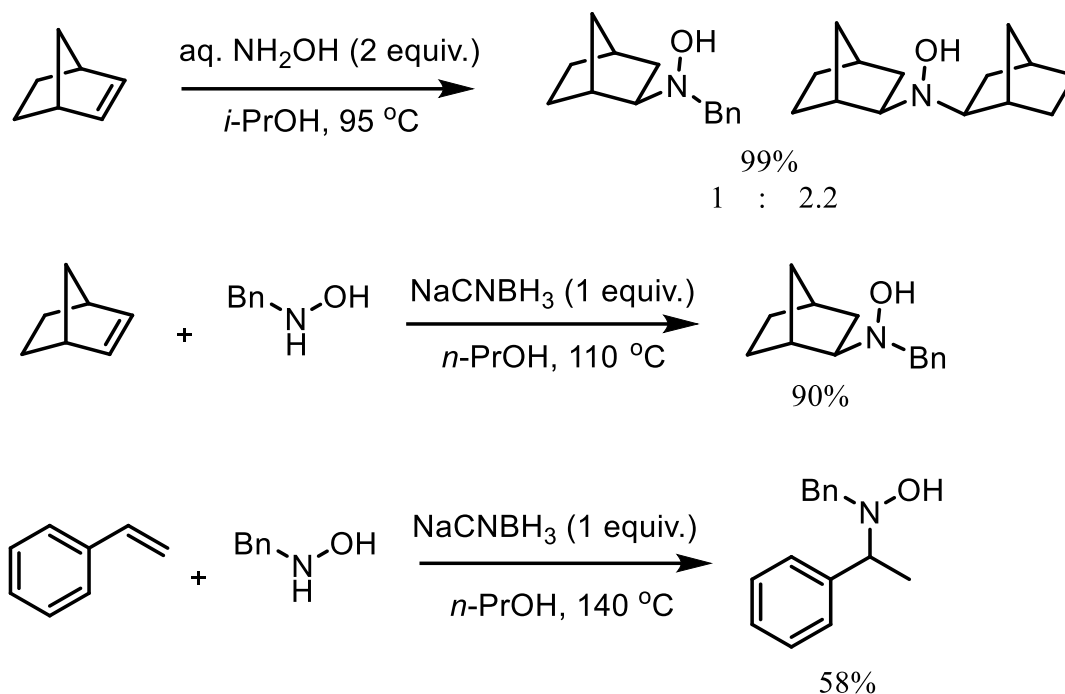
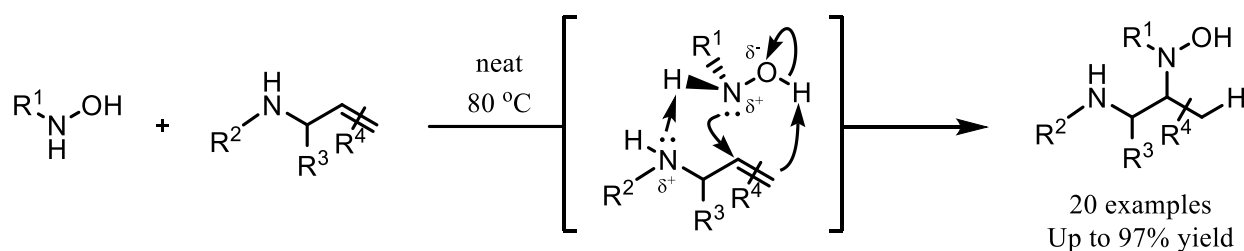


Figure 1.14 Initial examples of intermolecular Cope-type hydroamination of alkenes with aqueous hydroxylamine and *N*-alkylhydroxylamines

In 2012, upon further investigation of hydroamination reactions with hydroxylamines, our group was able to demonstrate that the reaction between *N*-alkylhydroxylamines and allylic amines in the absence of solvent resulted in the formation of Cope-type hydroamination products.²⁹ These were promising results given the good yields for reactions with unbiased alkenes. The observed increase in reactivity was attributed to stabilization by pre-association of reagents via H-bonding between the N-H

²⁹ Zhao, S-B.; Bilodeau, E.; Lemieux, V.; Beauchemin, A. M. *Org. Lett.* **2012**, *14*, 5082.

bond of the hydroxylamine and the lone pair of the allylic amine (Scheme 1.8). Although the yields obtained were good, the use of higher temperatures and longer reaction times were still required. However, the generation of hydroamination products was promising and validated further efforts to apply carbonyl catalysis methodologies.



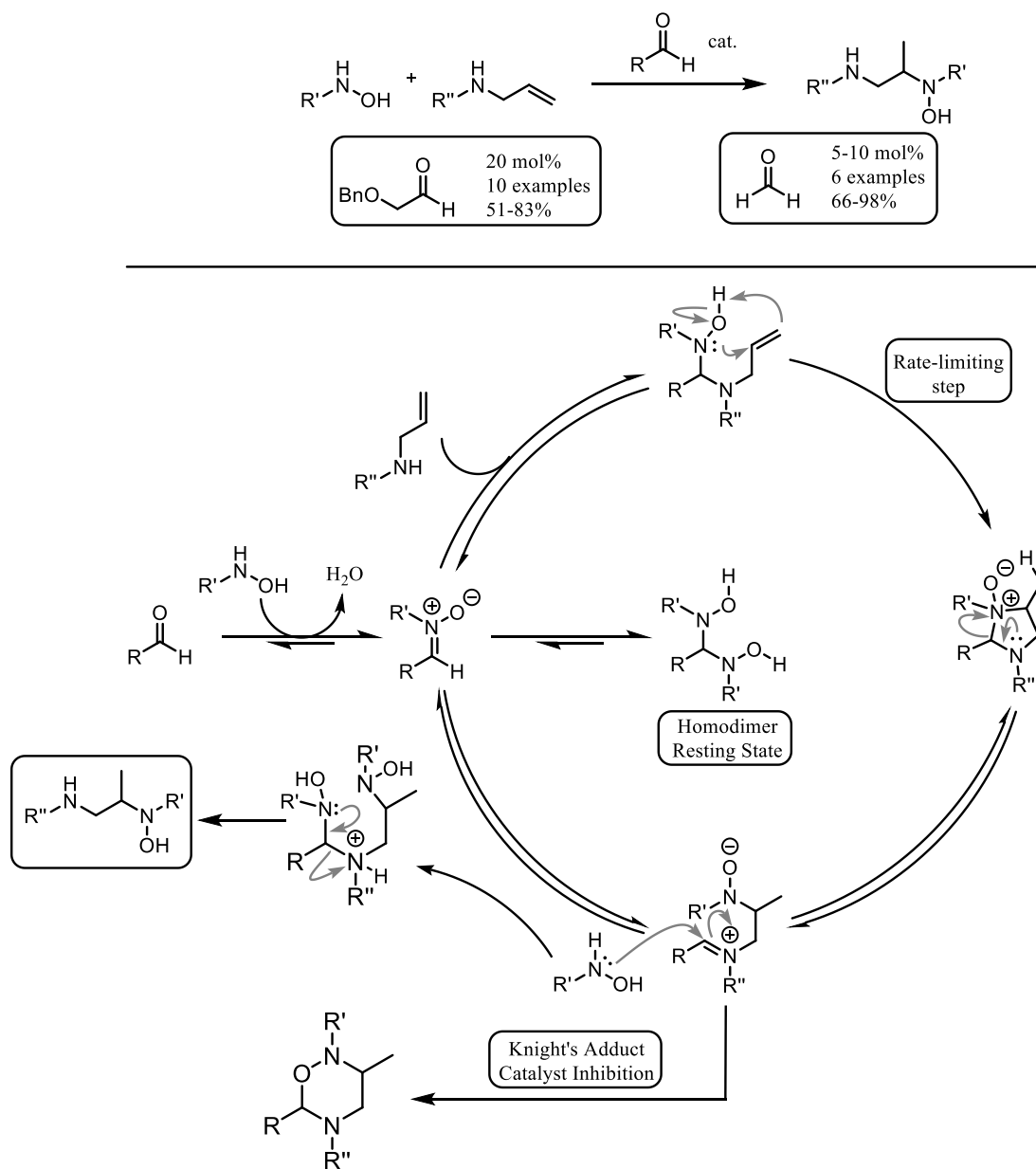
Scheme 1.8 Intermolecular Cope-type hydroamination of unbiased allylic amines promoted via hydrogen bonding

Expanding upon these initial hydroamination results, our group was able to demonstrate, in 2011 and 2012, the use of aldehydes as catalysts for the intermolecular hydroamination of allylic amines, thus validating the hypothesis of catalysis through temporary intramolecularity. Over the course of these studies, our understanding of the proposed catalytic cycle was improved by identifying potential routes for catalyst inhibition, the existence of competitive amination formation and potential rate-limiting step for the reaction. The revised catalytic cycle and overview of the scope of the reactions explored can be found in Figure 1.15.³⁰ After initial aldehyde screening, α -benzyloxyacetaldehyde was found to be the most effective catalyst, with catalyst loading of 20% allowing the efficient hydroamination of terminal allylic amines in decent yields. This lower catalyst loading allowed for efficient hydroamination product formation, while limiting the competitive formation of the 6-membered heterocycle, Knight's adduct. Furthermore, it was determined

³⁰ MacDonald, M. J.; Schipper, D. J.; Ng, P. J.; Moran, J.; Beauchemin, A. M. *J. Am. Chem. Soc.* **2011**, *133*, 20100.

that excess allylamine (1.5 equivalents) promoted product formation, due to favouring mixed aminal formation and limit competitive hydroxylamine homodimer formation. In 2012, further mechanistic studies (deuterium kinetic isotope effect studies) allowed for the determination of the most likely rate-limiting step, the hydroamination. During the course of these studies, a more efficient aldehyde catalyst was discovered: formaldehyde. Formaldehyde allowed for lower catalyst loadings (5-10%) and overall better product yields than α -benzyloxyacetaldehyde.³¹

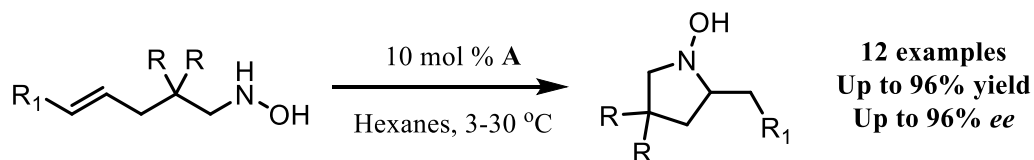
³¹ Guimond, N.; MacDonald, M. J.; Lemieux, V.; Beauchemin, A. M. *J. Am. Chem. Soc.* **2012**, *134*, 16571.



From the inception of the idea of using aldehydes as catalysts to promote temporary intramolecularity for hydroaminations, it was postulated that the use of chiral aldehydes could potentially induce asymmetry in the products. This approach seemed feasible and in

parallel, Jacobsen and coworkers reported the first enantioselective intramolecular thiourea-catalyzed Cope-type hydroamination (see Figure 1.16).³²

Jacobsen



R= H, Me

R₁= H, Ph, Substituted Aryl

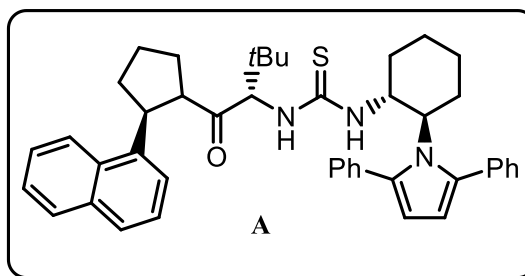


Figure 1.16 Enantioselective intramolecular thiourea-catalyzed Cope-type hydroamination

It was postulated that in the context of aldehyde catalyzed hydroamination, a transient stereocentre could be formed during hemiaminal formation. Following the condensation of the hydroxylamine to the aldehyde, a highly diastereoselective 1,2-addition of the allylic amine would follow, leading to transfer of the stereocentre through the bicyclic transition state associated with Cope-type hydroamination (see Figure 1.17).

³² Brown, A. R.; Uyeda, C.; Brotherton, C. A.; Jacobsen, E. N. *J. Am. Chem. Soc.* **2013**, *135*, 6747.

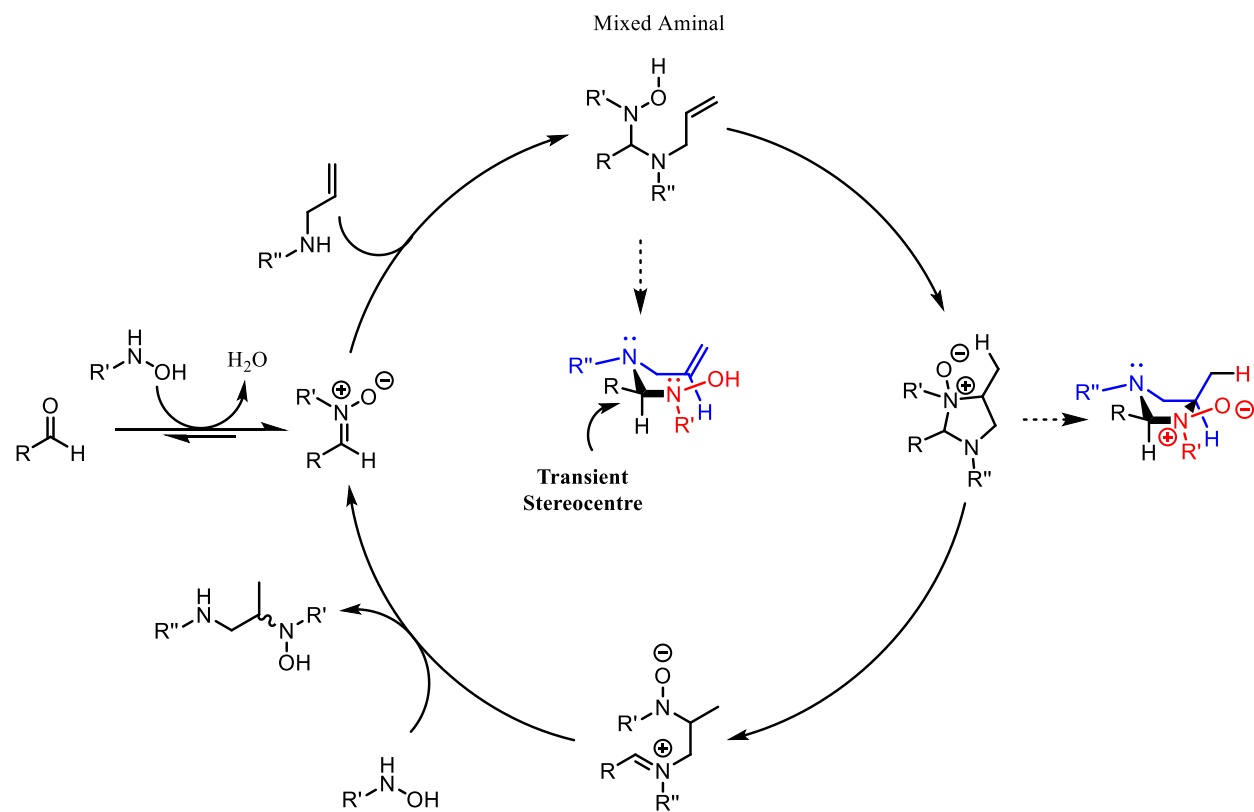
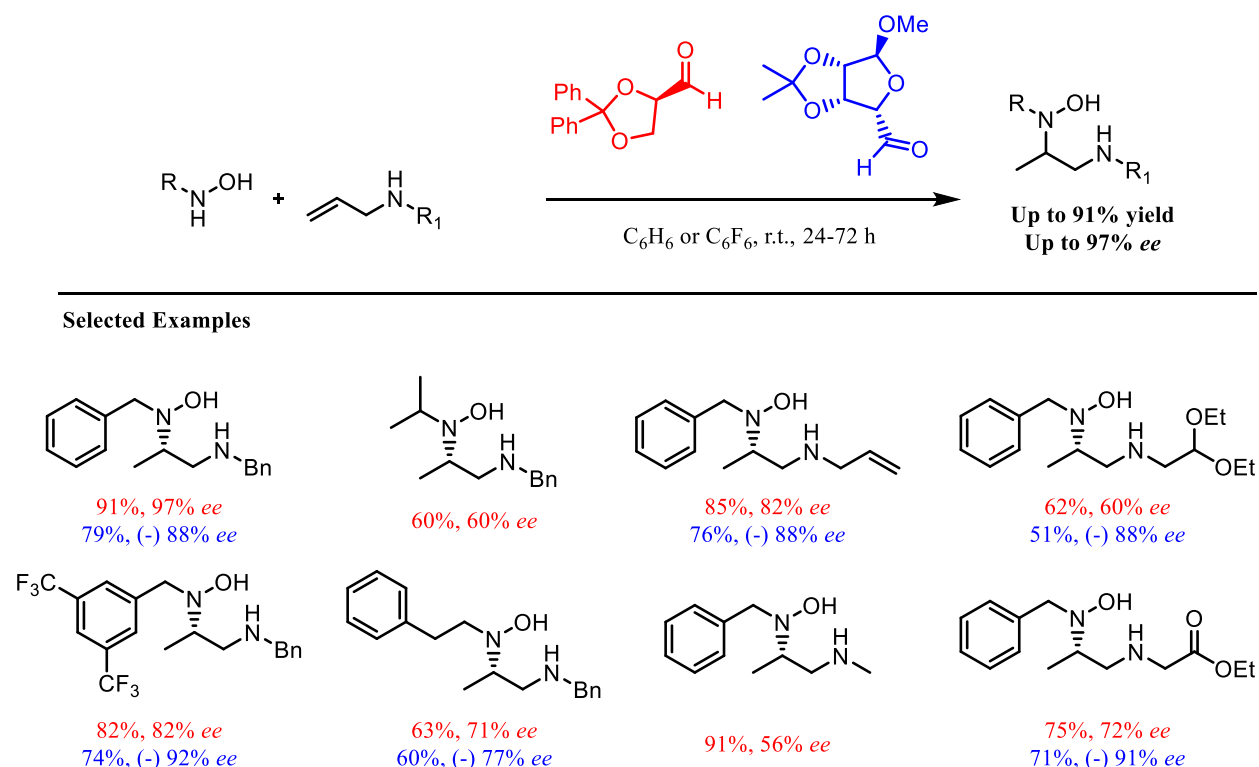


Figure 1.17 Basis for enantioselective aldehyde catalyzed Cope-type hydroamination

Following an initial aldehyde scan and conditions scan, it was found that two different chiral aldehydes (both adjacent to 5-membered rings) allowed access to both enantiomers of the diamine products in good yields and with excellent selectivities (see Table 1.1).³³

³³ MacDonald, M. J.; Hesp, C. R.; Schipper, D. J.; Pesant, M.; Beauchemin, A. M. *Chem. Eur. J.* **2013**, *19*, 2597–2601.

Table 1.1 Scope of asymmetric hydroaminations catalyzed by chiral aldehydes^a



^a Conditions: 1 equiv. hydroxylamine, 1.5 equiv. allylamine, 0.2 equiv. catalyst, solvent (1M), under argon, reported isolated yields, % *ee* determined by HPLC.

The obtained selectivities represent some of the highest reported for asymmetric hydroaminations of unactivated alkenes. Further studies are required in order to expand upon the substrate scope to more substituted alkenes and other nucleophilic analogs of allylic amines (alcohols and thiols), thus requiring further catalyst development and mechanistic studies. Even given the limitations of this system, it does represent the potential for organocatalysts to induce asymmetry solely through temporary intramolecularity.

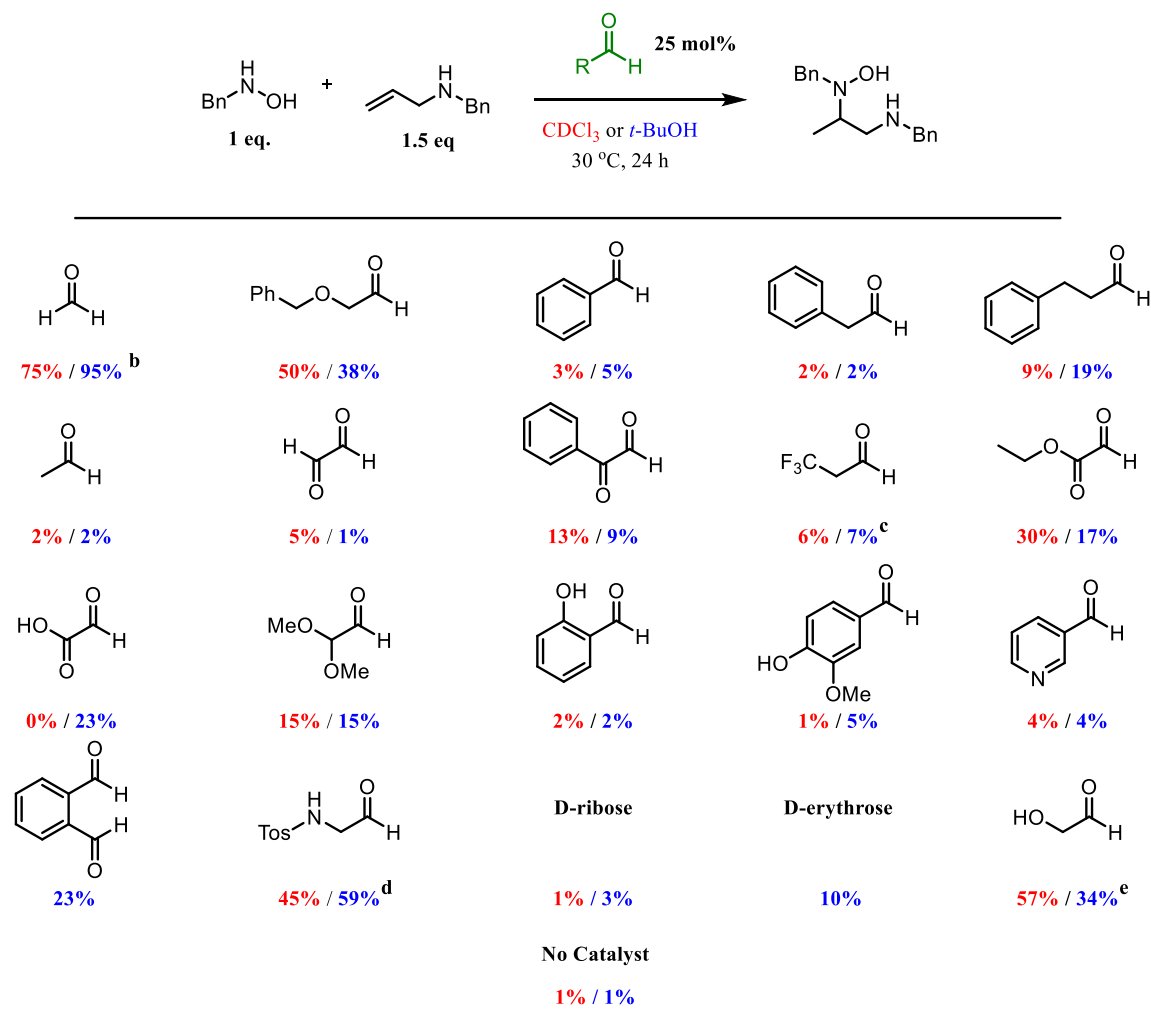
Chapter 2 – Further Studies of Cope-Type Hydroamination Reactions of Unactivated Alkenes

2.1 Comprehensive Aldehyde Scan

During the course of these initial studies into aldehyde catalysis of hydroamination, many conditions were used. Depending on the substrate course or the aldehyde studied, varying temperatures, solvents, catalyst loading were employed. Therefore, a more comprehensive and consistent aldehyde scan was required in order to ensure that initial findings and hypotheses held true, and that a true comparison of catalytic efficiency of different aldehydes was performed. Furthermore, we wanted insight into other potential classes of aldehydes which might not have been explored in earlier experiments, notably many aromatic aldehydes as well as other small electron deficient aldehydes. In order to accomplish this scan, two solvents, CHCl_3 and *t*-BuOH, were chosen in order to achieve a certain range of polarity; *t*-BuOH had previously been determined to be an excellent solvent in the case of formaldehyde (due to potential stabilization via hydrogen bonding, coupled with low nucleophilicity). The various aldehydes were tested with a 25 mol % loading, with a ratio of 1:1.5 of *N*-benzylhydroxylamine to *N*-benzylallylamine. As previously mentioned, the allyl amine was used in excess due to the inverse order relationship observed in the earlier mechanistic studies with α -benzyloxyacetaldehyde. This hydroxylamine and

allylamine pair were chosen due to their relatively low background reactivity.³⁴ The results of this scan are summarized in Table 2.1, with yields determined by NMR using an internal standard.

Table 2.1 Comprehensive aldehyde scan in CHCl₃ and *t*-BuOH ^a



^a Conditions: Allylamine (1.5 equiv.), hydroxylamine (1 equiv.), aldehyde (0.25 equiv.), *t*-BuOH/CDCl₃ (1M), 30°C.

^b Formalin (37 wt%) used as the formaldehyde source.

^c Hydrate form used.

³⁴ MacDonald, M. J. "An Organocatalytic Tethering Strategy: Aldehyde-Catalyzed Cope-type Hydroaminations of Allylic Amines" PhD Thesis, University of Ottawa, 2015.

^d α -N-tosyl aldehyde used without further purification.

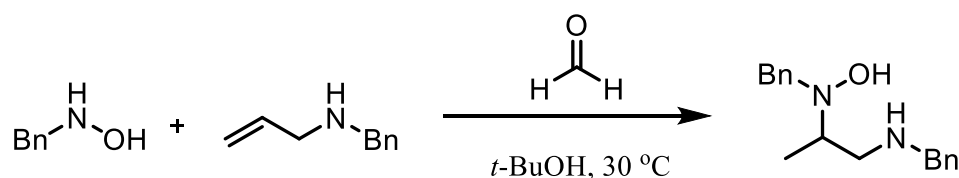
^e Glycolaldehyde used as a dimer.

This comprehensive aldehyde scan mostly reconfirmed that formaldehyde was the most efficient catalyst for this reaction, as well as highlighting solvent effects; α -benzyloxyacetaldehyde was also found to be efficient with better reactivity in CHCl_3 . Most of the aromatic aldehydes (aromatic ring in the α -position) which were examined were found to have very low reactivity, most likely due to their higher stability. This is exemplified in the comparison of benzaldehyde and hydrocinnamaldehyde, as the aliphatic chain is extended, the obtained yield increases. Some notable new aldehydes which were found to be moderately effective are glycolaldehyde and an α -N-Tosyl aldehyde, although not surpassing the efficiency of formaldehyde in this case. Surprisingly, some of the small electron deficient aldehydes (such as 2,2-Dimethoxyacetaldehyde and 3,3,3-Trifluoropropanal) only displayed very low reactivity, potentially due to their hydrate forms being utilized or the hydroxylamine homodimer being too stable. A few carbohydrate aldehydes were also tested and although their reactivity was fairly low, their use as potential catalyst could have implications for the field of prebiotic chemistry. The importance of carbohydrates as potential catalyst for prebiotic chemistry has more recently been highlighted by Blackmond *et al.* in their work studying enantioenrichment in amino acid synthesis, which is driven by chiral sugars.³⁵ Overall, this aldehyde scan reconfirmed most of our previous hypotheses, while also providing a system by which future potential aldehydes can be compared and examined.

³⁵ Recent development in prebiotic chemistry: Wagner, A. J.; Zubarev, D. Y.; Aspuru-Guzik, A.; Blackmond, D. G. *ACS Cent. Sci.* **2017**, *3*, 322–328.

After reconfirmation of formaldehyde being a superior catalyst, we became interested in evaluating the catalyst loading and testing the limits by which acceptable reactivity could still be achieved. To this effect the same methodology used for the comprehensive aldehyde scan was employed while using varying low formaldehyde loadings (see Table 2.2).

Table 2.2 Cope-type Hydroamination with Low Formaldehyde Loadings ^a



Entry	Formaldehyde Loading	Time	Yield ^b
1	1%	24 h	6%
2	1%	72 h	22%
3	5%	24 h	17%
4	5%	72 h	92%
5 ^c	5%	72 h	87%
6 ^d	5%	72 h	87%

^a Conditions: Allylamine (1.5 equiv.), hydroxylamine (1 equiv.), *t*-BuOH (1M), formalin used as formaldehyde source, 30°C.

^b Yields determined by NMR quantification using 1,4-Dimethoxybenzene as an internal standard.^c Paraformaldehyde used.

^d Paraformaldehyde used, addition of 0.3 equiv. H₂O.

Although catalysis and acceptable product yields were obtained with these low catalyst loadings, it should be noted that the reaction time to achieve comparable results was greatly increased. The very low loading of 1% did not result in very high yields, and this may be due to difficulty in handling small amounts of material. Longer reaction times could potentially lead to further increases in yield, however given the low cost of the catalyst, the

necessity for absolute catalyst efficiency is not as primordial. The trials with 5% loading led to similar results as the higher loading trials in the comprehensive aldehyde scan, after the longer reaction time. The use of formalin over paraformaldehyde did not have a dramatic effect on the reaction efficiency, nor did the addition of water when paraformaldehyde was used. While it was shown that low catalyst loadings for formaldehyde can still lead to acceptable reaction yields; the higher difficulties in handling, coupled with the longer reaction times necessary, limits the use of such low catalyst loadings.

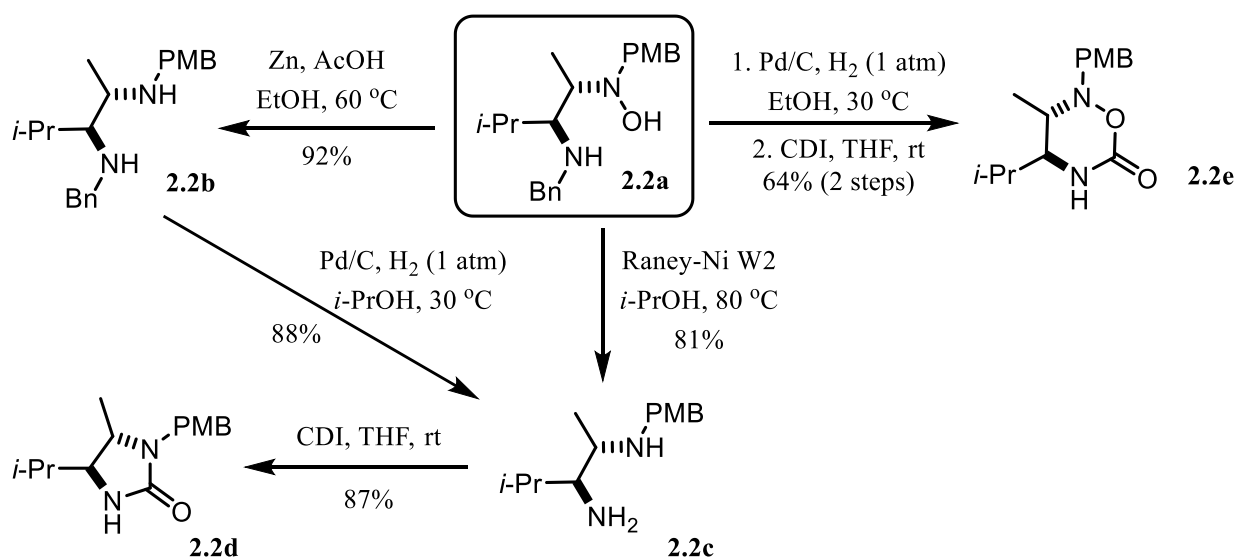
2.2 Derivatization of Hydroamination Products

In the scope of our group's study of diastereoselective hydroamination reactions, much effort was put into showcasing the utility and importance of the given products. 1,2-Diamine motifs are extremely important and prevalent in the fields of pharmaceutical chemistry, as well as in the development of chiral ligands.³⁶ The hydroamination products formed in our studies consisted of excellent candidates for further derivatization into such motifs, allowing these important class of molecule to be accessed efficiently from relatively simple precursors. The work to perform these derivatizations was undertaken in collaboration with Dr. Mohammad Mehdi Zahedi. Much of the efforts were concentrated on obtaining and modifying diamine motifs, but other considerable efforts were also put into the hydrolysis of cyclic hydroamination products (see Scheme2.1).³⁷

³⁶ (a) Lucet, D.; Le Gall, T.; Mioskowski, C. *Angew. Chem., Int. Ed.* **1998**, *37*, 2580. (b) Kotti, S. R. S. S.; Timmons, C.; Li, G. *Chem. Biol. Drug Des.* **2006**, *67*, 101. (c) Kim, H.; So, S. M.; Chin, J.; Kim, B. M. *Aldrichimica Acta* **2008**, *41*, 77.

³⁷ Hesp, C.; MacDonald, M.J.; Zahedi, M.M.; Bilodeau, D.A.; Shubin, Z.; Pesant, M.; Beauchemin, A.M. *Org. Lett.* **2015**, *17*, 5136–5139.

To undertake the main derivatization reactions envisioned in the scope of this study, a large quantity of a common hydroamination product (**2.2a**) was synthesized, which consisted of a differentially protected diamine precursor. To afford said diamine, the N-O bond was easily cleaved by treating with zinc dust under mild acidic conditions (**2.2b**). Following N-O bond cleavage, selective debenzoylation could be achieved through hydrogenation with palladium on carbon (**2.2c**). Alternatively, the diamine product could be accessed directly through treatment with Raney nickel, though purification following this method could be somewhat more difficult. These diamine motifs could then be further converted into imidazolidinone by treating them with 1,1'-carbonyldiimidazole (CDI) (**2.2d**). The initial hydroamination product could also be treated with CDI after selective debenzoylation to afford 6-membered heterocycles (**2.2e**).



Scheme 2.1 Derivatization of diamine motifs

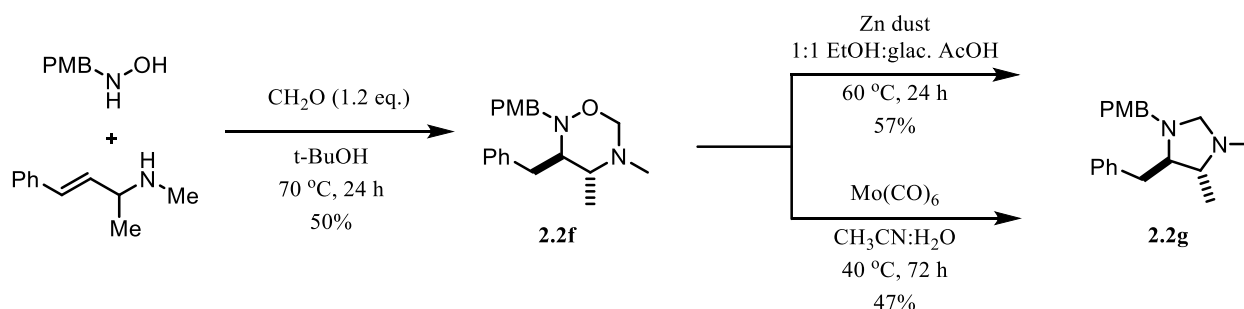
One of the limitations of this directed diastereoselective hydroamination reaction consisted of the substitution of the alkene. Although these hydroaminations proved difficult under catalytic conditions, the products could theoretically still be obtained in good yield by

using stoichiometric amounts of formaldehyde, thus creating 6-membered heterocycles. As previously discussed, these types of heterocycles had previously been reported by Knight, which his group was able to further convert into various diamine motifs.³⁸ To show the potential for hydrolysis of these structures, oxadiazinanes (**2.2f**) and (**2.2g**) were prepared by treating the appropriate hydroamination products with stoichiometric amounts of formaldehyde (see Schemes 2.2 and 2.3). Initial attempts to replicate Knight's hydrolysis (room temperature treatment with acid and Zn/HCl reduction) procedure were unsuccessful and led to either degradation of products or recovery of starting materials. Following these attempts, many other procedures were assessed. The first alternative tested consisted of treatment with Raney nickel and preliminary NMR analysis of crude reaction mixtures seemed to indicate hydrolysis of the heterocycle. However, difficulties were encountered in trying to successfully purify the obtained products and ultimately it was decided to attempt other procedures. Hydrogenation with palladium over carbon led to product decomposition and difficulties in purification. Attempted reduction via treatment with indium led to signs of Cope-elimination instead of the desired hydrolysis. Treatment of the oxadiazinane with strong basic conditions (*n*-BuLi) led to apparent alkylation of the starting material, while treatment with *m*CPBA led to apparent oxidation of the present nitrogen atoms. Many iterations of Mo(CO)₆ reductions were attempted in conjunction with Zn/AcOH reductions to achieve N-O bond cleavage. After purification of the products via preparatory thin layer chromatography and spectral analysis, it was discovered that the major product formed consisted of an imidazolidine (**2.2g**, see Scheme 2.2). Although the

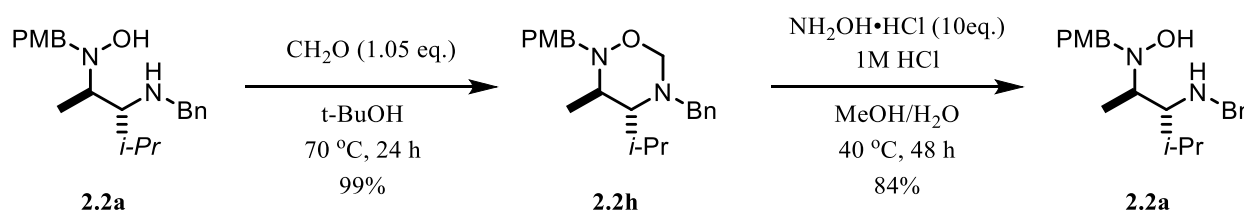
³⁸ (a) Bell, K. E.; Coogan, M. P.; Gravestock, M. B.; Knight, D. W.; Thornton, S. R. *Tetrahedron Lett.* **1997**, *38*, 8545.

(b) Gravestock, M. B.; Knight, D. W.; Malik, K. M. A.; Thornton, S. R. *J. Chem. Soc., Perkin Trans. 1* **2000**, 3292.

desired hydrolysis was not achieved with these procedures, this transformation could potentially be an effective way to access this class of heterocycles quickly and with high diastereocontrol. It should be noted however, that the scope of this transformation was not explored, therefore more inquiry is required to test this hypothesis. The conversion of the oxadiazinanes into the parent amino-hydroxylamine (**2.2a**) was finally achieved by following a procedure inspired by the work of Kang *et al.*, in which similar heterocycles were hydrolyzed.³⁹ Treatment of the oxadiazinane with $\text{NH}_2\text{OH}\cdot\text{HCl}$ under acidic conditions yielded the desired product in high yields with very few undesirable side products (see Scheme 2.3).



Scheme 2.2 Unexpected imidazolidine synthesis



Scheme 2.3 Hydrolysis of cyclic adducts

In summary, within the context of this study, our group was able to demonstrate the use of formaldehyde as an effective tethering organocatalyst to achieve highly

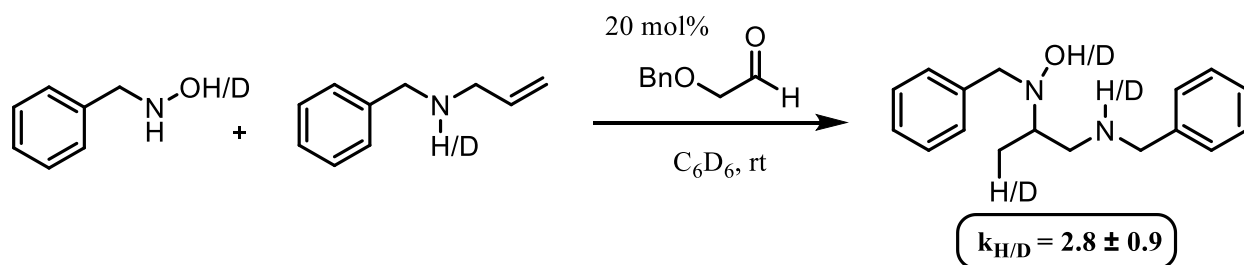
³⁹ Ziao, Z.; Yao, C.; Kang, Y. *Org. Lett.* **2014**, *16*, 6512–6514.

diastereoselective intermolecular Cope-type hydroamination reactions using both chiral allylic amines and chiral hydroxylamines. Furthermore, the efficiency and applicability of this methodology was demonstrated by derivatization of the obtained products. We were able to show that a variety of important 1,2-Diamine motifs and heterocycles could easily be accessed through simple transformations, thus highlighting the potential applications of this chemistry to the development of new pharmaceutical targets or chiral ligands. Although some difficulties were encountered during the hydrolysis of the oxadiazinanes, a potential route to imidazolidines was encountered, which could warrant further investigation.

2.3 Preliminary Kinetic Isotope Effect with Formaldehyde

Towards efforts to better understand the exact mechanism and catalytic cycle involved with the reverse Cope-type hydroamination reaction, our group became interested in measuring deuterium kinetic isotope effects (DKIE) in order to help elucidate the rate-determining step. DKIE helps in gaining an understanding of the hydrogen bond changes during this rate-determining step and involves comparing the rate of a reaction with a natural abundance of isotope versus the rate of a reaction with a fully deuterated species (k_H/k_D). The information gathered helps determine if a hydrogen/deuterium bond (X-H/X-D) is being broken during the rate-limiting step. To achieve this comparison, one reaction is run without the addition of deuterium, and monitored via NMR. A second reaction is then run, but all of the exchangeable protons are replaced by deuterium via several washes in MeOD. Preliminary DKIE experiments had already been conducted on α -benzyloxyacetaldehyde by Dr. Nicolas Guimond and Dr. Melissa MacDonald. It was

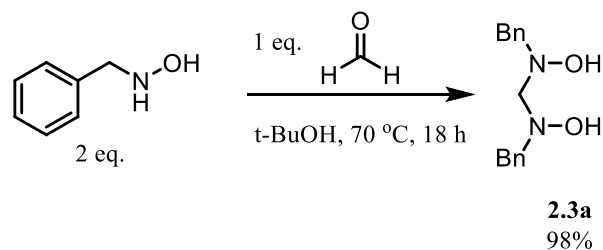
determined that for the case of this aldehyde, the DKIE measured was 2.8 ± 0.9 and therefore that the rate-limiting step was most likely the hydroamination step (see Scheme 2.4).³¹



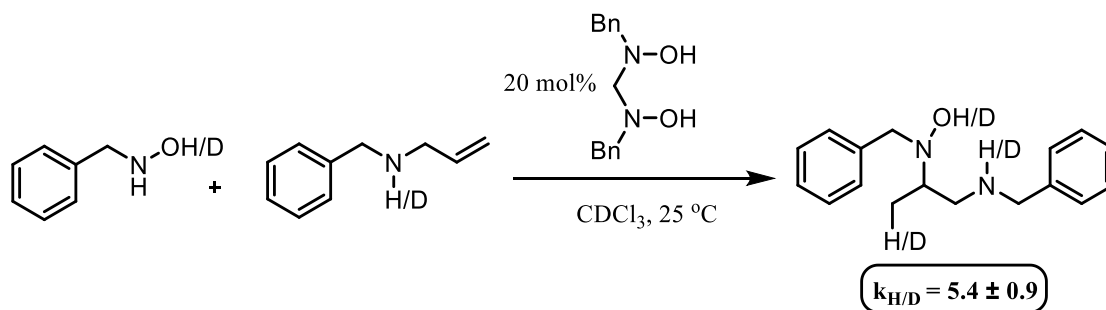
Scheme 2.4 Deuterium kinetic isotope effect experiment for α -benzyloxyacetaldehyde

As previously mentioned, after the discovery of α -benzyloxyacetaldehyde, formaldehyde was found to be a more effective catalyst and we wanted to confirm that a similar DKIE was to be observed in formaldehyde catalyzed reactions. However, difficulties arose for such a measurement to be obtained; given the sources of formaldehyde, paraformaldehyde and formalin, the previously used procedure for α -benzyloxyacetaldehyde could not be exactly replicated. Paraformaldehyde, being a long chain polymer, displays an induction or “cracking” period, in which formaldehyde monomer or shorter chain polymers are released; this causes monitoring of the reaction rate to be extremely sensitive to small variations and conditions and therefore not amenable to DKIE measurements. While, formalin consists of an aqueous solution of formaldehyde with methanol added as a stabilizer. This excess water and methanol consist of sources of exchangeable protons, which makes full deuterium exchange unreliable. Therefore, a different source of formaldehyde was to be determined in order to obtain accurate DKIE data. Some attempts were made towards the preparation of a formalin solution with deuterated water and paraformaldehyde, however such attempts proved too unreliable. An alternative was found when it was determined that the homodimer (homoaminal) of

benzylhydroxylamine (**1.33a**) with formaldehyde was a stable solid at room temperature, which allowed for easy handling and quantification of formaldehyde in solution, while avoiding the addition of excess water (see Scheme 2.5). In essence, this dimer, believed to be a resting state in the catalytic cycle, acts as a precursor to the active mixed aminal in the reaction. With a reliable formaldehyde source in hand, the reactions were run with and without deuterium exchange and the DKIE was determined to be 5.4 ± 0.9 (see Scheme 2.6). The observed DKIE is in line with the original hypothesis of the hydroamination step being the rate-limiting step in the catalytic cycle, due to being an indication of an H-bond being broken during that step. This results mirrors the obtained value for the previous trials with α -benzyloxyacetaldehyde. However, it should be noted that another potential candidate for rate-limiting step is the initial 1,2-addition. Further mechanistic investigation would be needed to properly determine this distinction, mostly accomplished by evaluating the equilibrium measurements for the various reversible steps of the catalytic cycle.



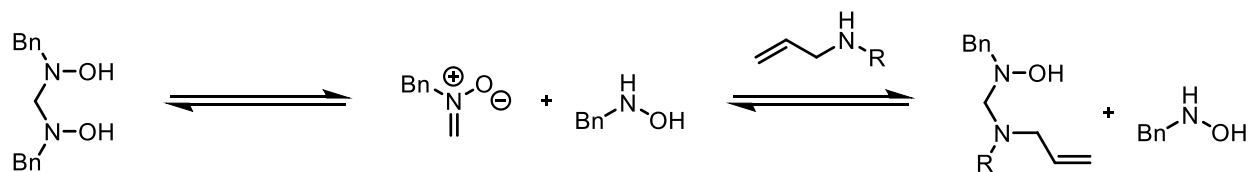
Scheme 2.5 Synthesis of benzylhydroxylamine homodimer



Scheme 2.6 Deuterium kinetic isotope effect experiment using a formaldehyde-hydroxylamine dimer as formaldehyde source

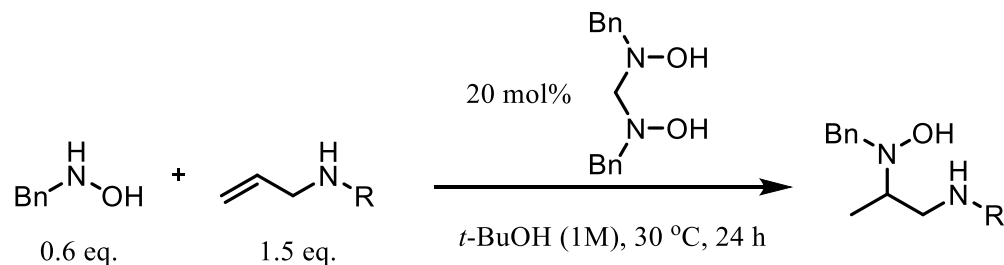
2.4 Hydroxylamine Dimer as a Precursor to Cope-type Hydroamination

After using the formaldehyde and hydroxylamine dimer **2.3a** in the DKIE experiments and determining that it was able to catalyze the hydroamination of allylic amines, we became interested in comparing its efficiency to that of formaldehyde catalyzed reactions. In theory, this dimer forms in solution under typical reaction conditions used for formaldehyde catalyzed hydroaminations and consists of a resting state for the catalyst. Hydroamination can take place once the allylic amine displaces one molecule of hydroxylamine, thus forming a mixed aminal that leads to the cyclic transition state allowing the C-N bond formation to take place (see Scheme 2.7).



Scheme 2.7 Formaldehyde hydroxylamine dimer as a precursor to active catalytic species

Therefore, we hypothesized that the dimer could act as a precursor to the active catalytic species in solution and would allow for easy handling and ease of formaldehyde quantification. Using similar conditions to the ones used for the comprehensive aldehyde scan, we set out to determine the catalytic efficiency of the formaldehyde homodimer with various representative allylic amines. The results of these experiments can be found in Table 2.3.

Table 2.3 Hydroamination of Allylic Amines Using a Formaldehyde Precursor Dimer

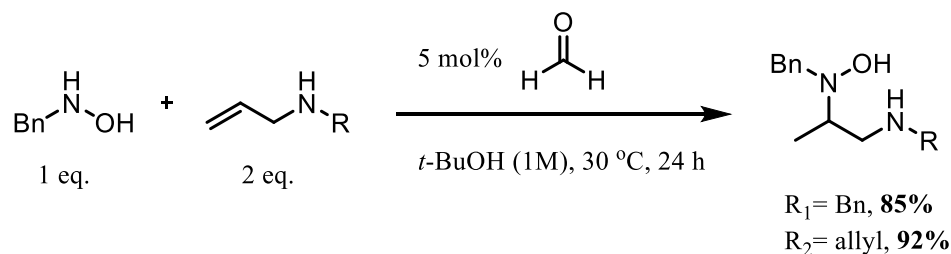
Entry	R	Modifications	Yield ^a
1	Bn	-	78%
2	Bn	CDCl ₃	75%
3	Bn	0.8 equiv. hydroxylamine	73%
4	Bn	1 equiv. hydroxylamine	52%
5	H	10% Dimer, 0.8 equiv. hydroxylamine, CDCl ₃	15%
6	H	10% Dimer, 0.8 equiv. hydroxylamine	14%
7	H	10% Dimer, 0.8 equiv. hydroxylamine, 0.05 equiv. H ₂ O	39%
8		10% Dimer, 0.8 equiv. Hydroxylamine, CDCl ₃	60%
9		10% Dimer, 0.8 equiv. hydroxylamine	30%
10		10% Dimer, 0.8 equiv. Hydroxylamine, 0.05 equiv. H ₂ O	74%
11		10% Dimer, 0.8 equiv. hydroxylamine, 0.5 equiv. H ₂ O	72%
12		0.1 equiv. H ₂ O	62%
13		0.5 equiv. H ₂ O	68%

^a Yields determined by NMR quantification using 1,4-Dimethoxybenzene as an internal standard.

Initial attempts were carried out with *N*-benzylallylamine under similar conditions than the hydroamination reactions conducted for the comprehensive aldehyde scan, with

slightly lower catalyst loading. The obtained yield of 78% for the reaction in *t*-BuOH (Entry 1) was much lower than the trials run for formaldehyde (formalin) catalyzed hydroamination between *N*-benzylallylamine and *N*-benzylhydroxylamine (i.e. 95% after 24 hours, see Table 2.1). Similar results were obtained when the solvent was changed to CDCl₃. When increasing the equivalents of *N*-benzylhydroxylamine (Entries 3,4), the yield expectedly decreased, as this favours the equilibrium reaction towards homodimer formation. Following these attempts with a known secondary amine, a simple primary amine, allylamine, was investigated. Initial attempts (Entries 5,6) resulted in very low yields of product. It was hypothesized that some additive found in the formalin solution used for other formaldehyde catalyzed hydroaminations was absent from these reaction conditions and could rescue some of the catalyst's/precursor's efficiency. Given that formalin consists of an aqueous solution, it was thought that the addition of water could assist in the hydrolysis of the homodimer and somehow facilitate the formation of the required mixed aminal with the allylamine. Upon addition of 0.05 equivalents of water to the reaction (Entry 7), the yield greatly improved, however remained moderate. Similar trials were conducted with another secondary allylamine, diallylamine (Entries 8 through 13). Once again, although initial yields were only low to moderate, the addition of water somewhat rescued catalytic efficiency. Increasing the equivalents of water added did not correlate to an increase in obtained yields. When compared to our group's initial results with formaldehyde catalyzed hydroamination (see Scheme 2.8), the obtained yields for the trials with **2.3a** were much lower, even given the higher catalyst loading.³¹ It is possible that other additives could help recover full catalytic efficiency, such as methanol and formic acid. To date, these additives have not yet been tested. Although the catalytic activity of the homodimer was lower than that of

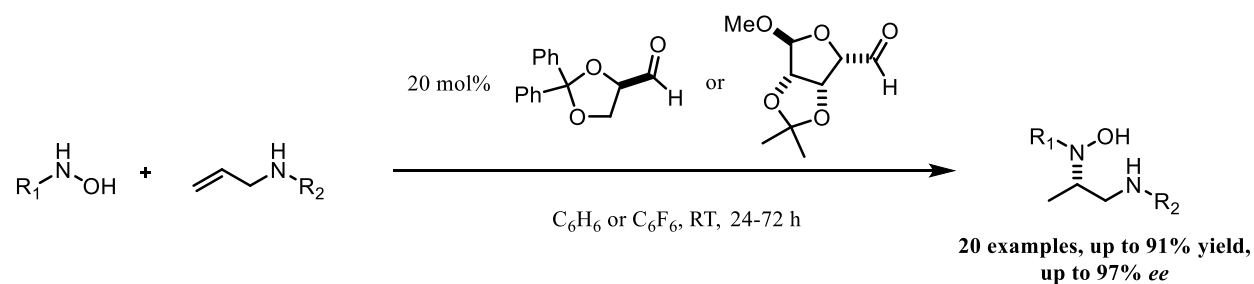
formaldehyde, it can still remain a useful tool for further mechanistic studies in which dry reaction conditions or accurate quantification of formaldehyde equivalency are needed.



Scheme 2.8 Formaldehyde catalyzed hydroamination of secondary allylamines

2.5 Synthesis of Enantiomerically Enriched Chiral Nitrones

In our group's previous work, we were able to demonstrate that simple organocatalysts were capable of inducing asymmetry solely through the promotion of temporary intramolecularity. Various chiral aldehydes were capable of catalyzing the Cope-type hydroamination of hydroxylamines and unactivated allylamines in good yields and high enantiomeric excess (see Scheme 2.9).³³ Although the obtained results were very promising, problems such as aldehyde epimerization and somewhat limited substrate scope remain to be overcome. Inspired by this methodology, we wished to expand upon enantioselective hydroamination reactions. In contrast to aldehyde catalyzed intermolecular enantioselective hydroamination, we wished to control the enantioselectivity of intramolecular hydroamination reactions via the application of chiral nucleophiles to appropriate nitrones; this work was done in collaboration with Dr. Mohammad Mehdi Zahedi.



Scheme 2.9 Asymmetric hydroaminations using chiral aldehydes

Instead of the chiral aldehyde transferring stereochemical information after creating a temporary tether between an allyl amine molecule and a hydroxylamine molecule, the stereochemical information would be transferred through the addition of a chiral nucleophile to a nitron. After the addition of the nucleophile, a bicyclic transition state allows for the facile hydroamination to take place, in a similar fashion to the aldehyde catalyzed intermolecular hydroaminations (see Figure 2.1). Following ring expansion and hydrolysis of the nucleophile, interesting enantiomerically pure heterocycles would be formed which could then in turn be further derived. Furthermore, this intramolecular hydroamination would hypothetically be assisted by the Thorpe-Ingold effect and substitution could greatly affect reaction efficiency.

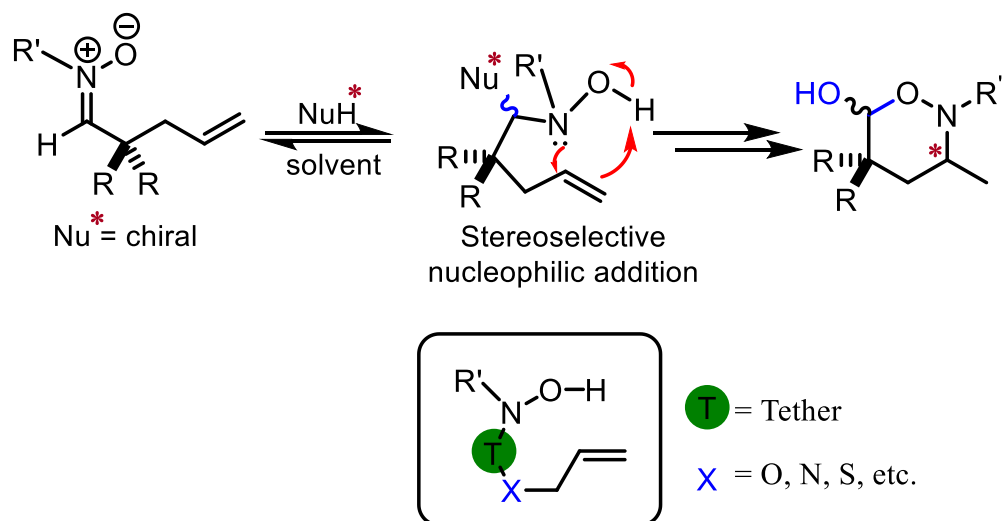
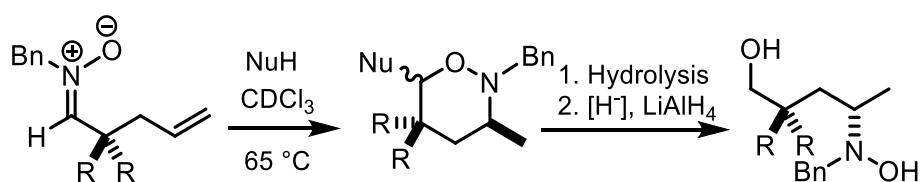


Figure 2.1 Asymmetric intramolecular hydroaminations controlled by chiral nucleophilic addition

An initial model system was developed to test out the initial hypotheses. A stable nitronium of *N*-benzylhydroxylamine and 4-Pentenal was synthesized and isolated, which could then be subjected to a variety of nucleophiles in order to confirm the formation of hydroamination products. In order to overcome purifications issues as well as facilitate determination of enantiomeric excess, the nucleophiles were hydrolyzed from the obtained heterocyclic products, which could then be subjected to reduction by LiAlH_4 in order to obtain linear primary alcohols. The results of the initial nucleophile scan can be found in Table 2.4. Primary amines, such as benzylamine seemed effective to promote hydroamination, while secondary amines did not result in product formation. In efforts to take advantage of the Thorpe-Ingold effect, the starting substrate was changed to 2,2-Dimethyl-4-pentenal. While product yield did not increase much with the application of benzylamine, it was found that thiols could be effective nucleophiles to promote hydroamination. With confirmation of hydroamination taking place, we wanted to

determine if enantioselectivity could be controlled via the use of chiral nucleophiles (Entries 7 and 8). Although overall yields remained acceptable, the obtained % *ee* remained quite low, only obtaining 23% *ee* with (*S*)-phenylalanine methyl ester. Due to chiral nucleophiles only offering moderate selectivities, we hypothesized that chiral nitrones could be used instead to transmit the stereochemical information.

Table 2.4 Intramolecular hydroamination of nitrones promoted by nucleophilic addition^a



Entry	R	Nucleophile	%Yield ^b	% <i>ee</i>
1	H	Benzylamine	65	-
2	H	Diethylamine	0	-
3	H	Pyrrolidine	0	-
4	Me	Benzylamine	63	-
5	Me	Benzylthiol	72	-
6	Me	Thiophenol	77	-
7	Me	(<i>S</i>)-alpha-Methylbenzyl amine	53	6
8	Me	(<i>S</i>)-Phenylalanine methyl ester	64	23

^a Performed by Dr. P. Zahedi. Conditions: Step 1: 0.11 mmol nitrone, 0.11 mmol nucleophile, 0.5 mL CDCl₃, 65 °C, 24 h. Step 2: 2 mL (1:0.5:8.5, HCl conc.: H₂O: THF), 1mL THF, rt, 3 h. Step 3: Under Ar., 0.4 mmol LiAlH₄, 0 °C to RT, 2h.

^b Isolated yields over three steps through prep. TLC; % *ee* determined by HPLC.

To test the ability of chiral hydroxylamines to transfer stereochemical information, (*R*)-1-Phenylethylhydroxylamine was synthesized and then condensed with 2,2-Dimethyl-4-pentenal to form a stable nitron. The obtained nitron was then subjected to the same conditions used for the initial nucleophile scan, using thiophenol as the nucleophile to promote hydroamination (see Figure 2.2). Upon analysis of the crude NMR spectra, it was determined that the desired 6-membered heterocycle was not obtained, instead showing evidence of the release of styrene. Upon purification of the crude reaction mixture, via preparatory thin layer chromatography, it was determined that the major product was the cyclic nitron **2.5a**. It was hypothesized that following nucleophilic addition and subsequent hydroamination, a Cope elimination could occur, causing the release of styrene and the formation of a cyclic hydroxylamine. The nitrogen's lone pair could then expel the nucleophile and thus a chiral cyclic nitron could be formed (see Figure 2.2).

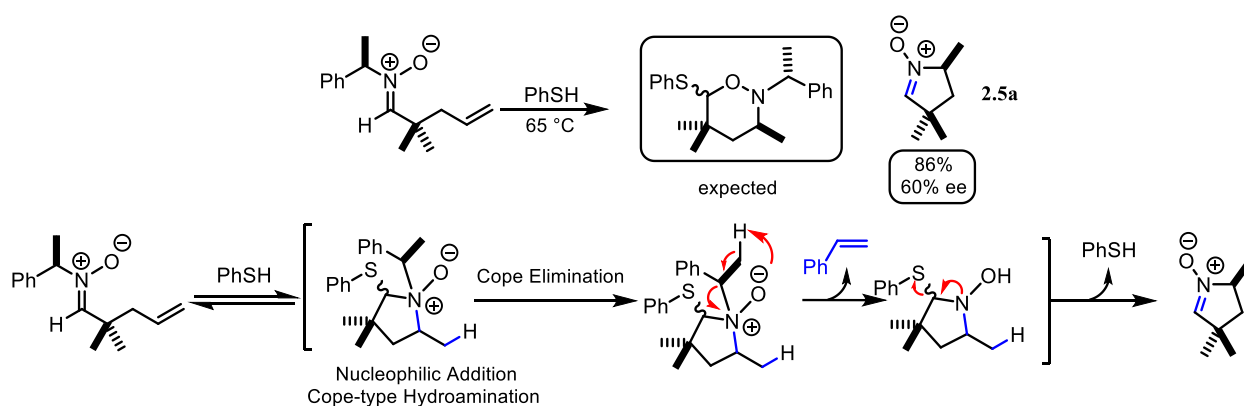
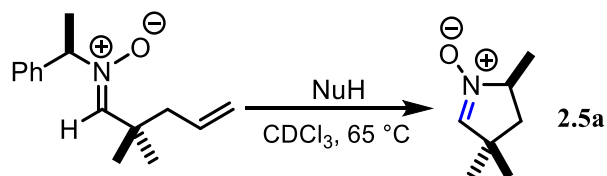
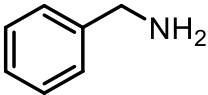
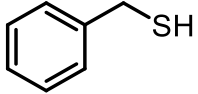
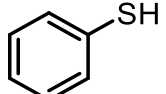
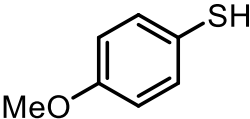
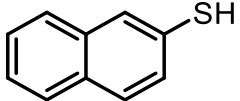

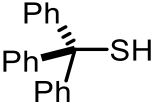
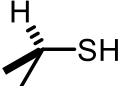


Figure 2.2 Synthesis of chiral cyclic nitron through application of nucleophiles

Following this unexpected result, a cursory nucleophile scan was conducted in order to confirm nitron formation and examine reaction efficiency and stereoselectivity (see Table 2.5). Thiols promoted this type of reactivity, while benzylamine did not promote hydroamination. Aromatic thiols gave good yields of the cyclic nitron with

4-Methoxybenzenethiol affording the highest yield (Entries 3-5), although enantioselectivity remained moderate. Aliphatic thiols, such as *tert*-butyl mercaptan and triphenylmethyl mercaptan (Entries 6 and 7), did not yield any desired product, most likely due to steric hindrance preventing initial nucleophilic attack. Less sterically hindered aliphatic thiols (Entries 2 and 8) allowed for product formation, while 2-propanethiol promoted the highest enantioselectivity with 70% *ee*. In order to improve enantioselectivity, further optimization of the conditions was undertaken.

Table 2.5 Nucleophilic scan for chiral cyclic nitron synthesis^a

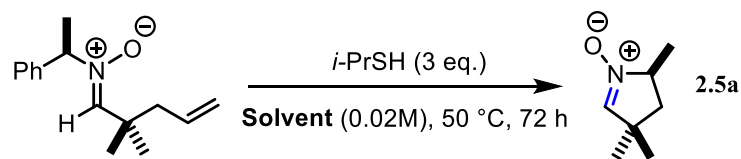
Entry	Nucleophile	% Yield	% <i>ee</i>
1		0	-
2		76	62
3		86	60
4		90	64
5		70	63
6		0	-
7		0	-
8		82	70

^a Performed by Dr. P. Zahedi.

An initial solvent scan was performed in order to determine reaction efficiency, as well as the feasibility of increasing enantioselectivity (See Table 2.6). Most polar solvents tried (Entries 1-4) generally yielded much lower efficiencies, while allowing for better solubility of some more polar nucleophiles. Non polar solvents (Entries 5-8) proved to be more effective to promote reactivity, with benzene and hexanes being the most effective.

Following the initial solvent scan, various other parameters such as temperature, reaction time and additives were explored (see Table 2.7). It was initially hypothesized that the addition of a strong base to the reaction mixture could help promote Cope elimination and nitrene formation, therefore potassium hydride was introduced to the reaction conditions. Initial attempts resulted in solubility issues, while not improving product yield (Entries 1 and 2). In order to improve solubility, the crown ether 18-crown-6 was added (Entries 3-5). While solubility of reagents greatly improved after this addition, improvements in yields remained modest, while enantioselectivities remained comparable to initial results (Entry 5). In order to improve enantioselectivity, trial reactions were run at lower temperature, while also reducing reaction time (Entries 6 and 7). While reactivity in benzene was greatly reduced at lower temperatures, reactivity in hexanes remained acceptable and comparable to higher temperature trials in the same solvent. Product yield remained similar without the addition of potassium hydride and 18-crown-6. It should be noted that reactions run at higher temperatures in hexanes led to starting material and product decomposition. In order to further investigate these effects a secondary nucleophile scan was conducted.

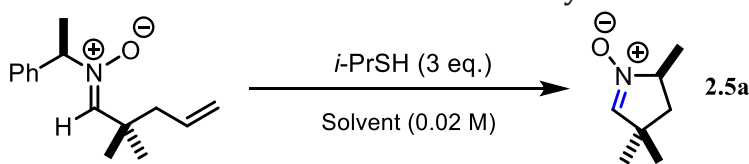
Table 2.6 Solvent scan for chiral cyclic nitron synthesis



Entry	Solvent	%Yield ^a
1	CH ₂ Cl ₂	8
2	<i>t</i> -BuOH	12
3	THF	8
4	CH ₃ CN	3
5	Toluene	17
6	CHCl ₃	14
7	C ₆ H ₆	25 ^b
8	Hexanes	28

^a Yields determined by NMR quantification using 1,3,5-trimethoxybenzene as an internal standard.

^b 70% *ee* determined by HPLC analysis.

Table 2.7 Additive and reaction conditions scan for chiral cyclic nitron synthesis

Entry	Solvent	Temperature (°C)	Time (h)	Additive	%Yield ^a
1	Benzene	50	72	1equiv. KH	17
2	Hexanes	50	72	1 equiv. KH	20
3	Benzene	50	72	1 equiv. KH, 1equiv. 18-crown-6	35
4	Benzene	50	24	1equiv. 18-crown-6	22
5	Tetrahydrofuran	50	24	1 equiv. KH, 1equiv. 18-crown-6	22 ^b
6	Benzene	30	24	1 equiv. KH, 1equiv. 18-crown-6	5
7	Hexanes	30	24	1 equiv. KH, 1equiv. 18-crown-6	26
8	Hexanes	50	24	1 equiv. KH, 1equiv. 18-crown-6	25
9	Hexanes	30	24	-	25

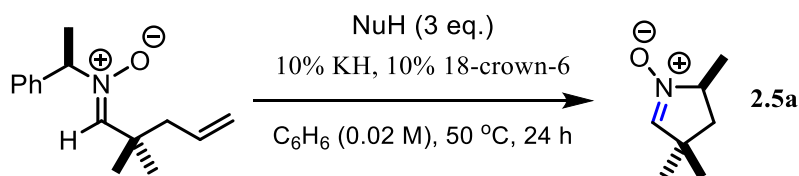
^a Yields determined after reaction work up by NMR quantification using 1,3,5-trimethoxybenzene as an internal standard.

^b 68% *ee* determined by HPLC analysis.

The secondary nucleophile scan was conducted to compare the reaction efficiency of various other nucleophiles and the effect of the addition of base (see Table 2.8). Aromatic thiols seem to increase the overall nitron product yields. However, the addition of base was unnecessary and slightly higher yields were obtained in base free conditions; reaction work up and product purification also greatly improved. Enantioselectivities were also slightly improved overall in base free conditions, with thiophenol providing the highest selectivity of 75% *ee*. However, the best result obtained consisted of the reaction being run in hexanes

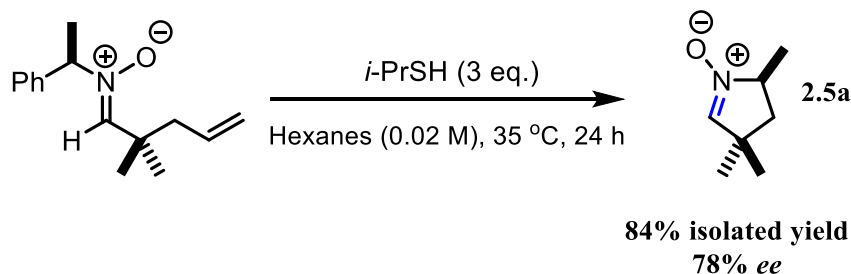
at lower temperature with 2-propanethiol (See Scheme 2.10). The achieved enantiomeric excess of 78% was acceptable, but higher selectivities were desired.

Table 2.8 Secondary nucleophile scan for chiral cyclic nitron synthesis



Entry	Nucleophile	%Yield ^a	% ee
1	<i>t</i> -BuSH	3 ^b	-
2	Thiophenol	41	-
3	Thiophenol ^c	51	75
4	4-Methoxybenzenethiol	44	-
5	4-Methoxybenzenethiol ^c	53	73
6	2-Naphthalenethiol	58	-
7	2-Naphthalenethiol ^c	60	69

^a Yields determined after reaction work up by NMR quantification using 1,4-Dimethoxybenzene as an internal standard. ^b Solubility issues, precipitate observed. ^c KH and 18-crown-6 free conditions.

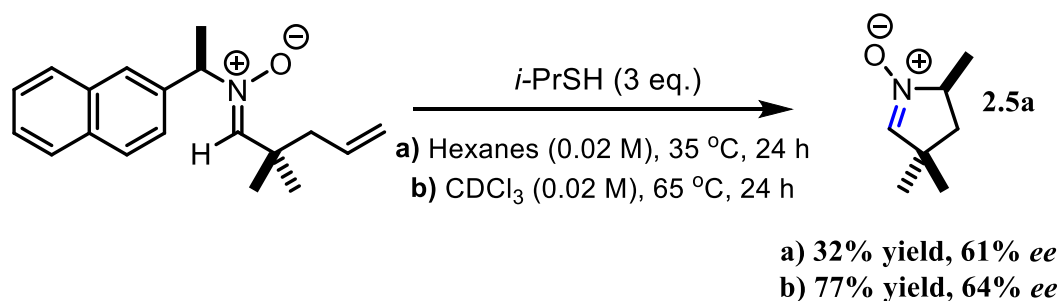


Performed by Dr. P. Zahedi.

Scheme 2.10 Optimized reaction conditions for chiral cyclic nitron synthesis

In efforts to increase enantioselectivity, another more sterically hindered enantiomerically pure hydroxylamine was synthesized; *N*-((1*R*)-1-Naphthalen-2-ylethyl) hydroxylamine (See Scheme 2.11). Although the formed nitron was stable, it did not result

in increased yields or enantioselectivities. Furthermore solubility issues were encountered when the reaction was run in hexanes. Another considered improvement consisted of taking greater advantage of the Thorpe-Ingold effect by changing the dimethyl groups to bulkier groups, which would ideally be cleavable after reaction completion (See Figure 2.3). Acetals and thioacetals were considered for this approach. Although much effort was put into the synthesis of such nitrones, their isolation proved difficult and competing hydroamination reactions observed upon attempted condensation reactions made their synthesis challenging and constituted a major issue given that the goal was to induce the hydroamination event with the addition of a nucleophile. Approaches to synthesize these nitrones in situ also yielded no beneficial results.



Scheme 2.11 Naphthalene nitron for synthesis of cyclic chiral nitron

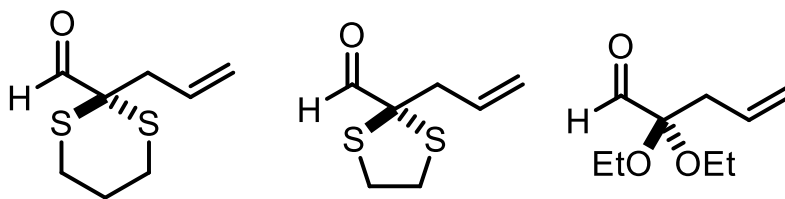


Figure 2.3 Sterically hindered aldehydes for cyclic chiral nitron synthesis

Although, the initial desired chiral heterocycles were not obtained through this methodology, an interesting and novel synthesis of enantiomerically enriched chiral

nitrones was achieved. Through a sequence of nucleophilic addition, Cope-type hydroamination and Cope elimination, enantiomerically pure nitrones could be converted into chiral cyclic nitrones. However, even given the optimization of conditions (nucleophile scan, use of non-polar solvents, lowering of temperature) the obtained stereoselectivities were modest. Furthermore, the substrate scope remained very limited given the need to take advantage of the Thorpe-Ingold effect. Considering the necessity for synthesizing enantiomerically pure hydroxylamines and acyclic nitrones, this suggested that this methodology would be unpractical and of narrow applicability and ultimately led to the conclusion that this line of investigation did not warrant further studies.

Chapter 3 – Small Peptide Catalysis and Mixed Aminals

3.1 Introduction to Small Peptide Catalysis

Since the late 1990s, small peptides have increasingly been exploited for their function as asymmetric catalysts to facilitate a variety of reactions such as epoxidations, acylations, phosphorylations, brominations, aldol reactions and many others.⁴⁰ Peptidic catalysts offer a wide diversity of functional and structural properties, which can be advantageous over traditional small molecule organocatalysts, which are much less modular. Recent advances in peptide synthesis have allowed for much quicker discovery and optimization of catalysts, which has greatly broadened the scope of reactions, while also improving enantioselectivities, regioselectivities and chemoselectivities, as well as allowing for decreased catalyst loadings.⁴¹ Such advances have allowed the Wennemers group to develop an array of small peptidic catalysts to catalyze a variety of reactions, most notably the conjugate addition between aldehydes and nitroolefins to provide chiral γ -nitroaldehydes, which could then be further modified into important motifs such as γ -amino acids, γ -butyrolactams and pyrrolidines.⁴² Among the best catalysts for this reaction are the tripeptides of the Pro-Pro-Xaa (where Xaa is a variable amino acid) motif (see Figure 3.1). These tripeptides have allowed for the catalysis of aldol reactions and conjugate addition of aldehydes to β -substituted, α,β -disubstituted and β,β -disubstituted nitroolefins;

⁴⁰ a) Davie E.A.C.; Mennen S.M.; Xu Y.; Miller S.J. *Chem. Rev.* **2007**, *107*, 5759- 5812. b) Wennemers H.; *Chem Commun* **2011**, *47*, 12036-12041.

⁴¹ Revell J.D; Wennemers H. *Curr. Opin. Chem. Bio.* **2007**, *11*, 269-278.

⁴² Reviews: a) Roca-Lopez, D.; Sadaba, D.; Delso, I.; Herrera, R. P.; Tejero, T.; Merino, P. *Tet. Asymm.* **2010**, *21*, 2561.; b) Mukherjee, S.; Yang, J. W.; Hoffmann, S.; List, B. *Chem. Rev.* **2007**, *107*, 5471.

excellent enantioselectivities of up to 99% *ee*, with catalyst loadings as low as 0.1 mol% (see Figure 3.2).⁴³

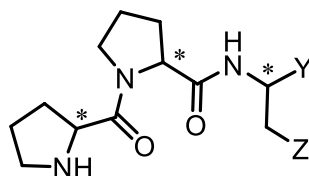


Figure 3.1 General Structure of Tripeptide Catalysts

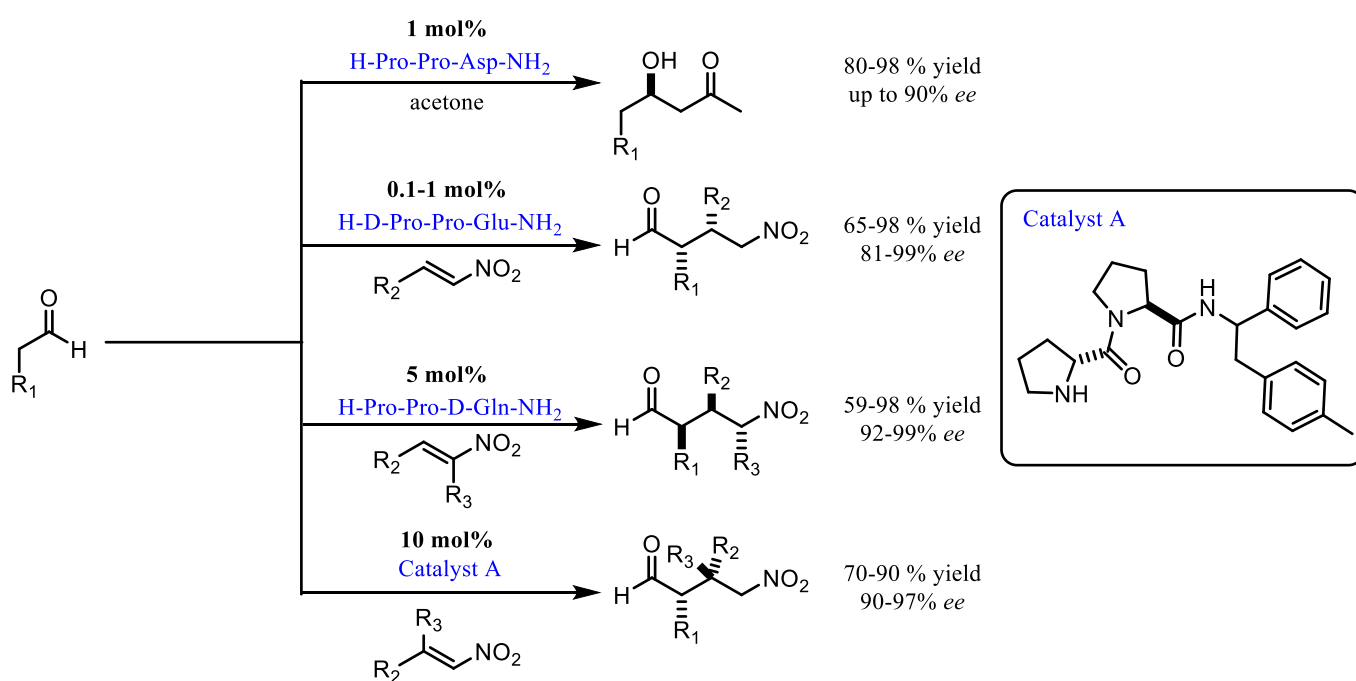


Figure 3.2 Overview of tripeptide catalyzed reactions by the Wennemers group

Functionalizations of such carbonyl compounds are widely used organocatalytic reactions and therefore a wide variety of organocatalysts have been developed, chiral

⁴³*Aldol reactions*: a) Krattiger, P.; Kovasy, R.; Revell, J.D.; Ivan, S.; Wennemers, H. *Org. Lett.* **2005**, *7*, 1101-1103. *Conjugate additions of aldehydes to nitroolefins*: b) Wiesner, M.; Revell, J.D.; Wennemers, H. *Angew. Chem. Int. Ed.* **2008**, *47*, 1871-1874. c) Wiesner, M.; Neuburger, M.; Wennemers, H. *Chem. Eur. J.* **2009**, *15*, 10103-10109. d) Duschmale, J.; Wennemers, H. *Chem. Eur. J.* **2012**, *18*, 1111-1120. d) Kastl, R.; Wennemers, H. *Angew. Chem. Int. Ed.* **2013**, *52*, 7228-7232. *Review*: e) Lewandowski, B.; Wennemers, H. *Curr. Op. Chem. Bio.* **2014**, *22*, 40-46.

secondary amines being amongst the most effective to catalyze the reaction of aldehydes and ketones with electrophiles.⁴⁴ Since pioneering work by Hajos and Parrish on intramolecular aldol reactions, proline catalysis has been widely studied to enable α -functionalizations of carbonyl compounds.⁴⁵ Most proposed reaction mechanisms consist of two main pathways, enamine catalysis and enol catalysis (see Figure 3.3). Through enamine catalysis, the secondary amine can form a nucleophilic enamine intermediate with the carbonyl substrate, which can then react with the chosen electrophile; coordination / activation of the electrophile and subsequent proton transfer is mediated by the carboxylic acid moiety of the catalyst. Another plausible mechanism consists of enol formation followed by coordination of substrates through noncovalent activation by the secondary amine. The Wennemers group's tripeptides take advantage of proline catalysis, while also taking advantage of the larger structural and functional flexibility of peptides.⁴⁶

⁴⁴ Mukherjee, S.; Yang, J.W.; Hoffmann, S.; List, B. *Chem. Rev.* **2007**, *107*, 5471 – 5569.

⁴⁵ Hajos, Z. G.; Parrish, D. R. *J. Org. Chem.* **1974**, *39*, 1615 – 1621.

⁴⁶ Bächle, F.; Duschmalé, J.; Ebner, C.; Pfaltz, A.; Wennemers, H. *Angew. Chem. Int. Ed.* **2013**, *52*, 12619 – 12623.

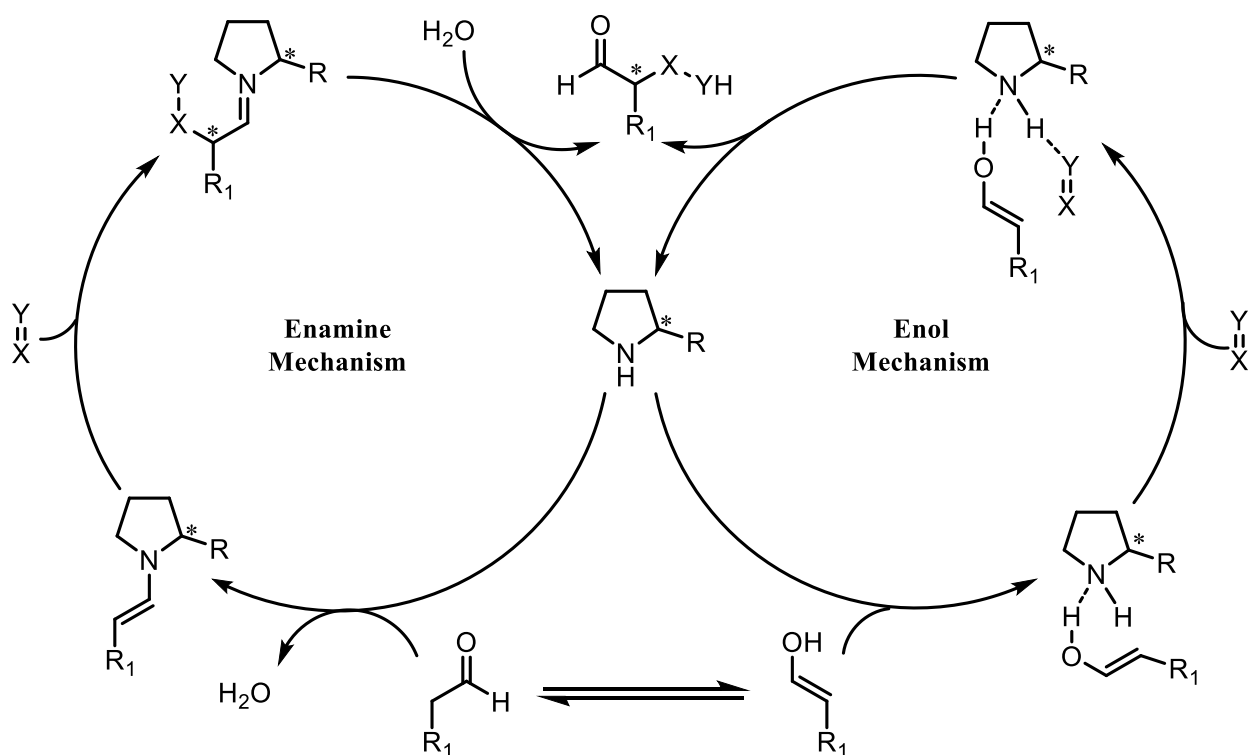


Figure 3.3 Mechanisms of proline organocatalyzed reactions

In comparison to proline catalysis, the distance between the reactive secondary amine of the tripeptide and the carboxylic acid moiety is much greater; approximately 3.7 Å in the case of proline and 7.3 Å in the case of the tripeptides (H-Pro-Pro-Asp-NH₂ in this example) (See Figure 3.4).⁴⁷ The Wennemers group hypothesized that this greater distance would not only allow the catalysis of 1,2-additions, but also of 1,4-additions. In the case of the 1,4-addition of aldehydes to nitroolefins, the carboxylic acid moiety is vital to the coordination of the electrophile through stabilizing interactions with the nitro group. The peptides' secondary structure coupled with the coordination of the electrophile allow for a

⁴⁷ Wiesner, M.; Revell, J.D.; Wennemers, H. *Angew. Chem. Int. Ed.* **2008**, *47*, 1871-1874.

very high level of stereocontrol. Given the peptides' ability to condense with aldehydes, our group hypothesized that amins could be formed to promote temporary intramolecularity between a variety of nucleophiles and electrophiles compatible with tripeptide catalysis.

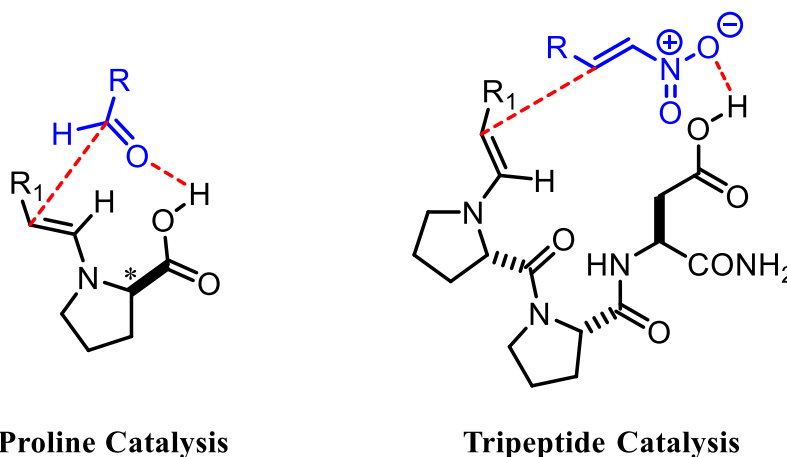


Figure 3.4 Comparison between proline catalysis and small peptide catalysis

3.2 Small Peptide Catalysis with Mixed Aminals

During a discussion with the Wennemers group, we envisioned a process by which an initial mixed aminal could be formed between the tripeptide catalyst and a nucleophile, through an initial condensation with aldehydes, namely formaldehyde (see Figure 3.5). Following aminal formation, an electron-deficient electrophile could be coordinated to the tripeptide through interactions with the carboxylic acid, which would then allow for a nucleophilic attack to occur. As is the case with the addition of aldehydes to nitroolefins, a proton transfer from the carboxylic acid group could then take place, followed by release of the desired product, regenerating an iminium intermediate. In theory, this approach would allow for the combination of the advantages of small peptide catalysis, with the advantages of catalysis through temporary intramolecularity; thus allowing for a great level of

stereocontrol, while also allowing for a broader scope of nucleophiles to participate in 1,4-addition.

Initial efforts to explore this reactivity centered on exploring the possibility of mixed aminal formation with various potential nucleophiles and pyrrolidine, serving as a model for the proline moiety found in the tripeptide catalyst. The nucleophiles were mixed with pyrrolidine and formaldehyde in equimolar amounts and the mixtures were allowed to reach equilibrium. The mixtures were then analyzed by NMR spectroscopy, to verify aminal formation in solution. A variety of amine nucleophiles of various degrees of nucleophilicity were examined under this preliminary study: aniline, *o*-Methoxyaniline, *p*-Toluenesulfonamide and Diphenylphosphinamide (see Figure 3.6).

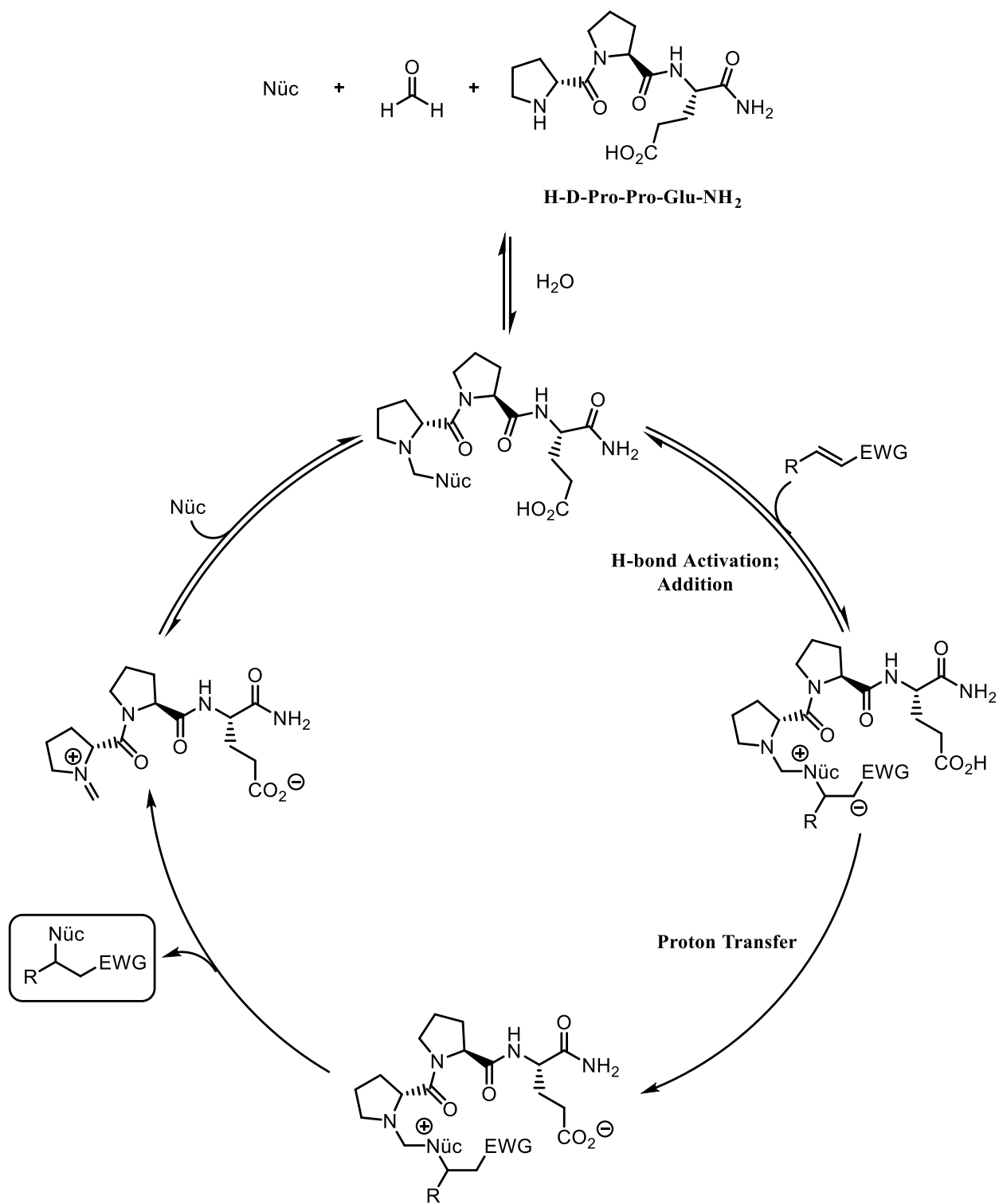


Figure 3.5 Suggested catalytic cycle for nucleophilic addition via peptide and amina catalysis

N-Benzylhydroxylamine and benzylamine were also considered, but were left out of the initial experiments due to their homodimers having been previously synthesized, therefore implying the possibility for aminal formation. Given the reversible nature of aminal formation and the potential for multiple species to arise in solution, only a cursory analysis of the ^1H and ^{31}P , when applicable, NMR spectra was performed. Analysis of the spectra revealed the appearance of new species in all examined examples. Aniline and *o*-methoxyaniline showed the appearance of many new species, some of which could be plausibly be mixed aminals. The sample with diphenylphosphinamide showed less species, but the formation of a new phosphorous containing compound was confirmed by ^{31}P NMR, indicating potential mixed aminal formation. The trial with toluenesulfonamide displayed very little reactivity, however further investigation was warranted to verify its reactivity with the peptide catalyst.

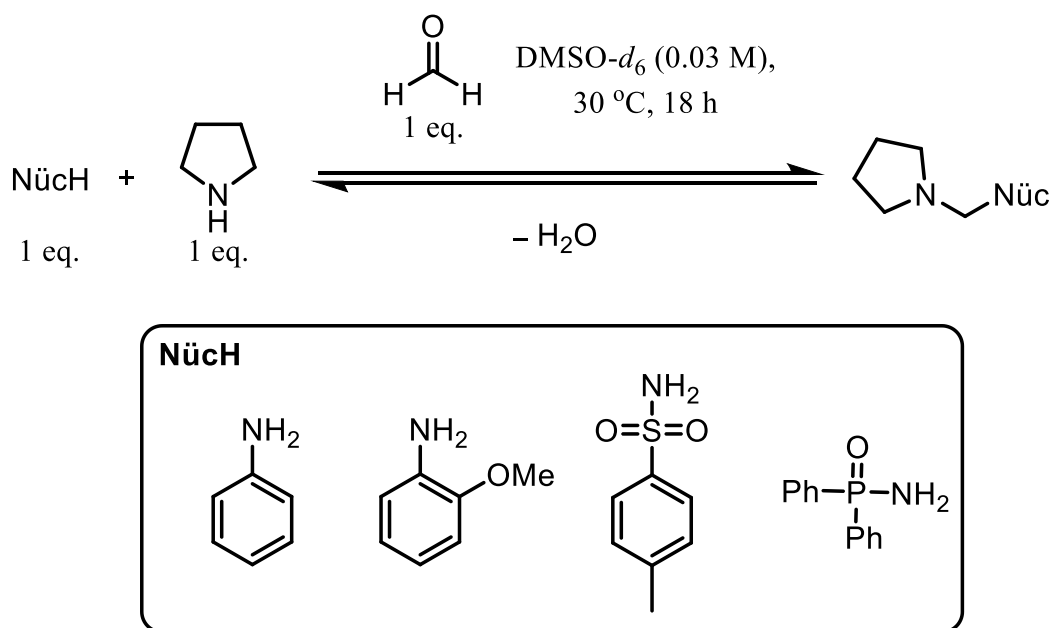


Figure 3.6 Mixed aminal formation with pyrrolidine as a model for tripeptide catalyst

Following evidence of potential mixed aminal formation, the background reactivity between various nucleophiles and potential electrophiles was examined. The initial electrophile chosen was β -Nitrostyrene, a model electrophile used by the Wennemer's group in their studies of 1,4-additions of aldehydes to nitroolefins (see Figure 3.7). Both aniline and *o*-methoxyaniline showed a high level of background reactivity with almost complete consumption of nitroolefin, while the weaker nucleophiles, Diphenylphosphinamide and toluenesulfonamide, showed very little to no reactivity with β -nitrostyrene. Although in all examined examples, full consumption of the electrophile was not observed, indicating the possibility of using peptide catalysis to improve reactivity and stereocontrol. Following the evaluation of background reactivity with β -nitrostyrene, the reactivity with β,β -disubstituted nitroolefins was examined, given their likely lower reactivity towards intramolecular nucleophilic addition due to higher steric hindrance. (1-Nitroprop-1-en-2-yl)benzene was chosen as a model substrate for this type of nitroolefin (see Figure 3.8). Following a preliminary analysis of the $^1\text{H-NMR}$ spectra for crude reaction mixtures with the chosen nucleophiles (aniline, *o*-Methoxyaniline and *N*-Benzylhydroxylamine), little to no background reactivity was observed with this disubstituted nitroolefin, indicating that it could serve as an ideal candidate for 1,4-addition test reactions with tripeptide catalysis.

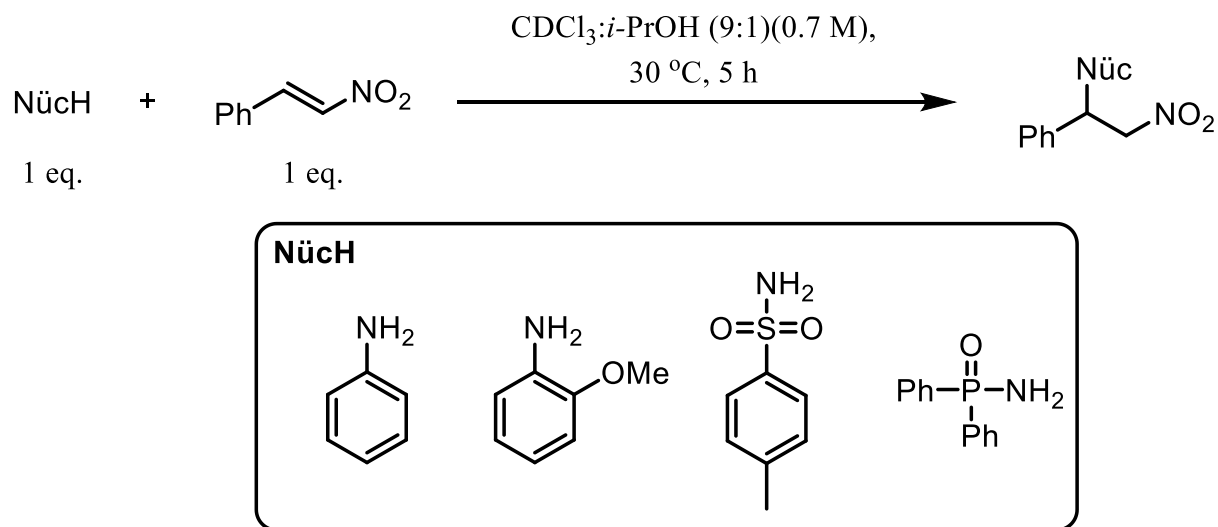


Figure 3.7 Preliminary study of background reactivity with β -nitrostyrene

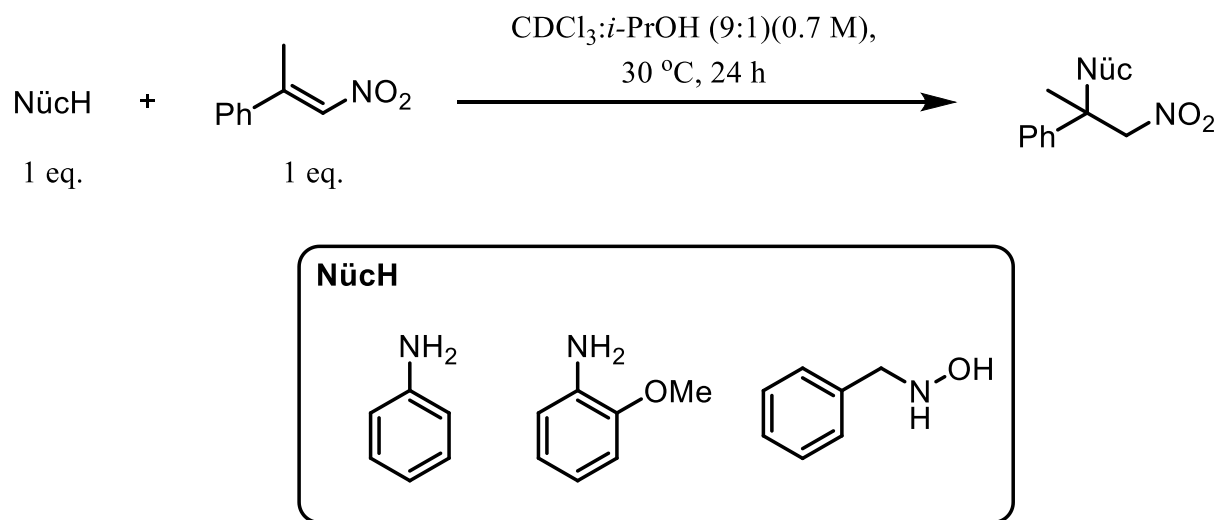


Figure 3.8 Evaluation of background with β,β -disubstituted nitroolefins for tripeptide catalysis

Following the examination of background reactivity of nitroolefins, the reactivity of a variety of electron-deficient electrophiles was also evaluated. These electron-deficient alkenes could serve as ideal candidates for this type of reaction given their higher propensity for 1,4-additions, as well as possibility for coordination to the small peptide catalyst. The reactivity of ethyl cinnamate, diethyl benzilidene, 2-Furanone and benzilidenemalononitrile

was examined against aniline and *N*-Benzylhydroxylamine, stronger nucleophiles (see Figure 3.9). In the case of reactions with *N*-Benzylhydroxylamine, most alkenes were almost completely consumed after the reaction time, with the reaction with ethyl cinnamate showing the least reactivity. Although, it should be noted that in none of the observed examples, did the reaction proceed to completion, potential allowing for rate improvements and stereocontrol by small peptide catalysis. As a general trend, the observed reactivity with aniline was much lower; with little to no reactivity observed with ethyl cinnamate, 2-Furanone and benzilidenemalononitrile and minimal product formation with diethyl benzilidene. With a better understanding of background reactivity of various potential nucleophiles and electrophiles, as well as potential aminal formation with the tripeptide catalyst, initial trial reactions could be undertaken.

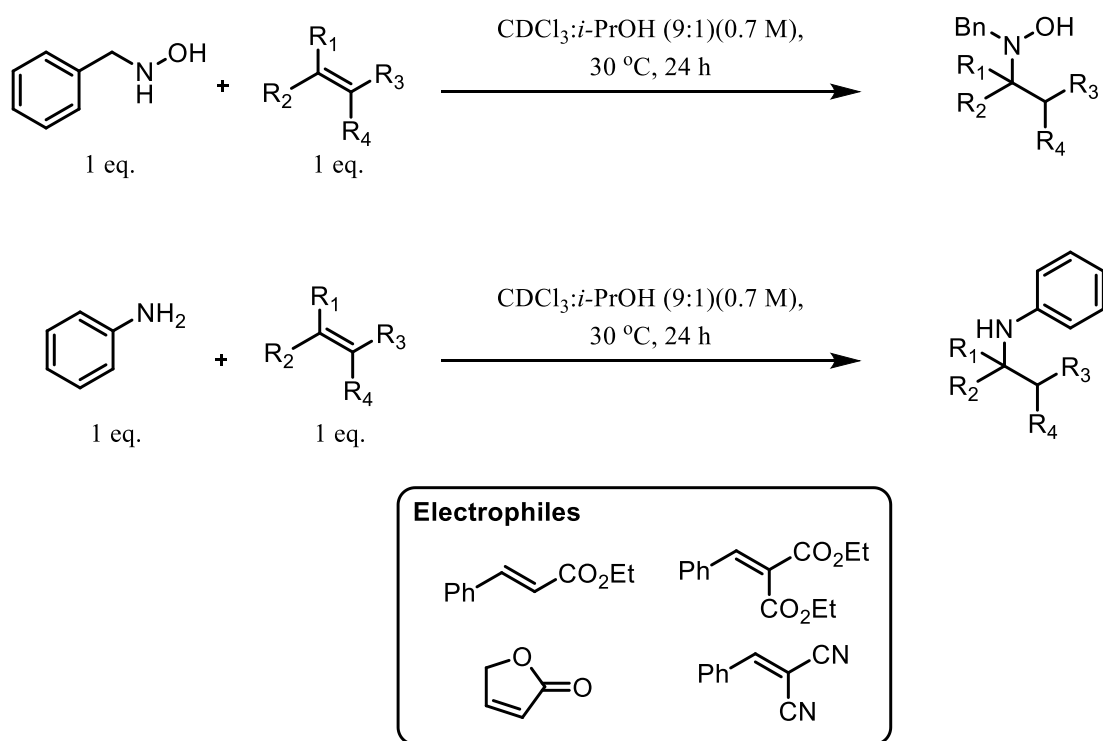
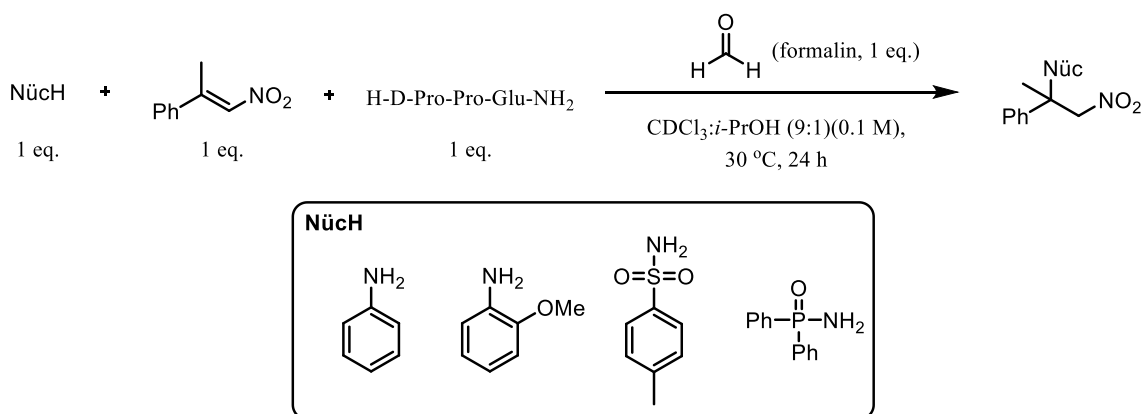


Figure 3.9 Evaluation of background reactivity between aniline and *N*-benzylhydroxylamine and various potential electrophiles for tripeptide catalysis

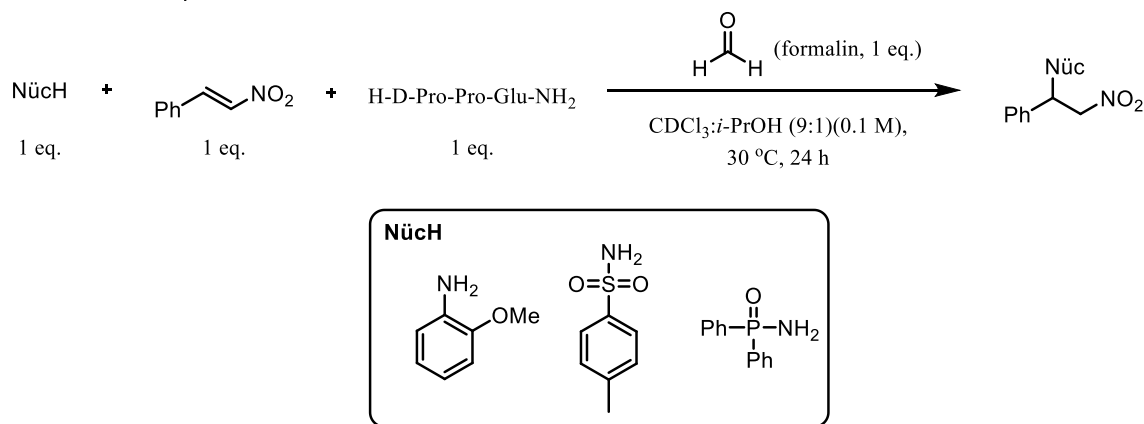
The initial test reactions with the Wennemers' tripeptide catalyst, H-D-Pro-Pro-Glu-NH₂, were conducted with 1-Nitroprop-1-en-2-yl)benzene as the chosen electrophile given its very low background reactivity with the nucleophiles of interest, as well as possessing the nitro group allowing for coordination to the peptide (see Figure 3.10). The chosen nucleophiles for these experiments consisted of the same series chosen for the initial background reactivity testing (see Figure 3.7). After some optimization of the reaction conditions and choosing a similar solvent system (CDCl₃:*i*-PrOH) previously used by the Wennemers group, reactions were run overnight, under stoichiometric conditions, and monitored by ¹H-NMR. After the elapsed reaction period, no desirable product formation was observed with any of the examined nucleophiles, similarly to the background reactions with this β,β-disubstituted nitroolefin. A new side product was isolated from the reaction with aniline, however it was not fully identified and characterized, given that it did not arise from 1,4-addition. Following trials with β,β-disubstituted nitroolefins, reactivity with the more reactive β-substituted nitroolefins was examined with nucleophiles which had shown little to no background reactivity with these electrophiles (see Figure 3.10). Once again under stoichiometric conditions, no desirable product formation between these nucleophiles and nitrostyrene was observed after a 24 hour period. The final trial reaction with the tripeptide catalyst was performed with *N*-benzylhydroxylamine, a nucleophile which had shown great background reactivity with nitrostyrene (see Figure 3.10). In order to attenuate background reactivity and potentially improve enantioselectivity, the temperature of the reaction was lowered to -15 °C and allowed to gradually warm to 4 °C over a 48 hour period. Furthermore, the equivalency of the tripeptide catalyst and formalin were slightly lowered to improve solubility of the mixture. While complete disappearance of

the nitroolefin and formation of nitrone were confirmed by analysis of the crude $^1\text{H-NMR}$ spectrum, the recovered product, after preparatory TLC purification, was found to be racemic. It was concluded that the resulting product formation was most likely due to innate background reactivity of the *N*-benzylhydroxylamine rather than through peptidic catalysis. Further investigations into this type of reactivity was discontinued, due to similar results being obtained by the Wennemers group.

a) Trial reactions with β,β -disubstituted nitroolefins



b) Trial reactions with β -substituted nitroolefins



c) Low temperature trial reactions with β -substituted nitroolefin

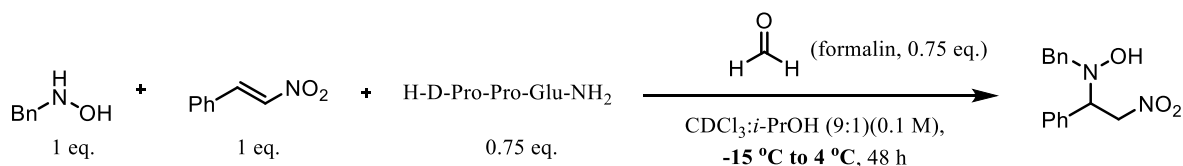


Figure 3.10 Investigations into aldehyde and small peptide dual-catalysis

Although investigations into the combination of small peptide catalysis with aldehyde catalysis did not result in desired product formation or enhanced enantioselectivities, these studies highlighted the potential for reversible mixed aminal formation to allow for new types of reactivity promoted through temporary intramolecularity. In the scope of this study, the background reactivity of multiple potential electrophiles and nucleophiles was evaluated, which could allow for calibration for future catalysis efforts. Furthermore, some preliminary evidence was collected to support the formation of new amins with formaldehyde and various nucleophiles, which could potentially be used in other types of aldehyde-catalyzed reactions. By broadening the scope of the nucleophiles and potential electrophiles for the combination of small peptide catalysis and aldehyde catalysis, and by potentially also modifying the structure and function of the small peptide catalysts used, it is possible that new novel productive reactivity could be developed.

Chapter 4 – Conclusions

4.1 Conclusions and Potential Future Studies

In the scope of this thesis, a broader understanding of aldehyde catalyzed Cope-type hydroamination and related reactions was achieved. We were allowed to highlight the strengths of catalysis acting solely through temporary intramolecularity, allowing a previously difficult intermolecular reaction to occur under very mild conditions. Aldehydes are shown to form mixed amins with hydroxylamines and allylic amines, which promotes their preassociation and therefore allows for a facile 5-membered transition state. This type of approach also allows for great stereocontrol of the formed products, through the application of chiral aldehydes or chiral reagents, thus highlighting the strengths of organocatalysis.

Initial studies performed involved comparing aldehyde catalytic efficiency in a model system in order to better understand previously observed reaction trends and potentially discover new highly effective catalysts; this was done in an effort to consolidate and contrast previous studies, in which conditions varied considerably. It was reconfirmed that formaldehyde consisted of an extremely effective catalyst for this transformation and that *t*-BuOH could have a particularly beneficial effect on the reaction. Following studies focused on other mechanistic aspects of the reaction, such as confirming the rate determining step through kinetic isotope effect studies and exploring the potential of using a precursor form of the catalyst, a hydroxylamine amination. Furthermore, hydroamination products were also

derived into an assortment of other chemical motifs, such as 1,2-Diamines; thus further demonstrating the relevance of these aldehyde catalyzed hydroaminations. It was also shown that difficult to obtain hydroamination products could be accessed through a sequence of using stoichiometric aldehyde (formaldehyde), followed by hydrolysis to afford the desired products. Future studies could focus on discovering new more robust aldehyde catalysts, especially for the enantioselective version of the reaction. Expanding upon preliminary results, it could also be considered to expand this type of catalysis through temporary intramolecularity to other reactions and substrates, such as the hydroamination of allylic alcohols or thiols, which has proven more difficult. Lastly, it is worth investigating the catalytic activities of small simple aldehydes and carbohydrates, as this could have many implications in the field of origin of life chemistry.

Wishing to expand upon enantioselective hydroamination reactions, exploratory studies were also conducted in order to develop a novel synthetic sequence to form enantiomerically enriched chiral nitrones. Although the initially desired chiral heterocycles were not obtained, we were able to explore the possibility of enantioselective hydroamination initiated by nucleophilic attack of appropriate nitrones. After only low selectivities were obtained using chiral nucleophiles, we explored the possibility of forming nitrones from enantiomerically pure hydroxylamines. The following sequence of nucleophilic addition (thiols), Cope-type hydroamination, followed by Cope elimination yielded the enantiomerically enriched cyclic nitrones. However, after much optimization, only modest selectivities were obtained, while requiring fairly complex synthesis of starting materials; therefore, further investigation was not warranted. Future studies into this type

of reactivity could focus on finding alternative chemical moieties to mimic the Thorpe-Ingold effect obtained from dimethyl substitution; acetals and thioacetals could be considered for their potential to be cleaved after synthesis of the nitrones.

Collaborative studies were also undertaken with the Wennemers group, in efforts to combine aldehyde catalysis with small peptide catalysis. Trying to expand upon the conjugate addition of aldehydes to nitroolefins achieved through small peptide catalysis, it was hypothesized that a wider scope of nucleophilic additions could be accessed through mixed aminal formation with aldehydes and the small peptide catalysts. In the scope of these studies, the potential for forming new mixed aminals between various nucleophiles and a small peptide catalyst was evaluated; preliminary data seemed to indicate the formation of such aminals, which could lead to the development of new aldehyde-catalyzed reactions. Studies were also undertaken to better understand the background reactivity between various nucleophile and electrophile pairings; allowing for some calibration for potential future studies of similar systems. Although the combination of both catalysts did not yield desired results, future efforts could focus on broadening the scope of potential nucleophiles and electrophiles, as well as examining the effects of varying the small peptide catalysts' structure and function.

Overall, the studies undertaken for this thesis allowed for a greater understanding of the strengths and weaknesses of organocatalytic strategies. Aldehydes have been shown to be excellent promoters of temporary intramolecularity, which has allowed for difficult intermolecular hydroamination reactions to occur. Further development of this strategy

could potentially allow for the catalysis of new reactions through temporary intramolecularity. Other studies could focus on expanding enantioselective hydroamination reactions and better understanding mechanistic aspects of the reaction, while also trying to discover new more robust chiral aldehyde catalysts. Aldehyde catalysis could also have exciting implications in the field of origin of life chemistry; further study and collaboration could help elucidate any potential roles.

Annex I

Claims to Original Research

- 1) Development of a method to compare aldehyde catalytic activity for intermolecular hydroaminations of unactivated alkenes
- 2) Measurement of kinetic isotope effect of formaldehyde catalyzed intermolecular hydroamination, using a catalytic precursor species
- 3) Derivatization of hydroamination products, including hydrolysis of 6-membered oxadiazinanes.
- 4) Synthesis of enantiomerically enriched chiral nitrones, using thiols.

Publications from This Work

Formaldehyde as Tethering Organocatalyst: Highly Diastereoselective Substrate and Reagent-Controlled Hydroaminations of Allylic Amines MacDonald, M. J.; Hesp, C. R.; Zahedi, M.M.; Bilodeau, D.A.; Pesant, M.; Zhao, S.; Beauchemin, A. M. *Org. Lett.* **2015**, *17*, 5136-5139.

Presentations from This Work

Poster Presentations

Bilodeau, D.; MacDonald, M.J.; Hesp, C.R.; Zhao, S.; Beauchemin, A.M. ***Organocatalytic Tether Formation: A Strategy Enabling Directed Intermolecular Amination Reactions.*** 24th Quebec-Ontario Mini-Symposium on Bioorganic and Organic Chemistry (November 8-10, 2013)

Bilodeau, D.; Zahedi, M.; MacDonald, M.J.; Hesp, C.R.; Pesant, M.; Zhao, S.; Beauchemin, A.M. **Formaldehyde as a Tethering Organocatalyst: Highly diastereoselective hydroamination of allylic amines.** International Symposium on Homogeneous Catalysis XIX (July 6-11, 2014)

Bilodeau, D.; Zahedi, M.M.; MacDonald, M.J.; Hesp, C.R.; Pesant, M.; Zhao, S.; Beauchemin, A.M. ***Organocatalytic Tether Formation: A Strategy Enabling Directed Intermolecular Amination Reactions.*** 22nd IUPAC International Conference on Physical Organic Chemistry (August 10-15, 2014)

Bilodeau, D.; Zahedi, M.M.; MacDonald, M.J.; Hesp, C.R.; Pesant, M.; Zhao, S.; Beauchemin, A.M. ***Organocatalytic Tether Formation: A Strategy Enabling Directed Intermolecular Amination Reactions.*** 98th Canadian Chemistry Conference and Exhibition (June 13-17, 2015)

Annex II

Experimental Section

General Information. All reactions were performed in flame-dried round bottom flasks under an argon atmosphere unless otherwise noted. Purification of reaction products was carried out by flash column chromatography using 40-63 μm silica gel. Analytical thin layer chromatography (TLC) was performed on aluminum sheets pre-coated with silica gel 60 F₂₅₄, cut to size. Visualization was accomplished with UV light followed by dipping in a potassium permanganate solution and heating. Infrared (IR) spectra were obtained as neat thin films on a sodium chloride disk and were recorded on a Bruker EQUINOX 55 Fourier transform infrared spectrometer (FTIR). ¹H spectra were recorded on Bruker AVANCE 300 or 400 MHz spectrometers at ambient temperature unless otherwise noted, and are reported in ppm using solvent as the internal standard (CDCl₃ at 7.26 ppm). Data are reported as: multiplicity (br = broad, s = singlet, d = doublet, t = triplet, q = quartet, m = multiplet), integration and coupling constant(s) in Hz. ¹³C NMR spectra were recorded at 75 or 100 MHz. Chemical shifts are reported in ppm from the residual solvent resonance employed as the internal standard (CDCl₃ at 77.0 ppm). High-resolution mass spectroscopy (HRMS) was performed on a Kratos Concept IIF mass spectrometer with an electron beam of 70 eV. High Performance Liquid Chromatography (HPLC) was performed on an Agilent 1200 series.

Materials. Unless otherwise noted, all deuterated solvents and reagents were used without further purification. Solvents were either distilled according to standard techniques or degassed prior to use.

NMR Yields. NMR yields were determined using 1,4-Dimethoxybenzene as an internal standard. These results are subject to the uncertainty of NMR integrations and the error resulting from the measurement of 1,4-Dimethoxybenzene. As a general rule, this data normally ranges anywhere from 5-10% and only reactivity trends are drawn as conclusions.

Table 2.1 Comprehensive aldehyde scan in CHCl₃ and *t*-BuOH

General Procedure for Comprehensive Aldehyde Scan

A microwave vial (2-5 mL) (*t*-BuOH reactions) or an NMR tube (CDCl₃ reactions) was loaded with a magnetic stir bar, *N*-benzylhydroxylamine (0.5 mmol, 1.0 equiv.), *N*-benzyl-*N*-allylamine (0.75 mmol, 1.5 equiv.), the appropriate solvent (CDCl₃ or *t*-BuOH, 1M with respects to hydroxylamine) and finally the aldehyde (0.125 mmol, 0.25 equiv.). The reaction was then stirred at 30 °C for 24 hours. The mixture was concentrated under reduced pressure. An NMR yield was then obtained by using an internal standard, 1,4-Dimethoxybenzene (0.125 equiv.) and comparing internal standard peaks to the newly formed product peak (1.14 ppm, 3H, doublet). An identical procedure was used when evaluating other aldehyde reactivity, such as data from Table 2.2 and 2.3; as well as Scheme 2.8.

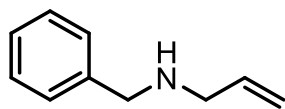
N-Hydroxylamines

N-Alkylhydroxylamines, including *N*-benzylhydroxylamine, were prepared by reductive amination of the corresponding oximes according to the modified method of House and Lee.⁴⁸ Modifications included vigorous stirring of the crude material in hot hexanes for the

⁴⁸ (a) House, H. O.; Lee, L. F. *J. Org. Chem.* **1976**, *41*, 863

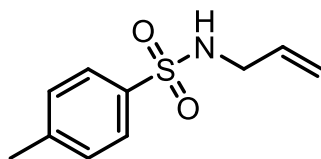
purposes of purification by recrystallization. All hydroxylamines prepared have been previously characterized in the literature.

N-Benzylallylamine



Allylamine (24.0 g, 421 mmol) was added to a 250 mL round-bottom flask equipped with a magnetic stir bar. Benzyl bromide (14.4 g, 84.1 mmol) was added dropwise over 15 minutes. The reaction was allowed to stir for an additional 2 hours before concentrating the mixture under reduced pressure. Diethyl ether (100 mL) and 2M NaOH (50 mL) were added to the residue. The aqueous portion was extracted twice more with diethyl ether (50 mL). The collected organic phases were then washed with water, brine, and dried over MgSO₄. The indicated compound was purified using a Kugelrohr distillation apparatus set to 110 °C, giving a colorless oil (8.87 g, 72%). ¹H NMR (300 MHz, CDCl₃) δ 7.29-7.17 (m, 5H), 5.97-5.83 (m, 1H), 5.19-5.02 (m, 2H), 3.75 (s, 2H), 3.23 (dt, *J* = 6.00 Hz, *J* = 5.9, 1.5 Hz, 2H). Spectral data was consistent with literature.⁴⁹

N-Allyl-4-methyl-1-benzenesulfonamide



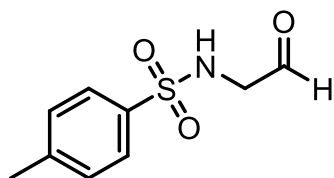
The protected allylamine was prepared via a modified procedure from *Studer et al.*⁵⁰ Allylamine (1.53 g, 26.7 mmol) and trimethylamine (2.98 g, 29.3 mmol) were dissolved in dichloromethane (13 mL) and added to a round-bottomed flask loaded with a magnetic stirrer. The mixture was cooled to 0 °C. Then, *p*-toluenesulfoamide chloride (5.60 g, 29.3 mmol) was dissolved in dichloromethane and added dropwise to the initial mixture over a

⁴⁹ Harvey, D. F.; Sigano, D. M. *J. Org. Chem.* **1996**, *61*, 2268-2272.

⁵⁰ Studer, A.; Amrein, S.; Timmerman, A. *Org. Lett.* **2001**, *3*, 2357.

period of 1 hour, after which the solution was allowed to warm to room temperature and stirred for 1 additional hour. The mixture was then washed with a solution of saturated ammonium chloride, followed by a saturated brine solution. The collected organic fractions were dried over MgSO_4 and concentrated under reduced pressure. The compound was purified via flash column chromatography using 30% EtOAc/70% Hexanes mixture. The compound was obtained in quantitative yield (5.64 g, 99%). Spectral data was consistent with literature.

N-(2-Oxoethyl)-4-methyl-1-benzenesulfonamide

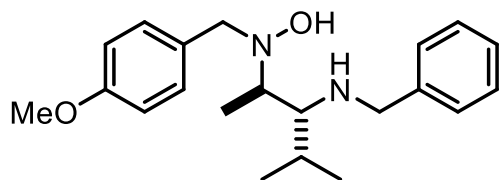


The protected aldehyde was synthesized according to procedure by *Aggarwal et al.*⁵¹ A solution of *N*-allyl-4-methyl-1-benzenesulfonamide (1.00 g, 4.74 mmol) was dissolved in a mixture of anhydrous methanol (4.6 mL) and anhydrous DCM (46 mL) then treated with ozone at $-78\text{ }^\circ\text{C}$ with stirring until the solution maintained a blue colouration. The solution was then degassed with nitrogen and treated with zinc (0.55 g, 8.41 mmol) and concentrated acetic acid (0.91 mL) then stirred for 3 hours at $-78\text{ }^\circ\text{C}$ then allowed to warm to room temperature and stirred for a further 18 hours under nitrogen. The reaction mixture was then filtered through Celite and concentrated under reduced pressure to give the product as a white gummy solid (0.97 g, 96%), the crude material was used without further purification. ^1H NMR (300 MHz, CDCl_3) δ 9.57 (s, 1H), 7.81-7.68 (m, 2H), 7.36-7.29 (m, 2H), 3.94 (d, $J=4.81\text{ Hz}$, d), 2.45 (s, 3H).

⁵¹ Aggarwal, V. K.; Unthank, M. G.; Hussain, N.; *Angew. Chem. Int. Ed.* **2006**, *45*, 7066.

Scheme 2.1, 2.2 and 2.3 Derivatization of Hydroamination Products

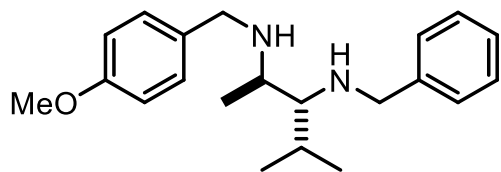
(±)-N-Benzyl-2-(hydroxy(4-methoxybenzyl)amino)-4-methylpentan-3-amine (2.2a)



N-(4-Methoxybenzyl)hydroxylamine (3.2 g, 0.021 mmol), *N*-benzyl-4-methylpent-1-en-3-amine (2.0 g, 0.010 mmol) were dissolved in a solvent mixture

(CDCl₃ in *t*-BuOH 20% v/v, 13 mL) under inert atmosphere. Formaldehyde (240 μL, 0.003 mmol, 37% w/w) was added and the vessel was sealed and heated to 50 °C. After 48 hours the reaction mixture was concentrated, and fractionated by FCC (pre-treated 500 mL silica gel with 55 mL NH₄OH solution 28-30% w/w, 20% ethyl acetate in hexane) to give the titled compound (2.36 g, 69%) as a white solid. ¹H NMR (400 MHz, CDCl₃) δ 7.31-7.21 (m, 7H), 6.85 (d, *J* = 9 Hz, 2H), 3.90 (d, *J* = 13 Hz, 1H), 3.83 (d, *J* = 7 Hz, 1H), 3.81 (d, *J* = 7Hz), 3.79 (s, 3H), 3.61 (d, *J* = 13 Hz), 2.81 (dq, *J* = 7 and 7 Hz, 1H), 2.33 (dd, *J* = 5 and 5 Hz, 1H), 1.97-1.89 (m, 1H), 1.17 (d, *J* = 7 Hz, 3H), 0.93 (d, *J* = 7 Hz, 3H), 0.90 (d, *J* = 7 Hz, 3H) ¹³C NMR (100MHz, CDCl₃) δ 158.7 (C), 140.3 (C), 130.5 (C), 130.2 (CH×2), 128.45 (CH ×2), 128.40 (CH ×2), 127.1 (CH ×2), 113.6 (CH ×2), 67.2 (CH), 60.1 (CH), 59.8 (CH₂), 55.5 (CH₂), 55.2 (CH₃), 30.3 (CH), 20.4 (CH₃), 18.0 (CH₃), 10.5 (CH₃); IR (film): 2964, 2831, 1612, 1512, 1247, 1035 cm⁻¹. HRMS (EI): Exact mass calcd for C₂₁H₃₀N₂O₂ [M]⁺: 342.2307. found: 342.2297.

(±)-N³-Benzyl-N²-(4-methoxybenzyl)-4-methylpentane-2,3-diamine (2.2b)

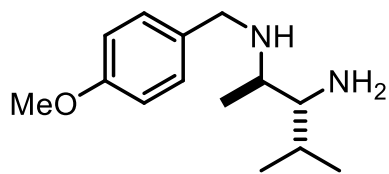


(±)-*N*-Benzyl-2-(hydroxy(4-methoxybenzyl)amino)-4-methylpentan-3-amine **2.2a** (0.200 g, 0.584 mmol) was dissolved in ethanolic solution of acetic acid (2

mL, 50% v/v). After 5 min, zinc powder (0.160 g, 2.52 mmol) was added to the reaction mixture at ambient temperature. The reaction vessel was sealed and heated to 60 °C. After 3

hours, the reaction mixture was cooled down to 0 °C and basified by using NaOH solution 4M to PH = 9-10. The reaction mixture was extracted twice by dichloromethane (60 mL). The combined organic layer was dried over Na₂SO₄ and concentrated under reduced pressure to give the titled compound as colorless oil (0.176 g, 92%). ¹H NMR (400 MHz, CDCl₃) δ 7.29-7.22 (m, 7H), 6.84 (d, *J* = 9 Hz, 2H), 3.93 (d, *J* = 13 Hz, 1H), 3.91 (d, *J* = 12 Hz, 1H), 3.80 (s, 3H), 3.79 (d, *J* = 12 Hz, 1H), 3.60 (d, *J* = 13 Hz, 1H), 2.62 (dq, *J* = 7 and 6 Hz, 1H), 2.31 (dd, *J* = 7 and 4Hz, 1H), 2.03-1.95 (m, 1H), 1.18 (d, *J* = 6 Hz, 3H), 1.01 (d, *J* = 7 Hz, 3H), 0.86 (d, *J* = 7 Hz, 3H) ¹³C NMR (100 MHz, CDCl₃) δ 158.8 (C), 140.9 (C), 129.5 (CH), 129 (C), 128.4 (CH×2), 128.2 (CH×3), 127 (CH), 113.9 (CH×2), 67.5 (CH), 55.4 (CH₂), 55.3 (CH₃), 54.9 (CH), 50.3 (CH₂), 29.6 (CH), 21.0 (CH₃), 17.1 (CH₃), 16.9 (CH₃); IR (film): 2964, 1610, 1581, 1512, 1245, 1033 cm⁻¹. HRMS (ESI): Exact mass calcd for C₂₁H₃₁N₂O [M+H]⁺: 327.2431. Found: 327.2437.

(±)-N²-(4-Methoxybenzyl)-4-methylpentane-2,3-diamine (2.2c)



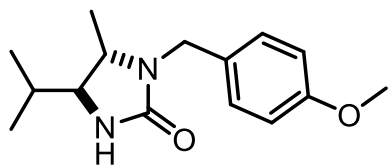
From hydroxylamine **2.2a**:

A suspension of Raney nickel (W2; 1.5 mL settled volume) in *i*-PrOH (4 mL) was added to (±)-*N*-Benzyl-2-(hydroxy(4-methoxybenzyl)amino)-4-methylpentan-3-amine **2i** (0.100 g, 0.292 mmol) and the mixture was heated at 80 °C with vigorous stirring. After 4 hours, the mixture was decanted and the solid was suspended in *i*-PrOH (4 mL) and heated at 80 °C with vigorous stirring for several min. This washing procedure was repeated four times. The combined organic layers were filtered through Celite®, concentrated, and fractionated by prep. TLC (48% EtOAc in hexanes, 2% NH₄OH solution 28-30% w/w) to give the titled compound as a pale yellow oil (0.056 g, 81%). ¹H NMR (400 MHz, CDCl₃) δ 7.25 (d, *J* = 7 Hz, 2H), 6.85 (d, *J* = 7 Hz, 2H), 3.87 (d, *J* = 13 Hz, 1H), 3.79 (s, 3H), 3.59 (s, 3H), 2.49 (dq, *J* = 7 and 6 Hz, 1H), 2.27 (dd, *J* = 7 and 4

Hz, 1H), 1.84 (m, 1H), 1.73 (bs, 3H), 1.09 (d, $J = 6$ Hz, 3H), 0.91 (d, $J = 7$ Hz, 3H), 0.79 (d, $J = 7$ Hz, 3H) ^{13}C NMR (100 MHz, CDCl_3) δ 158.6 (C), 133.0 (C), 129.4 ($\text{CH}\times 2$), 113.8 ($\text{CH}\times 2$), 61.7 (CH), 55.2 (CH₃), 55.1 (CH), 50.8 (CH₂), 29.1 (CH), 20.9 (CH₃), 16.9 (CH₃), 15.3 (CH₃); IR (film): 2958, 1612, 1512, 1242, 1174, 1033 cm^{-1} . HRMS (ESI): Exact mass calcd for $\text{C}_{14}\text{H}_{25}\text{N}_2\text{O}$ $[\text{M}+\text{H}]^+$: 237.1967. Found: 237.1969.

Also prepared from diamine 2.2b: To the solution of (\pm)-*N*³-benzyl-*N*²-(4-methoxybenzyl)-4-methylpentane-2,3-diamine **2.2b** (0.050 g, 0.150 mmol) in isopropanol, was added Pd/C (0.015 g, 10% w/w). The reaction mixture was stirred at 30 °C under H_2 . After 18 hours, the reaction mixture was passed through a pad of Celite® using ethanol. The organic layer was concentrated under reduced pressure to give the desired compound as colorless oil (0.032 g, 88%).

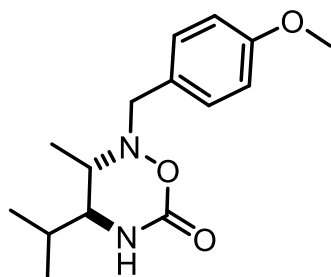
(\pm)-4-Isopropyl-1-(4-methoxybenzyl)-5-methylimidazolidin-2-one (**2.2d**)



Carbonyldiimidazole (0.068 g, 0.42 mmol) was added to a solution of (\pm)-*N*²-(4-methoxybenzyl)-4-methylpentane-2,3-diamine **2.2c** (0.050 g, 0.21 mmol) in THF (2 mL) under inert atmosphere at ambient temperature. After 3 hours, the reaction mixture was concentrated under reduced pressure and fractionated by PTLC (19% EtOAc in hexane, 1% NH_4OH solution 28-30% w/w) to give the titled compound as a colorless oil (0.048 g, 87%). ^1H NMR (400 MHz, CDCl_3) δ 7.17 (d, $J = 8$ Hz, 2H), 6.85 (d, $J = 8$ Hz, 2H), 4.74 (d, $J = 15$ Hz, 1H), 4.5 (bs, 1H), 3.92 (d, $J = 15$ Hz, 1H), 3.80 (s, 3H), 3.20 (dq, $J = 6$ and 6 Hz, 1H), 2.96 (ddd, $J = 6, 6$ and 1 Hz, 1H), 1.56 (m, 1H), 1.16 (d, $J = 6$ Hz, 3H), 0.81 (d, $J = 7$ Hz, 6H) ^{13}C NMR (100 MHz, CDCl_3) δ 160.8 (C), 158.9 (C), 129.3 ($\text{CH}\times 2$), 129.2 (C), 113.9 ($\text{CH}\times 2$), 63.2 (CH), 55.3 (CH₃), 53.6 (CH), 43.9 (CH₂), 32.3 (CH), 19.6 (CH₃), 18.3 (CH₃), 17.6 (CH₃); IR (film): 2974, 1693, 1515,

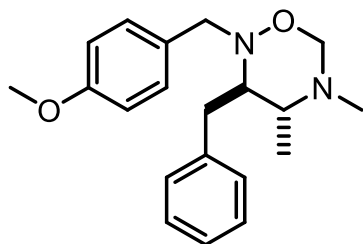
1463, 1248 cm^{-1} . HRMS (EI): Exact mass calcd for $\text{C}_{15}\text{H}_{22}\text{N}_2\text{O}_2$ $[\text{M}]^+$: 262.1681. Found: 262.1707.

(±)-4-Isopropyl-2-(4-methoxybenzyl)-3-methyl-1,2,5-oxadiazinan-6-one (2.2e)



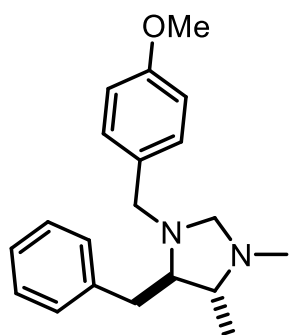
To an ethanolic solution of (\pm) -*N*-benzyl-2-(hydroxy(4-methoxybenzyl)amino)-4-methylpentan-3-amine **2.2a** (0.050 g, 0.146 mmol) was added Pd/C (0.015 g, 10% w/w). The reaction mixture was stirred at 30 °C under positive pressure of H_2 . After 18 hours, the reaction mixture was filtered through a pad of Celite® using ethanol (30 mL). The organic layer was concentrated under reduced pressure to give crude product (0.031 g). The crude mixture was taken up in dry THF (1 mL) under inert atmosphere and carbonyldiimidazole (0.038 g, 0.23 mmol) was added to the stirred solution. After 18 hours, the reaction mixture was concentrated under reduced pressure and purified by prep. TLC (20% EtOAc in hexane, 1% NH_4OH solution 28-30% w/w) to give the titled compound as a colorless oil (0.0260 g, 64%). ^1H NMR (400 MHz, CDCl_3) δ 7.27 (d, $J = 8$ Hz, 2H), 6.85 (d, $J = 8$ Hz, 2H), 5.95 (bs, 1H), 4.28 (d, $J = 13$ Hz, 1H), 3.83 (d, $J = 13$ Hz, 1H), 3.79 (s, 3H), 3.04 (dq, $J = 6.5, 4$ Hz, 1H), 2.81 (bs, 1H), 1.90 (m, 1H), 1.18 (d, $J = 6.5$ Hz, 3H), 0.92 (d, $J = 7$ Hz, 3H), 0.79 (bd, $J = 7$ Hz, 3H) ^{13}C NMR (100 MHz, CDCl_3) δ 159.2 (C), 155.3 (C), 130.4 ($\text{CH}\times 2$), 127.3 (C), 113.9 ($\text{CH}\times 2$), 63.5 (CH), 57.8 (CH_2), 55.3 (CH_3), 53.1 (CH), 31.2 (CH), 19.2 (CH_3), 17.6 (CH_3), 11.3 (CH_3); IR (film): 3259, 1712, 1514, 1409, 1247, 1031 cm^{-1} . HRMS (ESI): Exact mass calcd for $\text{C}_{15}\text{H}_{22}\text{N}_2\text{O}_3$ $[\text{M} + \text{Na}]^+$: 301.1523. Found: 301.0849.

(±)-(3R*,4R*)-3-Benzyl-2-(4-methoxybenzyl)-4,5-dimethyl-1,2,5-oxadiazinane (2.2f)



To a microwave vial is added a magnetic stir bar, *N*-(4-methoxybenzyl)hydroxylamine (0.591 g, 3.72 mmol), (±)-methyl[(3*E*)-4-phenylbut-3-en-2-yl]amine (0.623 g, 3.72 mmol) and *t*-BuOH (7.0 mL). Formaldehyde 37 wt % in water (0.332 mL, 4.46 mmol) was then added. The reaction was stirred at 50 °C in an oil bath for 72 hours. The title compound was purified by column chromatography (50% EtOAc in Hexanes) to yield a clear oil (0.575 g, 50%). ¹H NMR (400 MHz, CDCl₃) δ 7.33-7.21 (m, 7H), 6.87 (d, *J*=8.0 Hz, 2H), 4.45 (d, *J* = 12.0 Hz, 1H), 4.36 (d, *J* = 12.0 Hz, 1H), 4.22 (d, *J*=16.0 Hz, 1H), 3.81 (s, 3H), 3.59 (d, *J*= 16.0 Hz, 1H), 3.10 (dd, *J*= 16.0 and 4.0 Hz, 1H), 2.99 (ddd, *J* = 8.0, 4.0 and 4.0 Hz, 1H), 2.85 (dd, *J*= 16.0 and 4.0 Hz, 1H), 2.75 (dq, *J*= 4.0 and 4.0 Hz, 1H), 2.35 (s, 3H), 1.20 (d, *J*= 8.0 Hz, 3H) ¹³C NMR (100 MHz, CDCl₃) δ 158.6, 139.6, 130.1, 129.7, 129.2, 128.5, 126.2, 113.6, 86.1, 66.0, 58.7, 57.4, 55.3, 36.1, 34.8, 15.5; IR (film): 2956, 2927, 2837, 1612, 1512, 1452, 1244, 1037, 700 cm⁻¹; HRMS (EI): Exact mass calcd for C₂₀H₂₇N₂O₂ [M]⁺: 327.2067 found 327.2049.

Imidazolidine (2.2g)

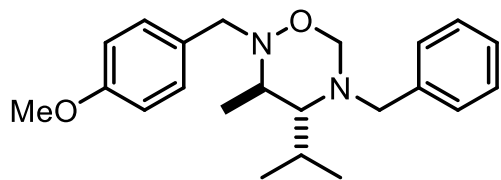


To a microwave vial is added a magnetic stir bar, (±)-(3*R**,4*R**)-3-benzyl-2-(4-methoxybenzyl)-4,5-dimethyl-1,2,5-oxadiazinane (0.050 g, 0.15 mmol), zinc dust (0.050 g, 0.77 mmol) and a 1:1 mixture of EtOH and glacial acetic acid (0.30 mL). The reaction was stirred at 60 °C in an oil bath for 24 hours. The title compound was purified by preparative TLC (50% EtOAc in Hexanes with 1% NH₄OH) to yield a clear oil (0.026 g, 57%). ¹H NMR (400 MHz, CDCl₃) δ 7.30-7.17 (m, 7H), 6.83 (d, *J*=8.0 Hz, 2H), 4.45 (d, *J* = 12.0 Hz, 1H),

3.80 (s, 3H), 3.79 (d, $J= 12.0$ Hz, 1H), 3.61 (d, $J= 8.0$ Hz, 1H), 3.57 (s, 2H), 3.18 (d, $J= 4.0$, 1H), 2.79-2.72 (m, 3H), 2.20 (s, 3H), 2.09 (dq, $J= 4.0$ and 4.0 Hz, 1H), 1.02 (d, $J= 8.0$ Hz, 3H), ^{13}C NMR (100 MHz, CDCl_3) δ 158.5, 139.5, 132.4, 129.8, 129.6, 128.2, 126.1, 113.6, 73.8, 66.8, 60.2, 55.3, 40.3, 38.2, 17.1; IR (film): 2960, 2840, 2770, 1612, 1510, 1452, 1240, 1036, 737, 700 cm^{-1} ; HRMS (EI): Exact mass calcd for $\text{C}_{19}\text{H}_{24}\text{N}_2\text{O}$ $[\text{M}]^+$: 311.2045 found 311.2123.

Alternatively: To a microwave vial is added a magnetic stir bar, (\pm)-(3*R**,4*R**)-3-benzyl-2-(4-methoxybenzyl)-4,5-dimethyl-1,2,5-oxadiazinane (0.100 g, 0.32 mmol) and $\text{Mo}(\text{CO})_6$ (0.084 g, 0.32 mmol) in acetonitrile (2.8 mL) and water (0.30 mL). The reaction was stirred at $40\text{ }^\circ\text{C}$ in an oil bath for 72 hours. The title compound was purified by preparative TLC (50% EtOAc in Hexanes with 1% NH_4OH) to yield a clear oil (0.047 g, 47%). Spectral data was in excellent agreement with the data shown immediately above, for the reaction using Zn/AcOH .

(\pm)-(2*S**,3*S**)-5-Benzyl-4-isopropyl-2-(4-methoxybenzyl)-3-methyl-1,2,5-oxadiazinane (2.2h)



To a microwave vial is added a magnetic stir bar, (\pm)-(2*S**,3*S**)-*N*-benzyl-2-(hydroxy(4-methoxybenzyl)amino)-4-methylpentan-3-amine (0.10 g,

0.29 mmol), paraformaldehyde (0.092 g, 0.31 mmol) and *t*-BuOH (7.0 mL). The reaction was stirred at $70\text{ }^\circ\text{C}$ in an oil bath for 18 hours. The title compound was not further purified, yielding a clear light yellow oil (0.109 g, 99%). ^1H NMR (400 MHz, CDCl_3) δ 7.32-7.25 (m, 6 H), 7.23-7.17 (m, 1 H), 6.90-6.76 (m, 2 H), 4.75 (d, $J= 11.0$ Hz, 1H), 4.35 (d, $J= 13.9$ Hz, 1 H), 4.16-4.16 (m, 1 H), 4.16 (d, $J= 11.0$ Hz, 1 H), 3.96 (d, $J= 13.5$ Hz, 1 H), 3.89-3.89 (m, 1 H), 3.89 (d, $J= 13.5$ Hz, 1 H), 3.77 (s, 3H), 3.59 (d, $J= 13.5$ Hz, 1 H), 3.02 (q, $J= 6.9$ Hz, 1H), 2.51-2.34 (m, 1 H), 2.12 (d, $J= 9.8$ Hz, 1 H), 1.41 (d, $J= 6.9$ Hz, 3 H), 1.00 (d, $J= 6.7$ Hz, 3 H), 0.80 (d, $J= 6.7$ Hz,

3 H) ^{13}C NMR (100 MHz, CDCl_3) δ 158.6, 140.6, 129.9, 129.5, 128.8, 128.1, 126.9, 113.6, 81.3, 70.5, 60.5, 58.1, 55.3, 54.7, 27.9, 21.2, 13.2; IR (film): 2907, 2867, 2851, 1612, 1512, 1244, 1035, 956, 731, 698 cm^{-1} ; HRMS (EI): Exact mass calcd for $\text{C}_{22}\text{H}_{30}\text{N}_2\text{O}_2$ $[\text{M}]^+$: 354.2307 found 354.2289.

Hydrolysis to form hydroamination product

To a microwave vial is added a magnetic stir bar, 5-benzyl-4-isopropyl-2-(4-methoxybenzyl)-3-methyl-1,2,5-oxadiazinane (0.050 g, 0.14 mmol), hydroxylamine hydrochloride (0.0980 g, 1.41 mmol) and methanol (0.56 mL). While stirring, distilled water (12.7 μL) and 1M HCl (14.1 μL) were added. The vial was then sealed and stirred in an oil bath at 40 $^\circ\text{C}$ for 24 hours. The mixture was then neutralized using a saturated solution of Na_2CO_3 (0.56 μL) and then extracted three times with dichloromethane (3 x 4 mL). The obtained organic layers were combined, dried over MgSO_4 and the solvent was removed under reduced pressure yielding a clear oil (0.0406 g, 84%). Based on the ^1H NMR obtained, in excellent agreement with the data shown for previously reported hydroamination product, the title compound was not purified further.

Scheme 2.6 Deuterium kinetic isotope effect experiment for formaldehyde

Protocol for the determination of DKIE values

In a flame-dried 10 mL round-bottomed flask was added 1,4-Dimethoxybenzene (the internal standard, 0.0173 g, 0.125 mmol, 0.25 equiv.), *N*-benzylhydroxylamine (0.0370 g, 0.300 mmol, 0.6 equiv.) and *N*-benzylhydroxylamine homodimer (0.0258 g, 0.100 mmol, 0.2 equiv.). The round-bottomed flask was sealed with a rubber septum and flushed with argon after which MeOD (0.5 mL) was added followed by allylbenzylamine (0.117 mL, 0.750 mmol,

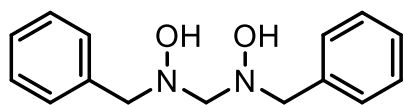
1.50 equiv.). The mixture was allowed to stir for 20 min at room temperature under argon. Then, the tube was placed under high vacuum to evaporate MeOD. It is important to be careful at this point because the solution bumps readily. Once most of the MeOD was removed, the tube was refilled with argon and another portion of 0.5 mL MeOD was added. It was stirred for 20 min and then removed under high vacuum. This cycle was repeated until the mixture was allowed to stir 3 x 20 min in MeOD. After removal of the last portion of MeOD, CDCl₃ (0.5 mL) was added. The mixture was then quickly transferred in a NMR tube and flushed with argon. The NMR tube was then taken to the spectrometer and heated to 298 K. Using a custom program made by our NMR professional, Dr. Glenn Facey, an 8 scan spectrum was acquired every 12 minutes for a period of 10 hours. The concentration of product formed was determined by integrating the product's peak ($\delta = 1.1$ ppm (d, 2H)) relative to the internal standard peak ($\delta = 6.08$ ppm). The exact same protocol was employed for the determination of the rate of the reaction with non-deuterated starting material except for the fact that MeOH was employed instead of MeOD. Also, the spectra were acquired over a period of 96 min instead of 10 hours.

Run	V ₀ H (M/s)	V ₀ D (M/s)	KIE
1	1.372 x 10 ⁻⁵	2.848 x 10 ⁻⁶	-
2	1.634 x 10 ⁻⁵	3.083 x 10 ⁻⁶	-
3	1.873 x 10 ⁻⁵	3.109 x 10 ⁻⁶	-
Average	1.626 x 10 ⁻⁵	3.014 x 10 ⁻⁶	5.4
Std. Dev.	0.251 x 10 ⁻⁵	0.144 x 10 ⁻⁶	0.9 (from error propagation analysis)

KIE= 5.4 ± 0.9

Table 2.3 Hydroamination of Allylic Amines Using a Formaldehyde Precursor Dimer

N-Benzylhydroxylamine



A dry 50 mL round-bottomed flask was loaded with 4.00 g (32.5 mmol, 2 equiv.) of N-benzylhydroxylamine and a magnetic stir bar. The hydroxylamine was then dissolved in 20.0 mL of *t*-BuOH and the mixture was heated to 70 °C. After 15 minutes of stirring and the solution became clear, 0.488 g (16.2 mmol, 1.0 equiv.) of paraformaldehyde was added. The mixture was allowed to stir for 18 hours. The mixture was then allowed to cool down to room temperature and excess solvent was removed under reduced pressure. The crude product was then recrystallized from EtOH in hexanes or 10% EtOAc in hexanes. The recovered light yellow/beige crystals were washed with cold hexanes and dried under high vacuum. Isolated yield: 91 % (3.81 g) of pure dimer was recovered. ¹H NMR (300 MHz, CDCl₃) δ 3.49 (s, 2H), 3.73 (s, 4H), 7.21-7.26 (m, 4H), 7.27-7.33 (m, 6H). ¹³C NMR (100 MHz, CDCl₃) δ 135.2, 130.1, 128.4, 127.5, 61.5.

General Procedure for Hydroaminations using Formaldehyde Precursor Dimer

A microwave vial (2-5 mL) was loaded with a magnetic stir bar, N-benzylhydroxylamine (0.3-0.4 mmol, 0.6-0.8 equiv.), N-benzyl-N-allylamine (0.0926 mL, 0.750 mmol, 1.5 equiv.), N-hydroxylamine homodimer (0.1-0.2 equiv.) and *t*-BuOH (0.5 mL, 1M with respect to hydroxylamine). Distilled H₂O was added in certain reactions, with total volume adjustments being made when necessary. The reaction was then stirred at 30 °C for 24 hours. The mixture was concentrated under reduced pressure. An NMR yield was then obtained by using an internal standard, 1,4-Dimethoxybenzene (0.125 equiv.) and comparing internal standard peaks to the newly formed product peak (1.14 ppm, 3H, doublet).

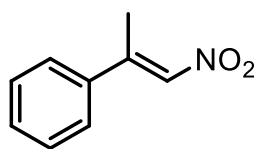
Figure 3.6 Mixed amination formation with pyrrolidine as a model for tripeptide catalyst

General procedure for pyrrolidine dimer investigations

A dry NMR tube was loaded with pyrrolidine (0.0133 mL, 0.16 mmol, 1.0 equiv.), the chosen nucleophile (0.16 mmol, 1.0 equiv.), formalin (0.0121 mL, 0.16 mmol, 1.0 equiv.) and DMSO-*d*₆ (0.500 mL). The reaction was stirred for 18 h at 30 °C. The reaction was then monitored by thin layer chromatography (30:70, EtOAc:Hex) and ¹H and ³¹P NMR when applicable.

Figure 3.7 and Figure 3.8 Preliminary study of background reactivity with nitroolefins

(E)-(1-Nitroprop-1-en-2-yl)benzene



Nitration was done following a procedure from *Maiti et al.*⁵² To an oven-dried 2-5 mL microwave vial, was added silver AgNO₂ (3.55 g, 23.1 mmol), TEMPO (0.48 g, 3.1 mmol) and 4.0 Å molecular sieves (2.31 g). Dichloroethane (28 μL) and prop-1-en-2-ylbenzene (1.0 mL, 7.7 mmol) was then added. The mixture was heated to 80°C and vigorously stirred for 18 hours. The mixture was allowed to cool to room temperature and then filtered through a bed of celite, which was washed with ethyl acetate. The filtrate was dried and concentrated under reduced pressure. The pure nitrated product was isolated by column chromatography through a silica gel column (mesh 60–120). Eluent: ethyl acetate/ petroleum ether (2:98 v/v); yellow solid; isolated yield: 84 % (0.069 g). ¹H NMR (400 MHz, CDCl₃) δ 2.29 – 3.07 (d, *J* = 1.5 Hz, 3H), 7.29 – 7.33 (q, *J* = 1.4, 1.4, 1.4 Hz, 1H), 7.41 – 7.49 (m, 5H). Obtained spectral data was consistent with data reported in literature.⁵²

⁵² Maity, S.; Manna, S.; Rana, S.; Naveen, T.; Mallick, A.; Maiti, D. *J. Am. Chem. Soc.* **2013**, *135*, 3355–3358.

General procedure for background reactivity with nitroalkenes

A dry NMR tube was loaded with nitroalkene (0.34 mmol, 1.0 equiv.), the chosen nucleophile (0.34 mmol, 1.0 equiv.), CDCl₃ (0.45 mL) and *i*-PrOH (0.05 mL)(0.7M with respect to nitroalkene). The reaction was stirred for 5-24h at 30°C. The reaction was then monitored by thin layer chromatography (30:70, EtOAc:Hex) and ¹H NMR to assess the consumption of starting materials and the appearance of new products.

Figure 3.9 Evaluation of background reactivity between aniline and *N*-benzylhydroxylamine and various potential electrophiles for tripeptide catalysis

General procedure for background reactivity with various electrophiles

A dry NMR tube was loaded with *N*-benzylhydroxylamine or aniline (0.34 mmol, 1.0 equiv.), the chosen electrophile (0.34 mmol, 1.0 equiv.), CDCl₃ (0.45 mL) and *i*-PrOH (0.05 mL)(0.7M with respect to nucleophiles). The reaction was stirred for 24h at 30°C. The reaction was then monitored by thin layer chromatography (30:70, EtOAc:Hex) and ¹H NMR to assess the consumption of starting materials and the appearance of new products.

Figure 3.10 Investigations into aldehyde and small peptide dual-catalysis

General procedure for small peptide trial reactions

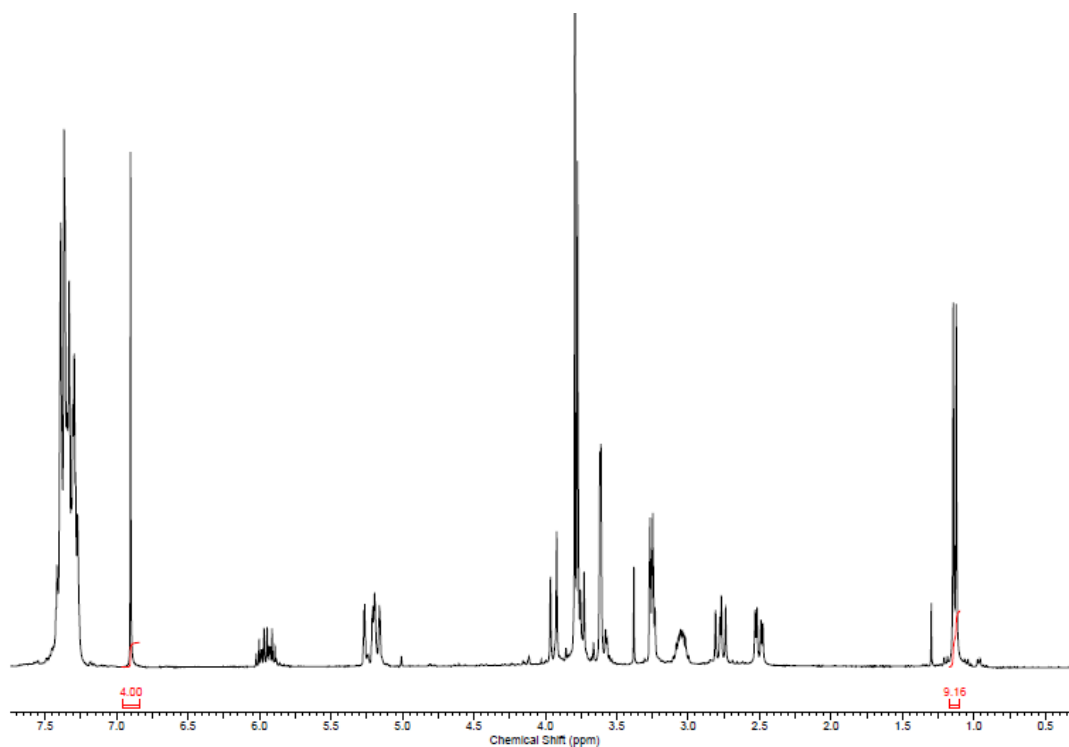
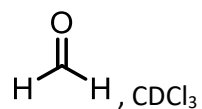
A dry NMR tube was loaded with nitroalkene (0.029 mmol, 1.0 equiv.), the chosen nucleophile (0.029 mmol, 1.0 equiv.), the small peptide catalyst (10 mg, 0.029 mmol, 1.0 equiv.), formalin (2.21 μL, 0.029 mmol, 1.0 equiv.), CDCl₃ (0.45 mL) and *i*-PrOH (0.05 mL). The reaction was stirred for 24 hours at 30 °C; although one trial reaction was run at lower temperature (-15 °C allowed to warm to 4 °C over 48h). The reaction was then monitored by thin layer chromatography (30:70, EtOAc:Hex) and ¹H NMR to assess the consumption of starting materials and the appearance of new products.

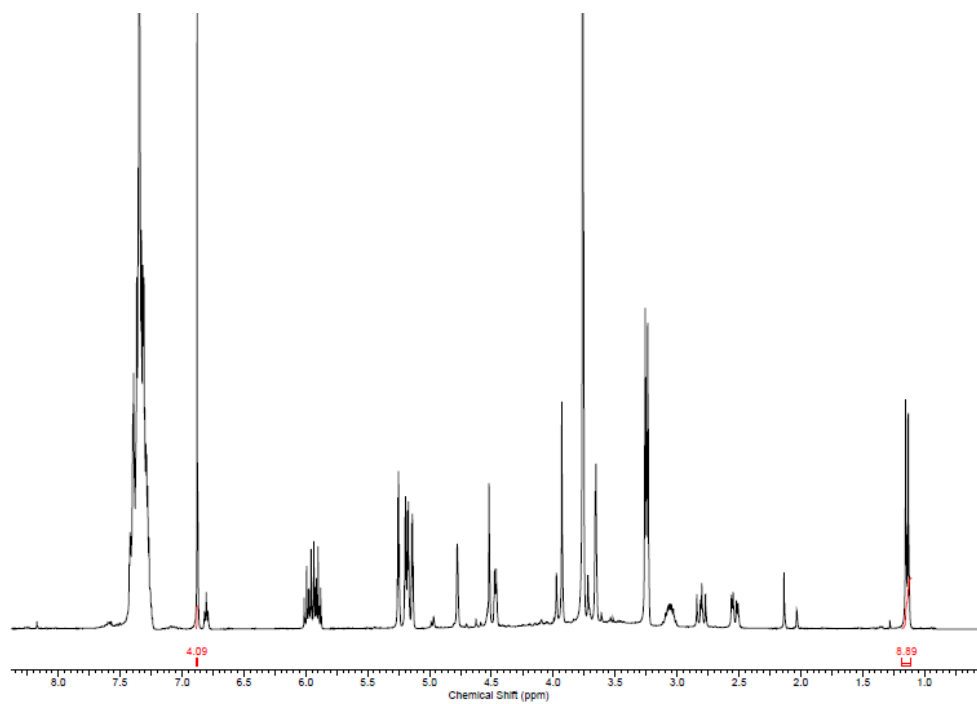
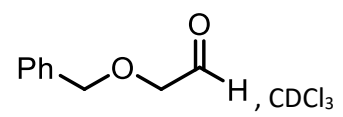
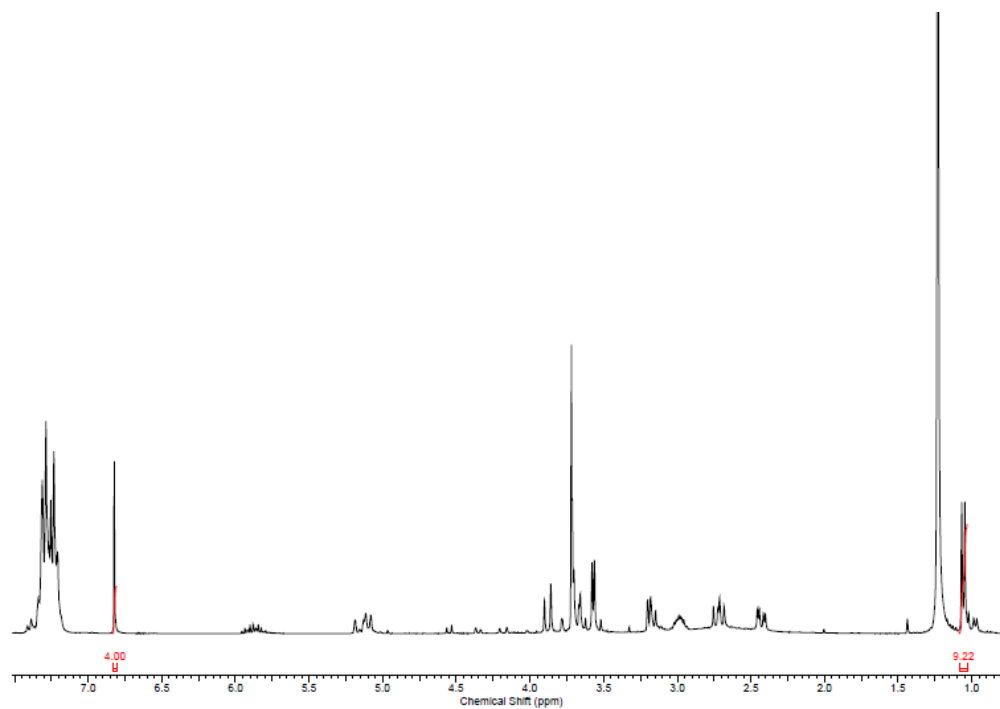
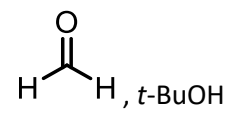
Annex III

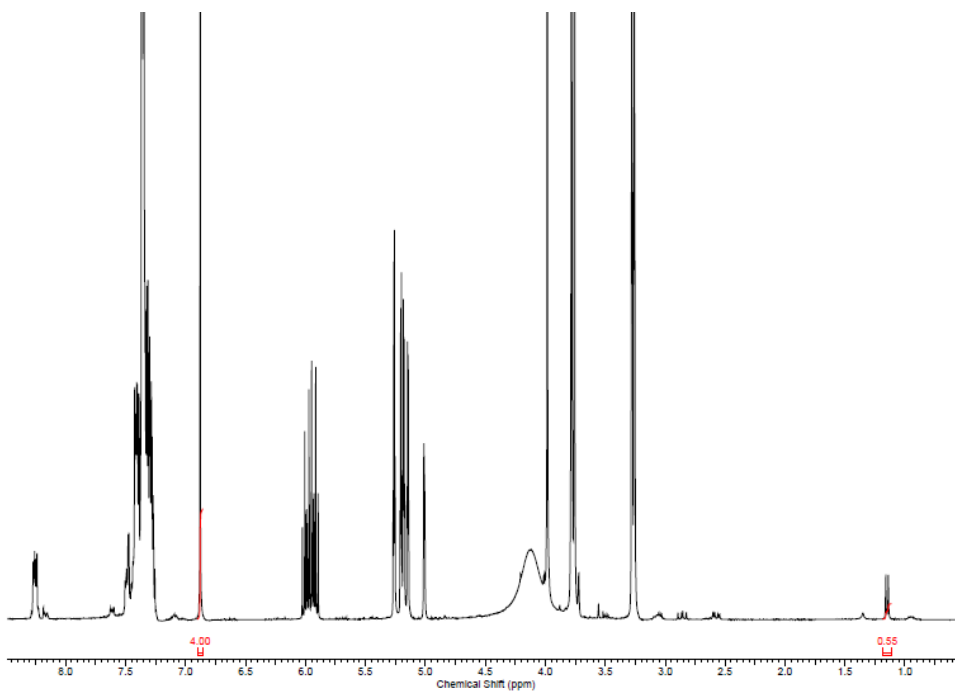
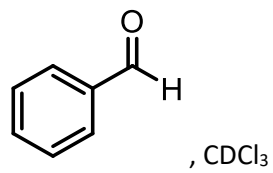
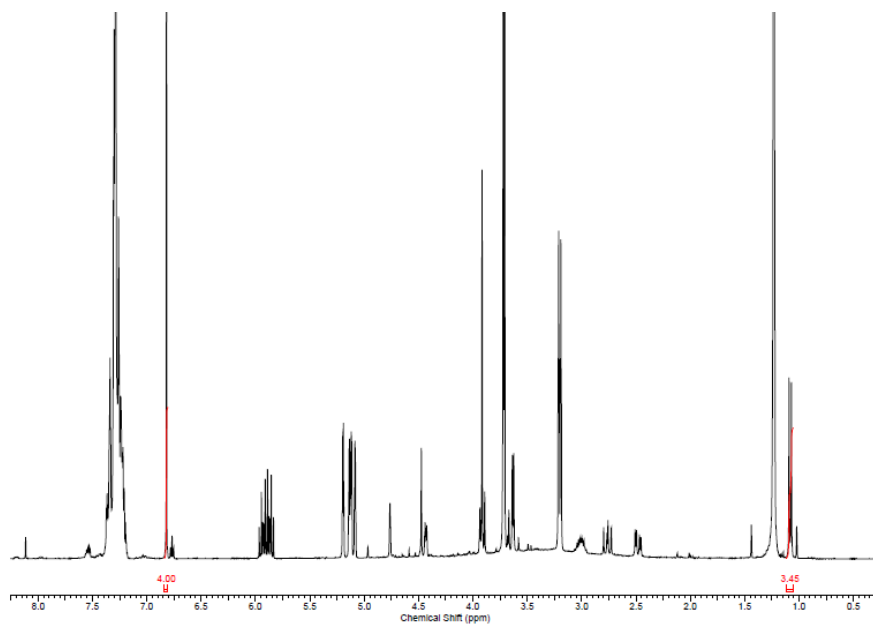
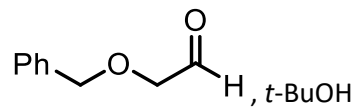
NMR Spectra and HPLC Data

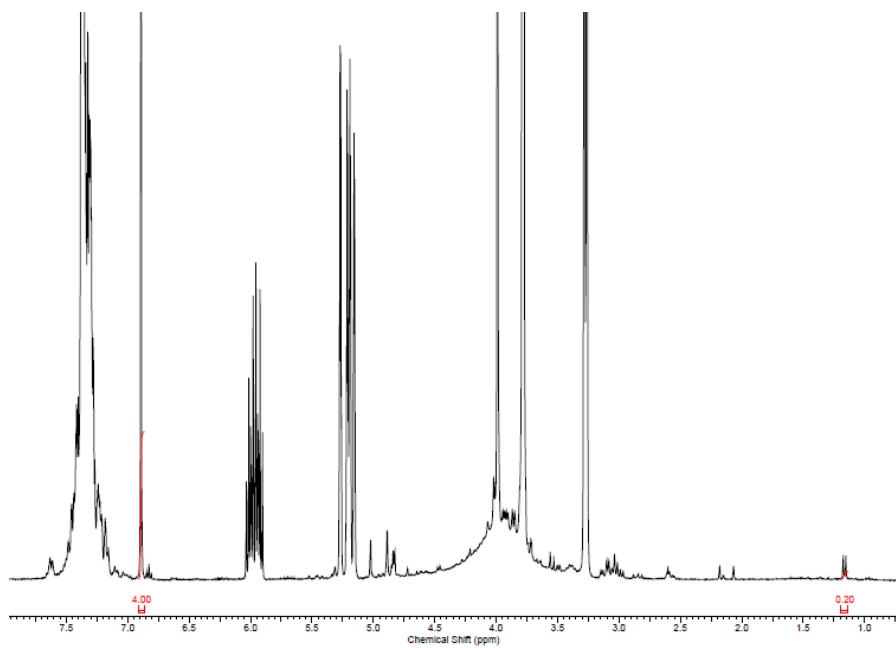
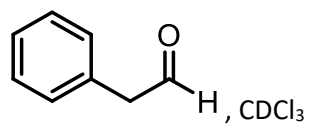
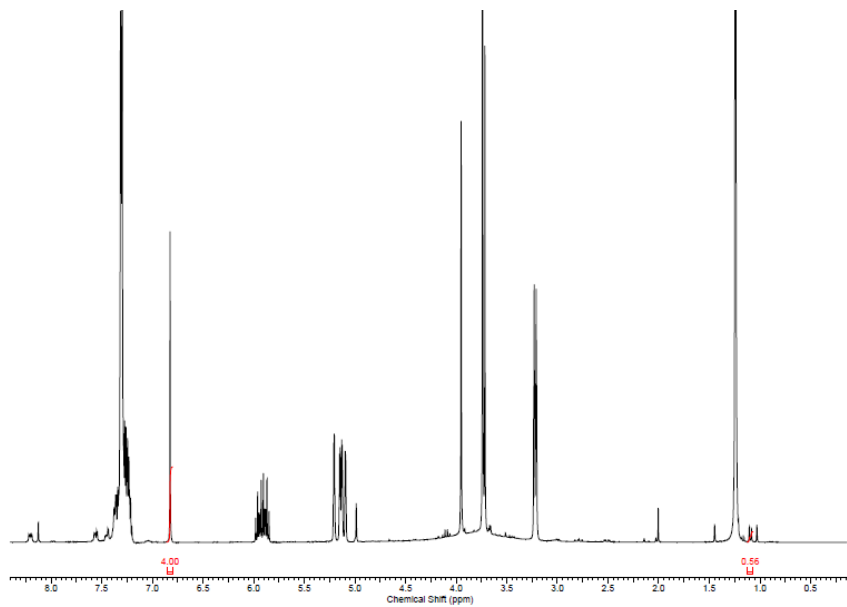
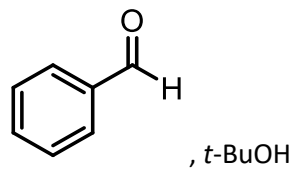
Table 2.1 Comprehensive aldehyde scan in CHCl_3 and $t\text{-BuOH}$

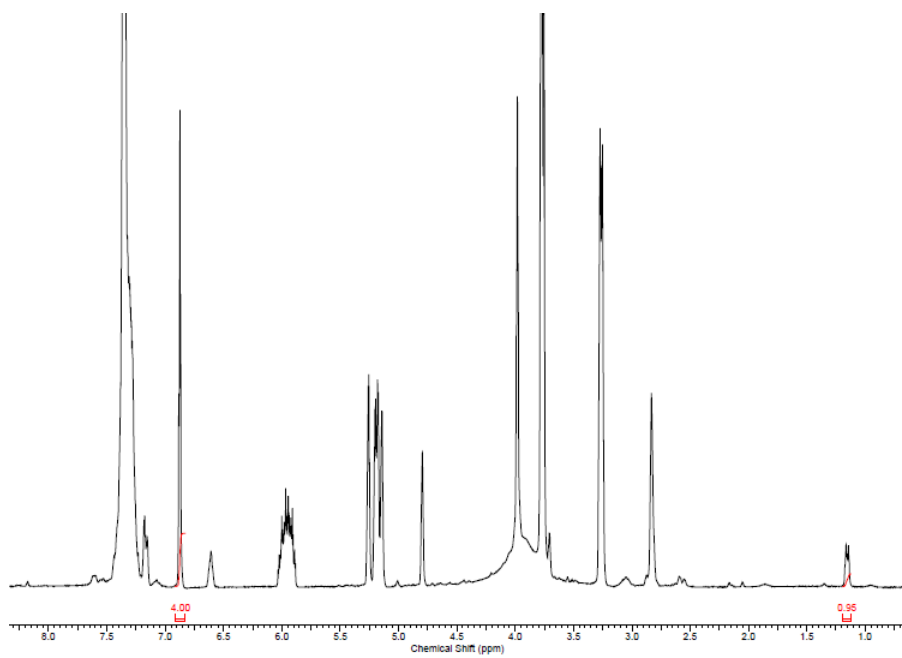
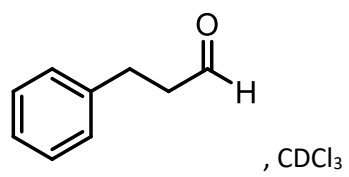
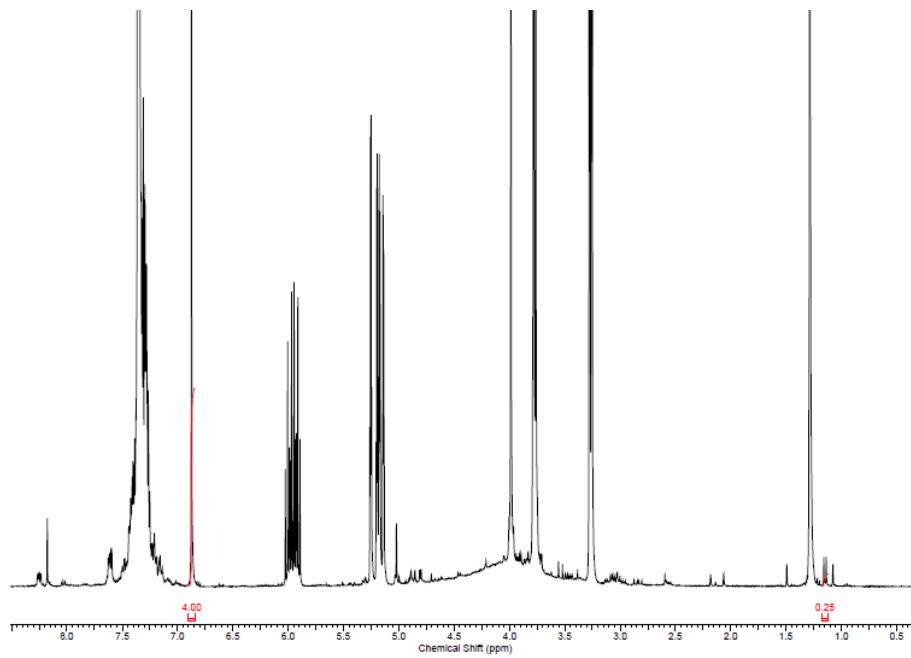
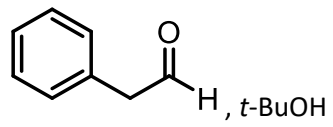
NMR yields were obtained by using an internal standard, 1,4-Dimethoxybenzene (0.125 equiv.) and comparing the internal standard peak (6.83 ppm, 4H, singlet) to the newly formed product peak (1.14 ppm, 3H, doublet). See Annex II for the full procedure.

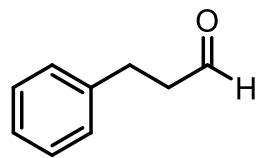




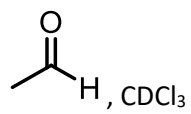
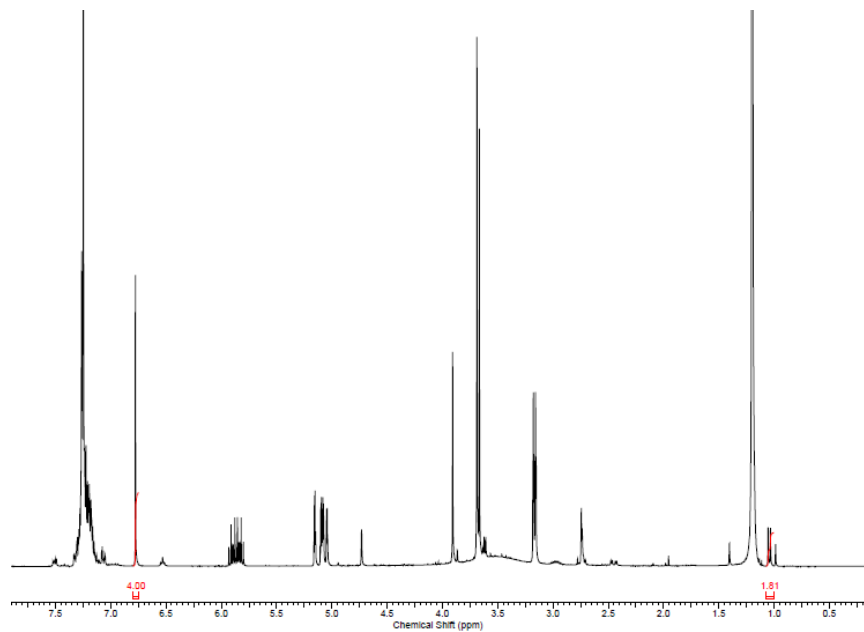




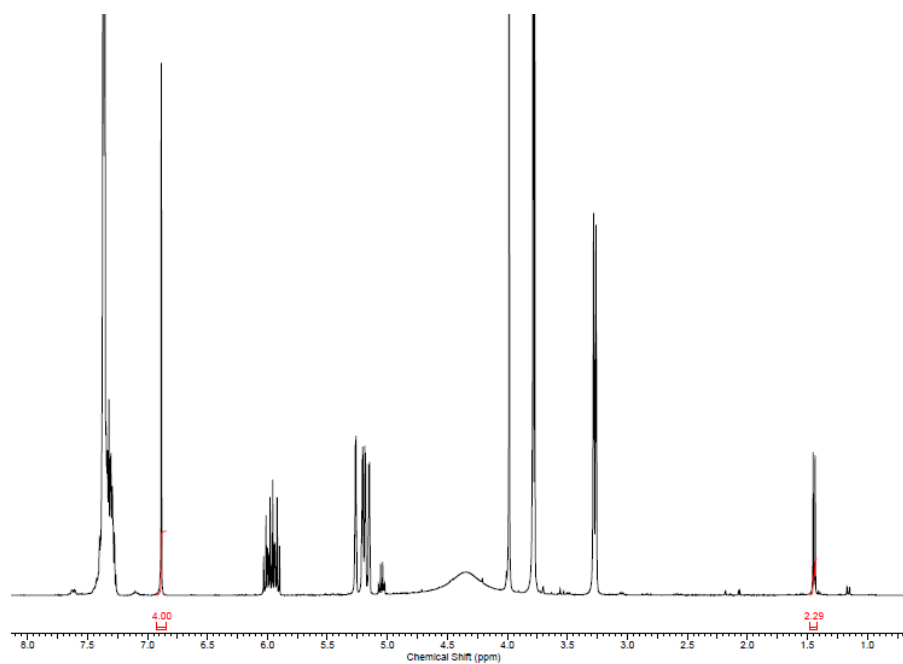


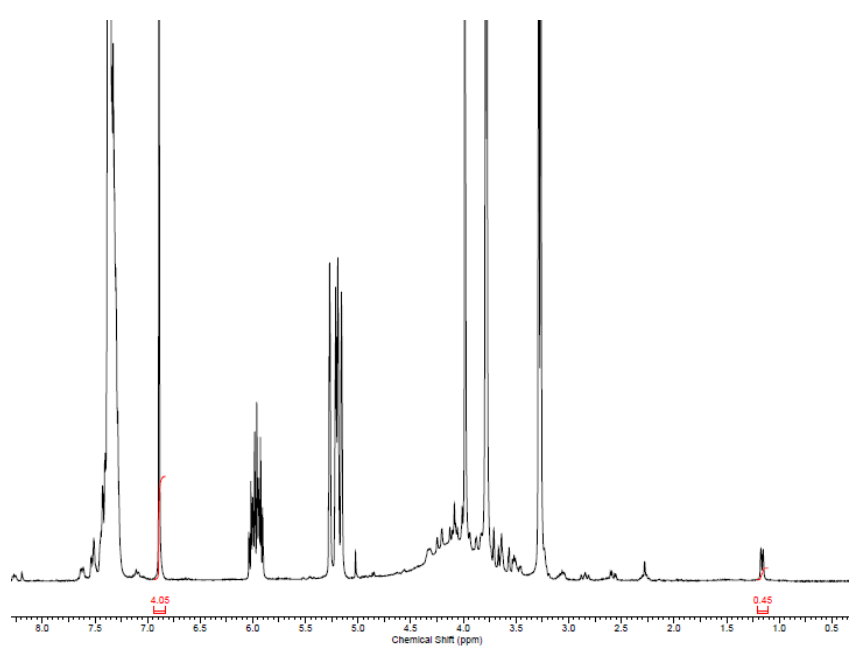
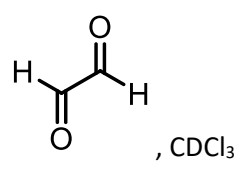
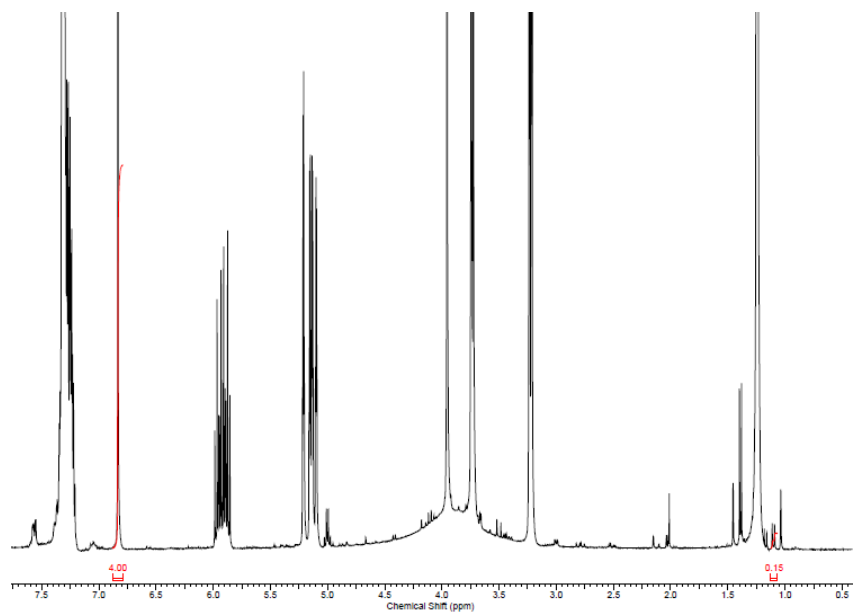
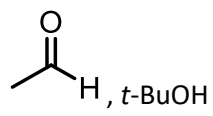


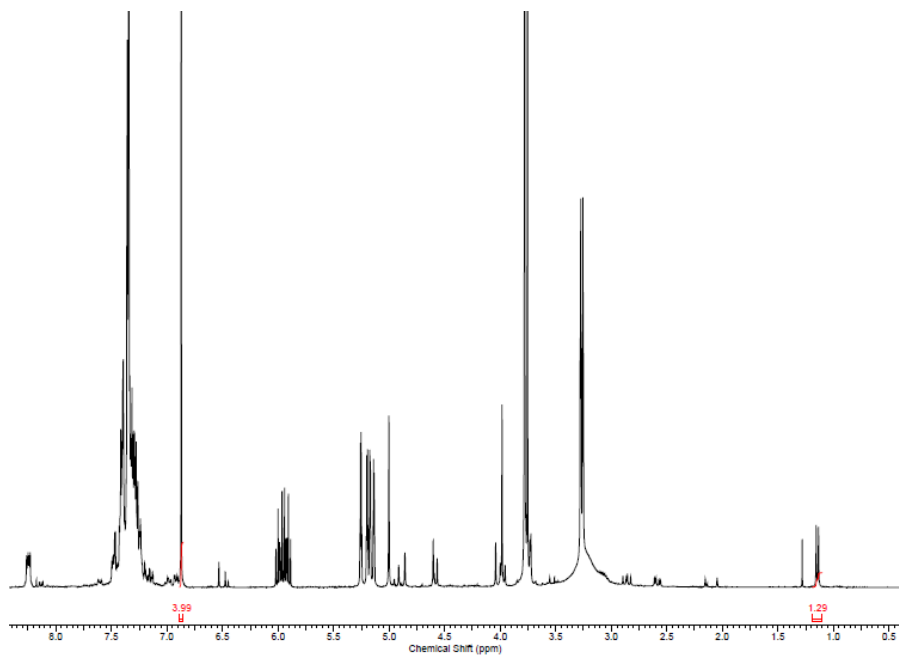
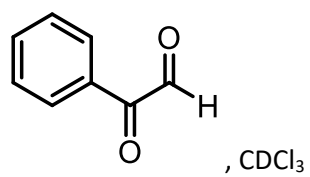
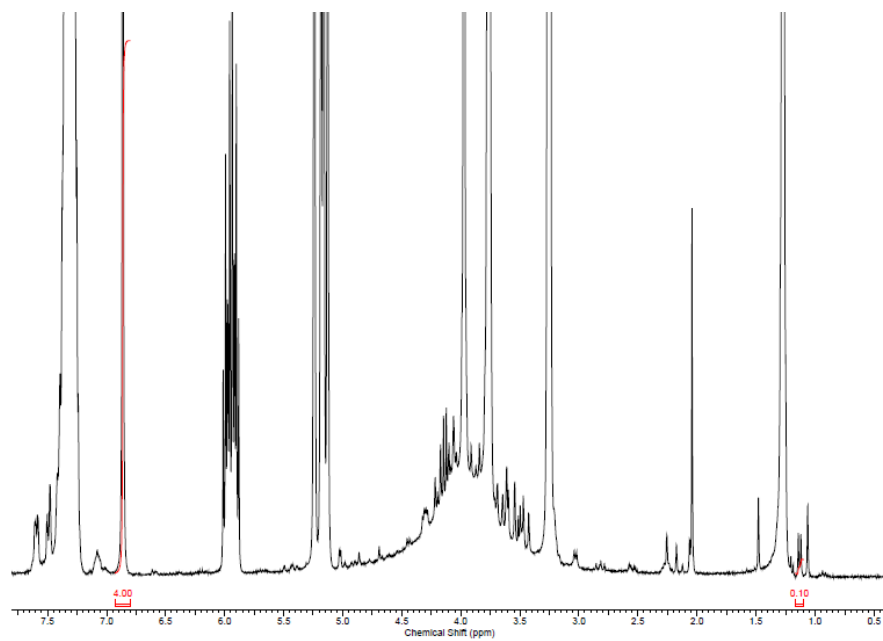
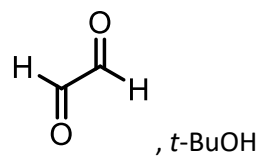
, *t*-BuOH

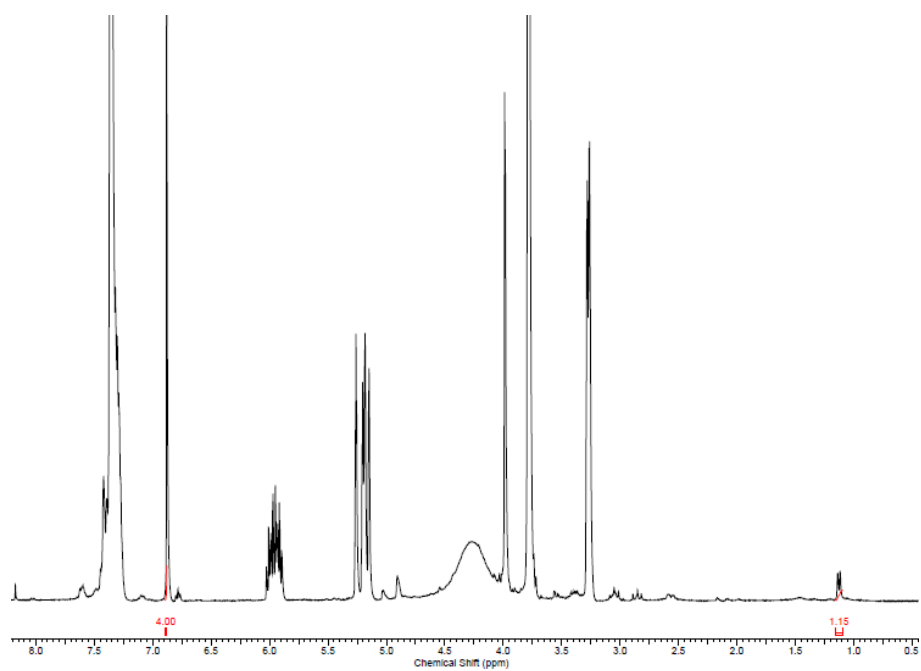
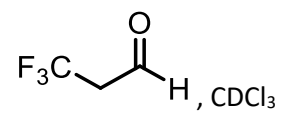
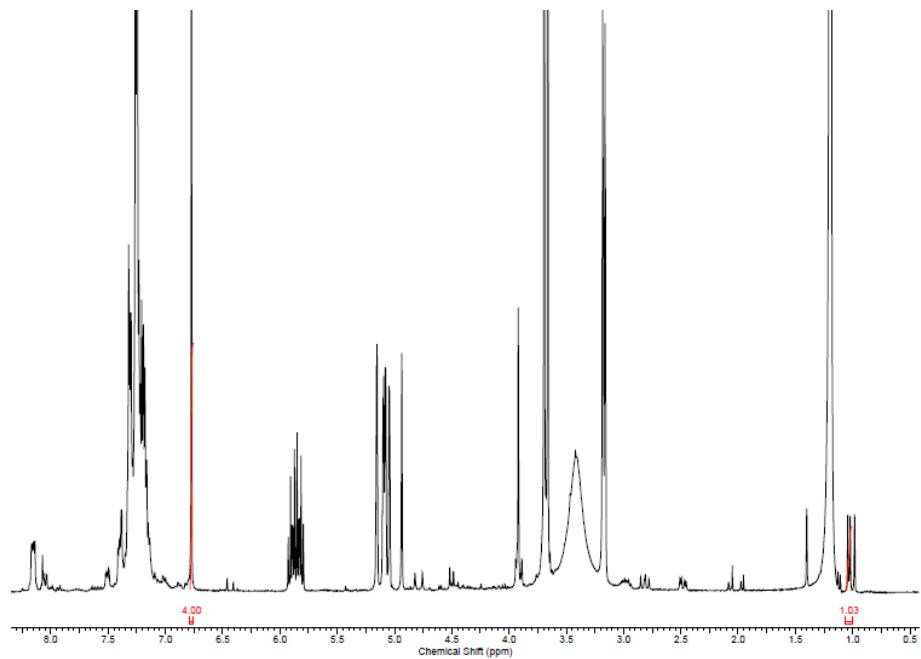
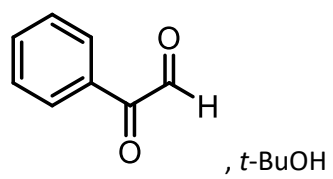


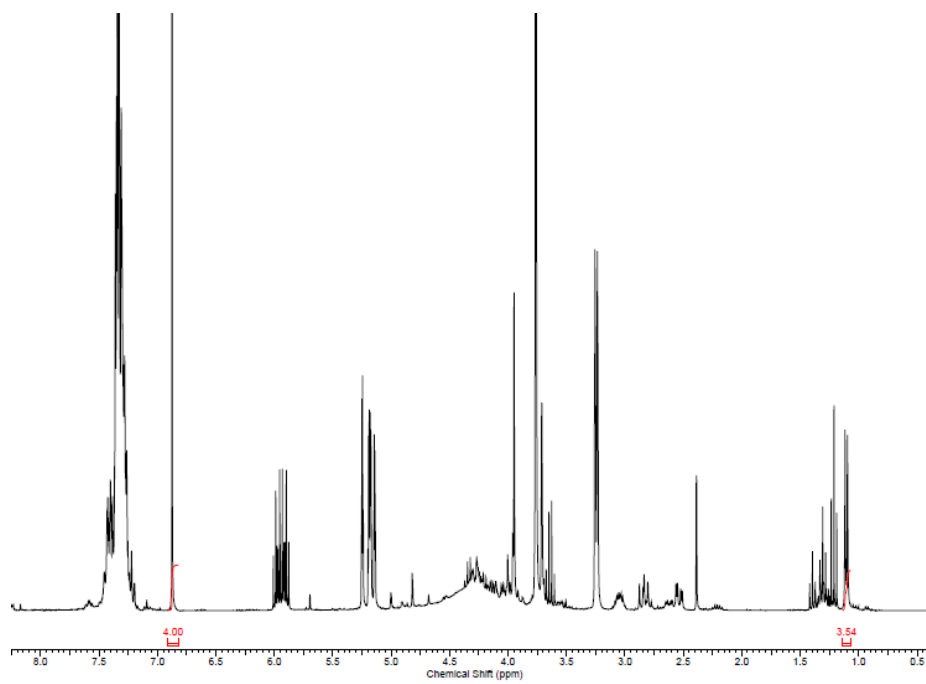
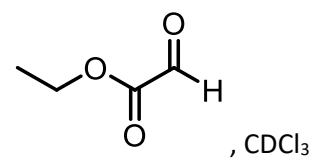
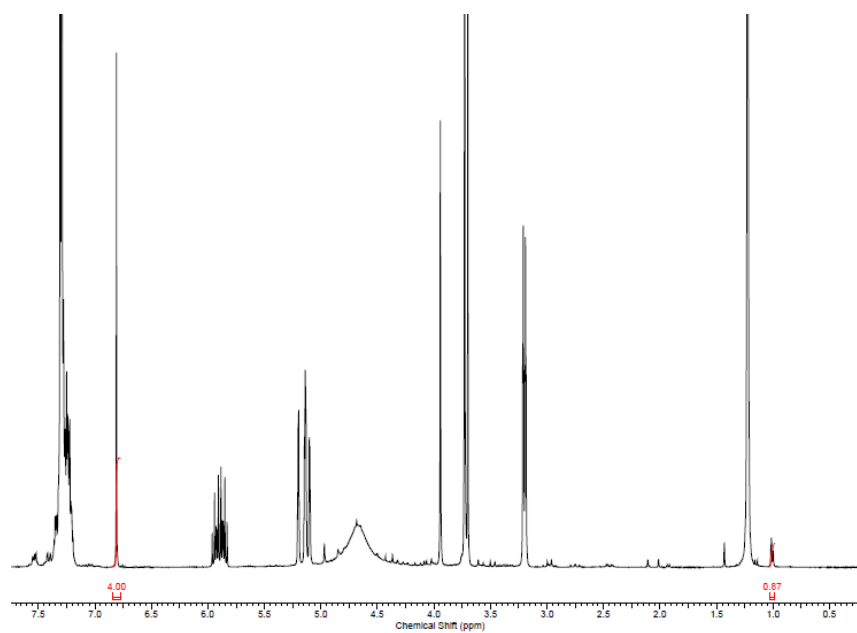
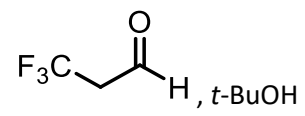
, CDCl₃

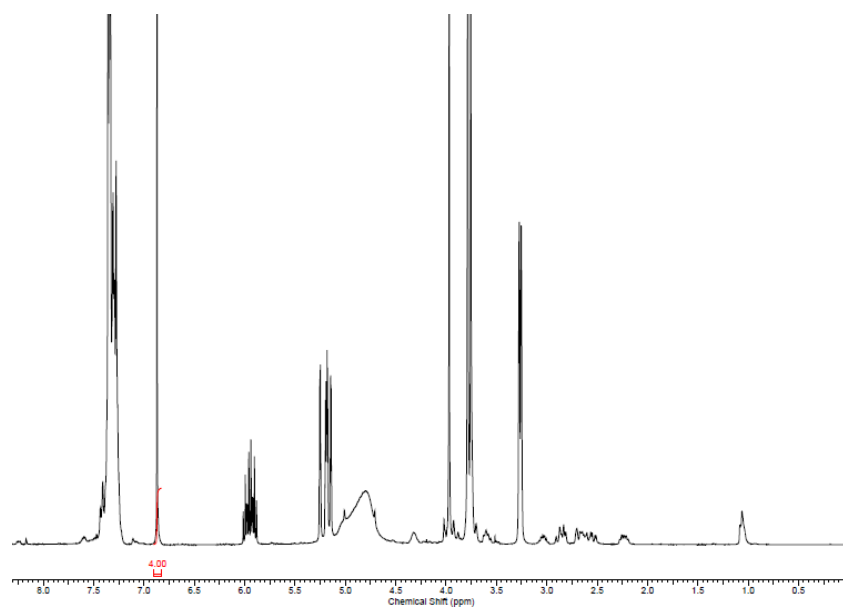
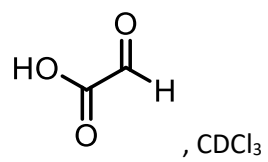
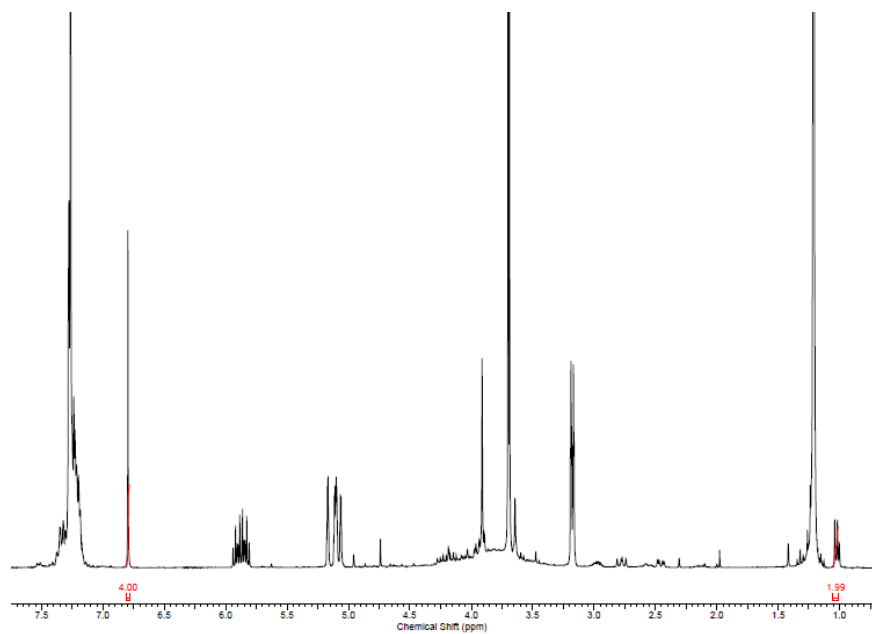
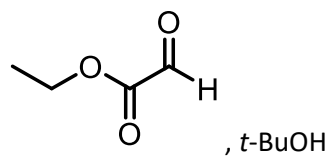


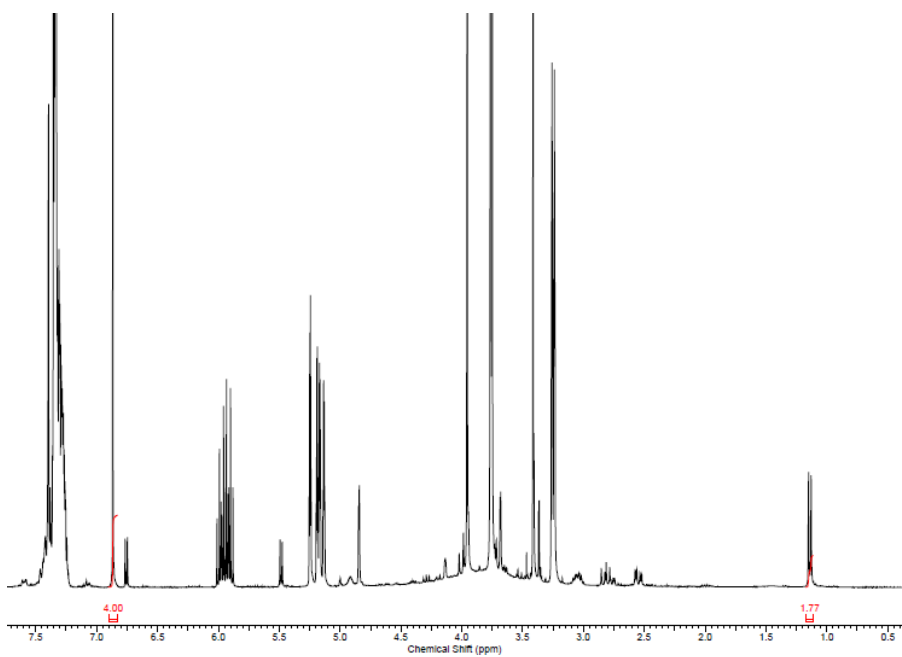
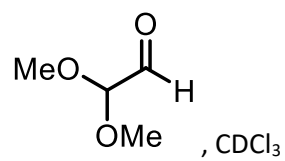
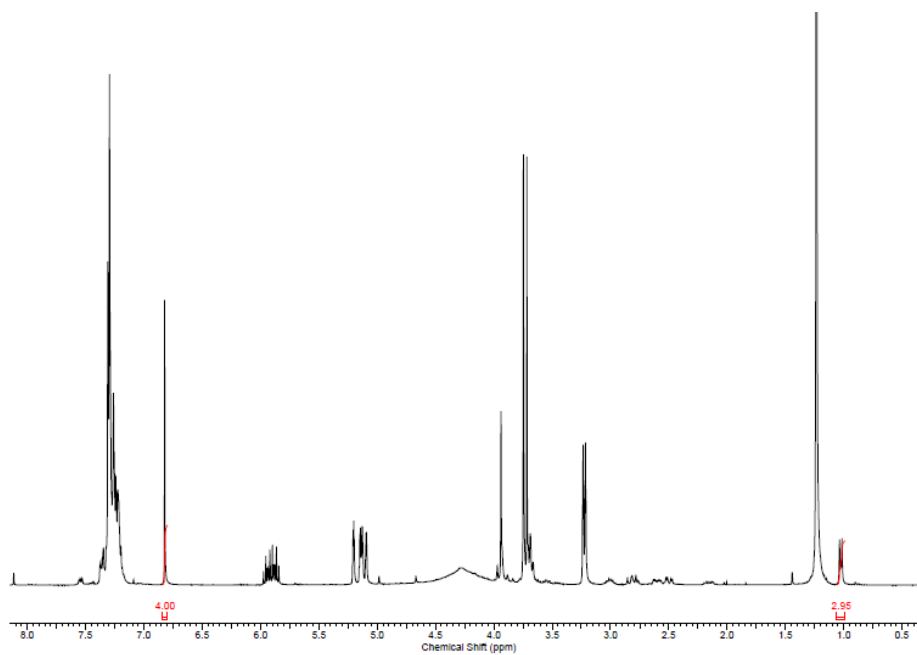
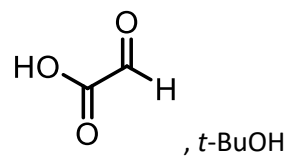


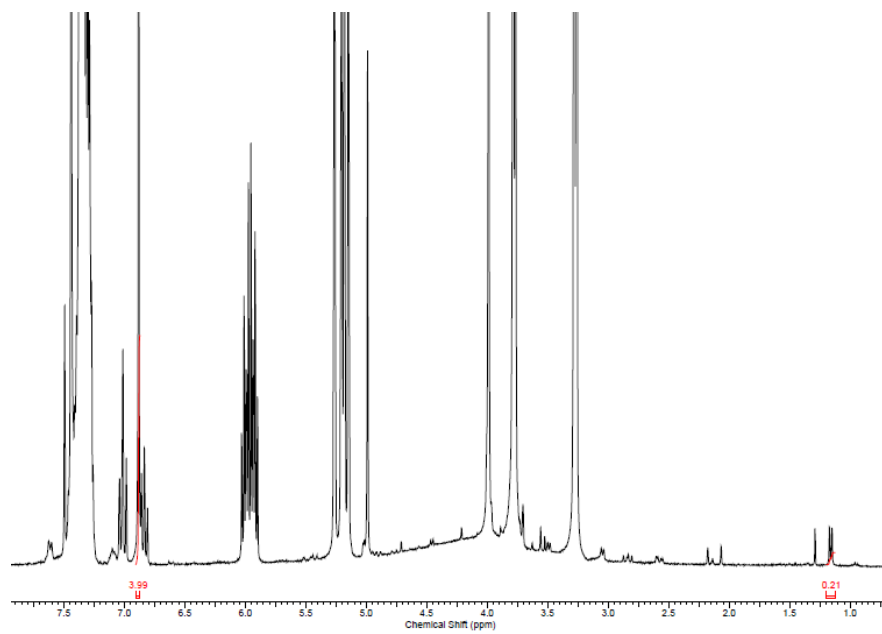
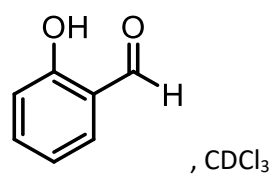
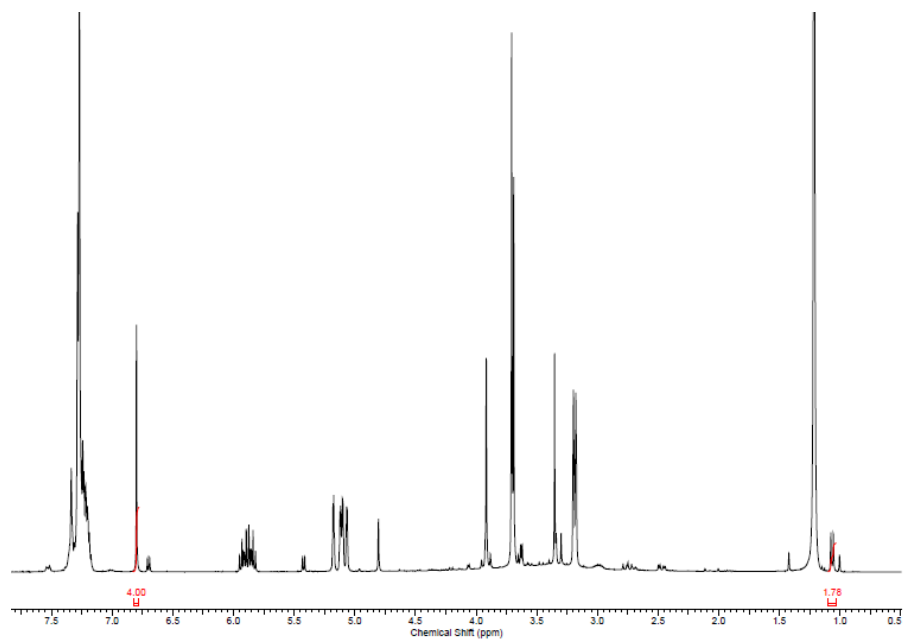
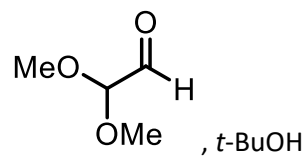


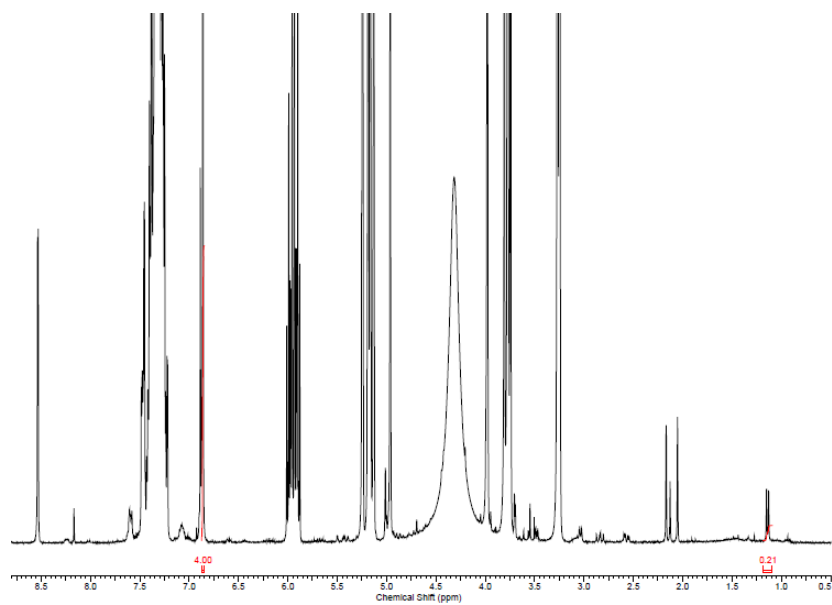
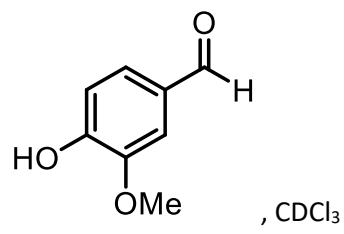
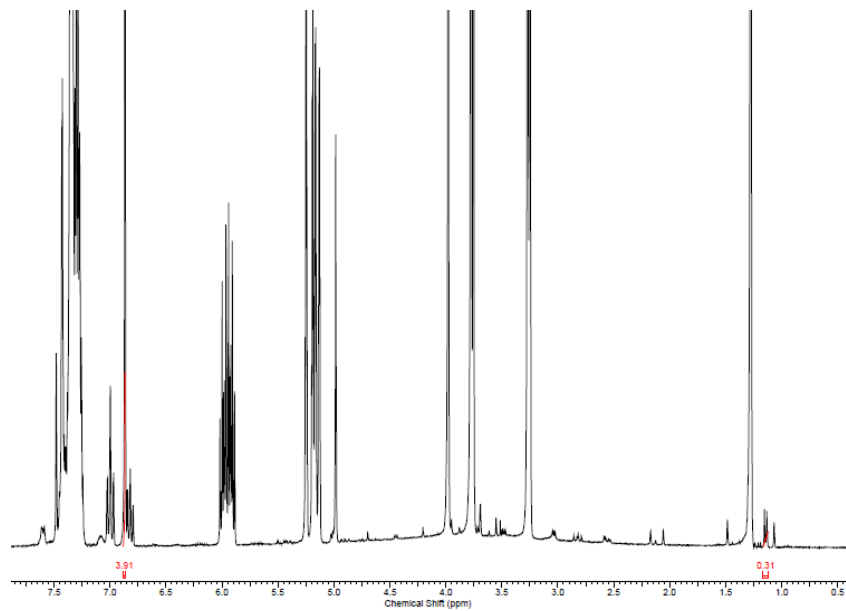
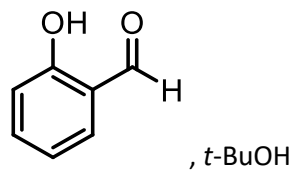


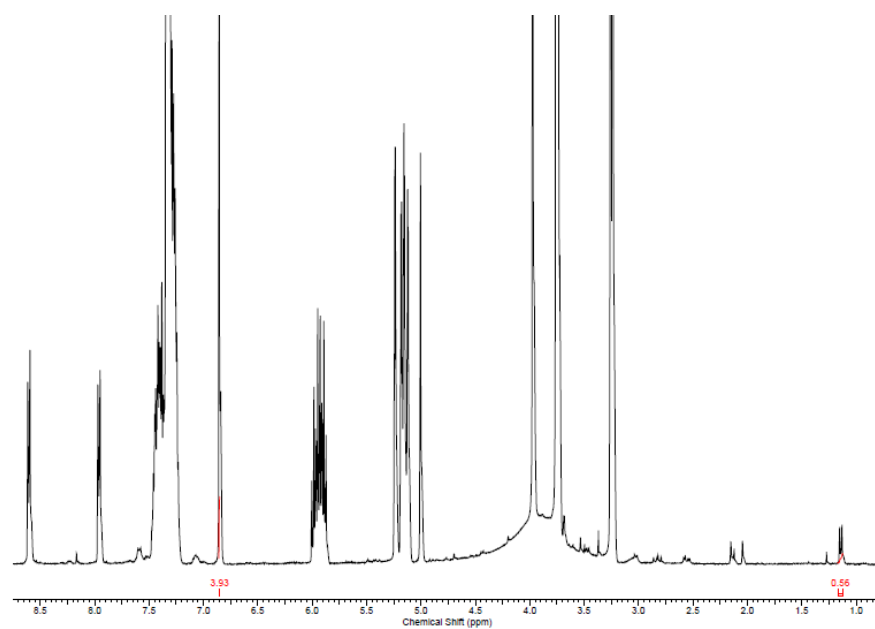
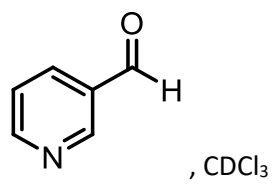
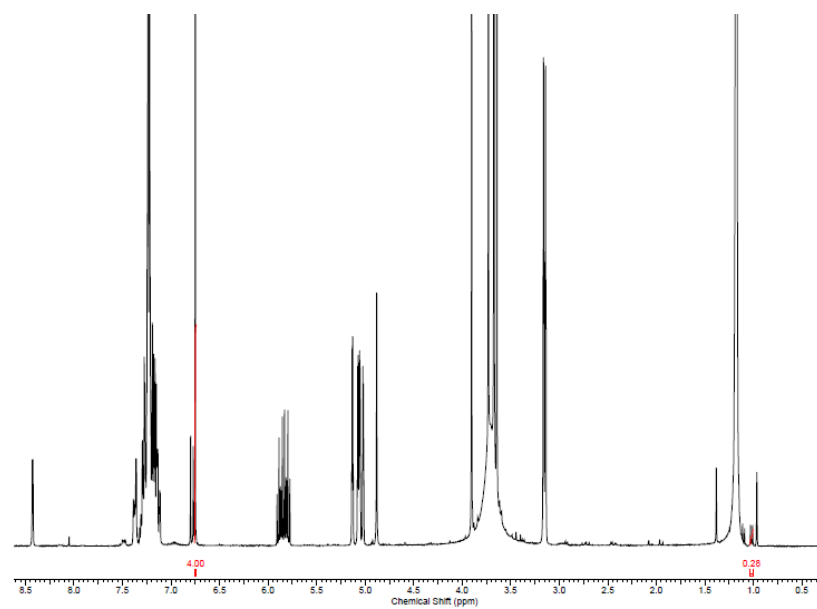
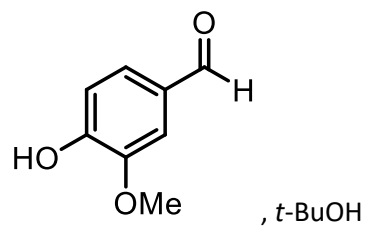


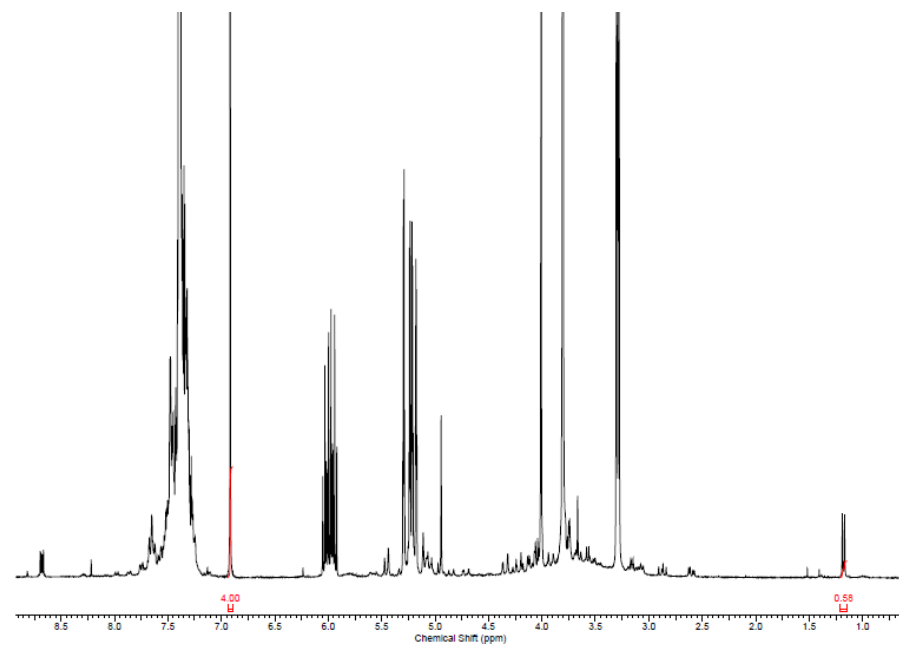
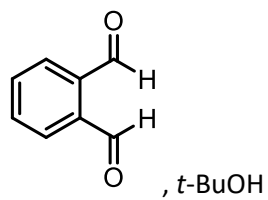
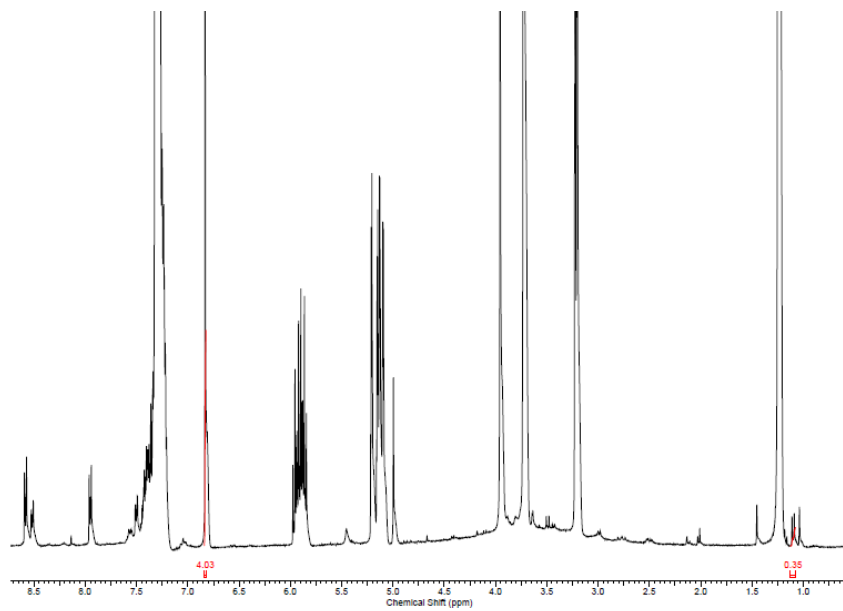
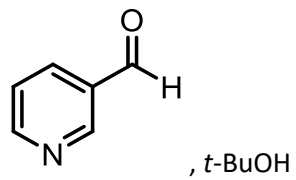


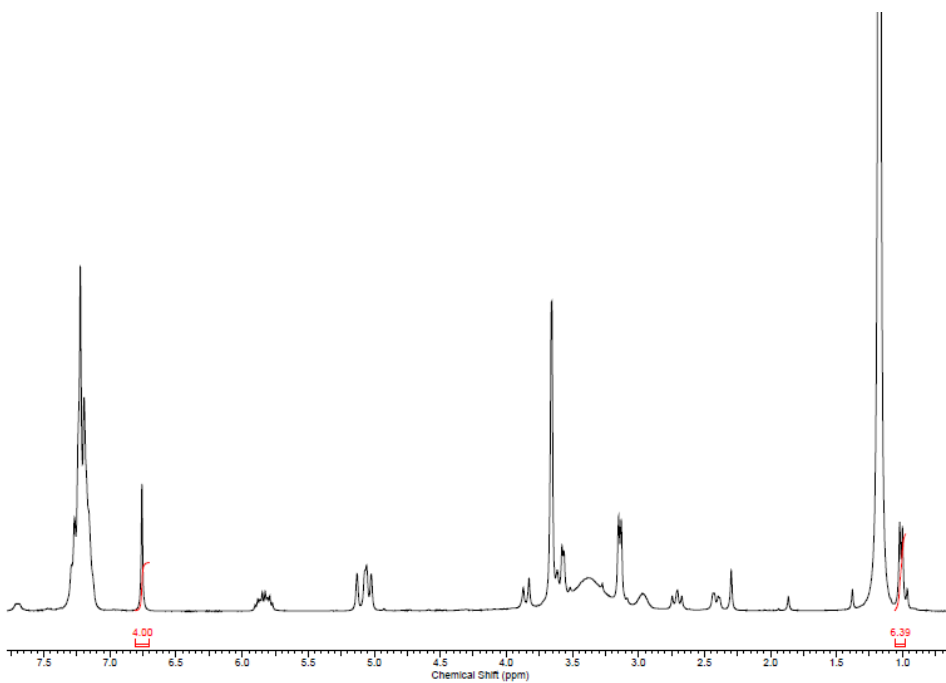
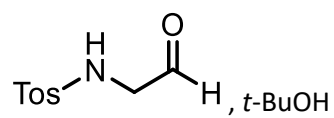
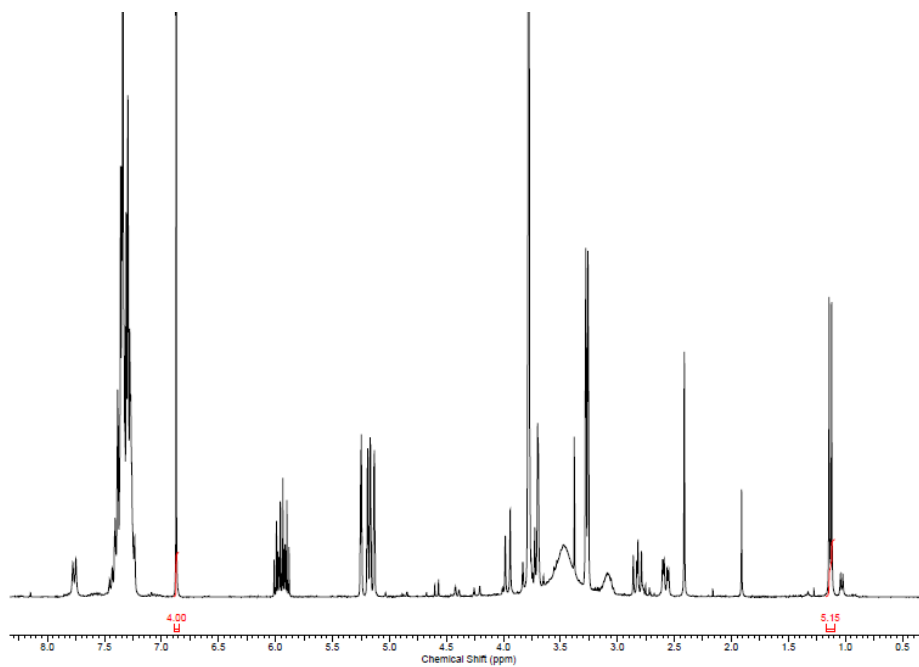
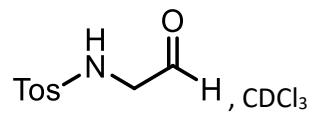




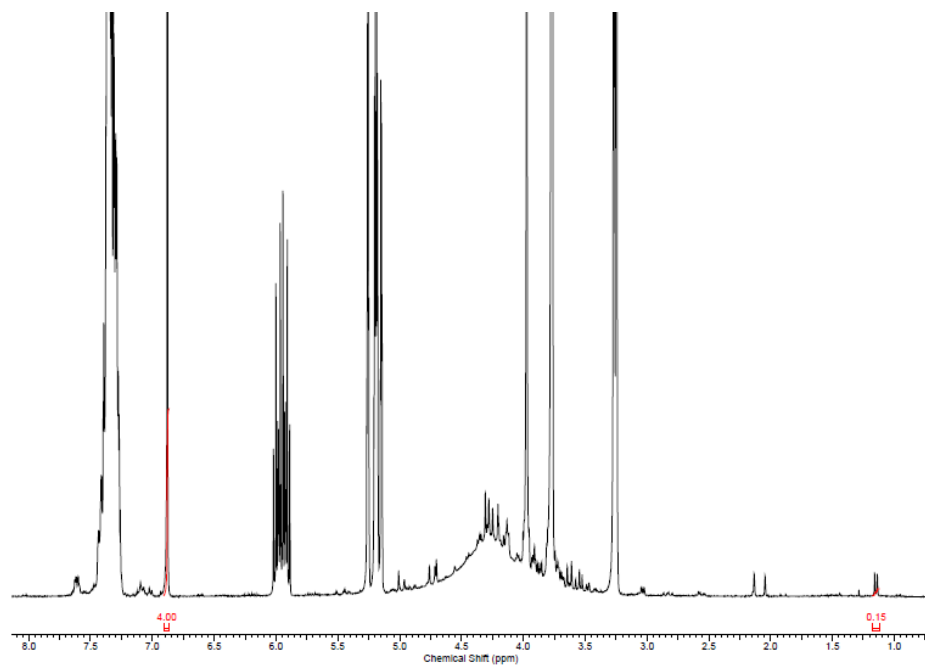




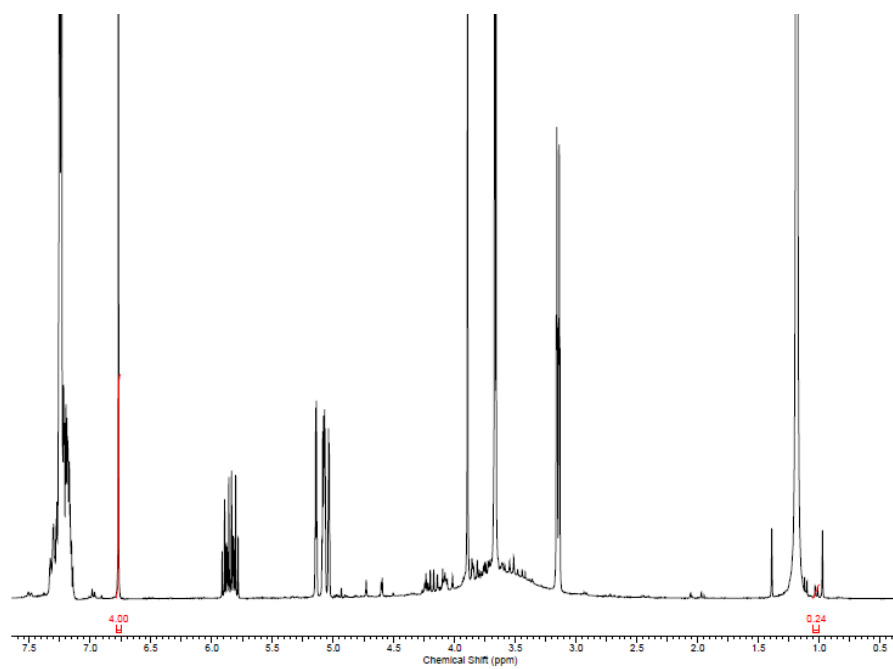




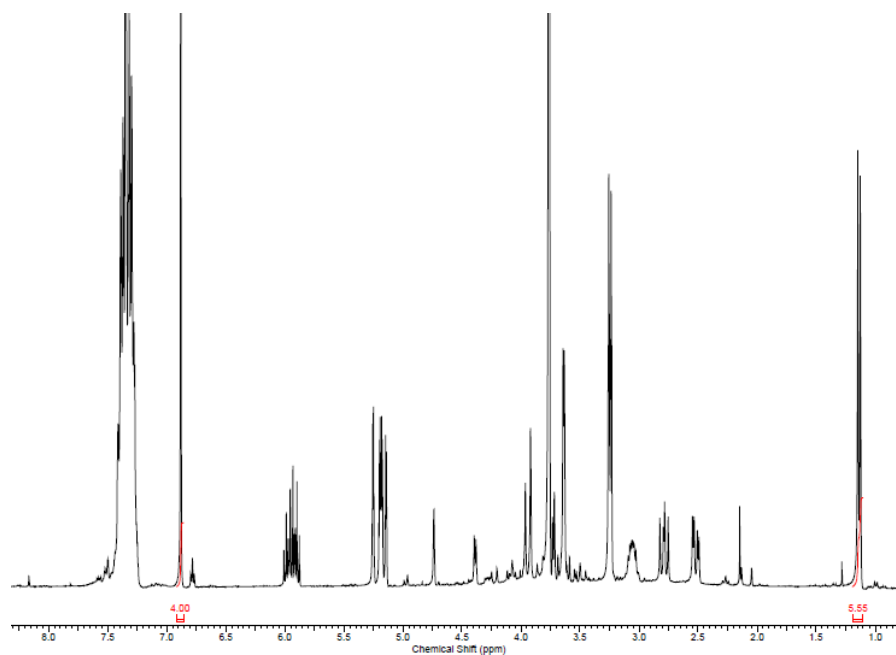
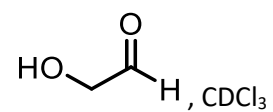
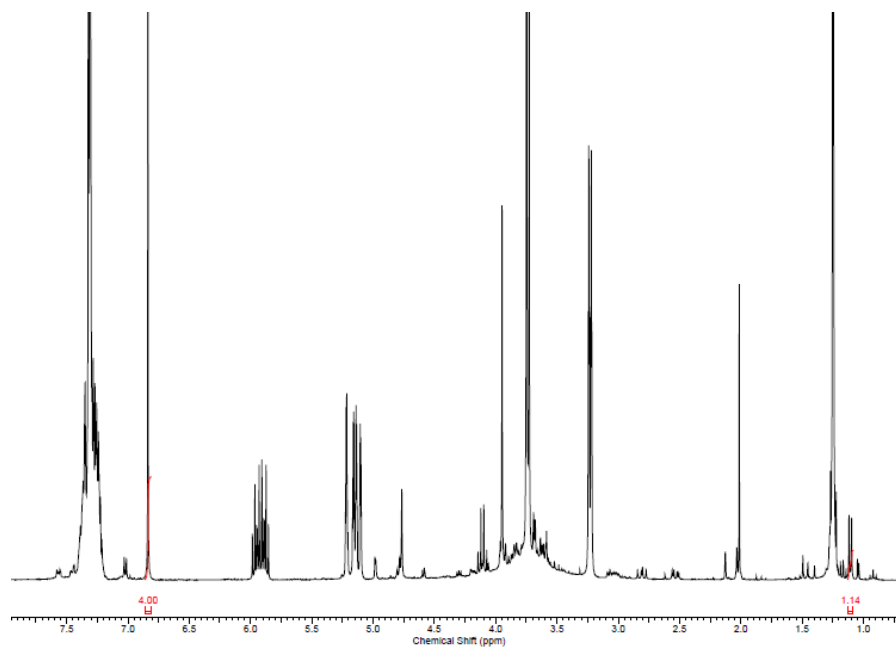
D-ribose, CDCl₃

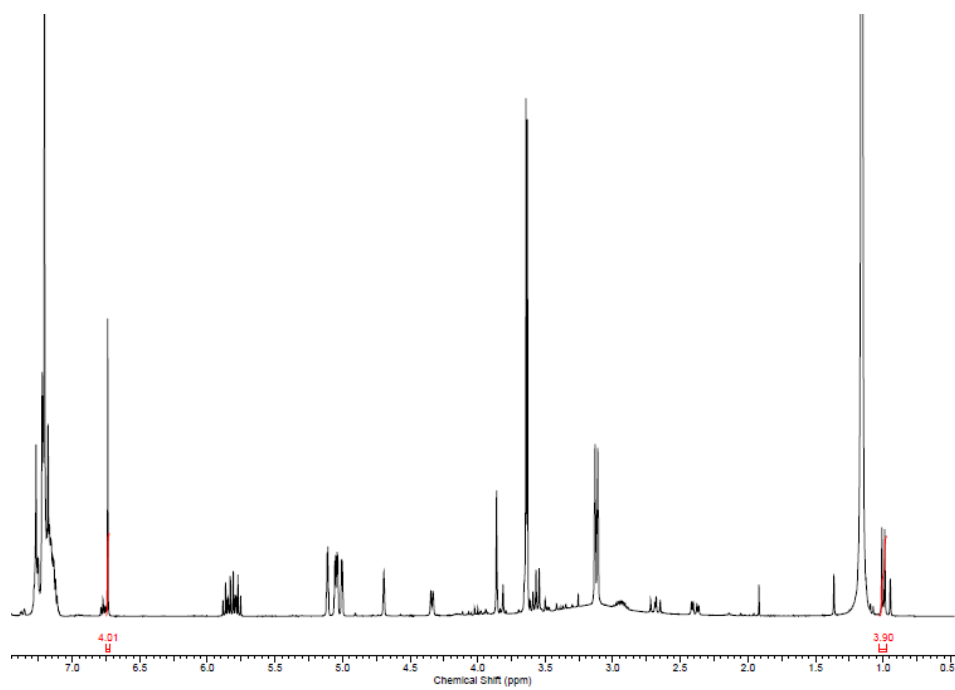
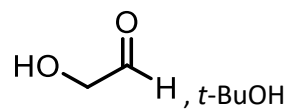


D-ribose, *t*-BuOH

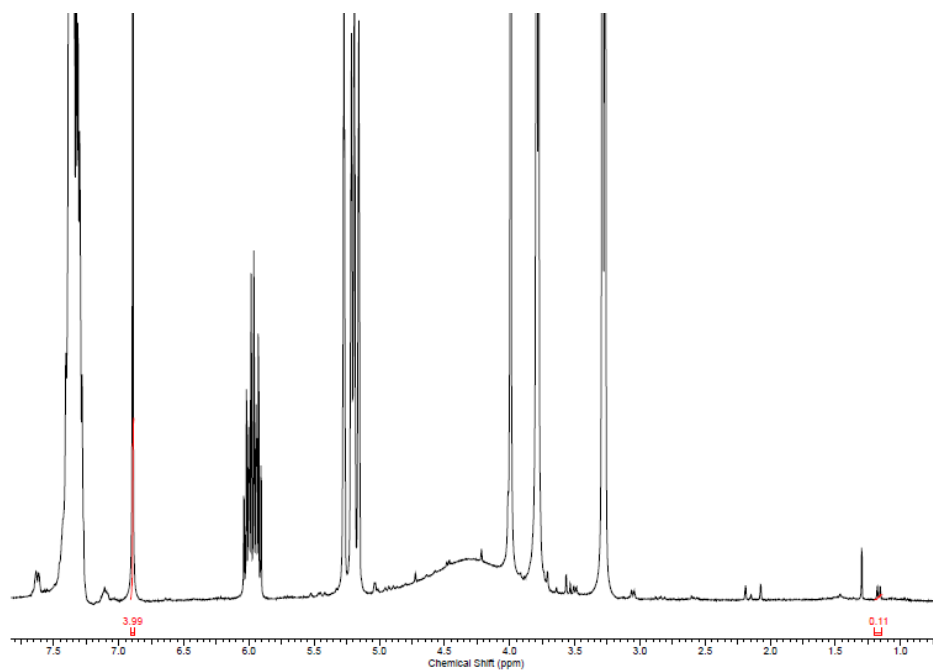


D-erythrose, *t*-BuOH





Blank, CDCl₃



Blank, *t*-BuOH

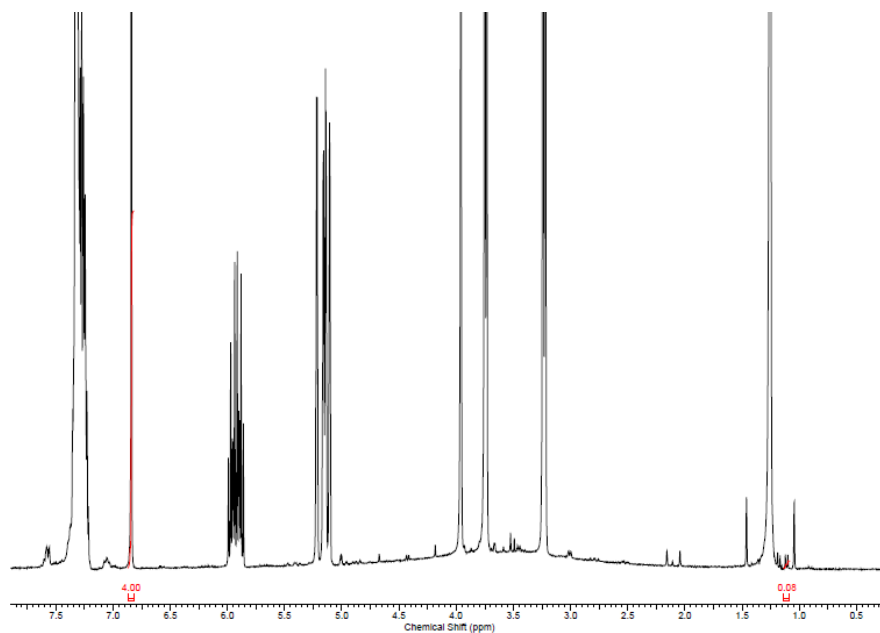
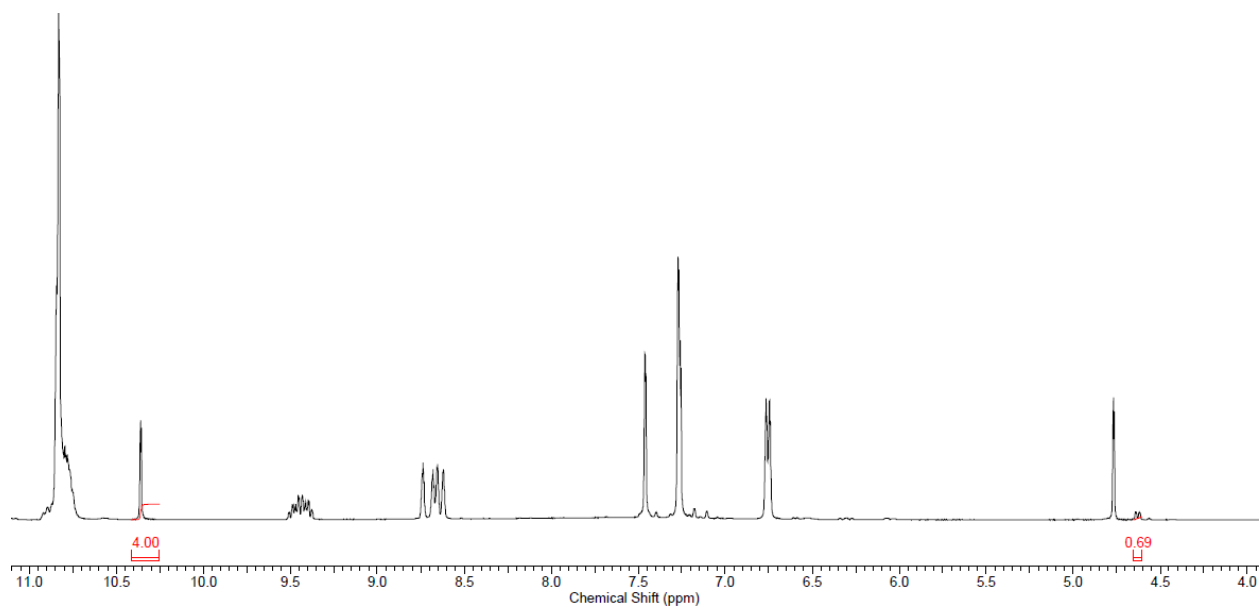


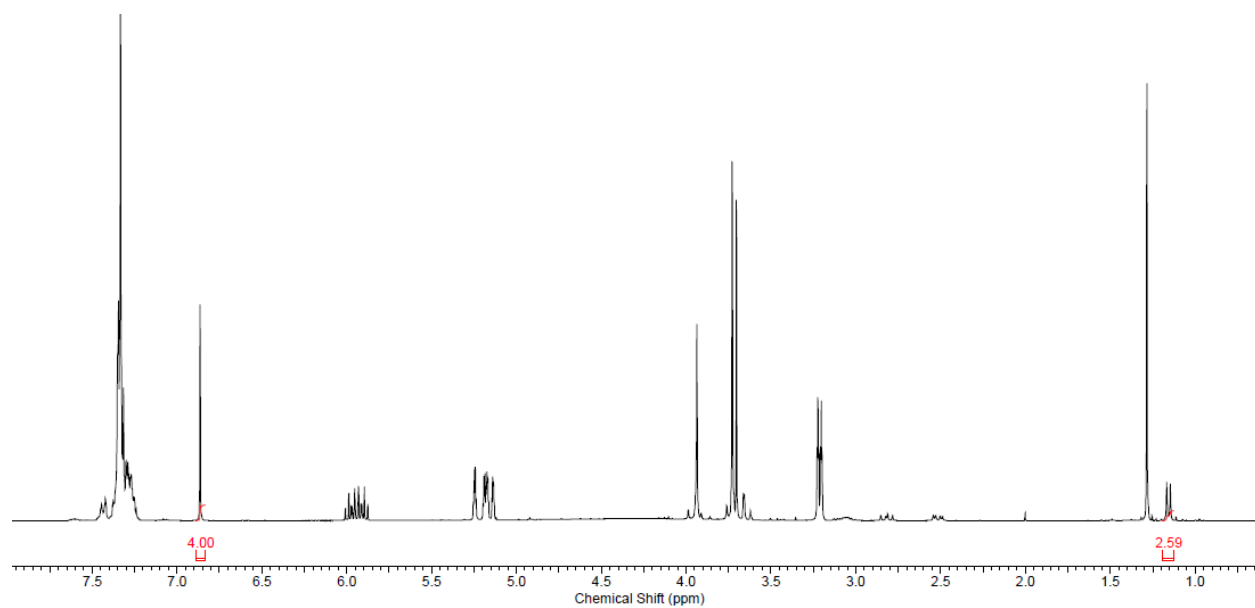
Table 2.2 Cope-type Hydroamination with Low Formaldehyde Loadings

NMR yields were obtained by using an internal standard, 1,4-Dimethoxybenzene (0.125 equiv.) and comparing the internal standard peak (6.83 ppm, 4H, singlet) to the newly formed product peak (1.14 ppm, 3H, doublet). See Annex II for the full procedure.

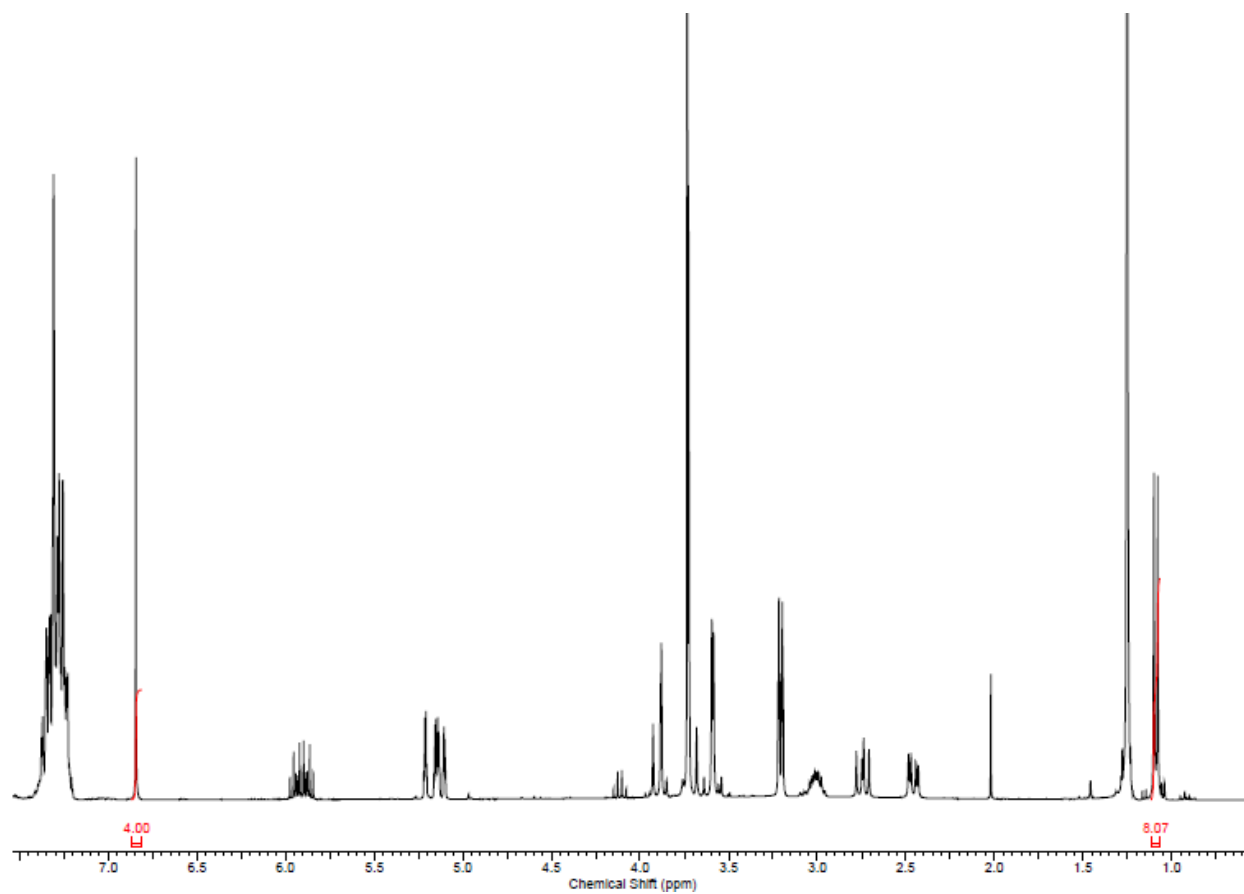
Entry 1



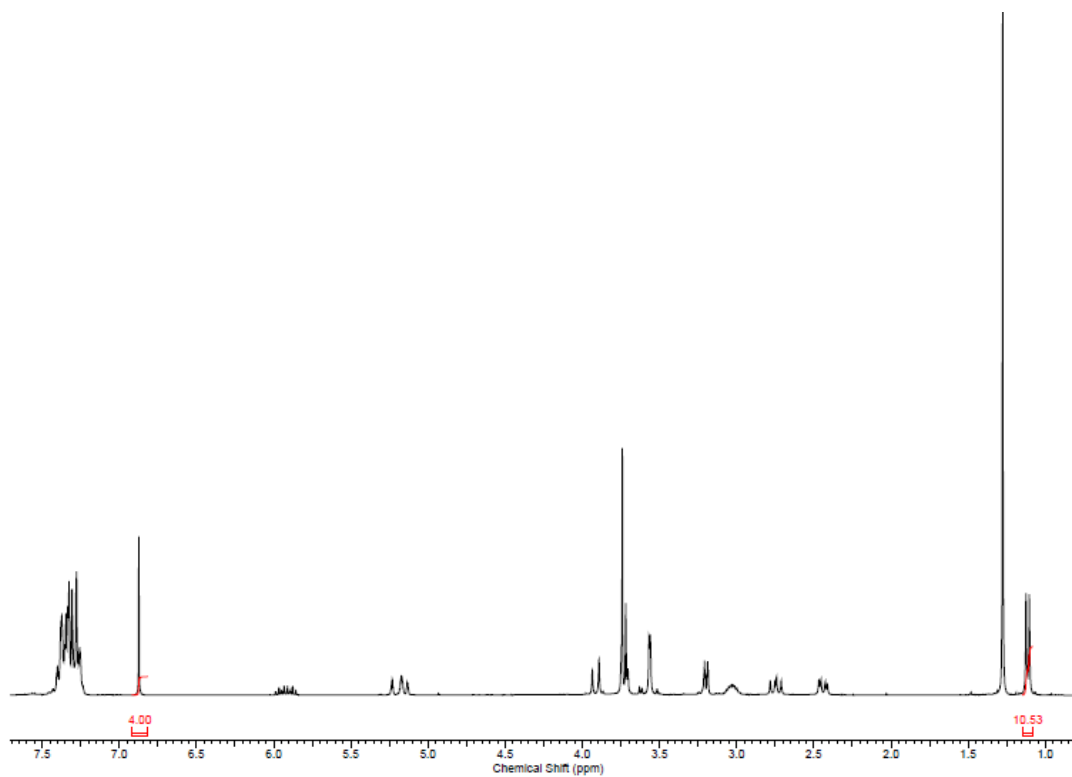
Entry 2



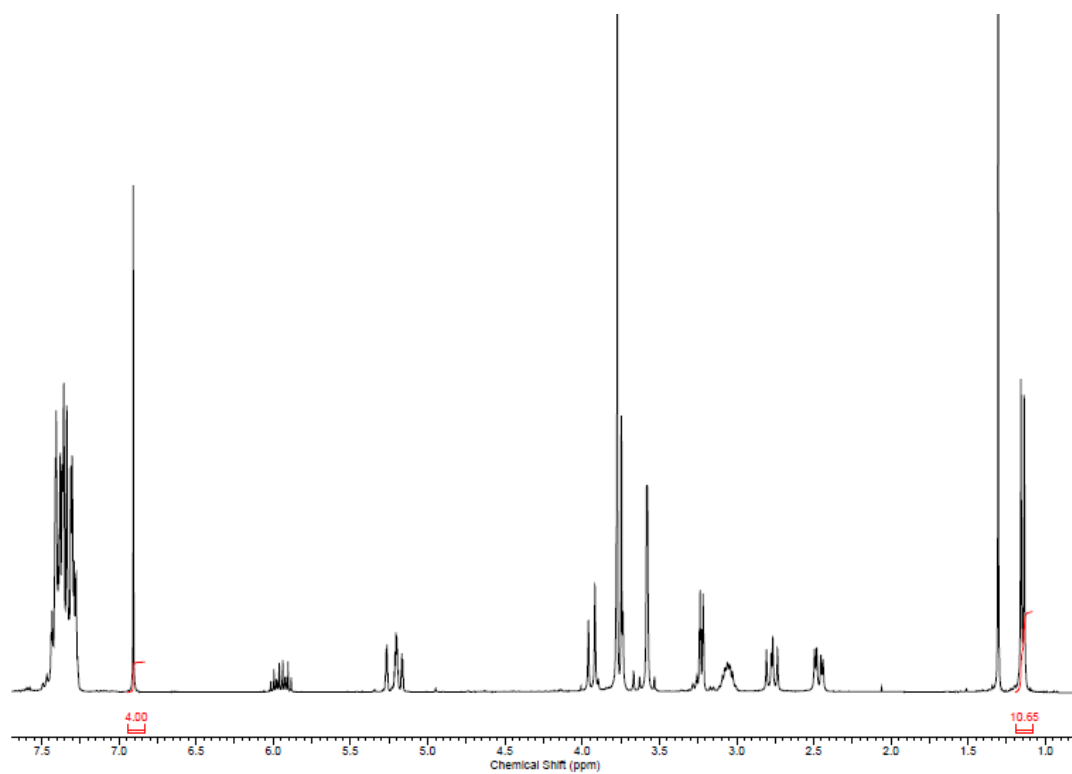
Entry 3



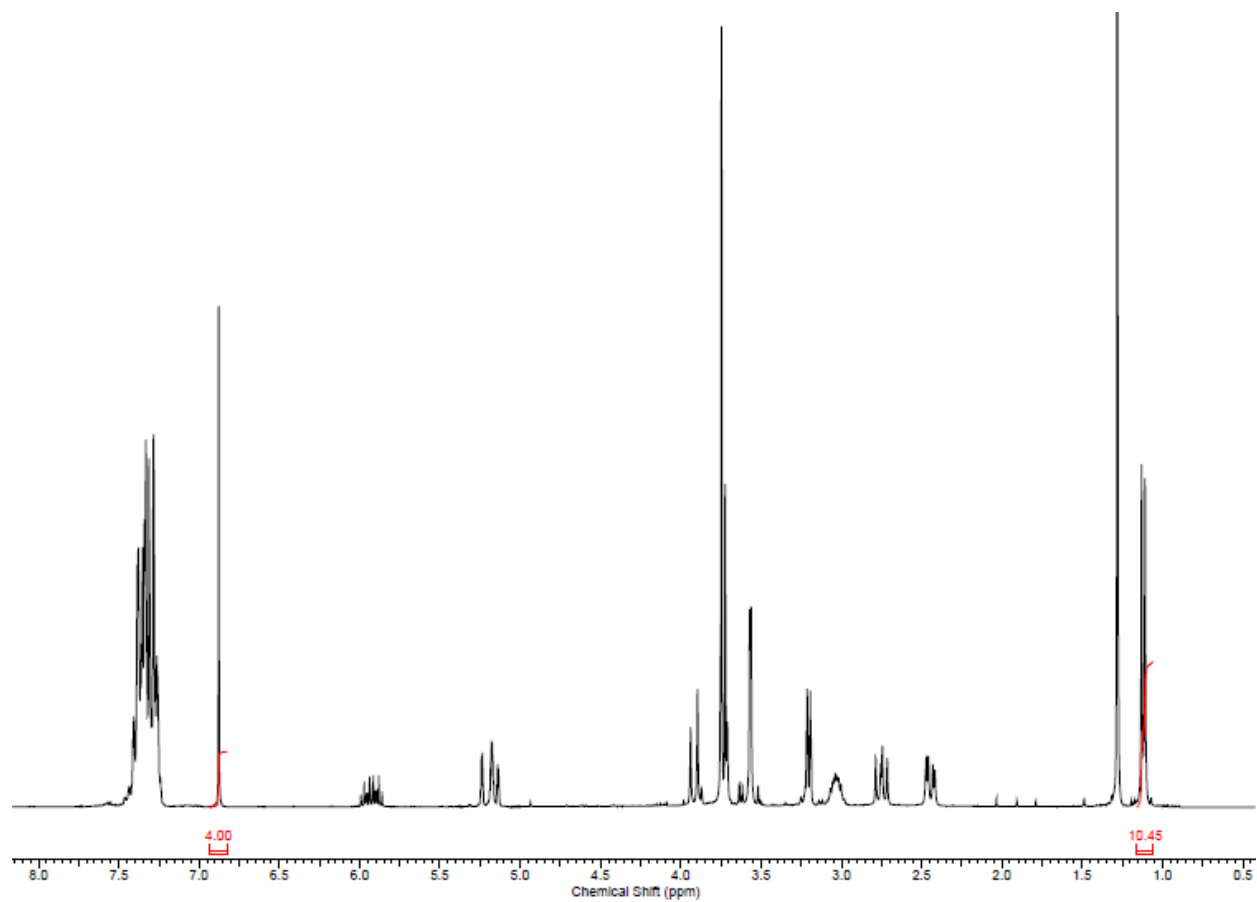
Entry 4



Entry 5

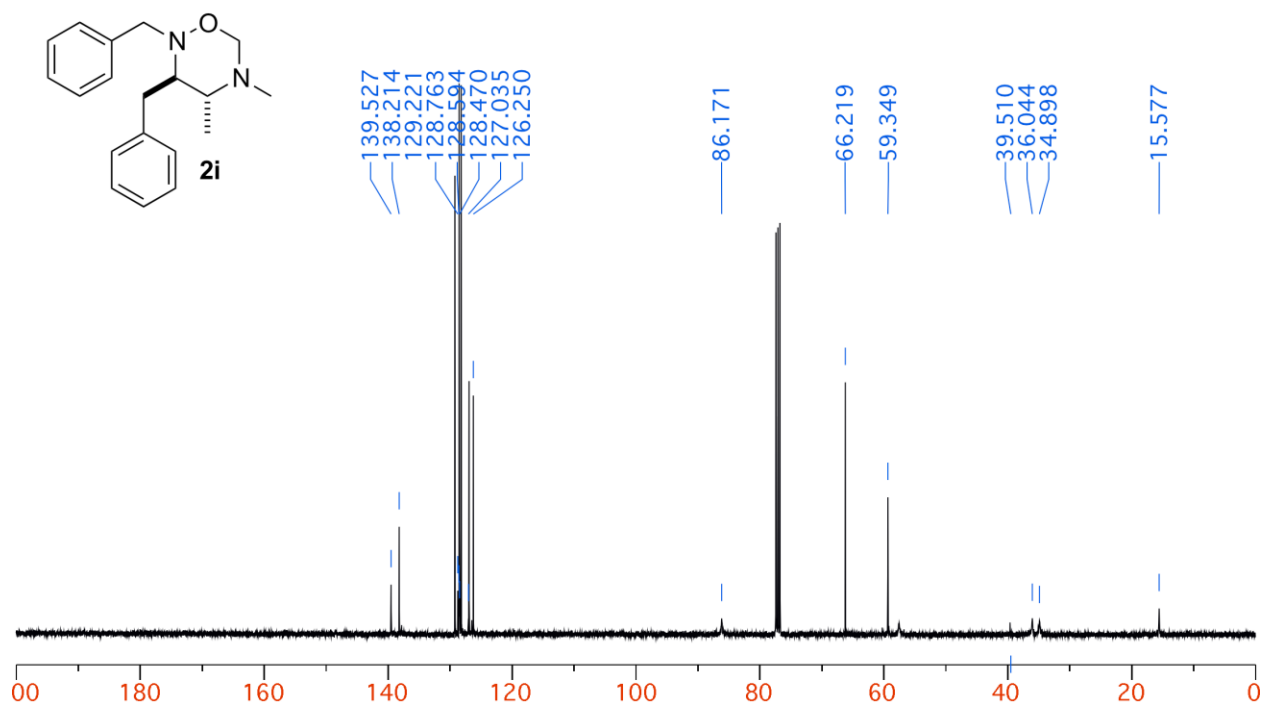
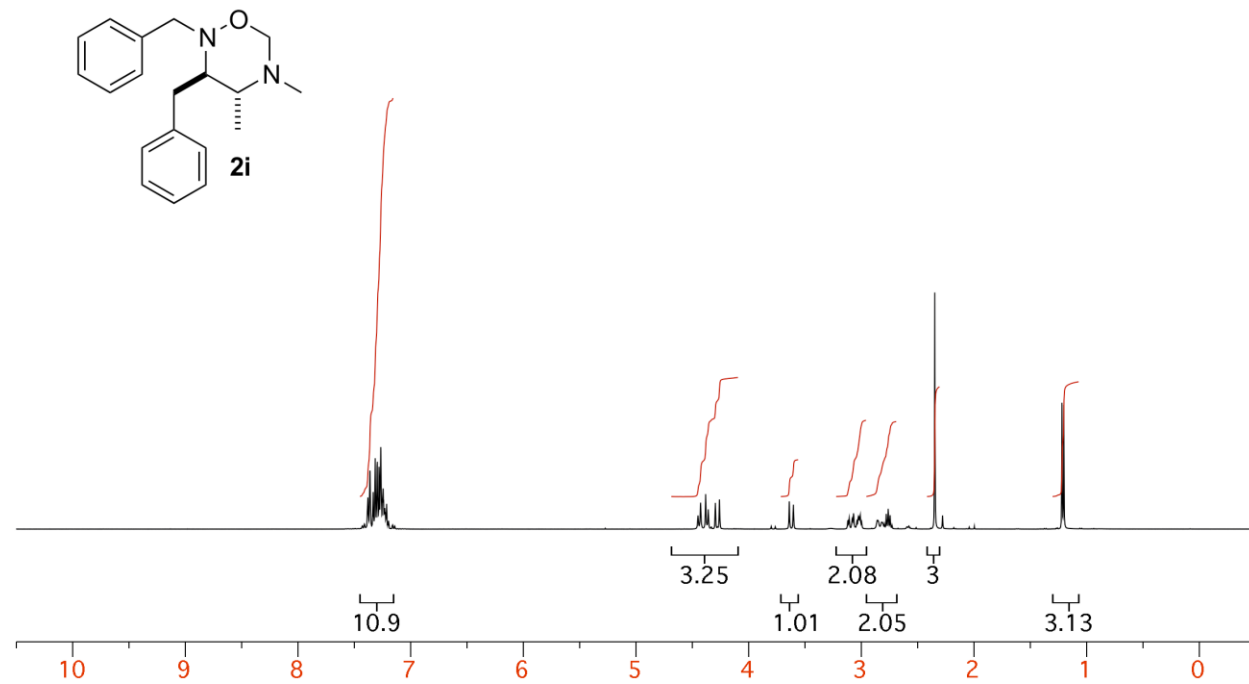


Entry 6

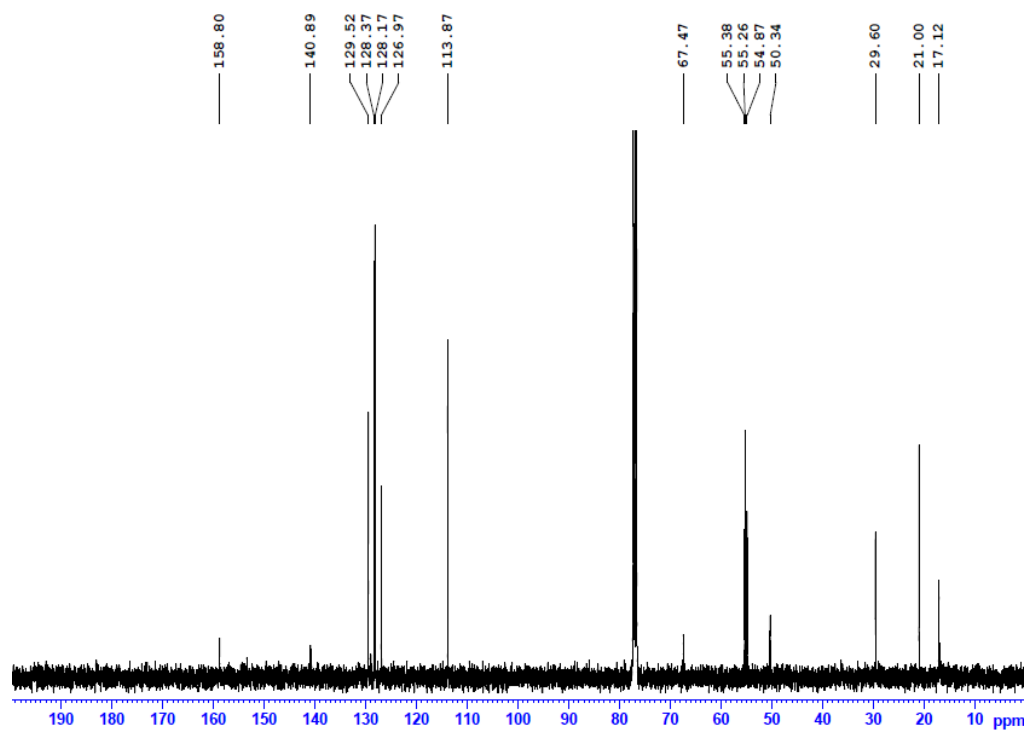
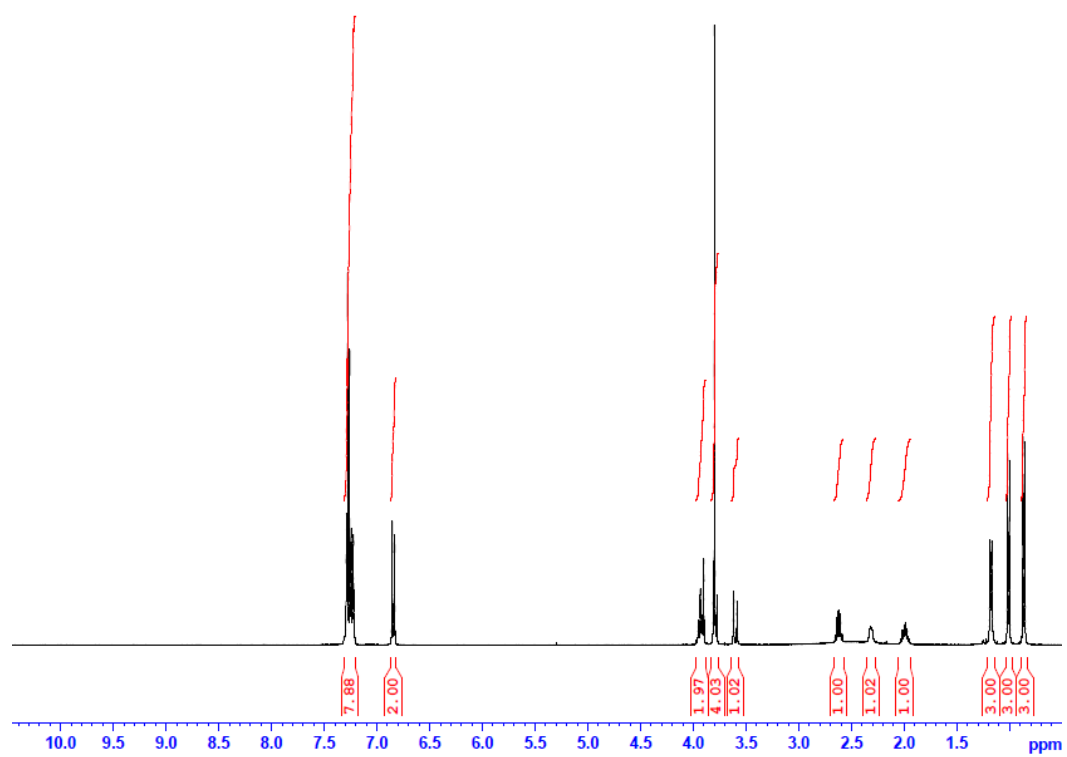


Scheme 2.1 Derivatization of diamine motifs

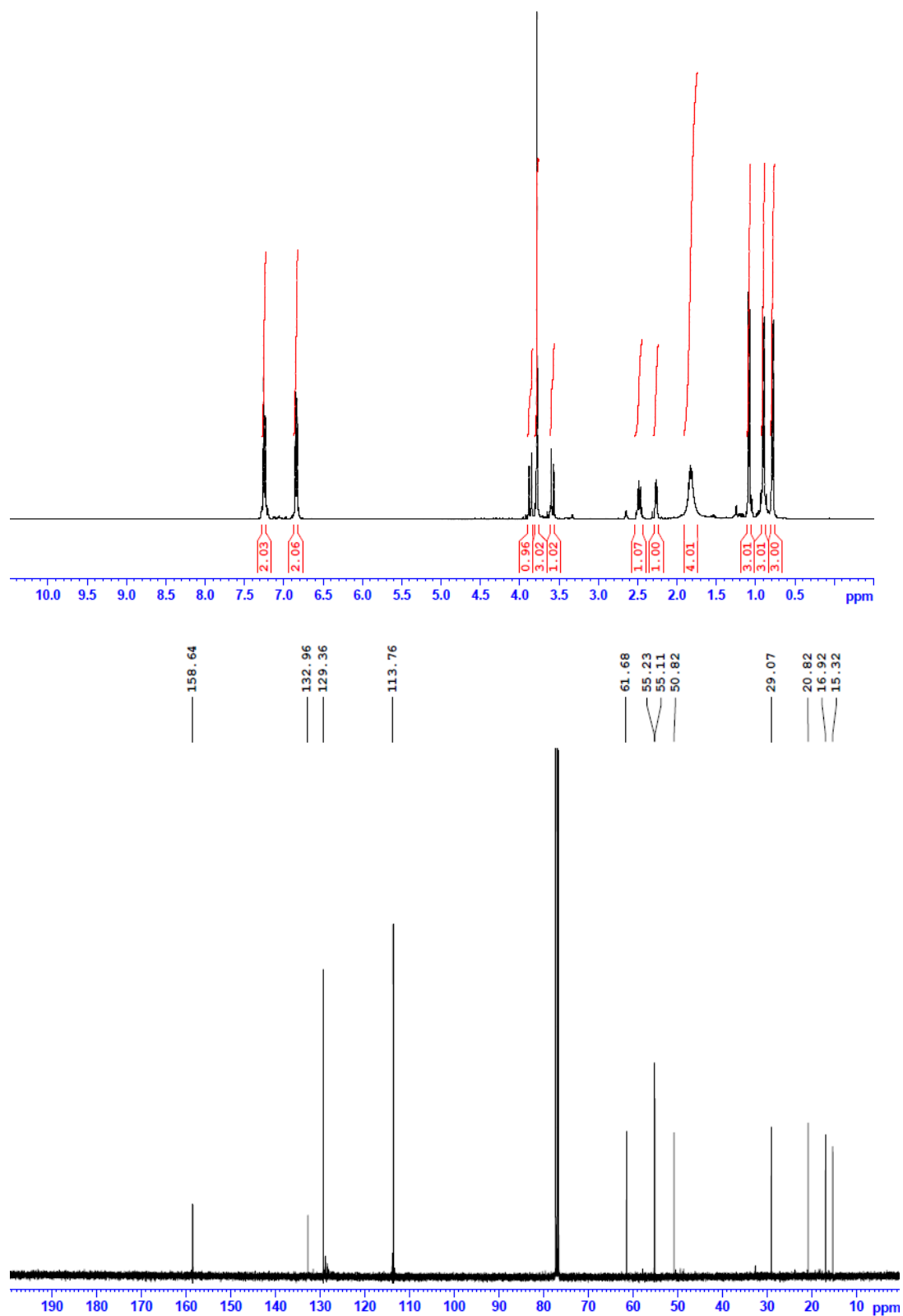
(±)-N-Benzyl-2-(hydroxy(4-methoxybenzyl)amino)-4-methylpentan-3-amine (2.2a)



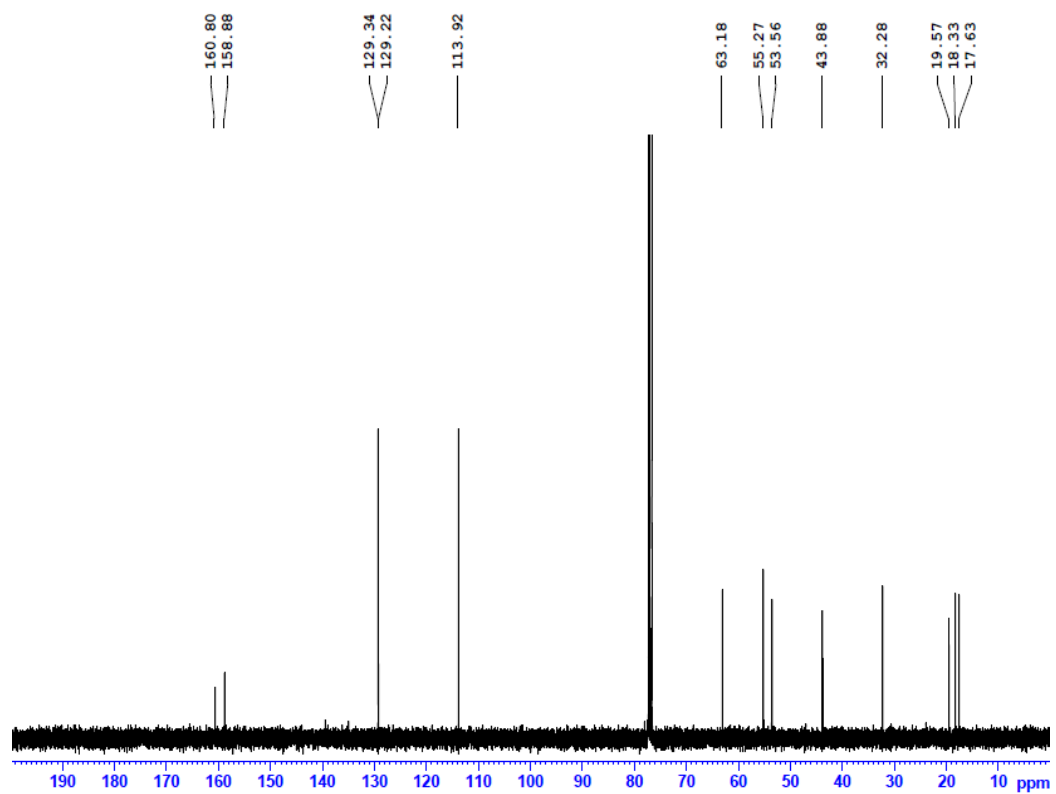
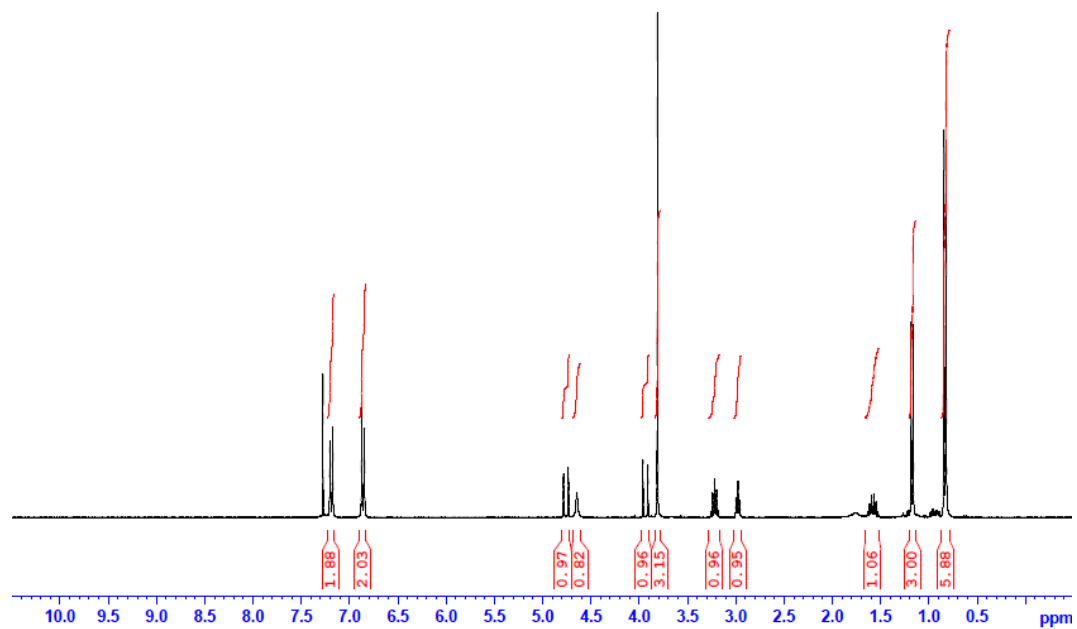
(±)-N³-Benzyl-N²-(4-methoxybenzyl)-4-methylpentane-2,3-diamine (2.2b)



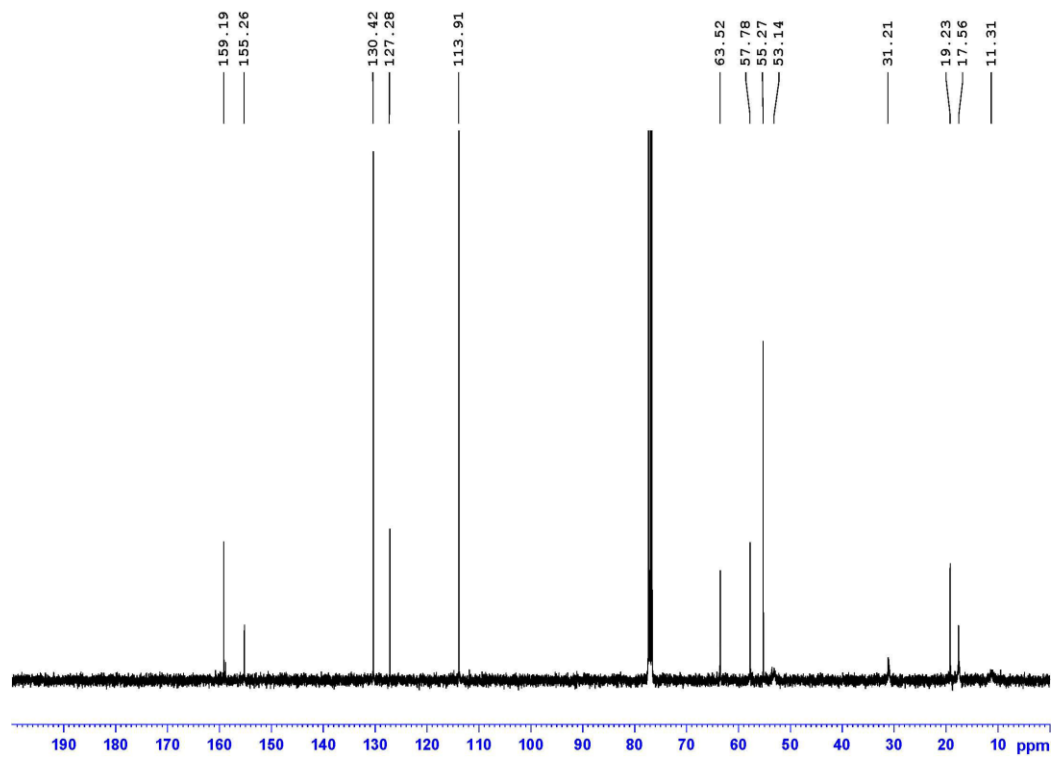
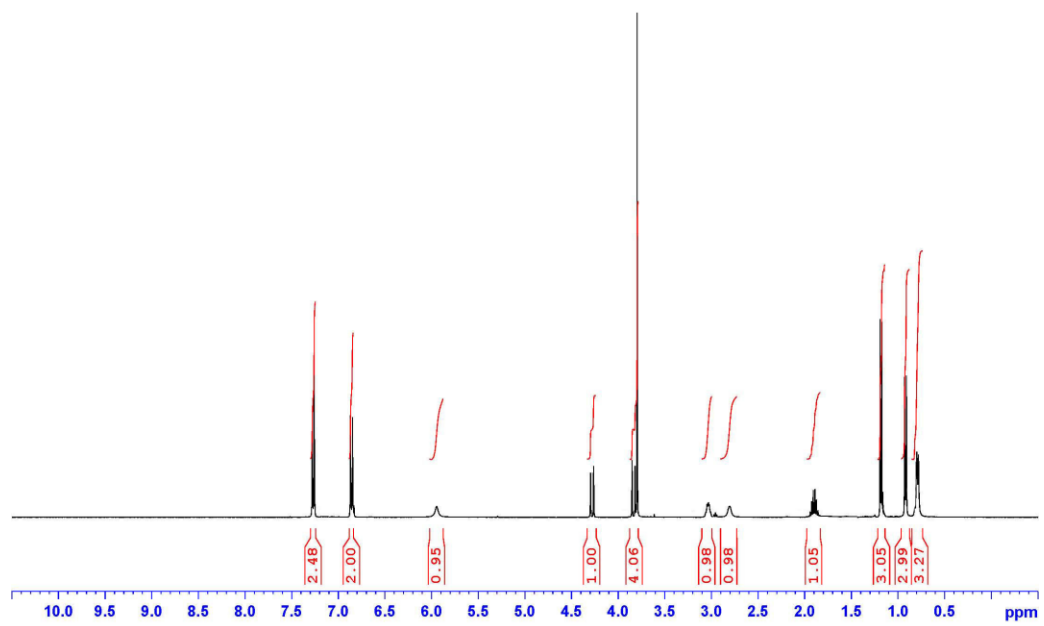
(±)-N²-(4-Methoxybenzyl)-4-methylpentane-2,3-diamine (2.2c)



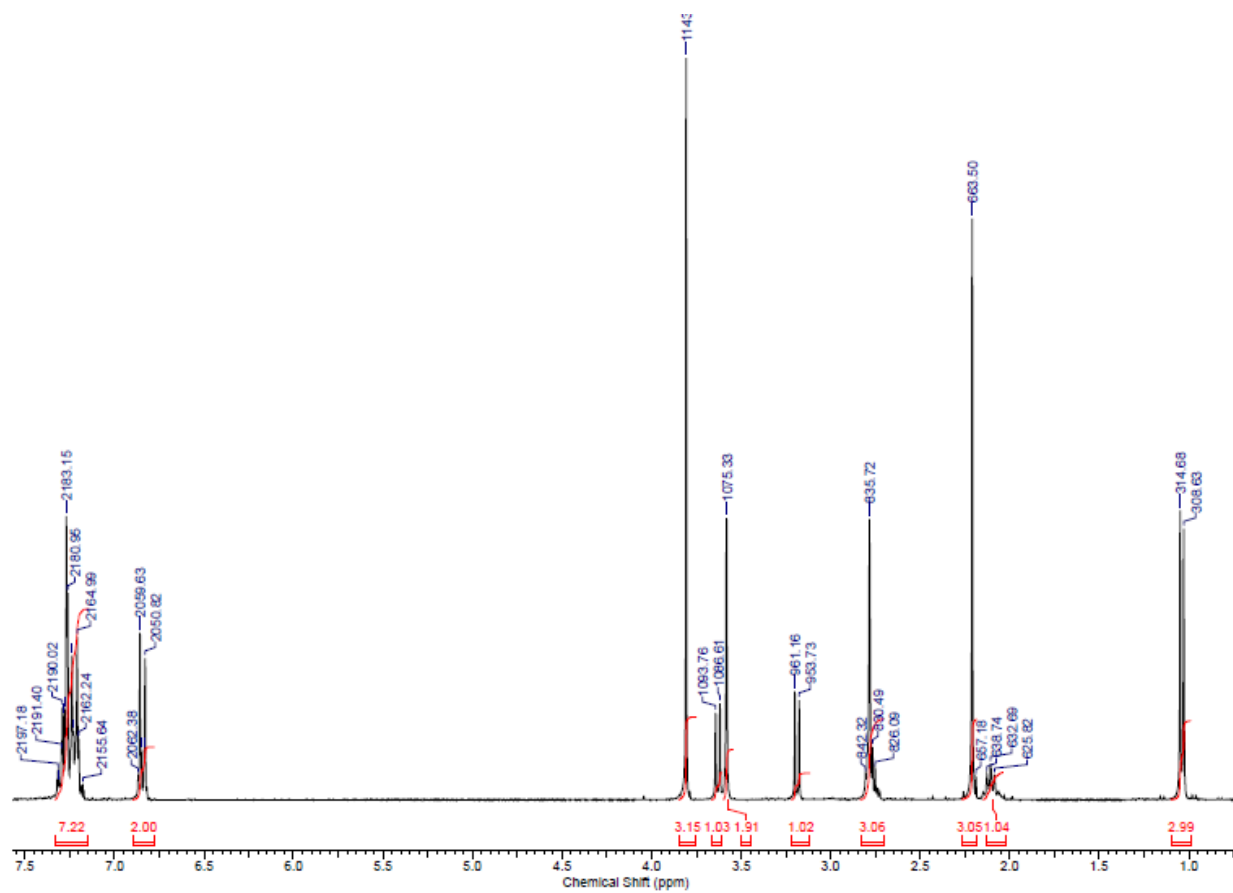
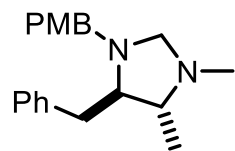
(±)-4-Isopropyl-1-(4-methoxybenzyl)-5-methylimidazolidin-2-one (**2.2d**)

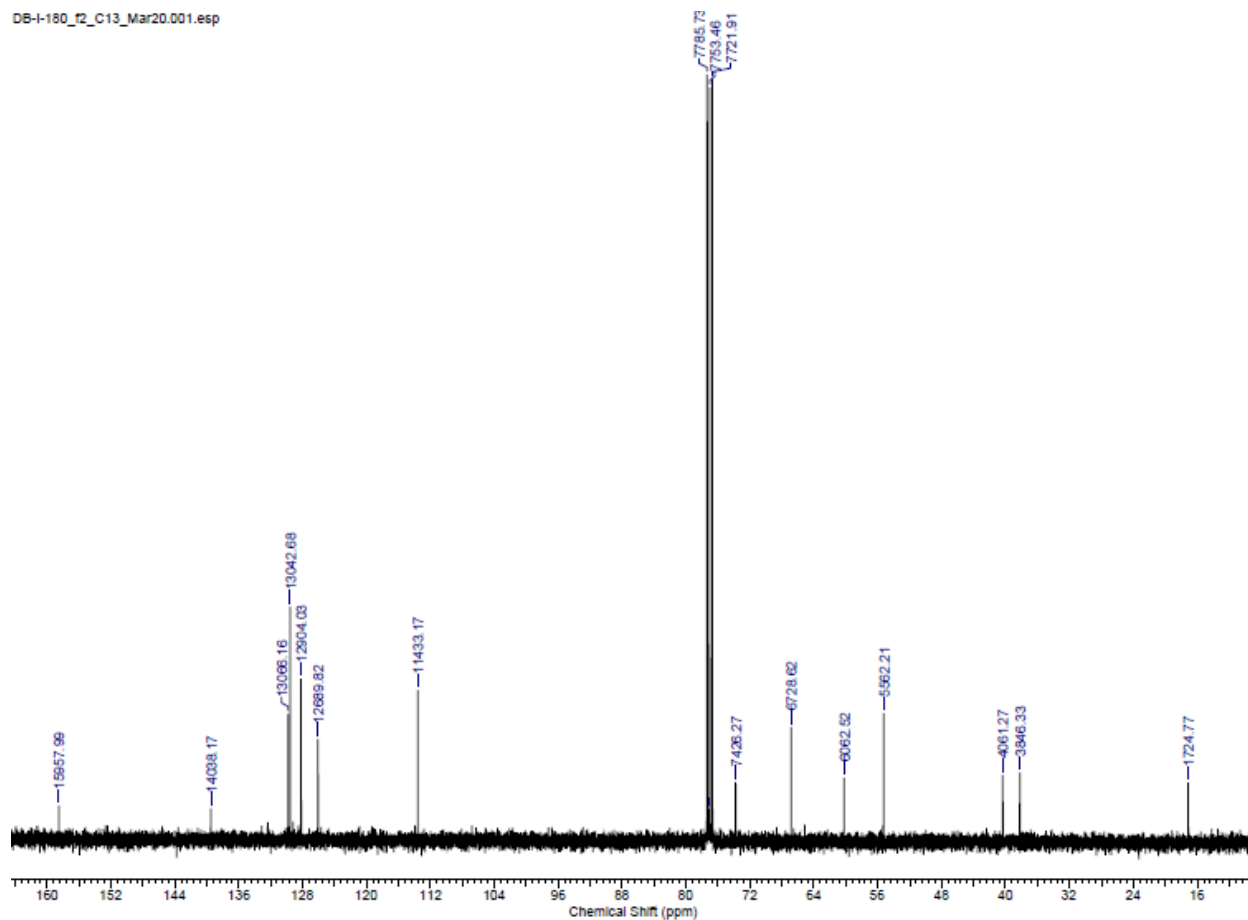


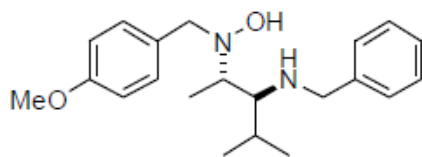
(±)-4-Isopropyl-2-(4-methoxybenzyl)-3-methyl-1,2,5-oxadiazinan-6-one (**2.2e**)



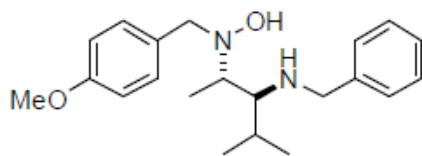
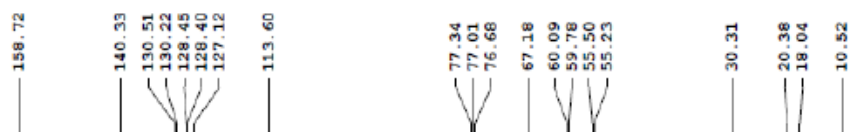
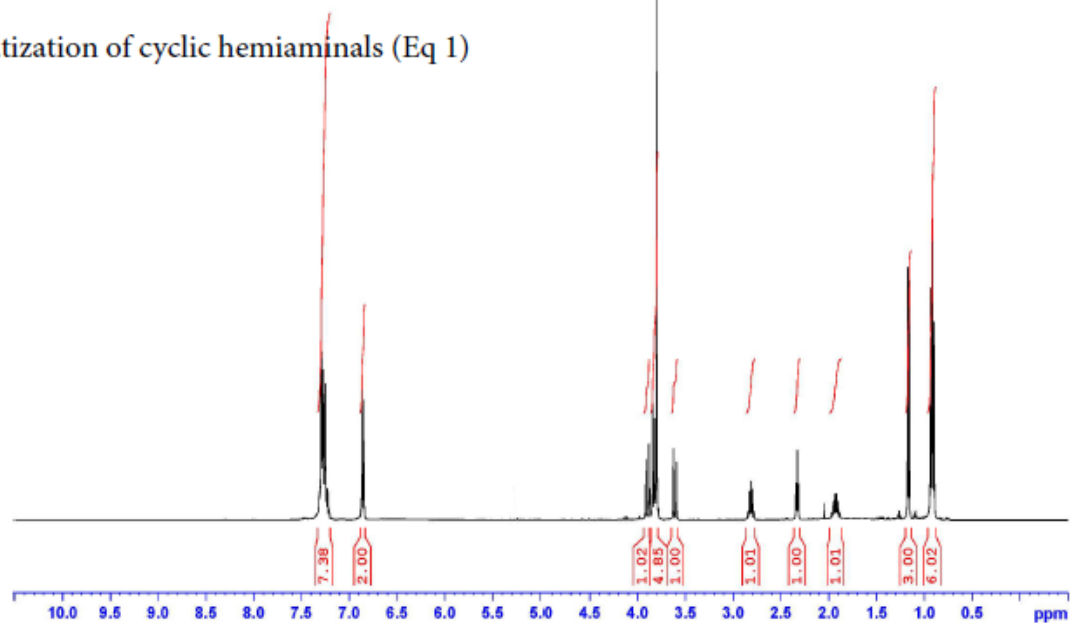
Imidazolidine (2.2g)



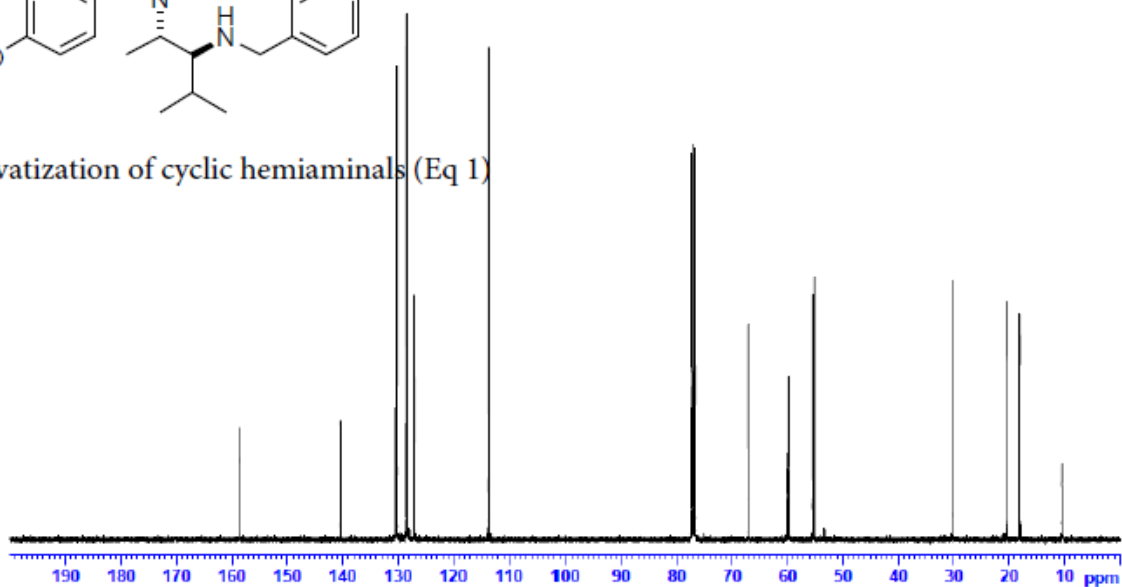




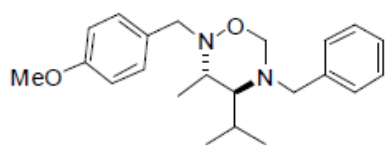
Derivatization of cyclic hemiaminals (Eq 1)



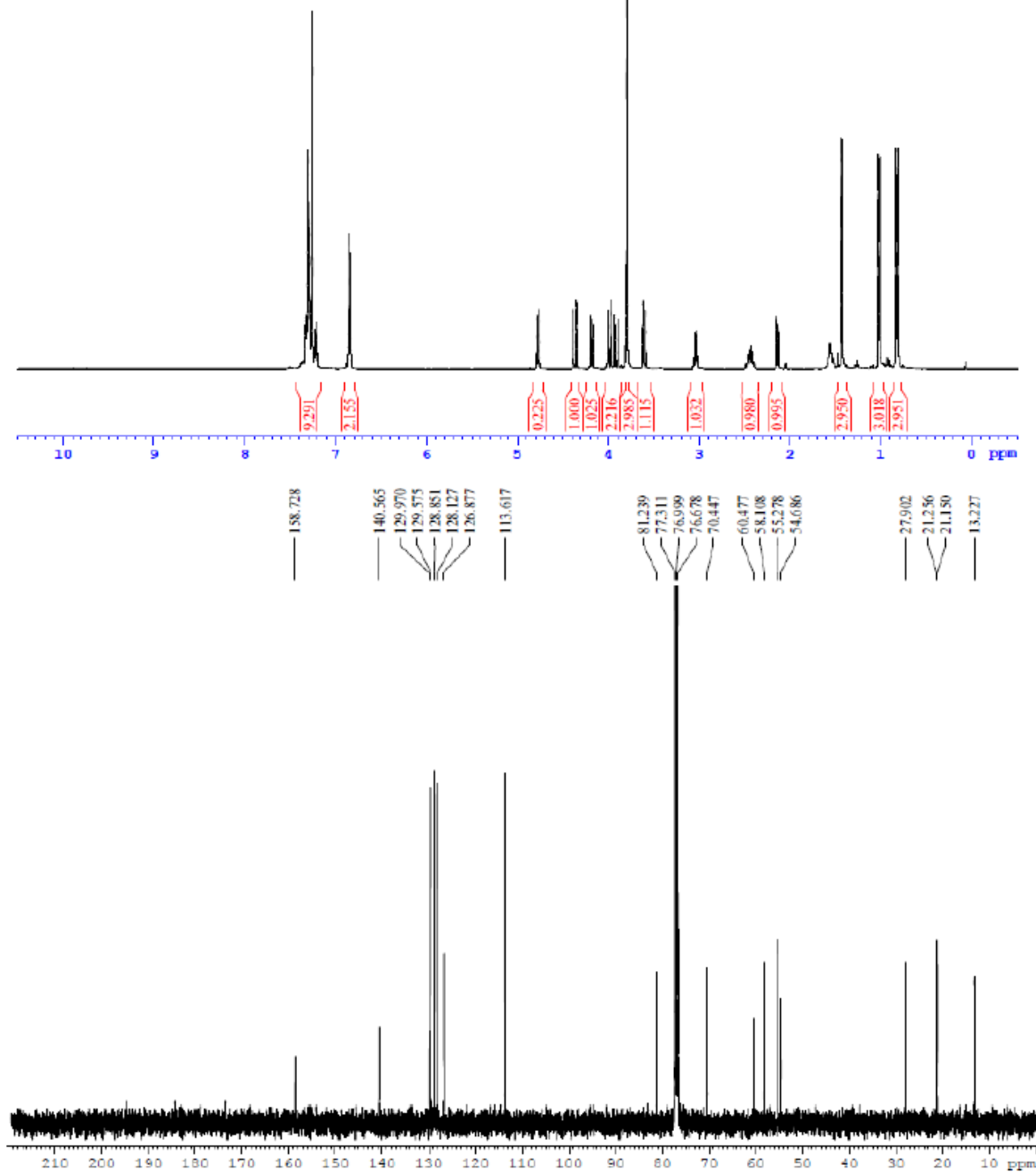
Derivatization of cyclic hemiaminals (Eq 1)



Scheme 2.3 Hydrolysis of cyclic adducts



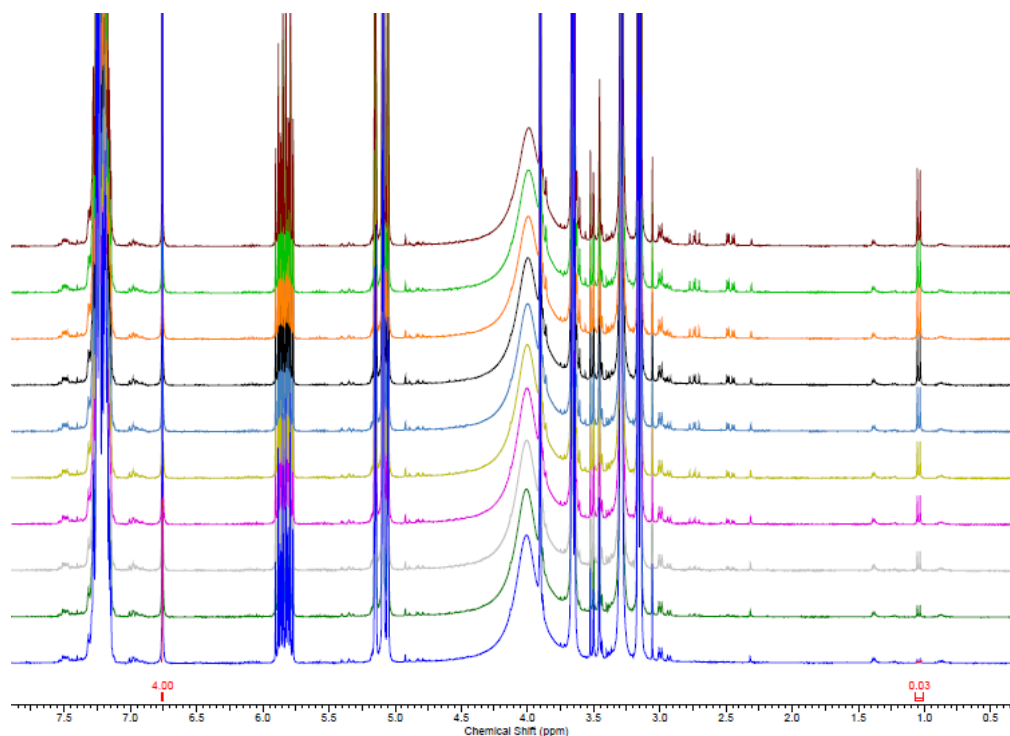
Derivatization of cyclic hemiaminals (Eq 1)



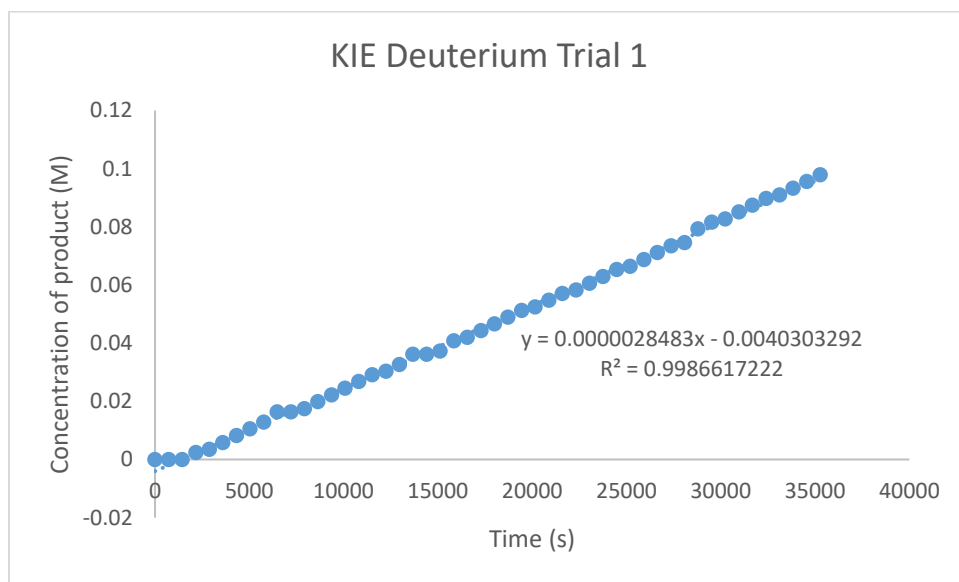
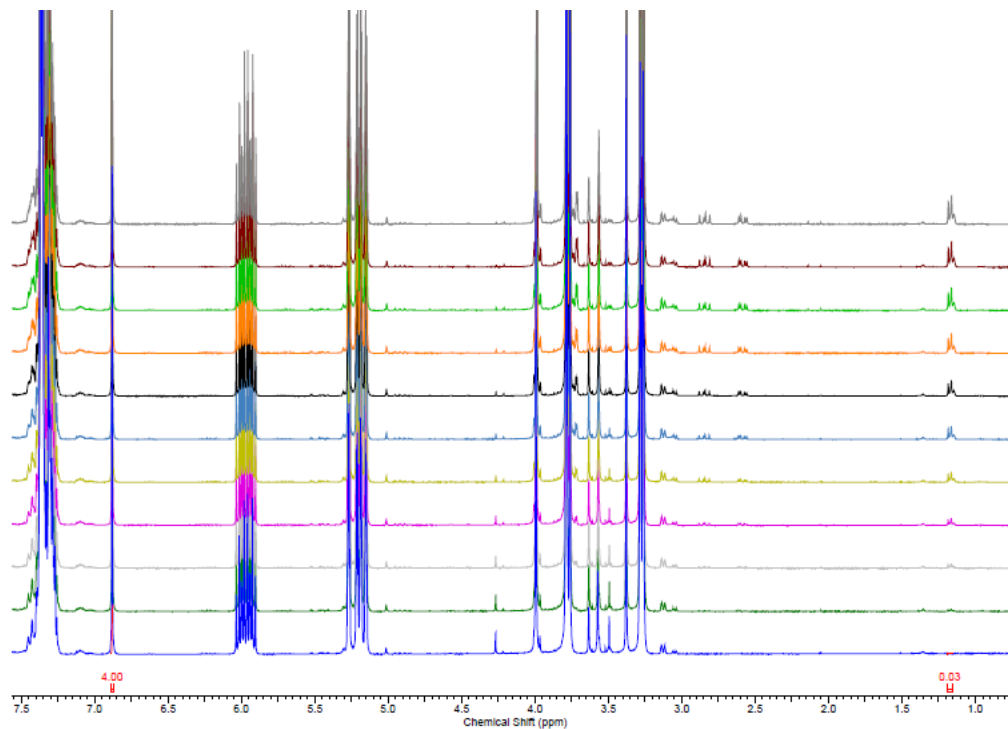
Scheme 2.6 Deuterium kinetic isotope effect experiment for formaldehyde

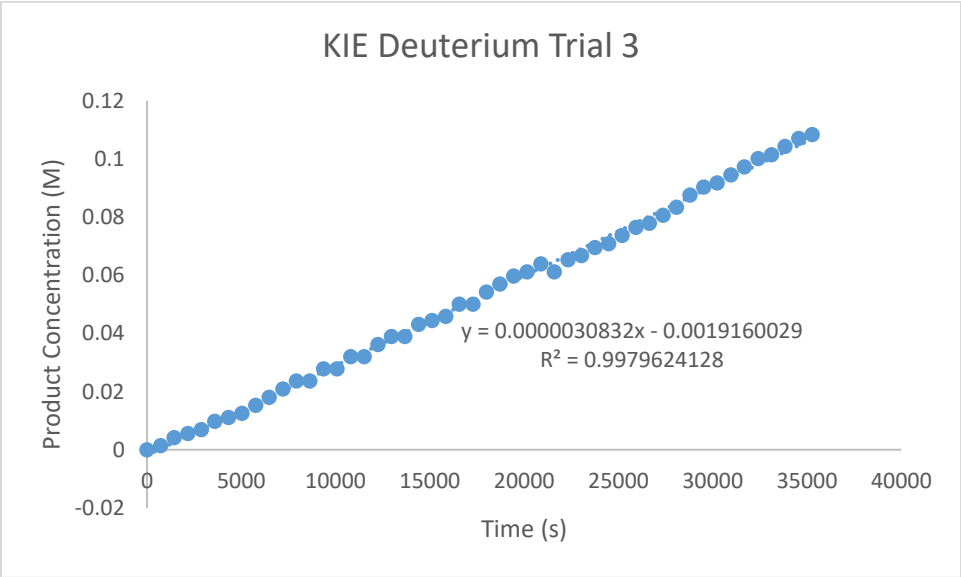
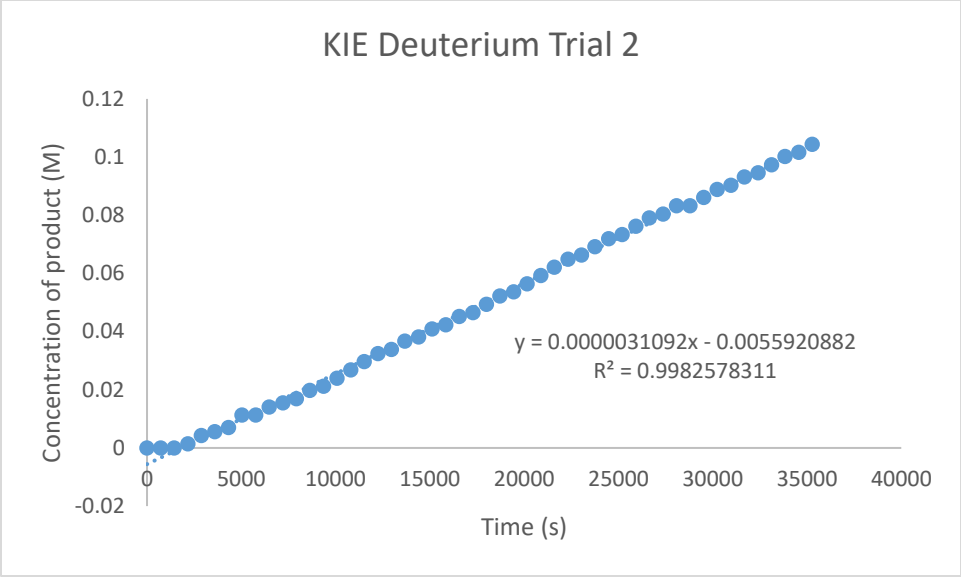
NMR samples were taken to the spectrometer and heated to 298 K. Using a custom program made by our NMR professional, Dr. Glenn Facey, an 8 scan spectrum was acquired every 12 minutes for a period of 10 hours. The concentration of product formed was determined by integrating the product's peak ($\delta = 1.1$ ppm (d, 2H)) relative to the internal standard peak ($\delta = 6.83$ ppm, 4H). The exact same protocol was employed for the determination of the rate of the reaction with non-deuterated starting material except for the fact that MeOH was employed instead of MeOD. Also, the spectra were acquired over a period of 96 min instead of 10 hours. The concentration of product was then plotted against reaction time, in order to obtain a rate constant (slope of curve) ($n=3$). See Annex II for full procedure.

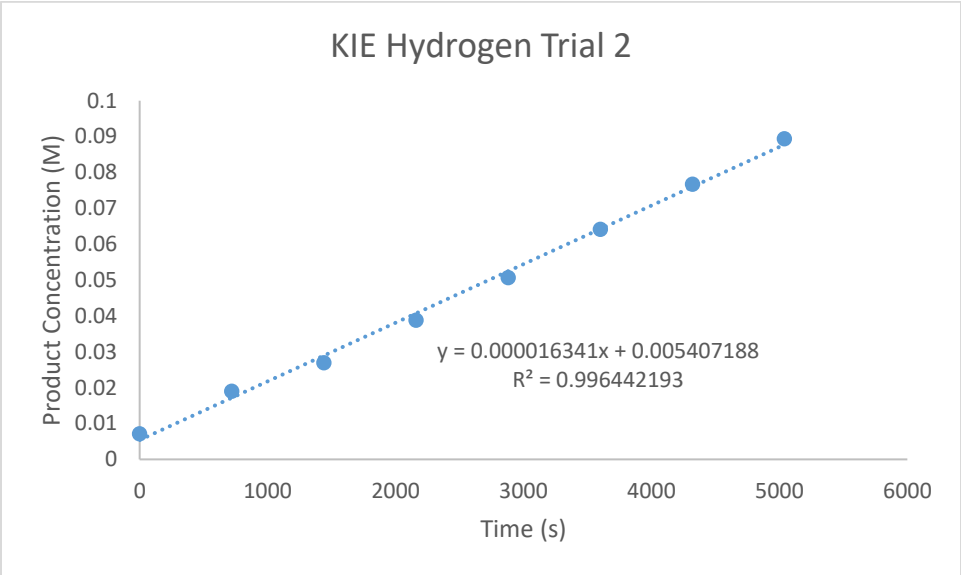
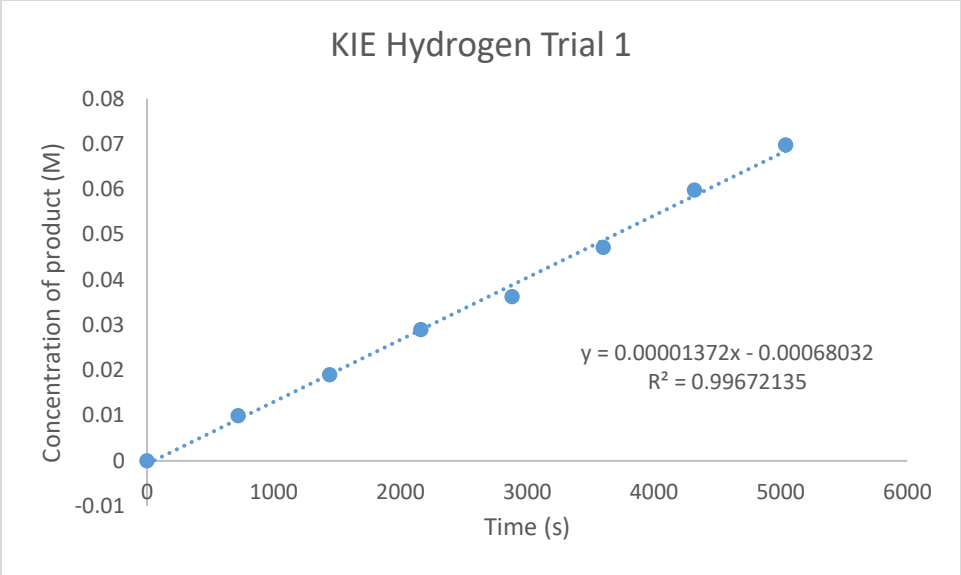
Representative KIE-H Spectra



Representative KIE-D Spectra







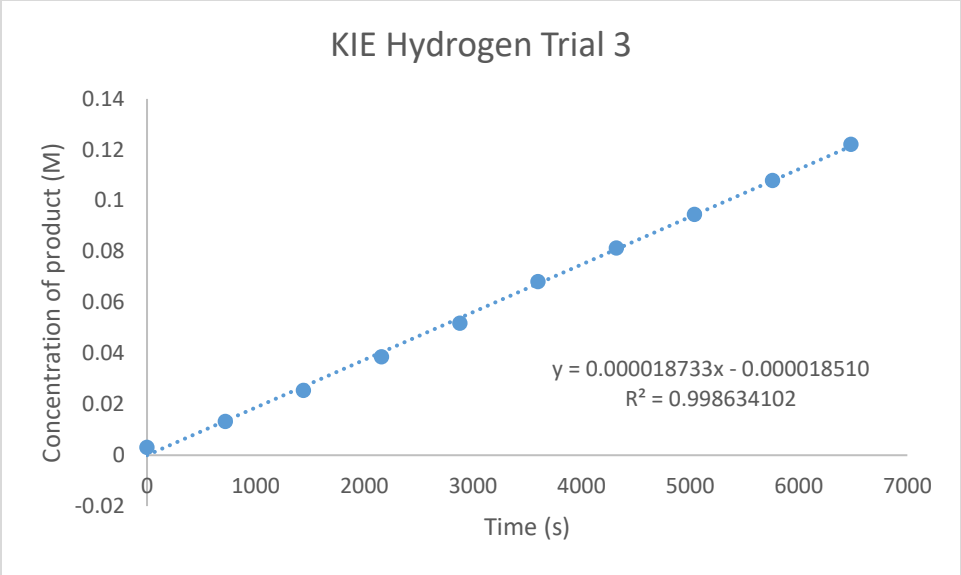
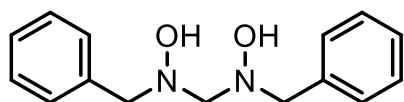
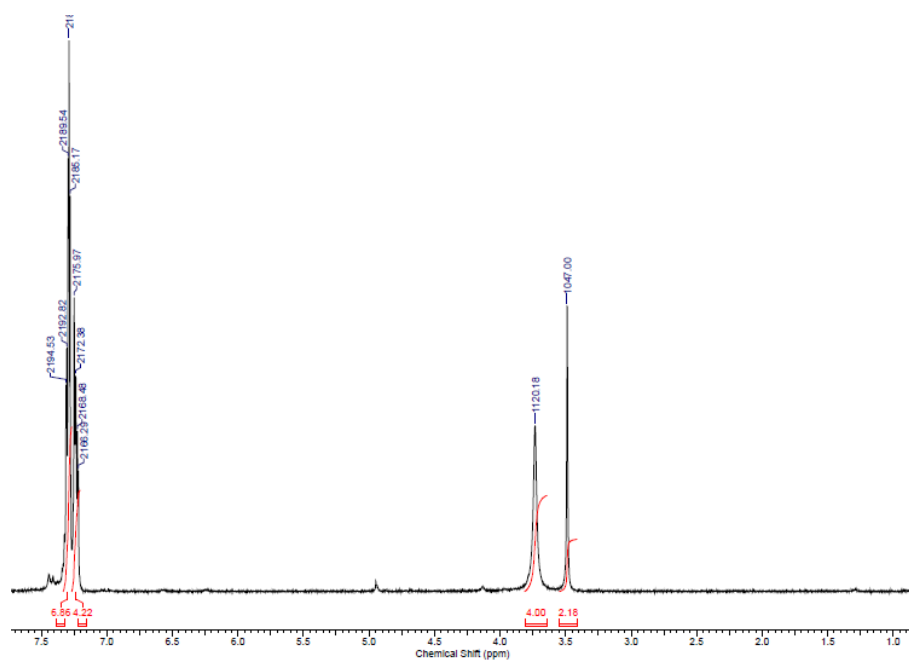


Table 2.3 Hydroamination of Allylic Amines Using a Formaldehyde Precursor Dimer

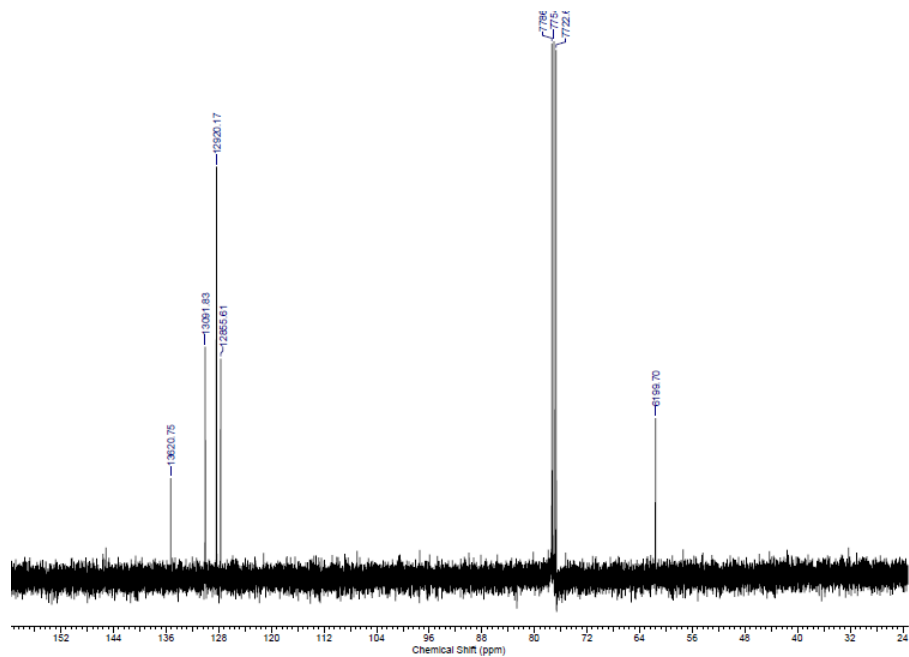
NMR yields were obtained by using an internal standard, 1,4-Dimethoxybenzene (0.125 equiv.) and comparing the internal standard peak (6.83 ppm, 4H, singlet) to the newly formed product peak (1.14 ppm, 3H, doublet). See Annex II for the full procedure.



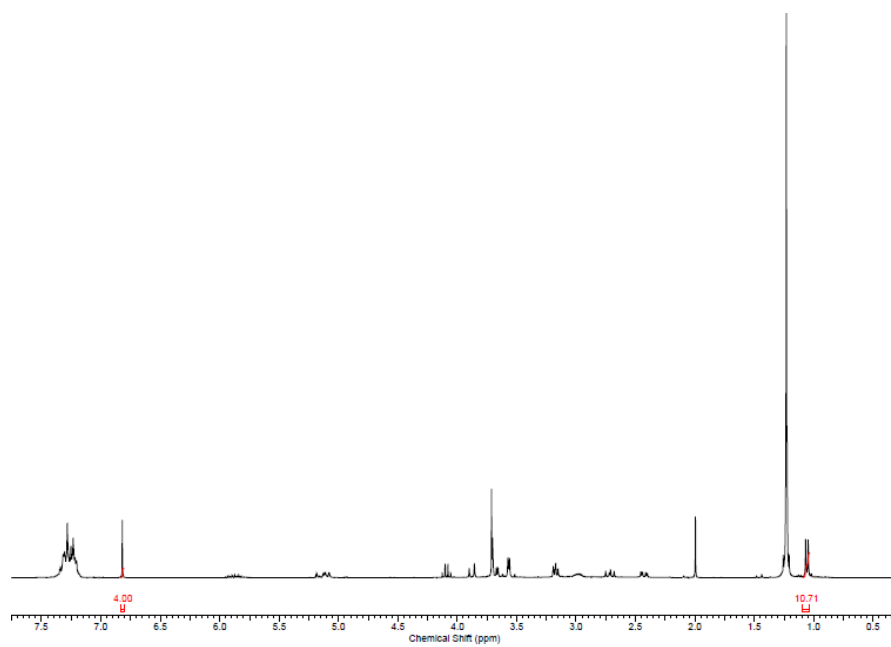
^1H , 300 MHz, CDCl_3



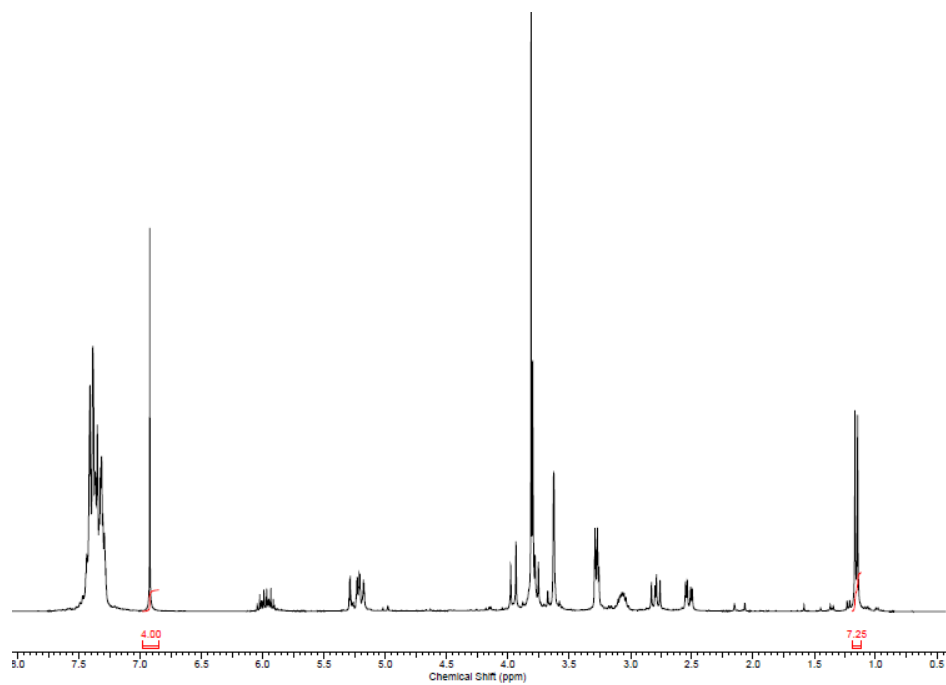
^{13}C , 100 MHz, CDCl_3



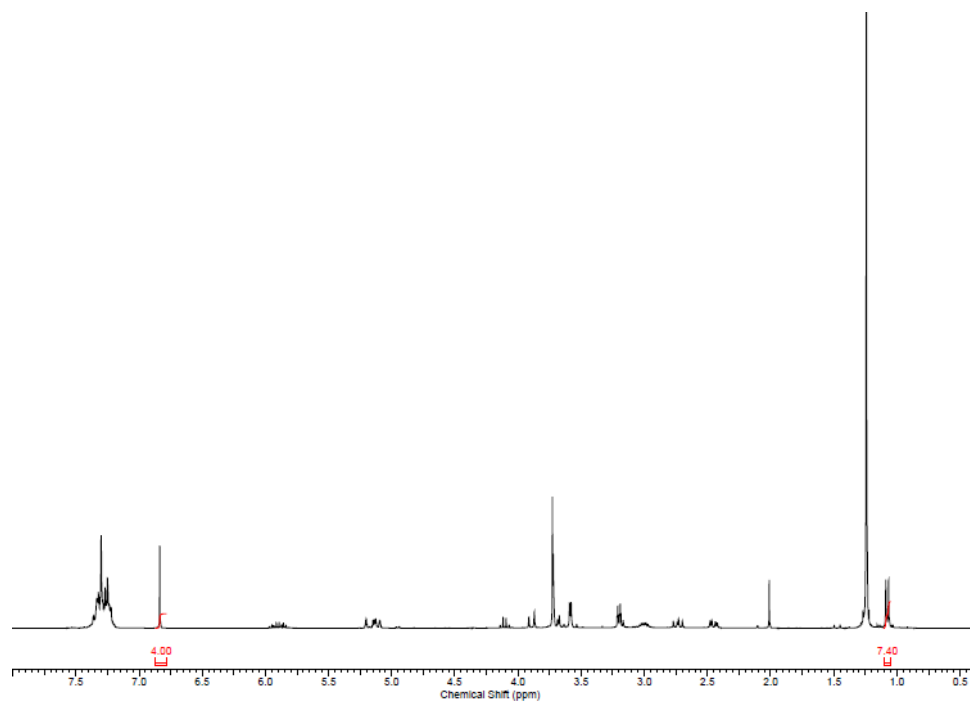
Entry 1



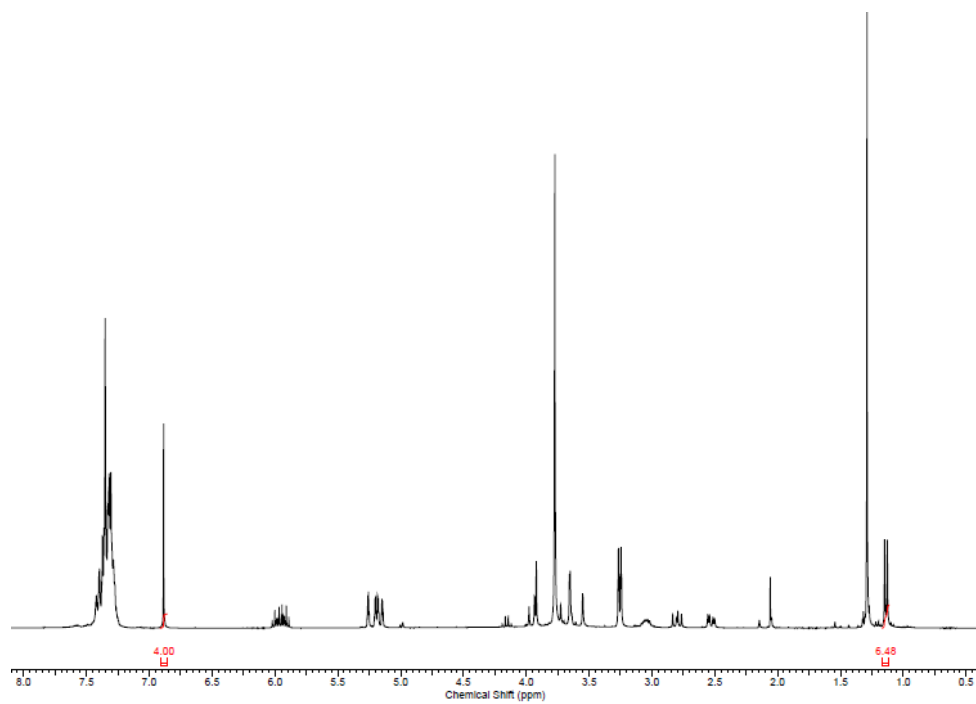
Entry 2



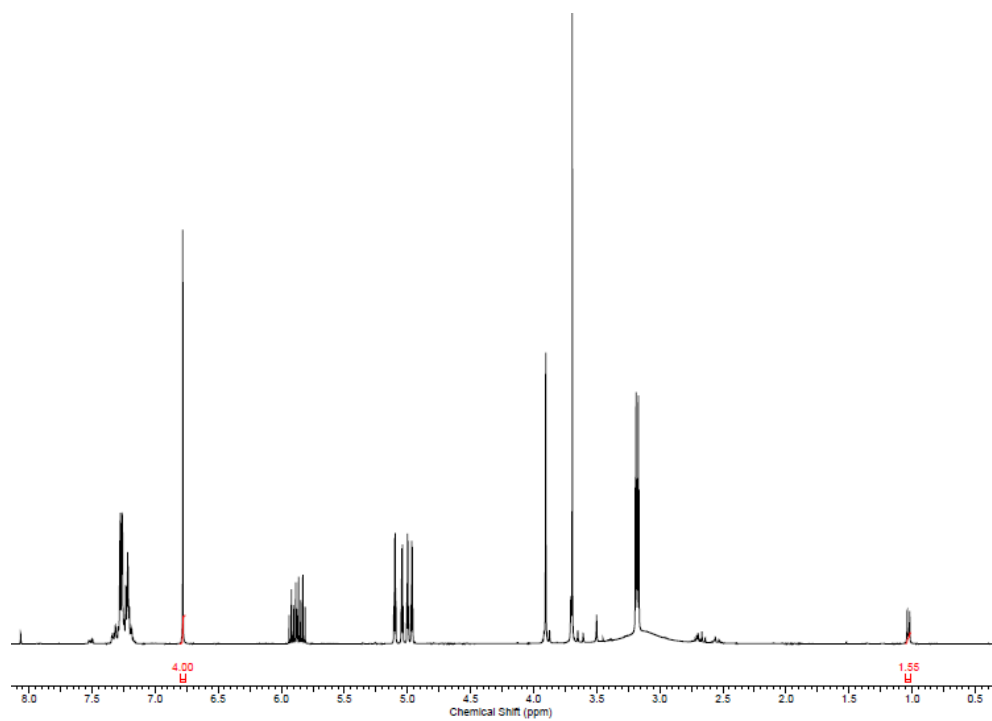
Entry 3



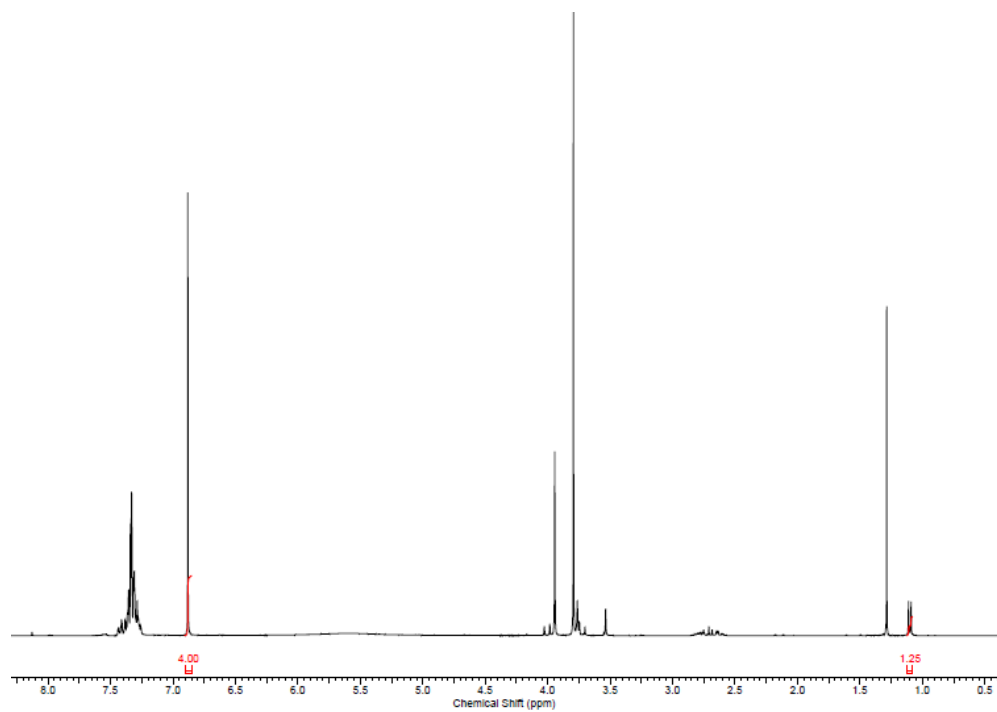
Entry 4



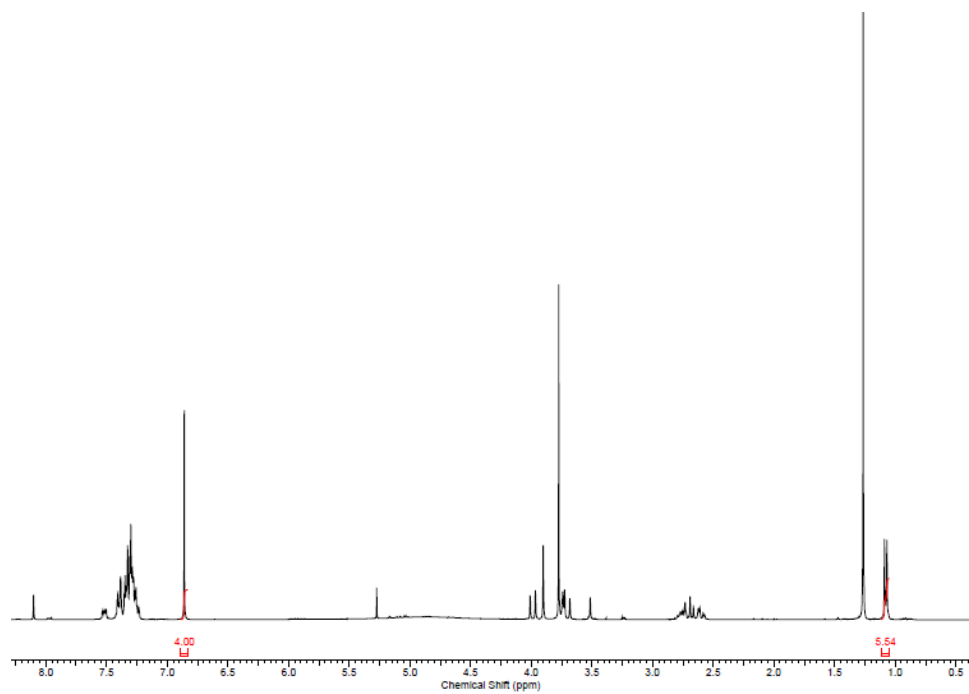
Entry 5



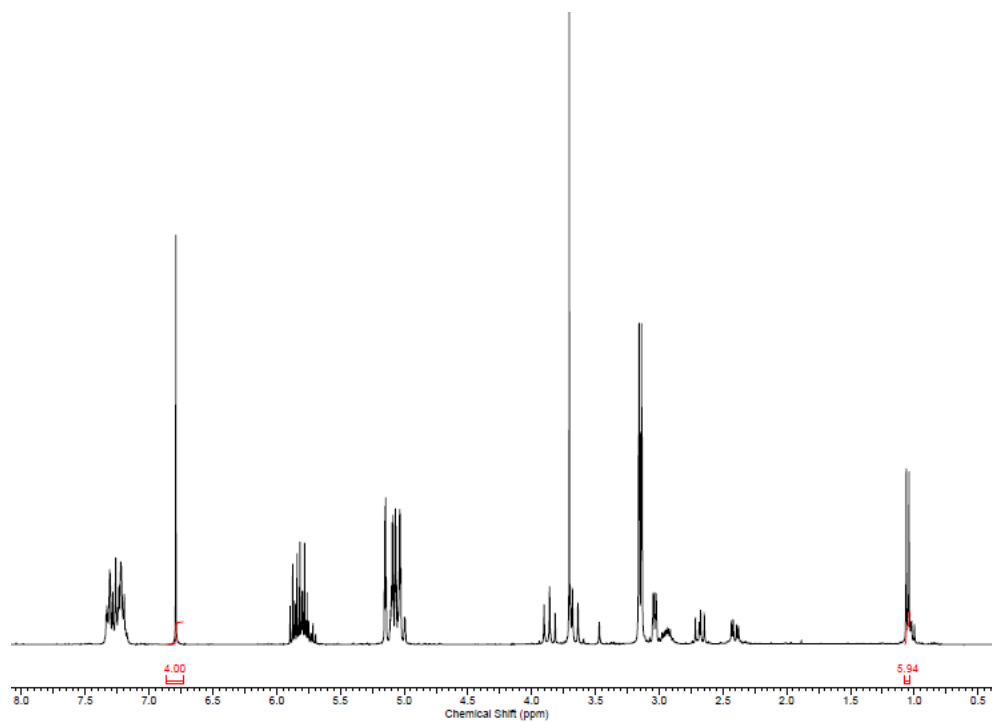
Entry 6



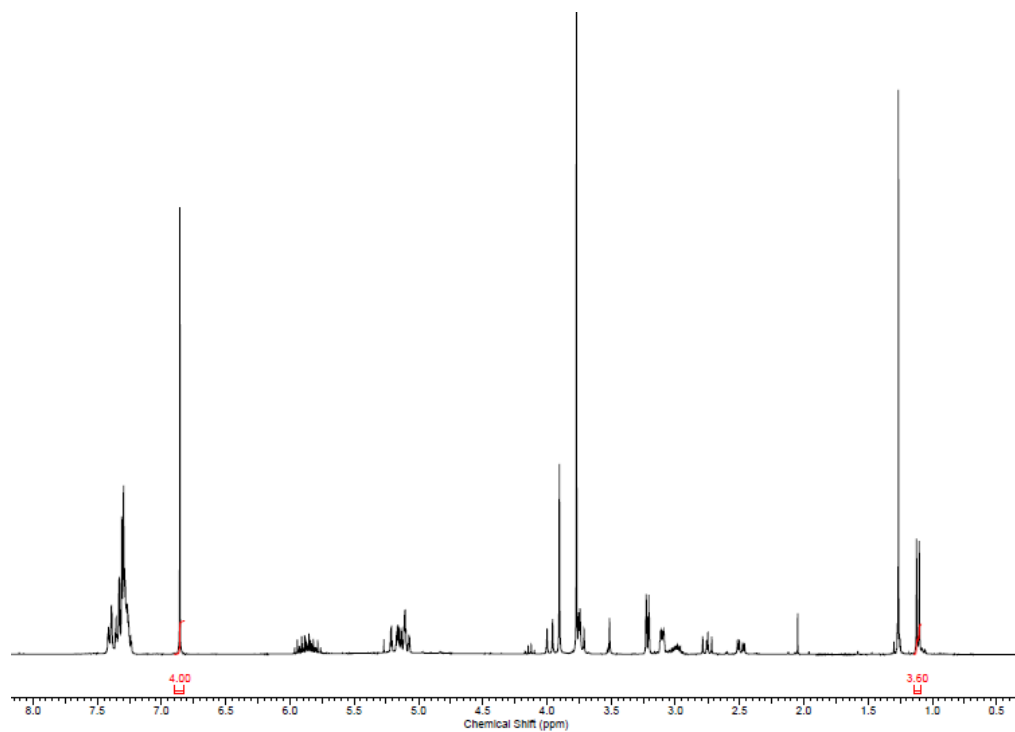
Entry 7



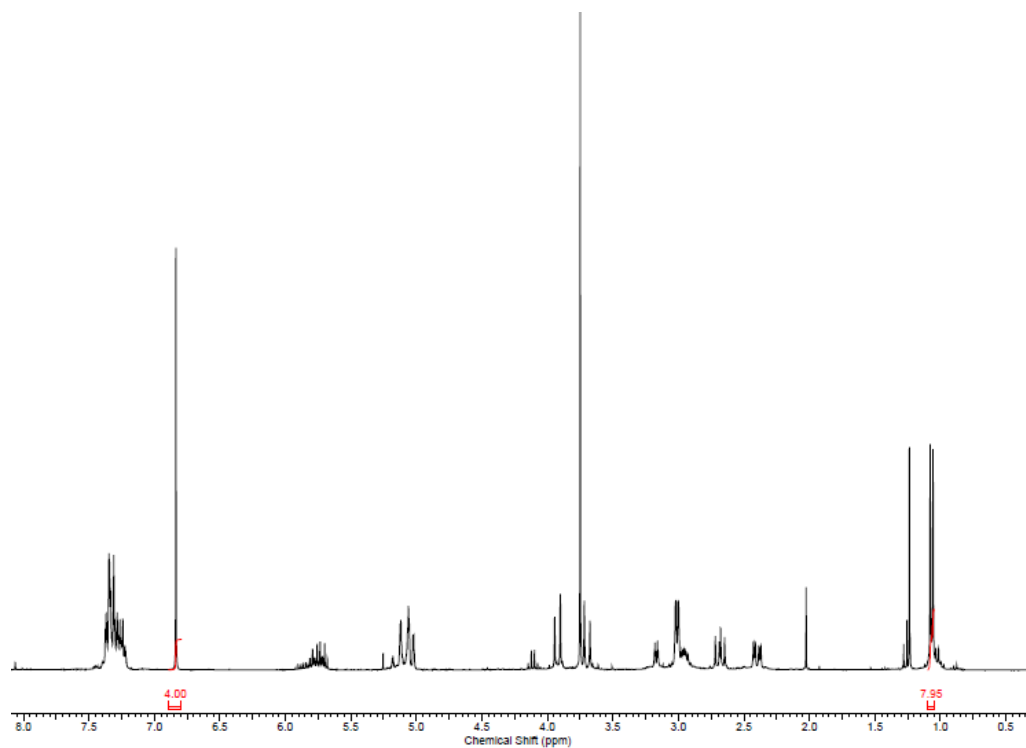
Entry 8



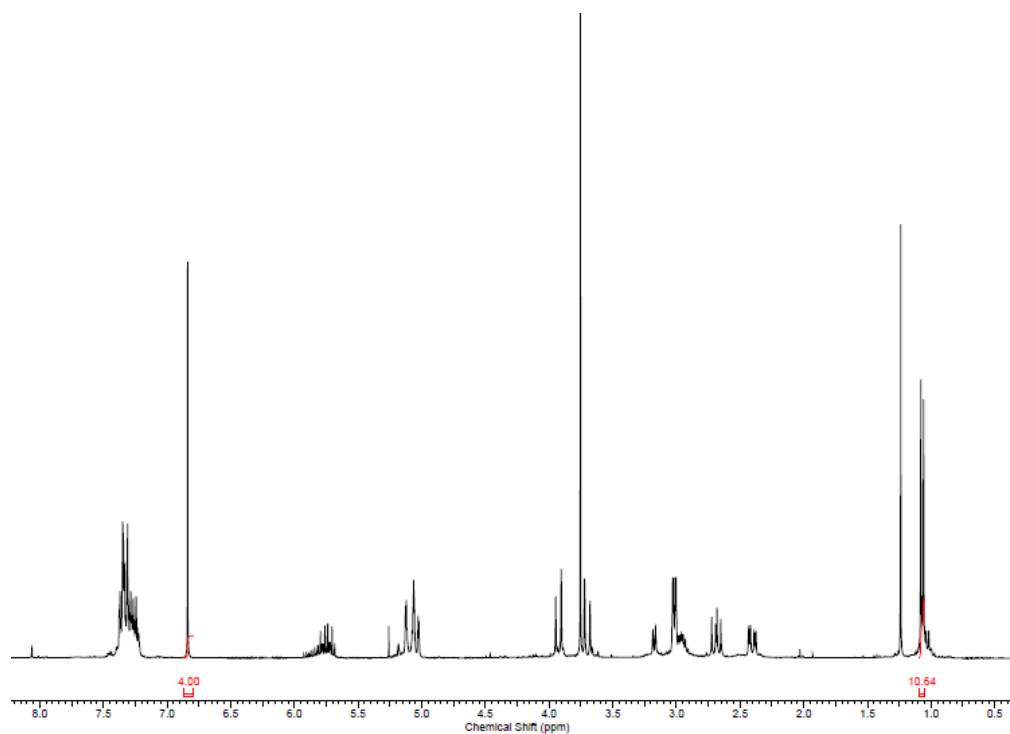
Entry 9



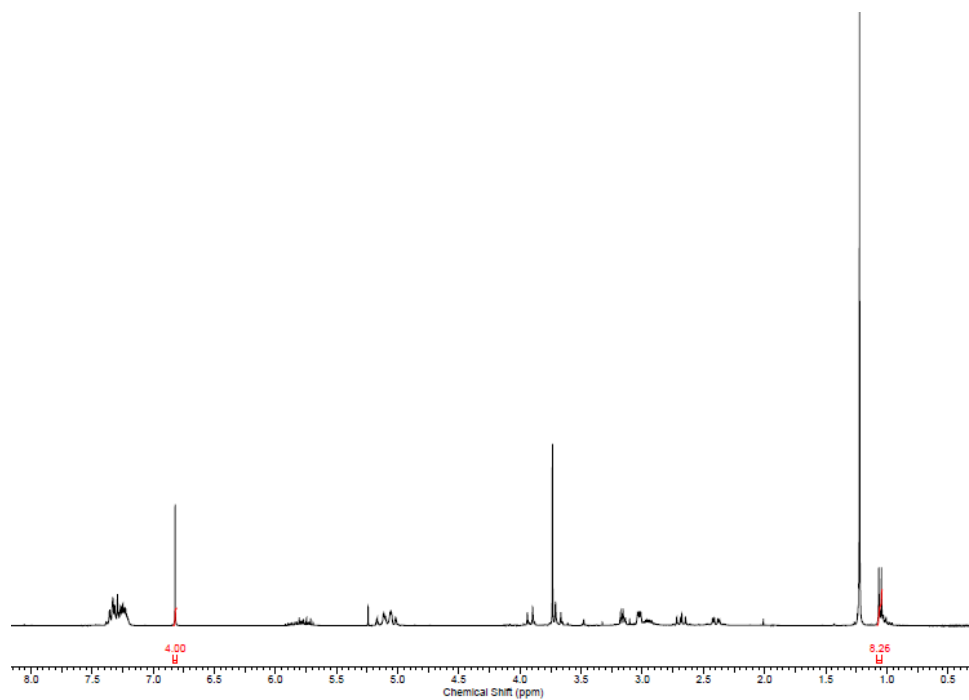
Entry 10



Entry 11



Entry 12



Entry 13

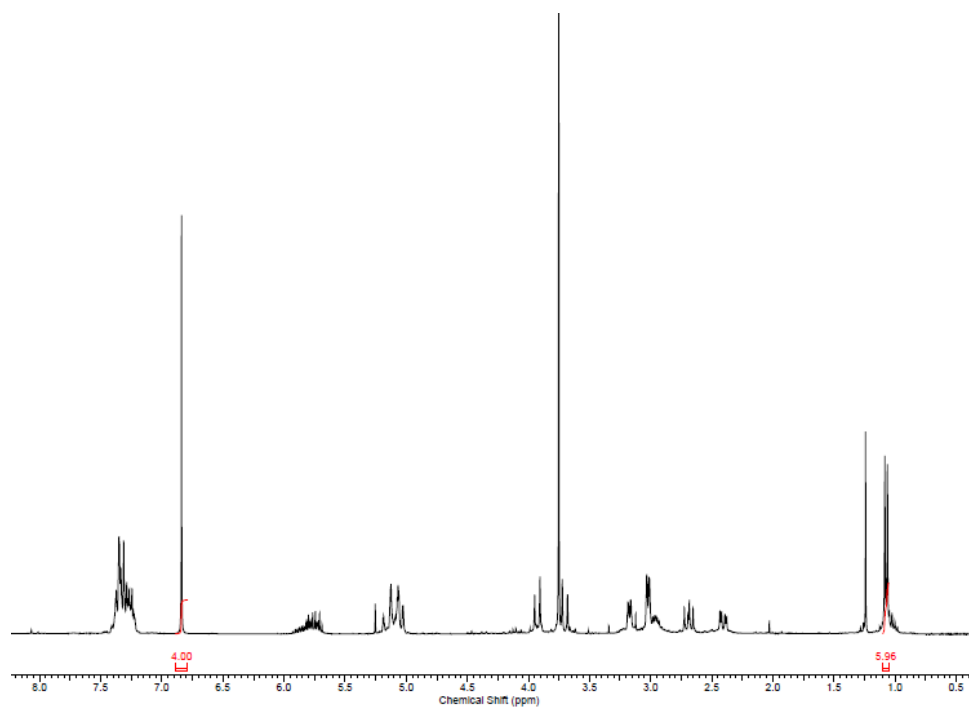
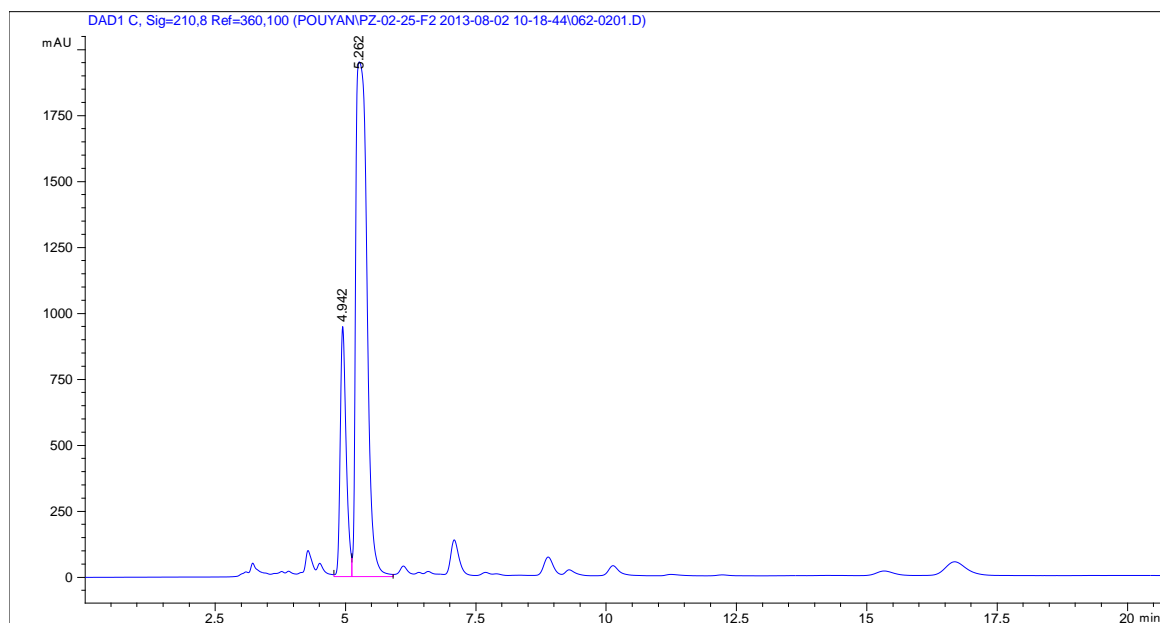


Table 2.4 Intramolecular hydroamination of nitrones promoted by nucleophilic addition

HPLC Data

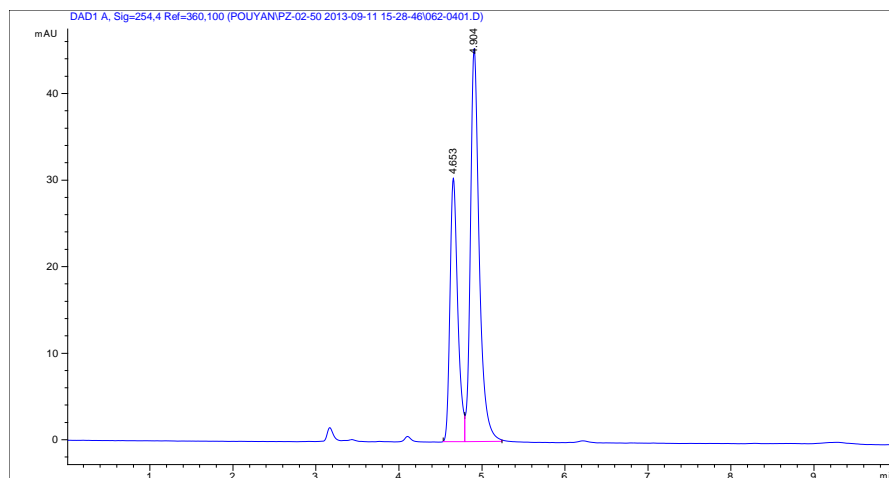
HPLC data used to obtain % *ee*, by comparing obtained area of peaks for each separated enantiomer. The solvent system used is listed for each entry.

Entry 7 (10% *i*-PrOH:90% Hexanes)



Peak	Time	Area	Height	Width	Area %	Symmetry
1	4.942	7524.2	948.1	0.1186	20.530	0.674
2	5.262	29125.2	1951.4	0.2401	79.470	0.465

Entry 8 (10% *i*-PrOH:90% Hexanes)

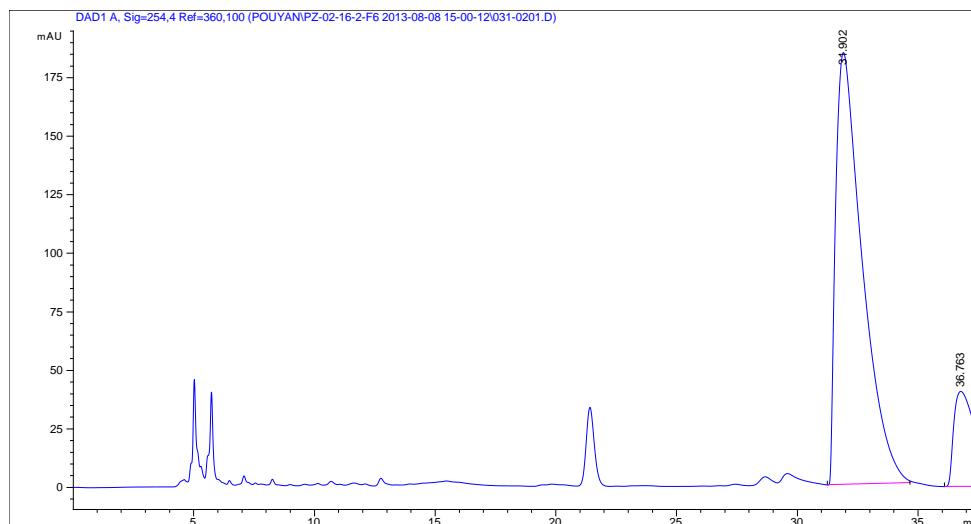


Peak	Time	Area	Height	Width	Area %	Symmetry
1	4.653	198.3	30.5	0.0979	37.109	0.708
2	4.904	336.2	45.5	0.1102	62.891	0.673

Table 2.5 Nucleophilic scan for chiral cyclic nitron synthesis

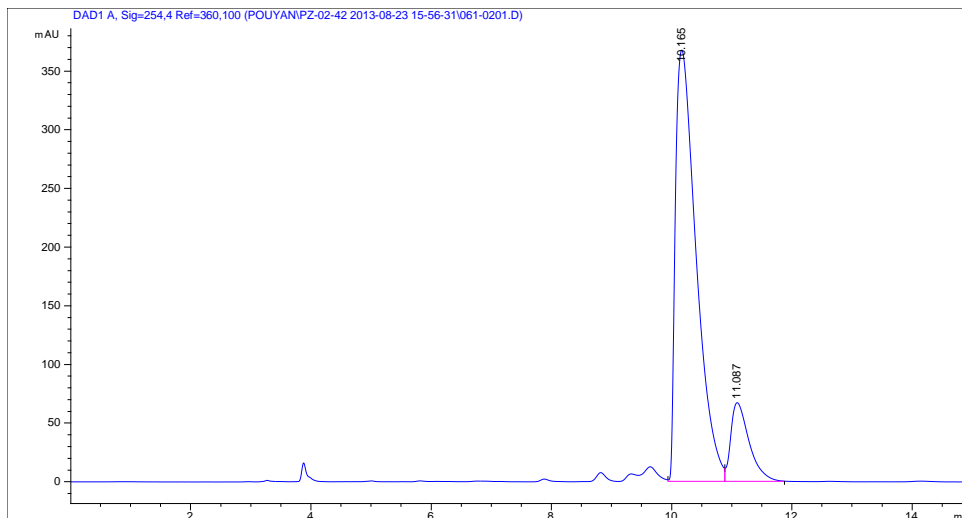
HPLC Data

Entry 2 (5% *i*-PrOH:95% Hexanes)



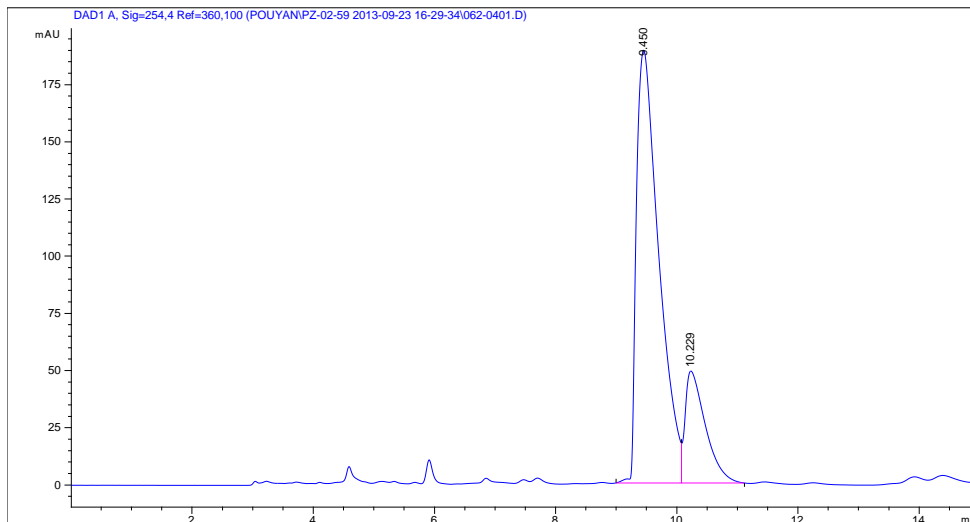
Peak	Time	Area	Height	Width	Area %	Symmetry
1	31.902	14171.5	184.6	1.1278	85.633	0.374
2	4.904	336.2	45.5	0.1102	62.891	0.673

Entry 3 (5% *i*-PrOH:95% Hexanes)



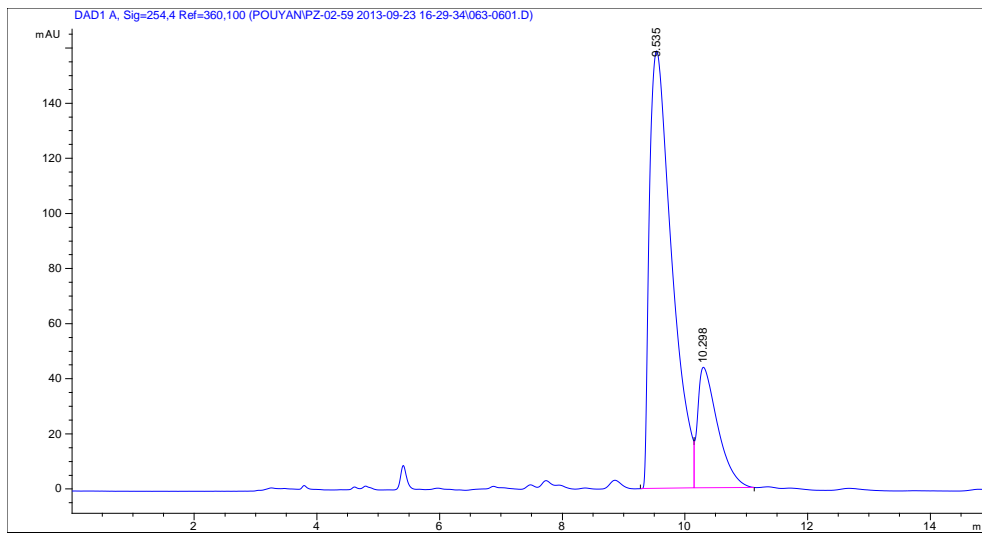
Peak	Time	Area	Height	Width	Area %	Symmetry
1	10.165	8829.4	367.8	0.3701	86.044	0.402
2	11.087	1432.1	67.2	0.3228	13.956	0.5

Entry 4 (5% *i*-PrOH:95% Hexanes)



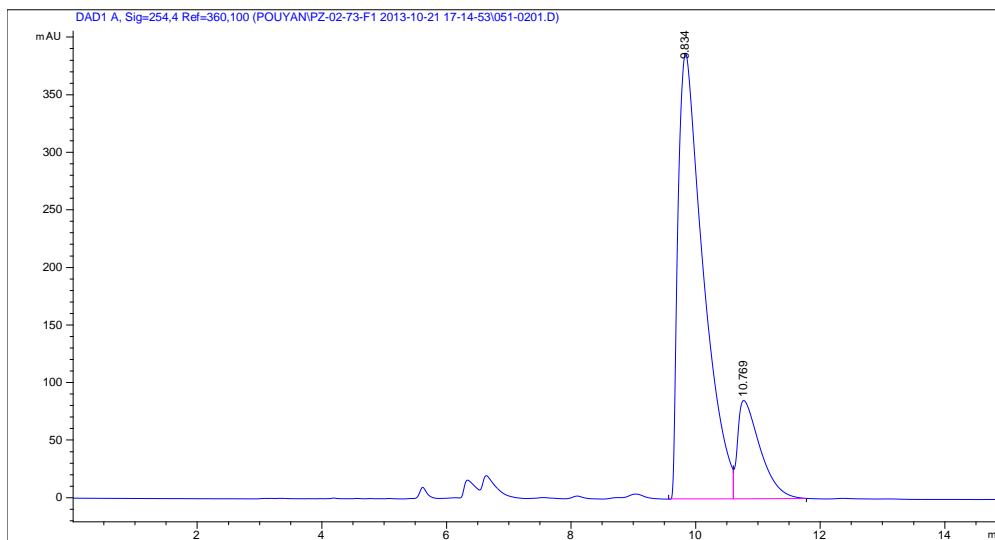
Peak	Time	Area	Height	Width	Area %	Symmetry
1	9.45	4861.9	189.2	0.3858	81.000	0.431
2	10.229	1140.5	49	0.3476	19.000	0.363

Entry 5 (5% *i*-PrOH:95% Hexanes)



Peak	Time	Area	Height	Width	Area %	Symmetry
1	9.535	4029.4	158.8	0.384	80.154	0.426
2	10.298	997.7	43.8	0.3417	19.846	0.376

Entry 8 (5% *i*-PrOH:95% Hexanes)

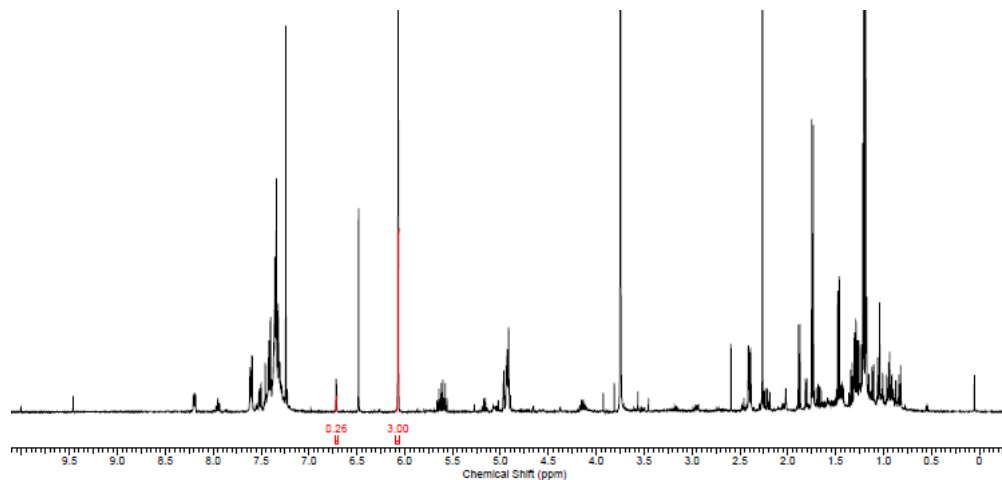


Peak	Time	Area	Height	Width	Area %	Symmetry
1	9.834	10849.7	387.3	0.4168	83.374	0.385
2	10.769	2163.6	85.5	0.3793	16.626	0.344

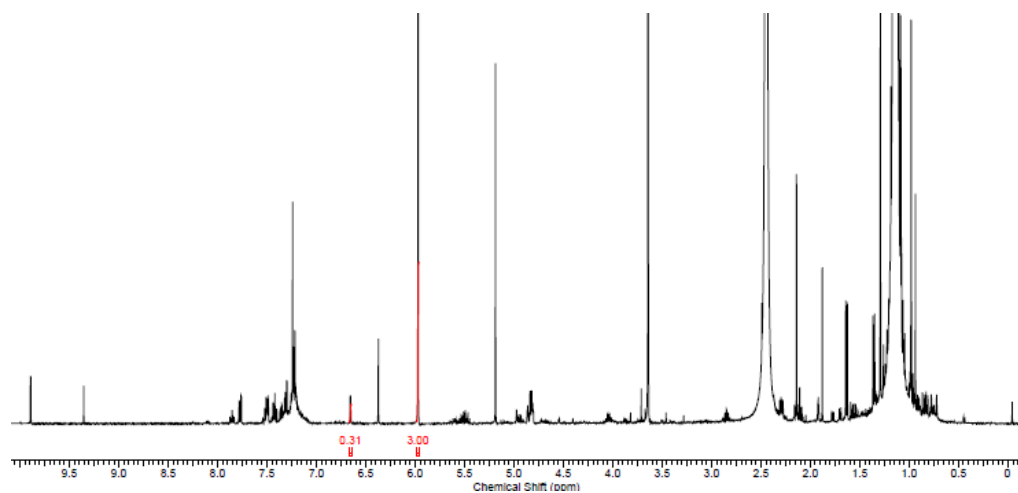
Table 2.6 Solvent scan for chiral cyclic nitron synthesis

NMR yields were obtained by using an internal standard, 1,3,5-trimethoxybenzene (0.125 equiv.) and comparing the internal standard peak (6.08 ppm, 3H, singlet) to the newly formed nitron-proton product peak (6.74 ppm, 1H, doublet).

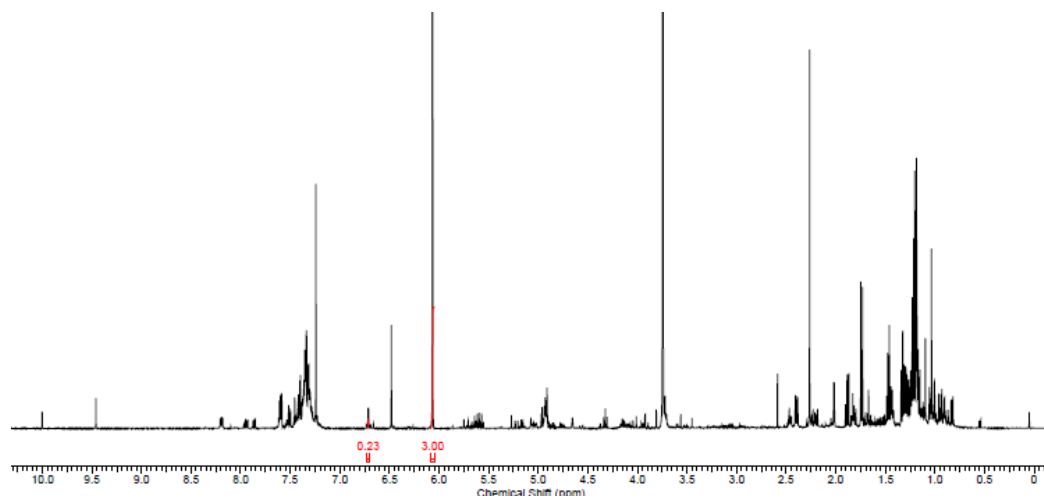
Entry 1



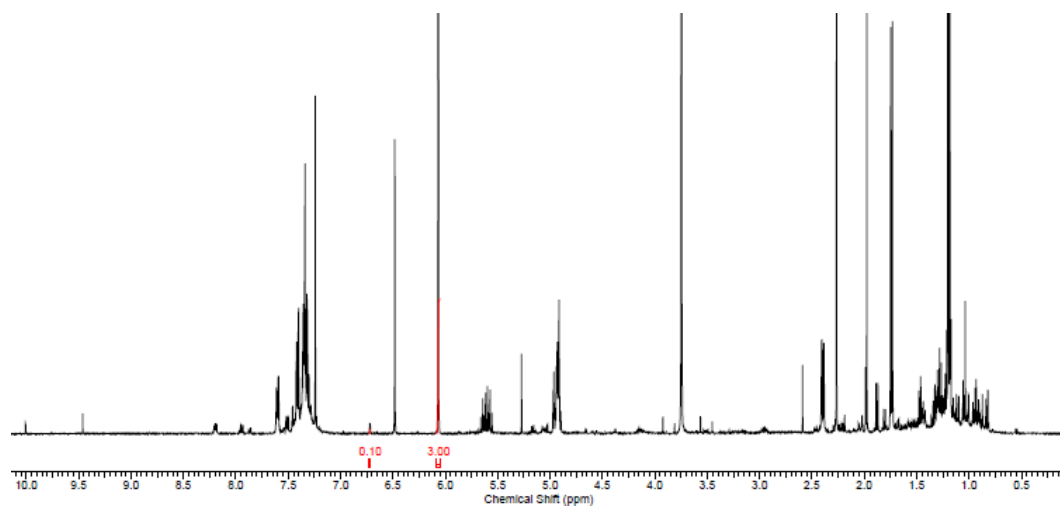
Entry 2



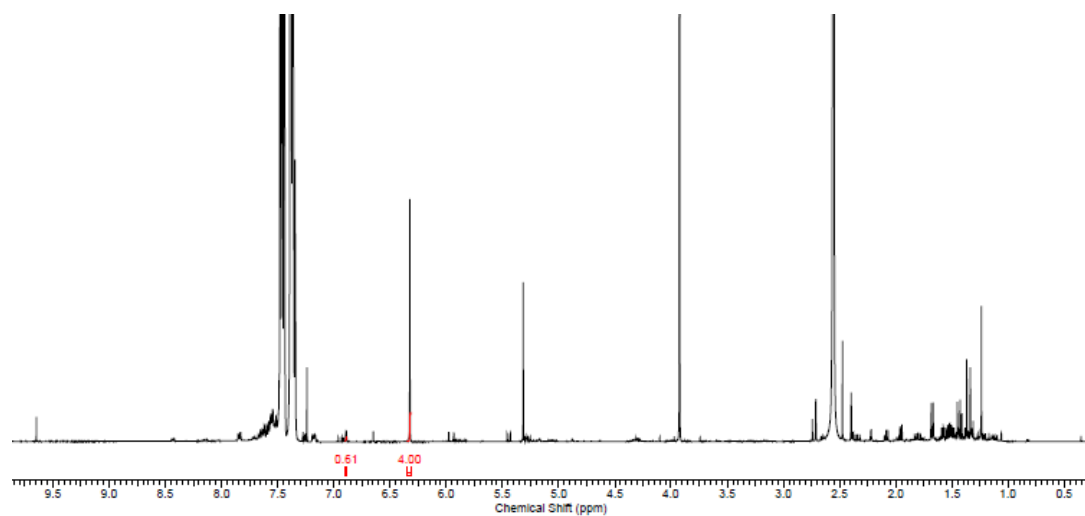
Entry 3



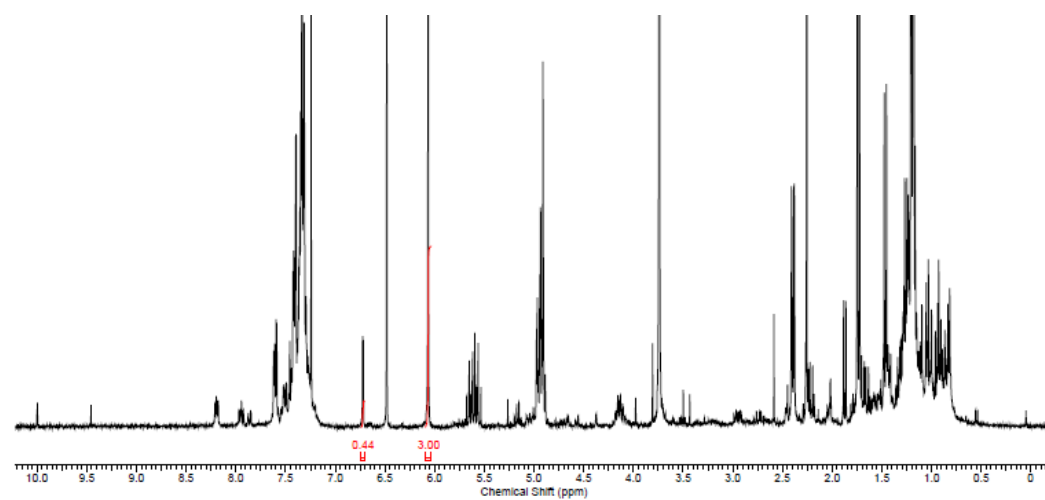
Entry 4



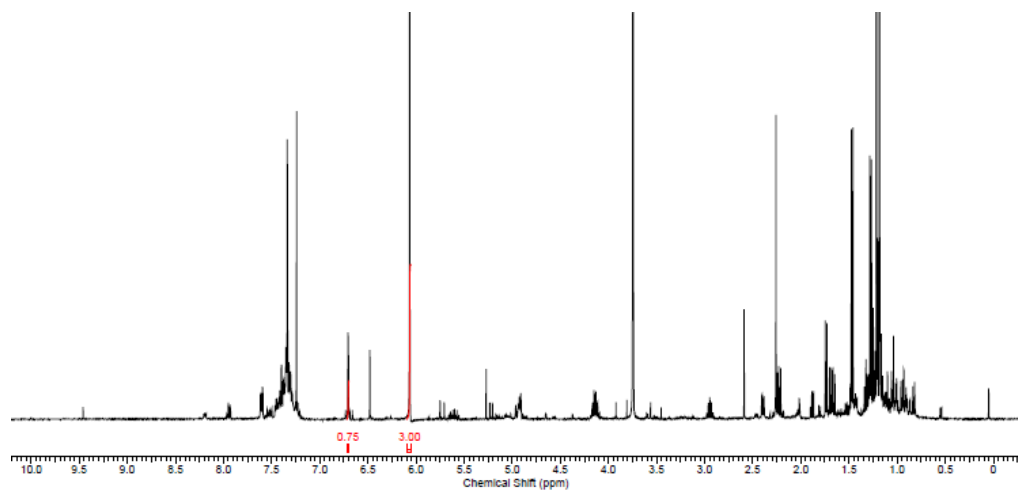
Entry 5



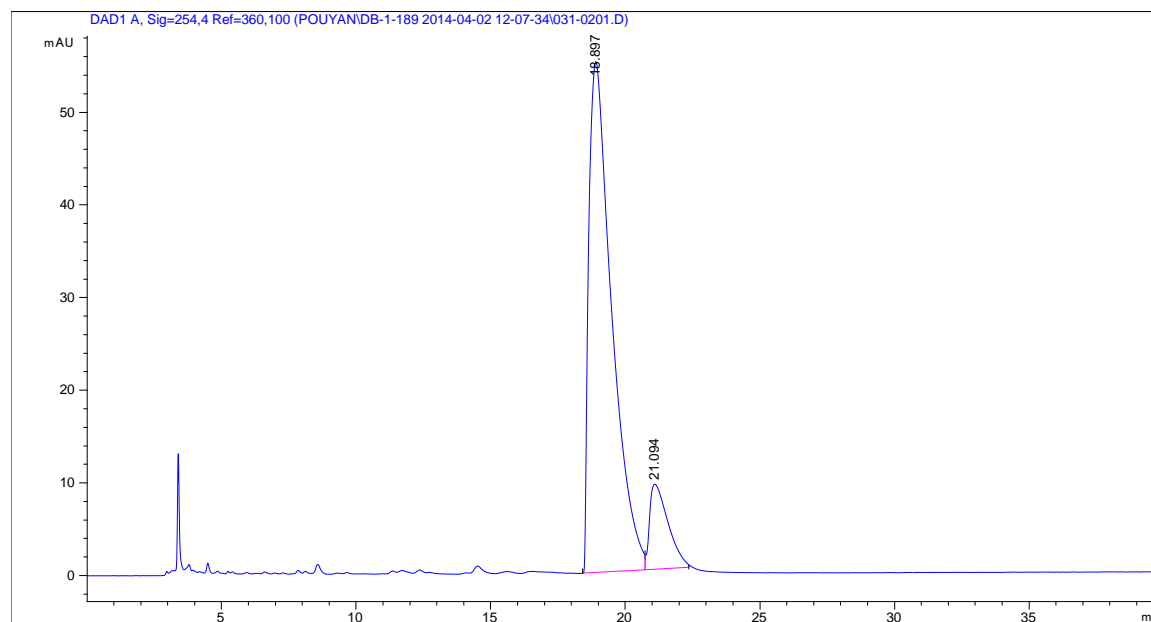
Entry 6



Entry 7



Entry 7 (5% *i*-PrOH:95% Hexanes)



Peak	Time	Area	Height	Width	Area %	Symmetry
1	18.897	3260.6	55.1	0.8719	88.136	0.398
2	21.094	438.9	9.2	0.6392	11.864	0.381

Entry 8

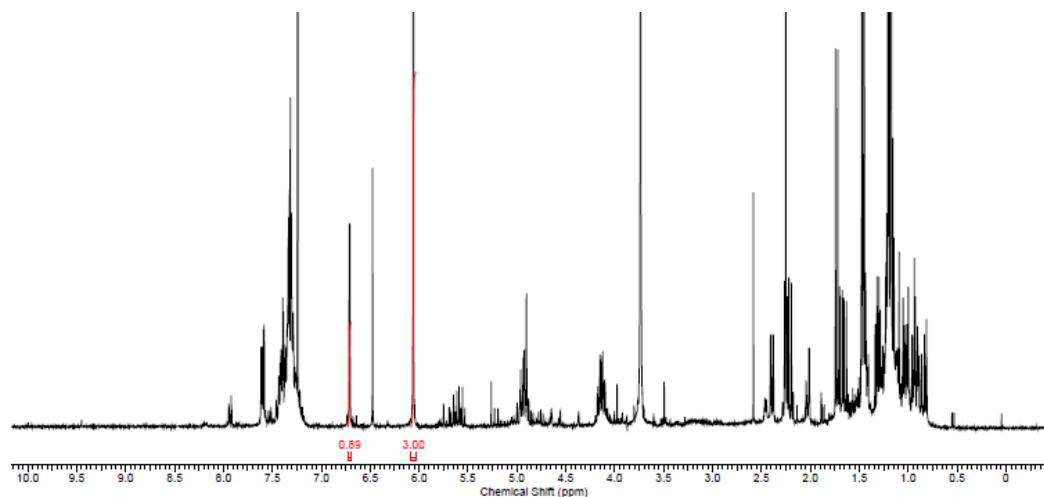
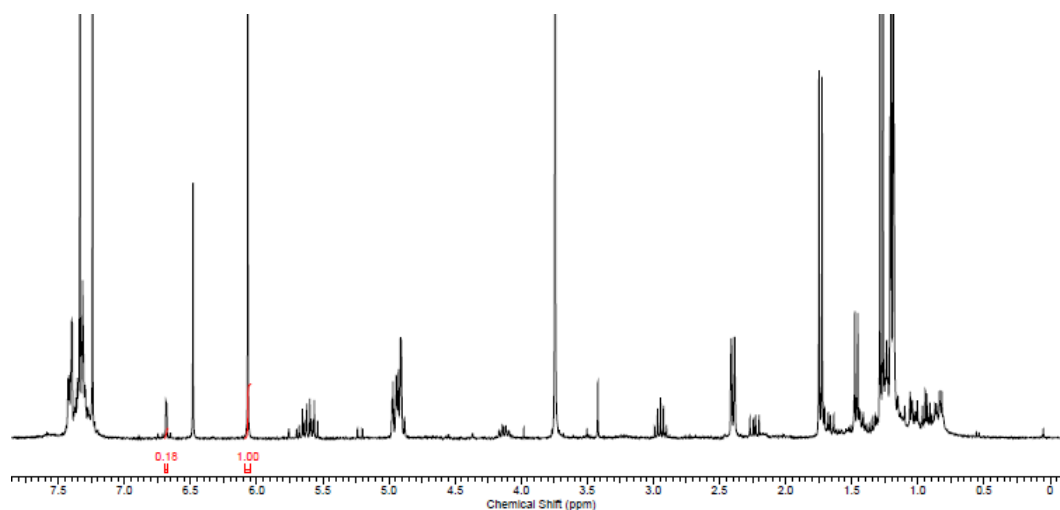


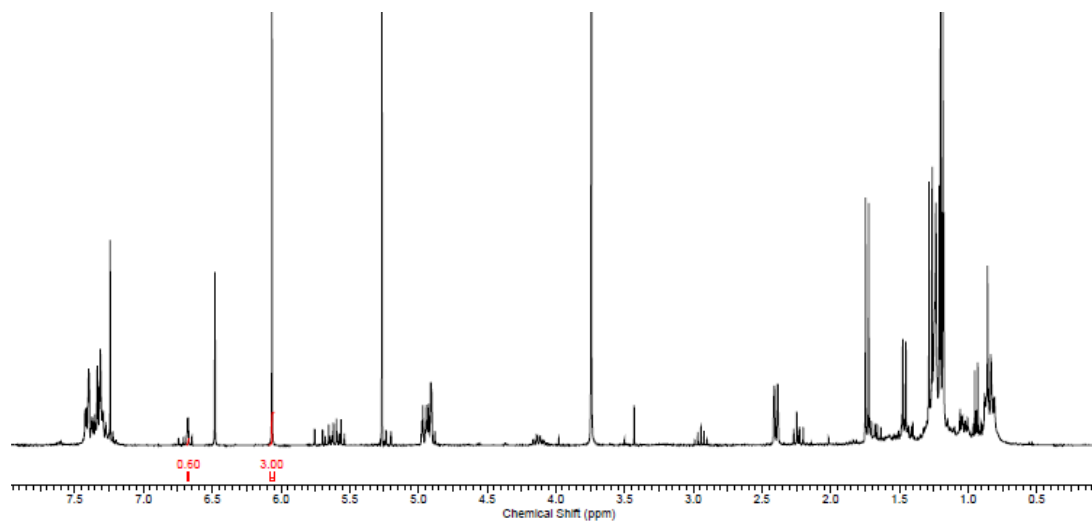
Table 2.7 Additive and reaction conditions scan for chiral cyclic nitron synthesis

NMR yields were obtained by using an internal standard, 1,3,5-trimethoxybenzene (0.125 equiv.) and comparing the internal standard peak (6.08 ppm, 3H, singlet) to the newly formed nitron-proton product peak (6.74 ppm, 1H, doublet). HPLC data shown for applicable entries.

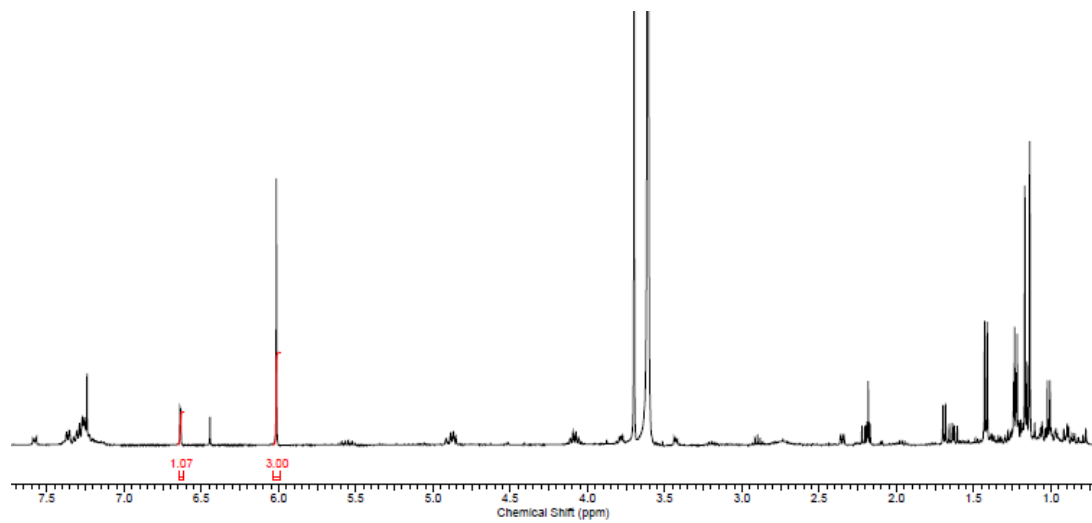
Entry 1



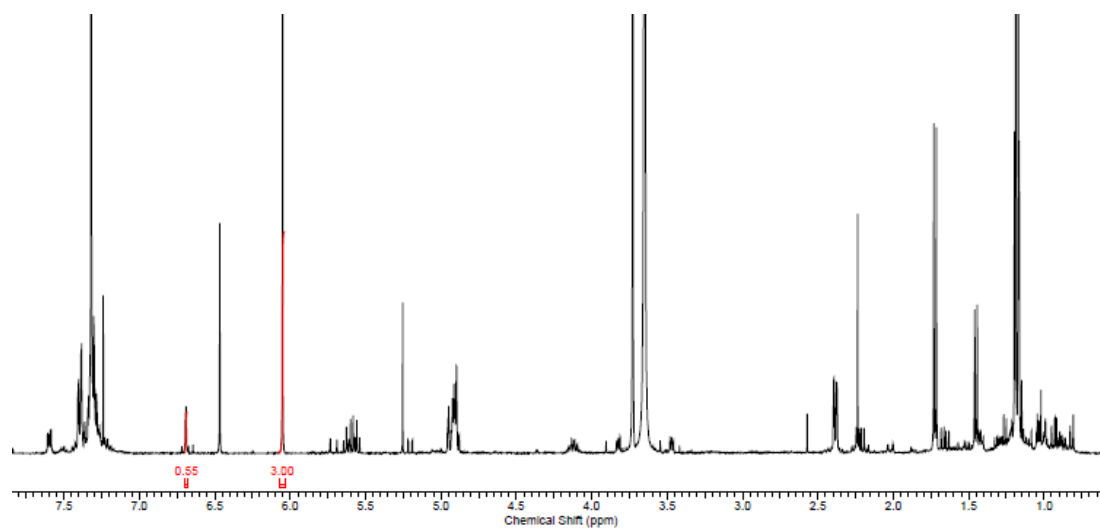
Entry 2



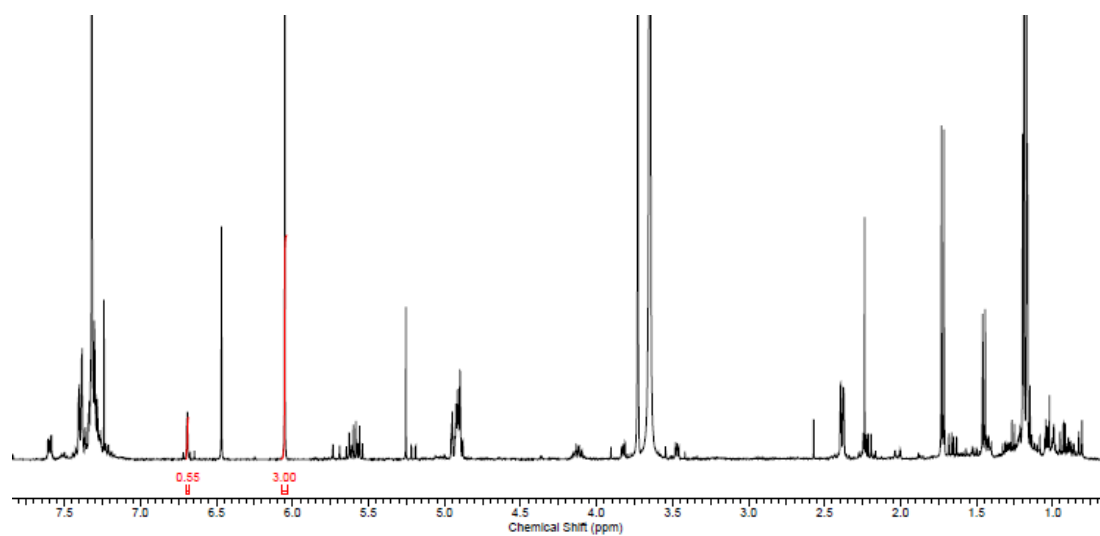
Entry 3



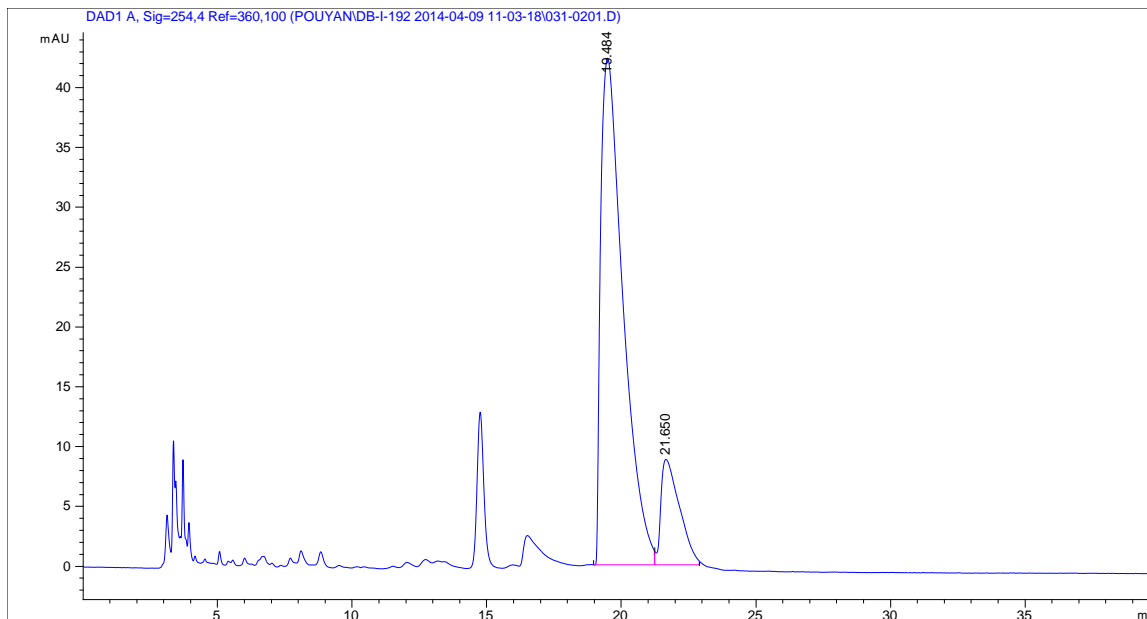
Entry 4



Entry 5

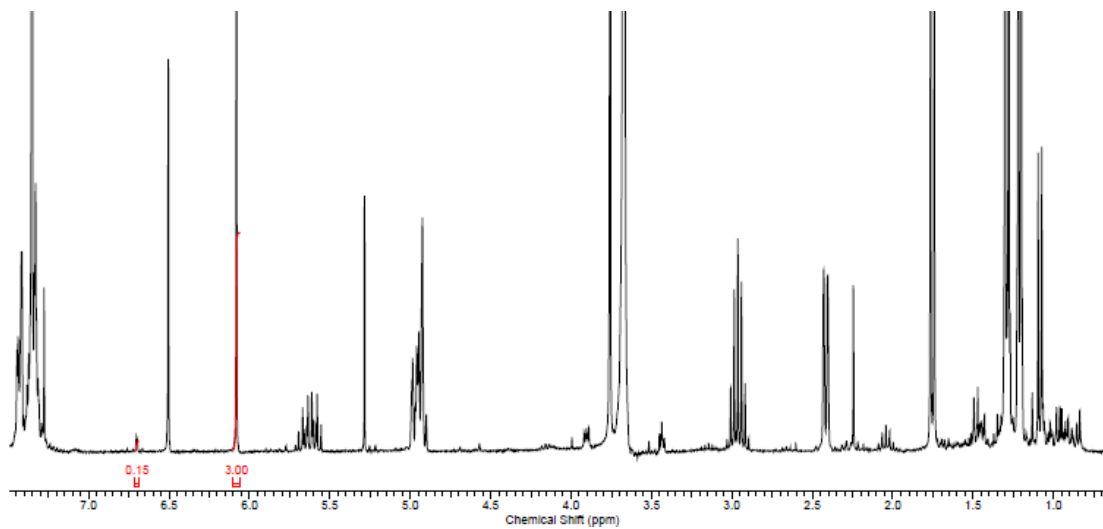


Entry 5 (5% *i*-PrOH:95% Hexanes)

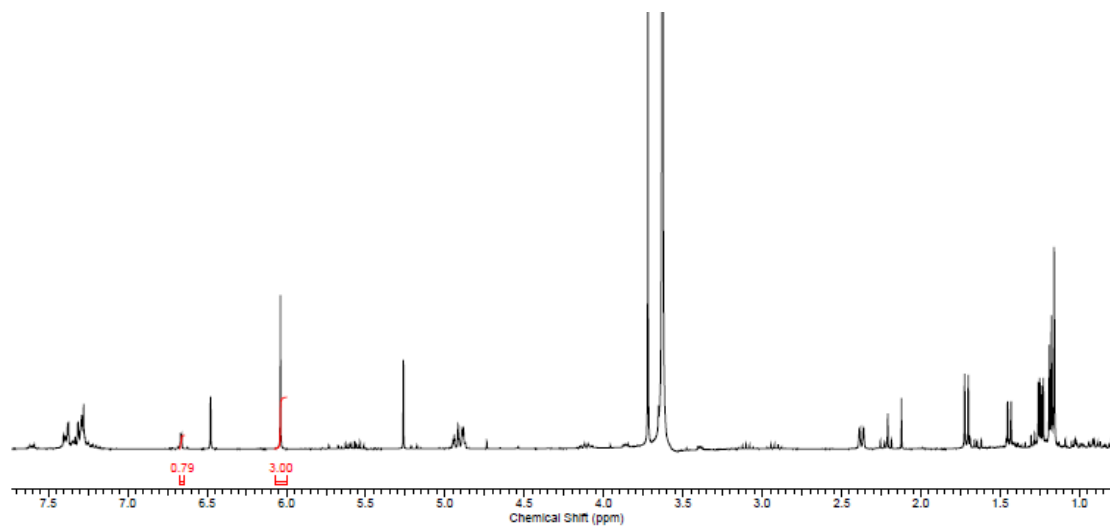


Peak	Time	Area	Height	Width	Area %	Symmetry
1	19.484	2450	42.3	0.867	85.215	0.402
2	21.65	425.1	8.8	0.6723	14.785	0.358

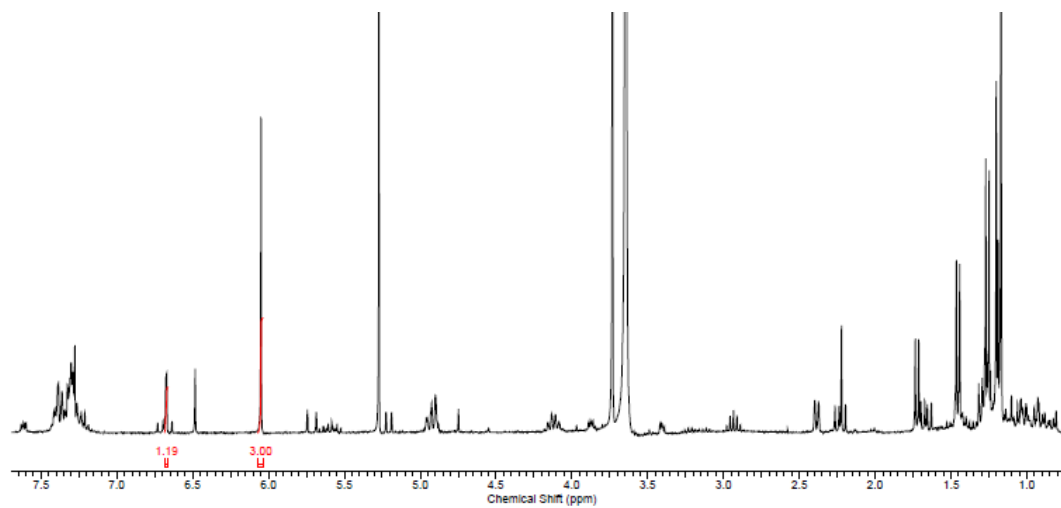
Entry 6



Entry 7



Entry 8



Entry 9

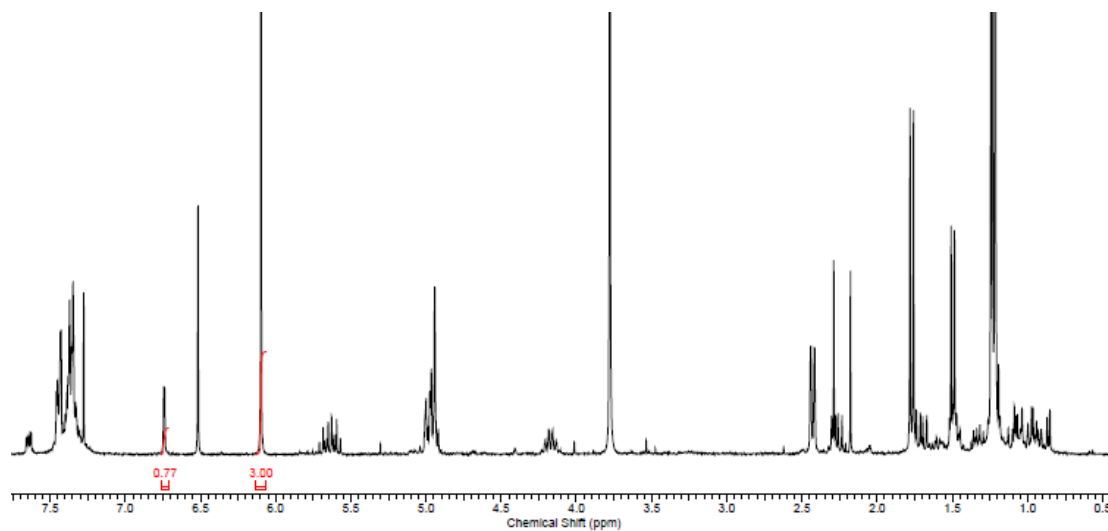
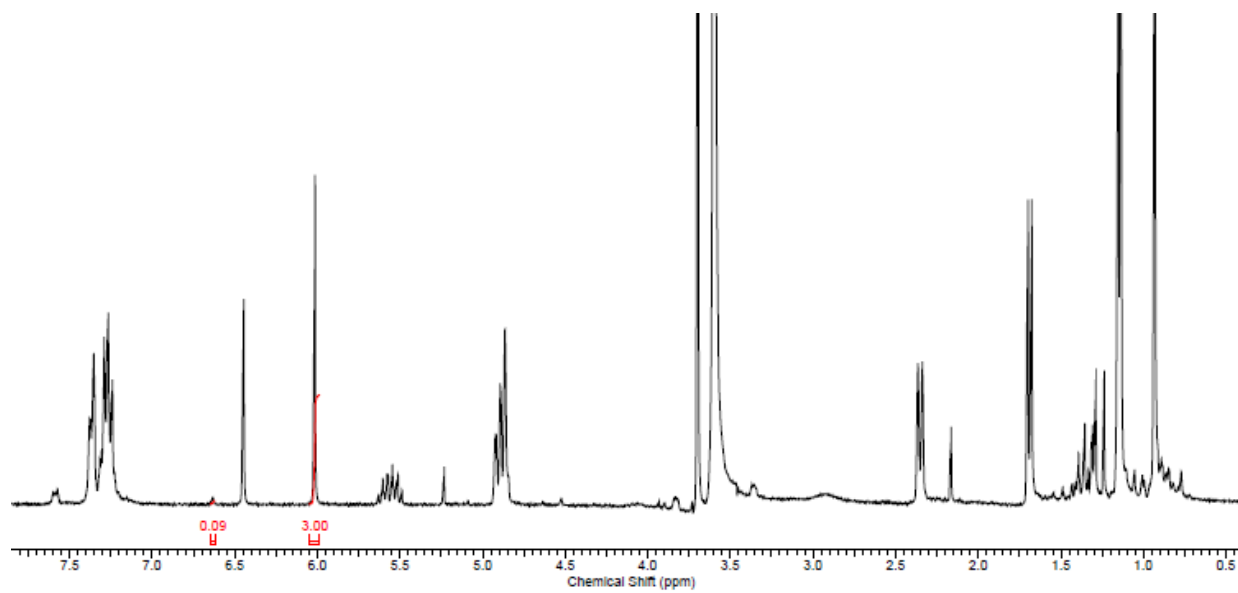
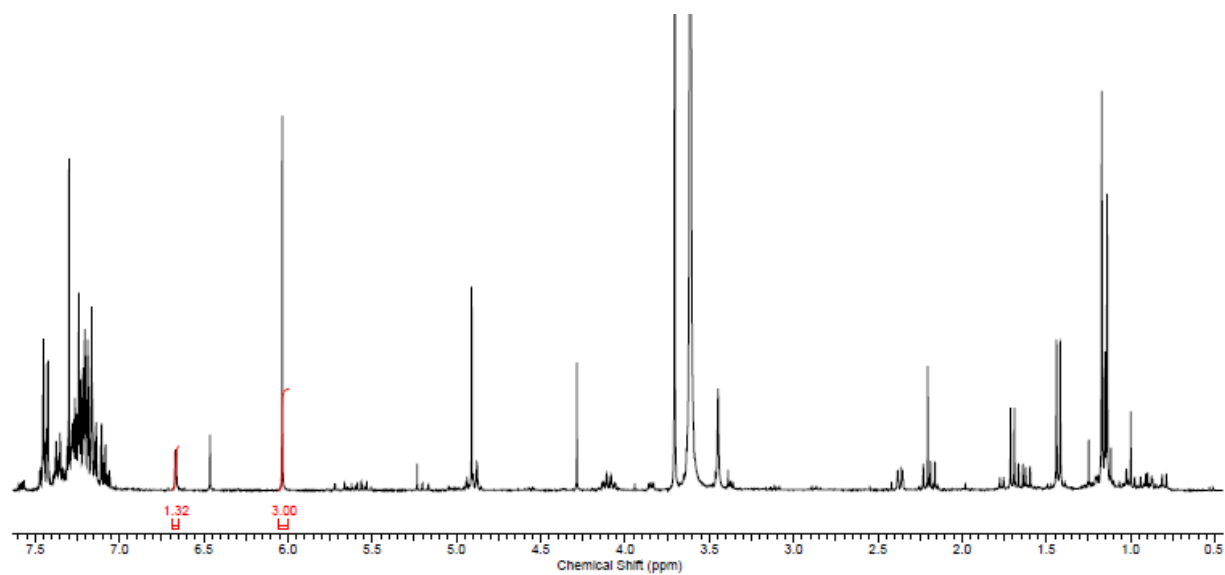


Table 2.8 Secondary nucleophile scan for chiral cyclic nitron synthesis

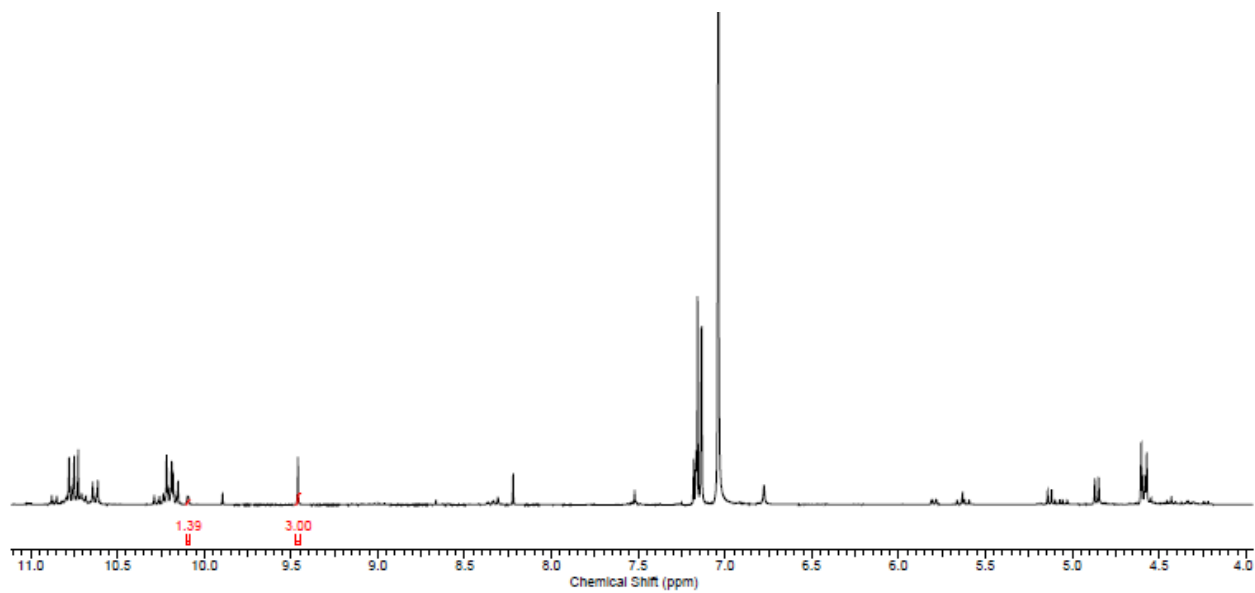
Entry 1



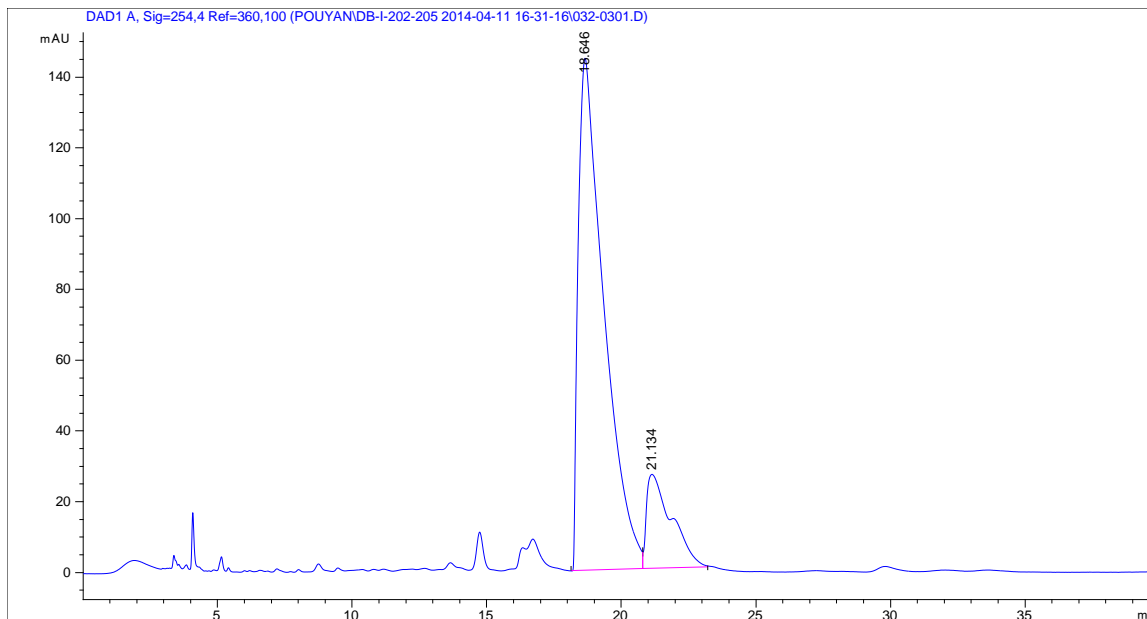
Entry 2



Entry 3

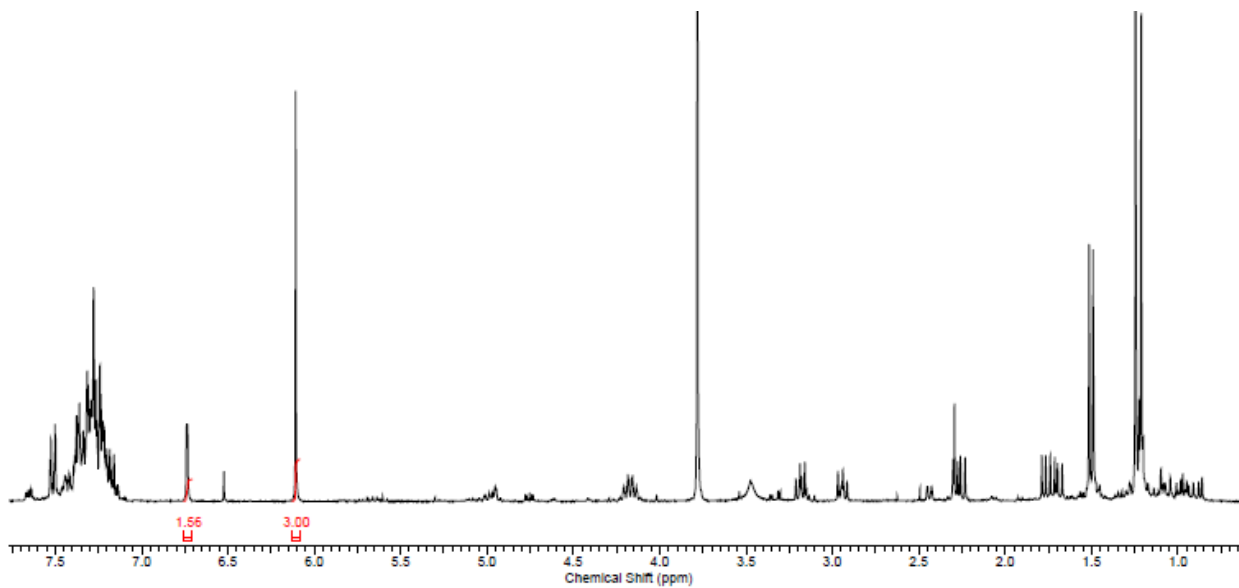


Entry 3 (5% *i*-PrOH:95% Hexanes)

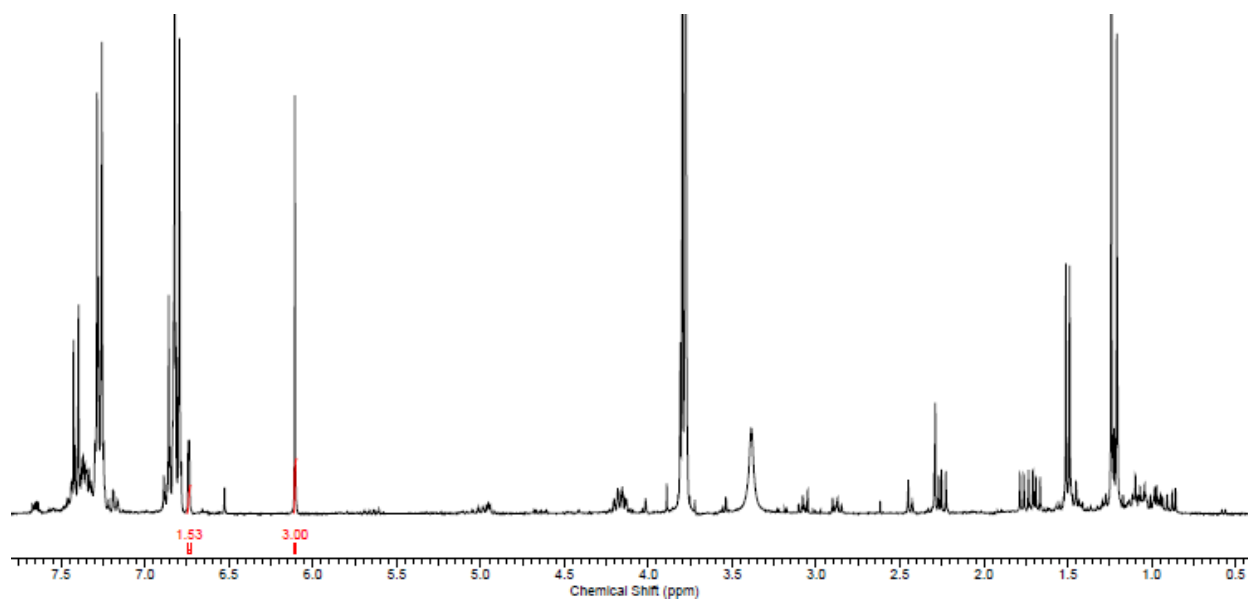


Peak	Time	Area	Height	Width	Area %	Symmetry
1	18.646	9605.4	144.8	0.9401	84.837	0.329
2	21.134	1716.8	26.6	0.9084	15.163	0.26

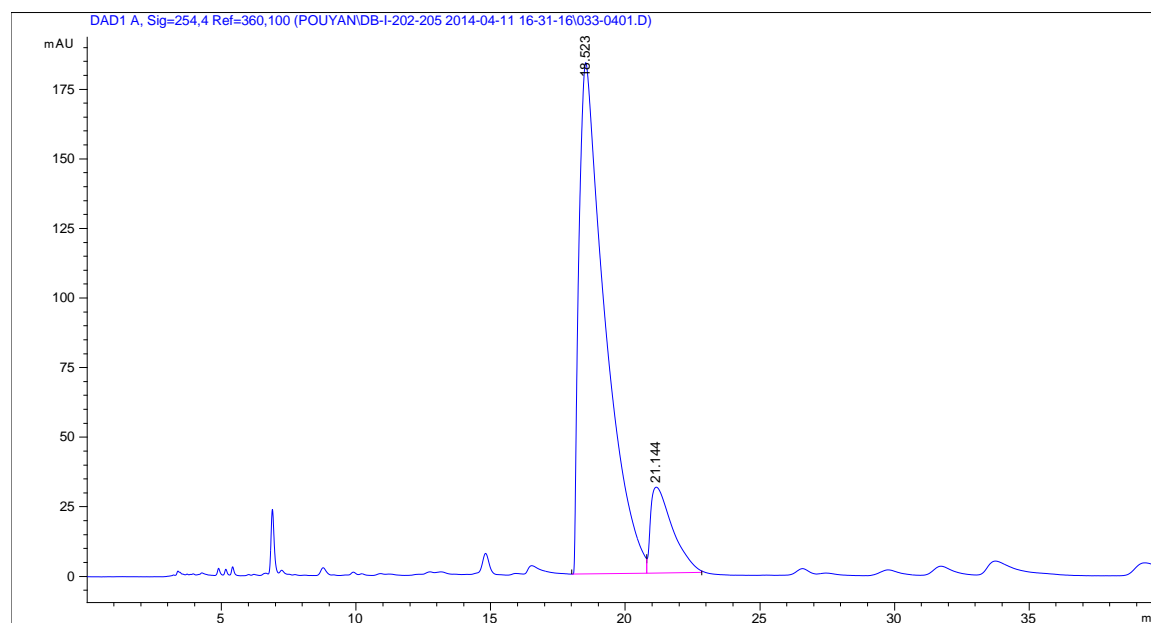
Entry 4



Entry 5

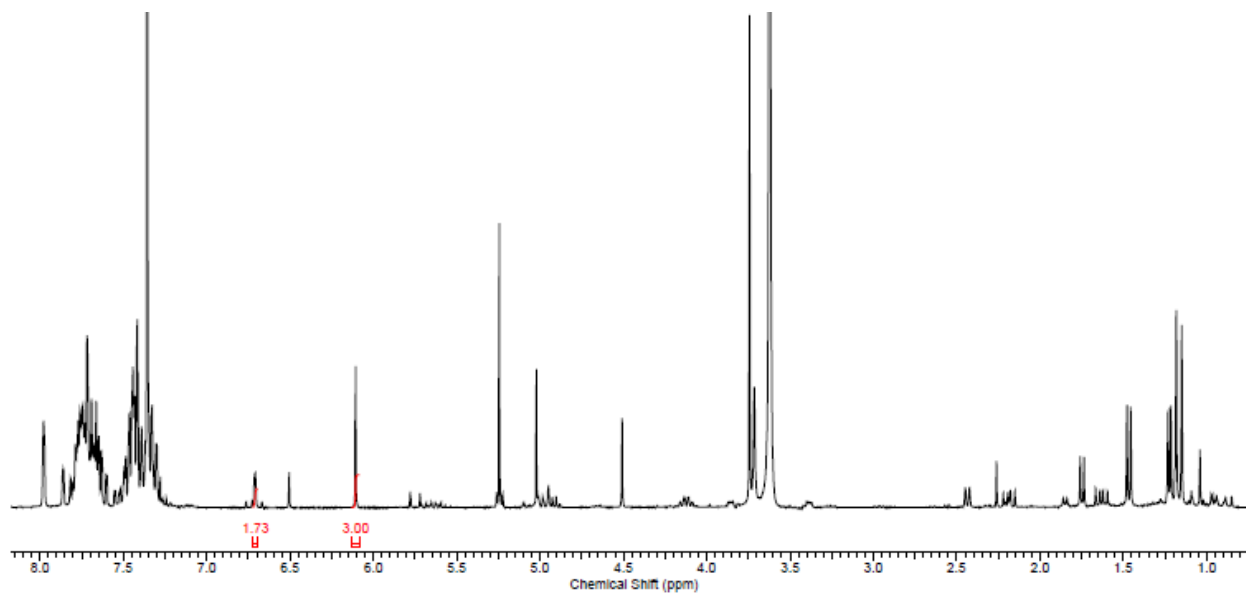


Entry 5 (5% *i*-PrOH:95% Hexanes)

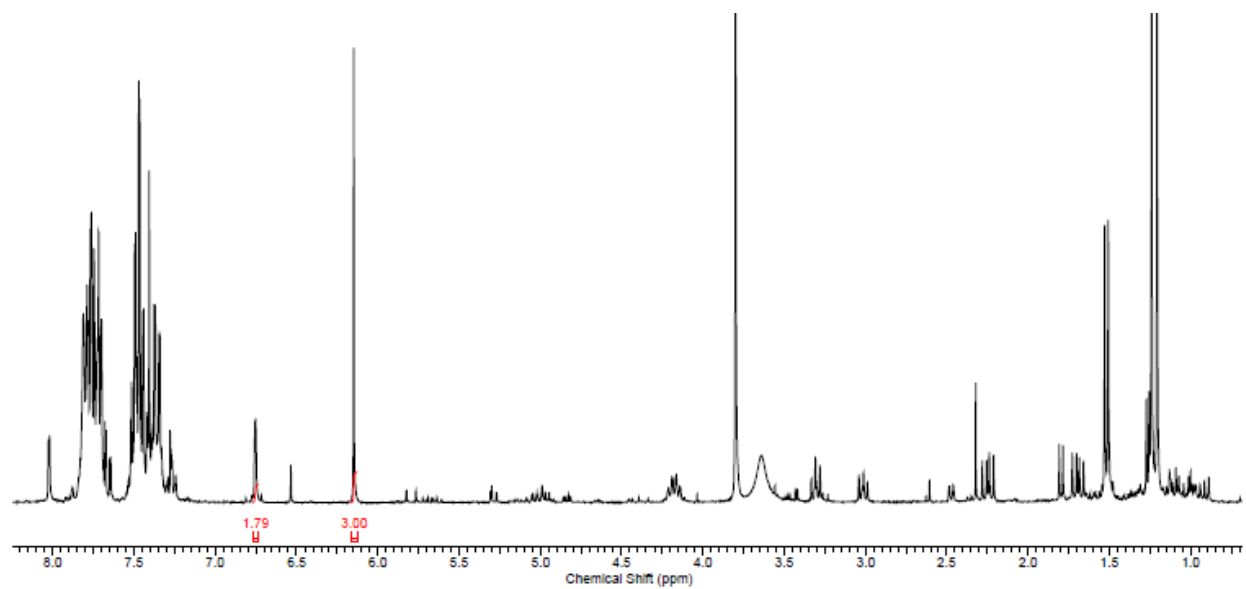


Peak	Time	Area	Height	Width	Area %	Symmetry
1	18.523	12373.3	183.7	0.9637	87.552	0.32
2	21.144	1759.2	30.9	0.8206	12.448	0.323

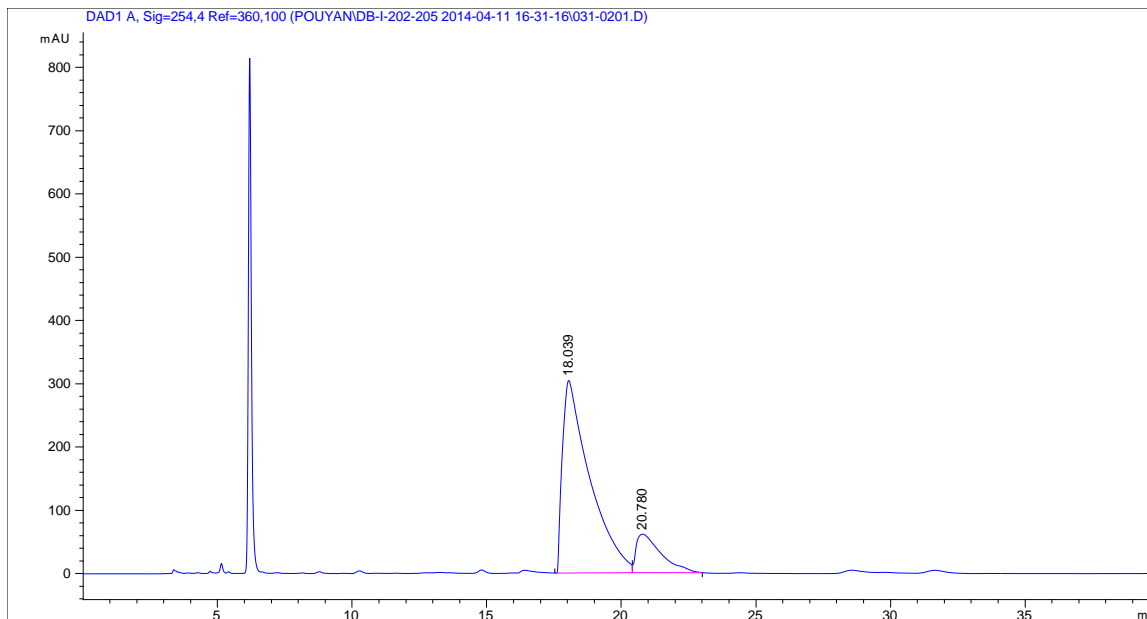
Entry 6



Entry 7



Entry 7 (5% *i*-PrOH:95% Hexanes)



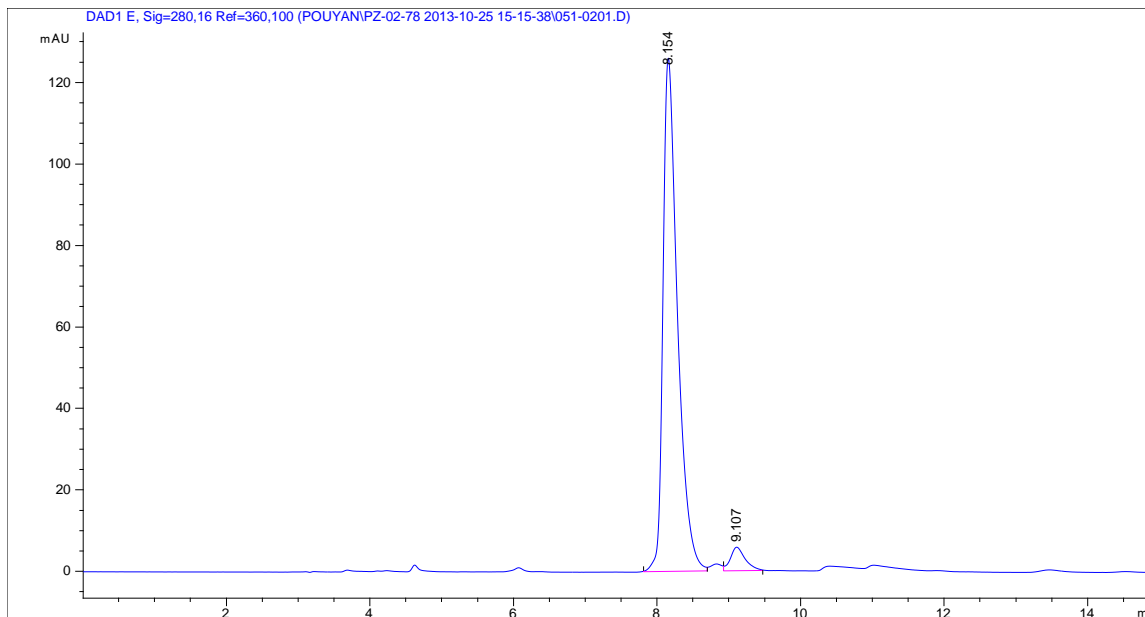
Peak	Time	Area	Height	Width	Area %	Symmetry
1	18.039	21518.5	304.3	0.9891	84.384	0.278
2	20.78	3982.3	61.4	0.9311	15.616	0.309

Scheme 2.10 Optimized reaction conditions for chiral cyclic nitron synthesis

HPLC Data

HPLC data used to obtain % *ee*, by comparing obtained area of peaks for each separated enantiomer. The solvent system used is listed for each entry.

(5% *i*-PrOH:95% Hexanes)



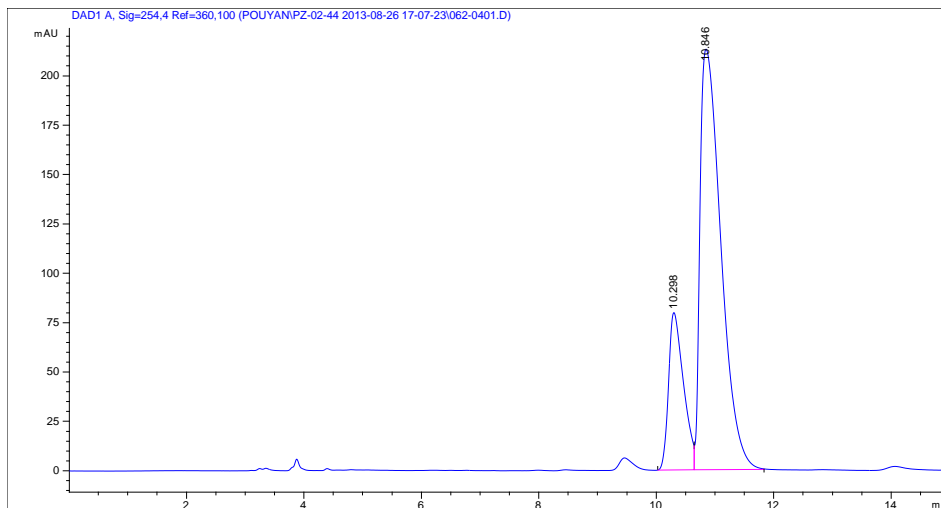
Peak	Time	Area	Height	Width	Area %	Symmetry
1	8.154	1776.4	126.1	0.2104	95.469	0.537
2	9.107	84.3	5.8	0.2126	4.531	0.694

Scheme 2.11 Naphthalene nitron for synthesis of cyclic chiral nitron

HPLC Data

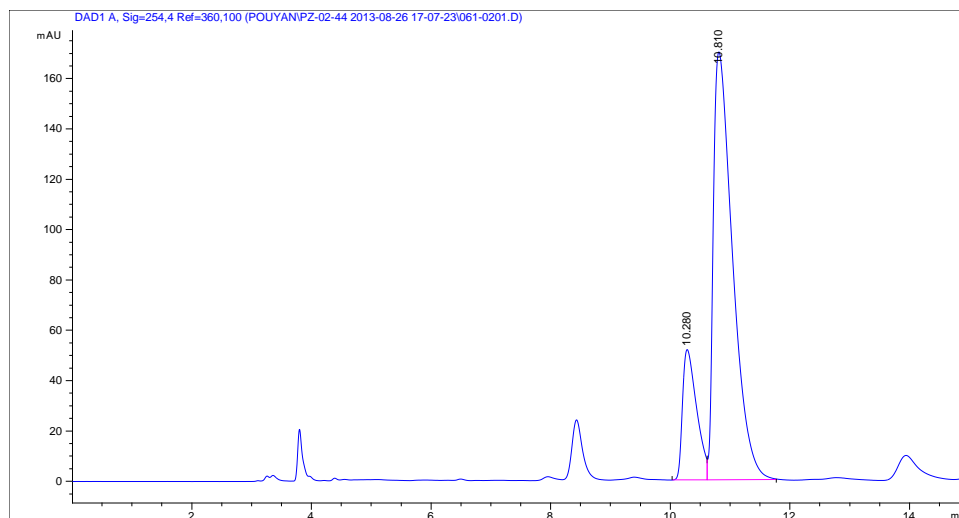
HPLC data used to obtain % *ee*, by comparing obtained area of peaks for each separated enantiomer. The solvent system used is listed for each entry.

Conditions a) Hexanes (5% *i*-PrOH:95% Hexanes)



Peak	Time	Area	Height	Width	Area %	Symmetry
1	10.298	1411.2	79.7	0.2645	21.135	0.529
2	10.846	5266.2	213	0.3884	78.865	0.377

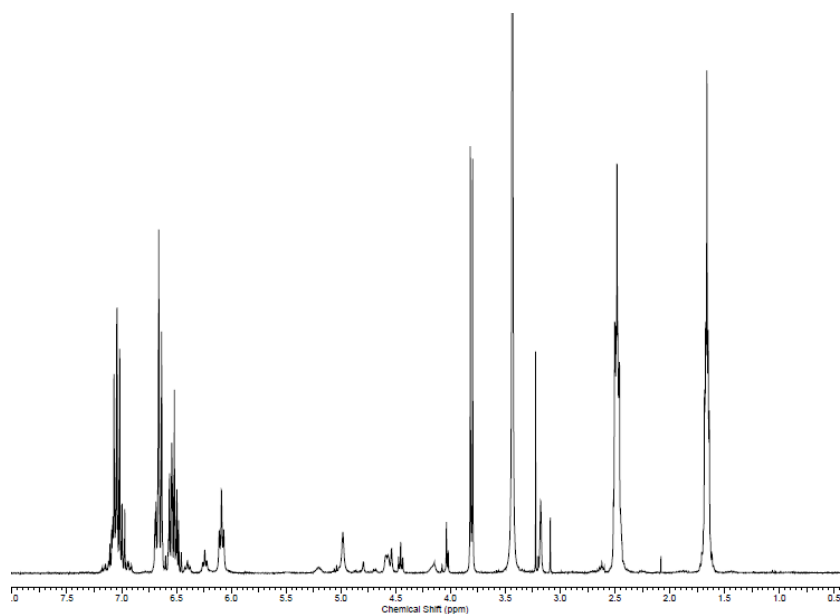
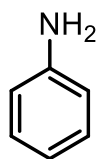
Conditions b) CDCl₃ (5% *i*-PrOH:95% Hexanes)

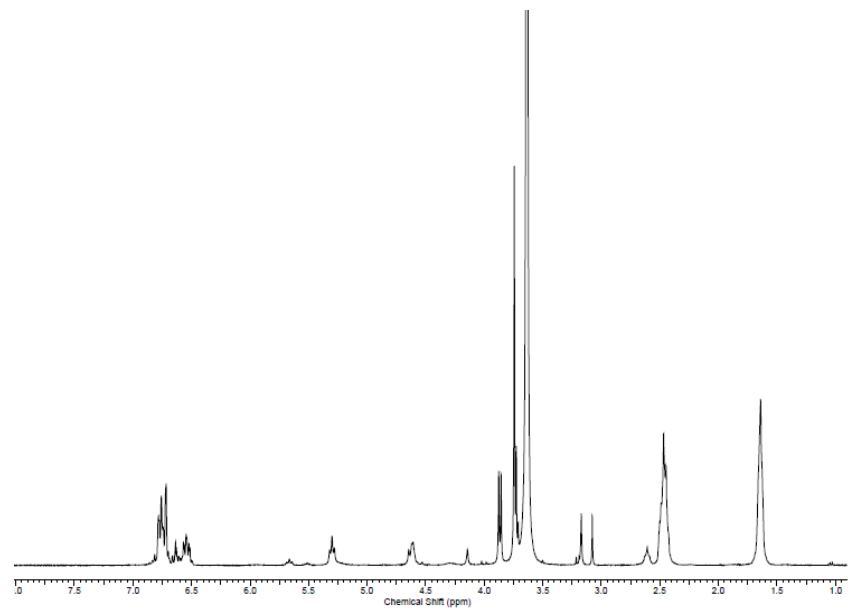
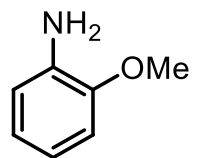


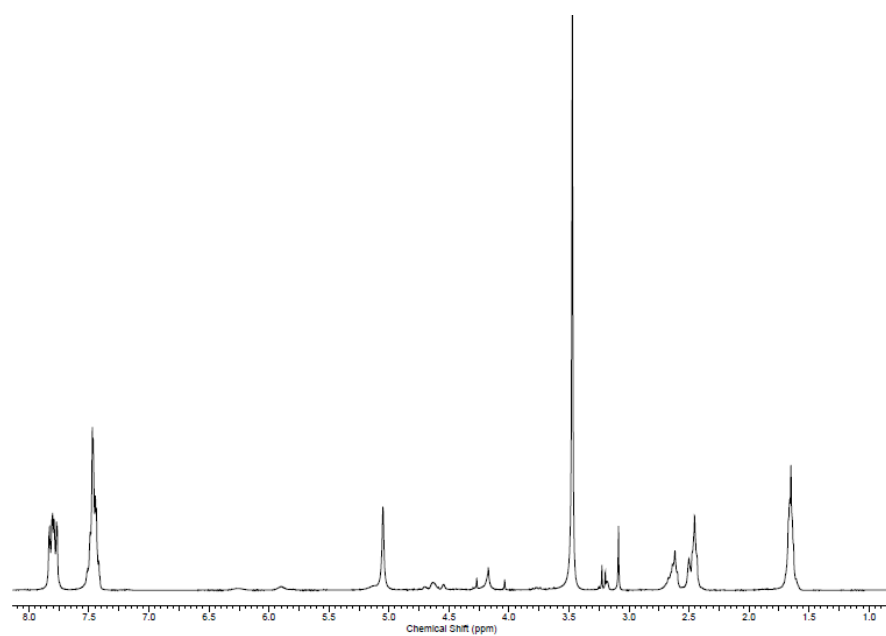
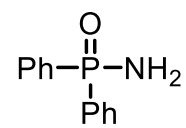
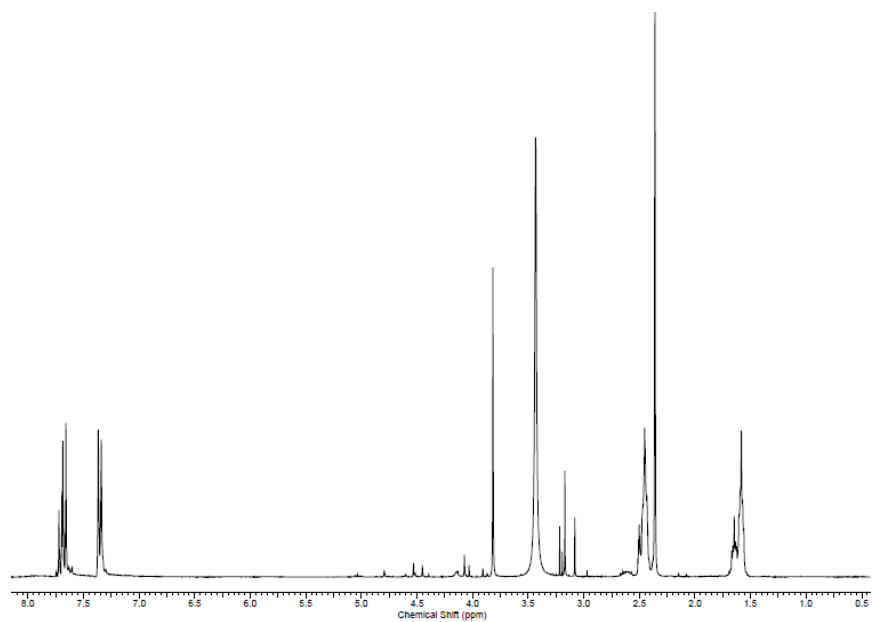
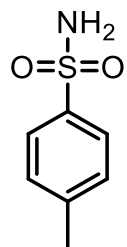
Peak	Time	Area	Height	Width	Area %	Symmetry
1	10.28	852.4	51.8	0.2499	18.303	0.463
2	10.81	3804.8	170.1	0.343	81.697	0.375

Figure 3.6 Mixed aminal formation with pyrrolidine as a model for tripeptide catalyst

All presented NMR spectra, correspond to crude NMR spectra of unpurified products/mixtures. The spectra were analyzed for the appearance of new product peaks, which could show potential formation of mixed aminal formation.







31P Spectrum for phosphiamide

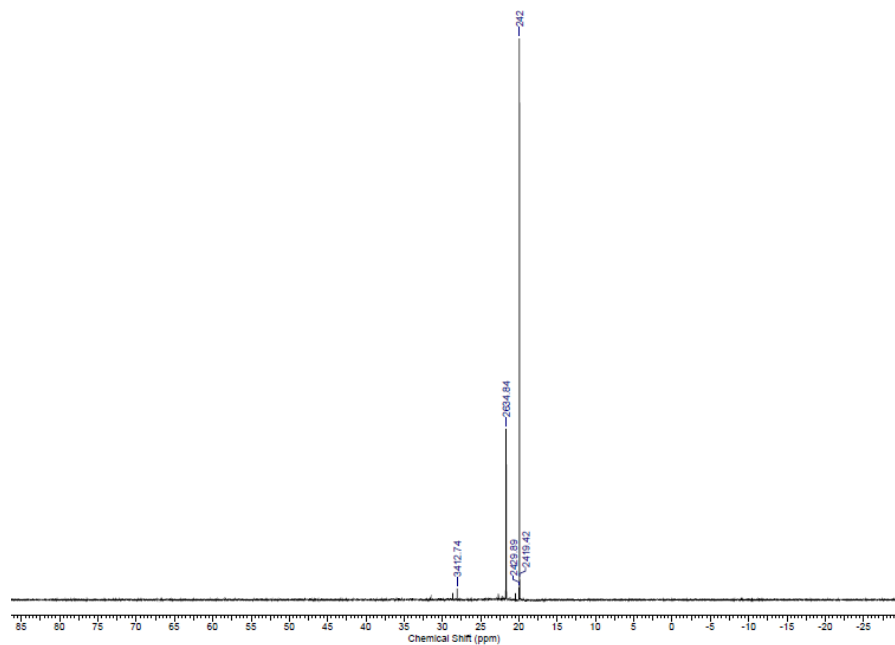
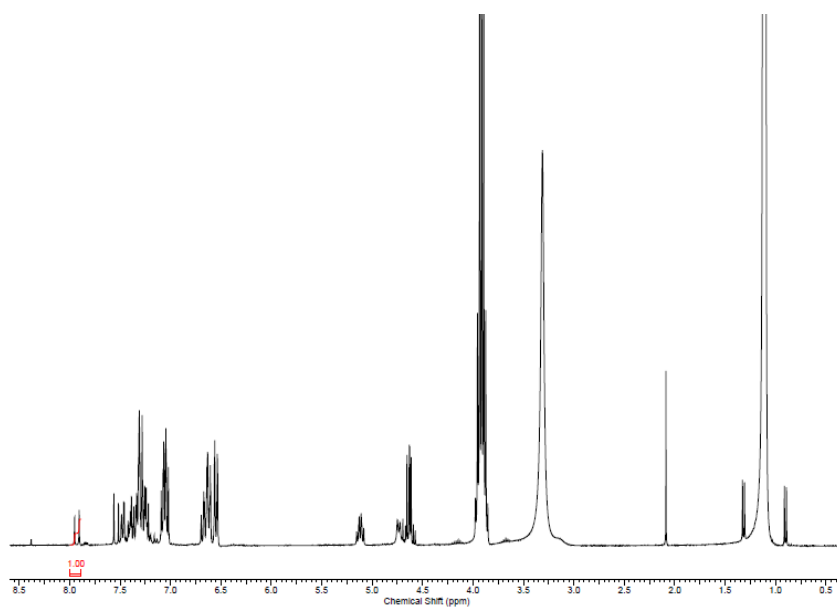
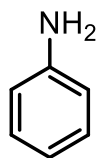
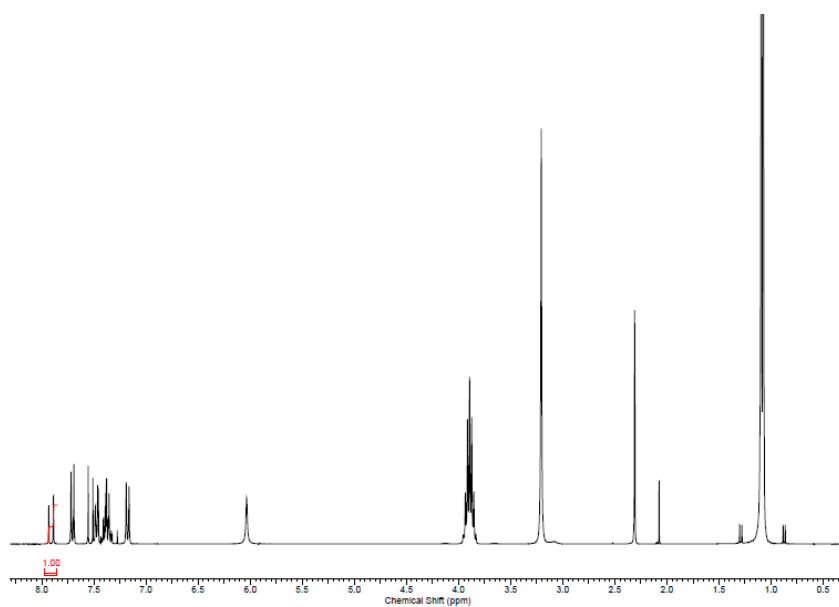
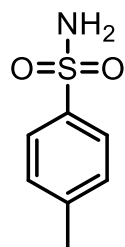
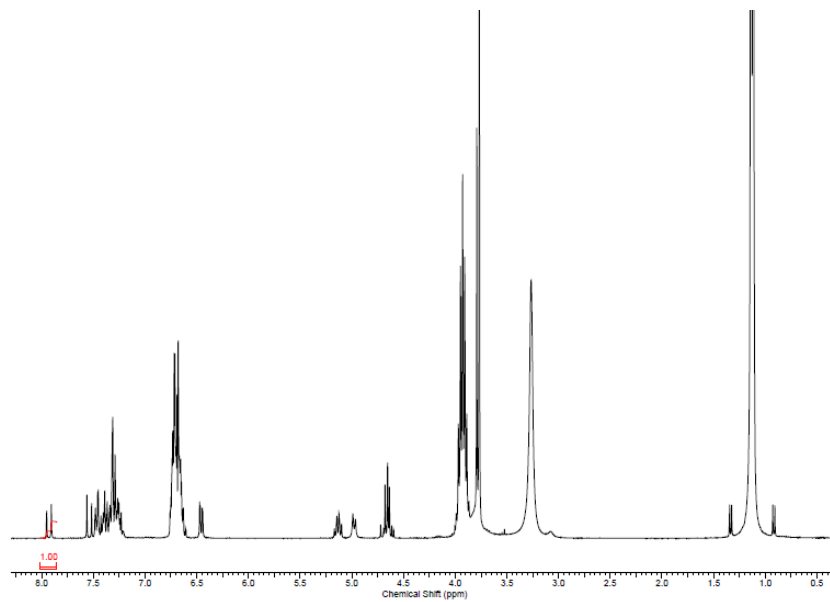
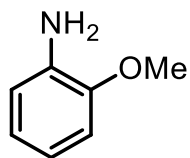


Figure 3.7 Preliminary study of background reactivity with β -nitrostyrene

Crude reaction NMR spectra are shown to monitor the disappearance of alkene peaks for the evaluated electrophiles, in order to assess levels of background reactivity under reaction conditions. Where applicable the appearance of new potential product peaks was analyzed. The same holds true for Figures 3.8, 3.9 and 3.10.





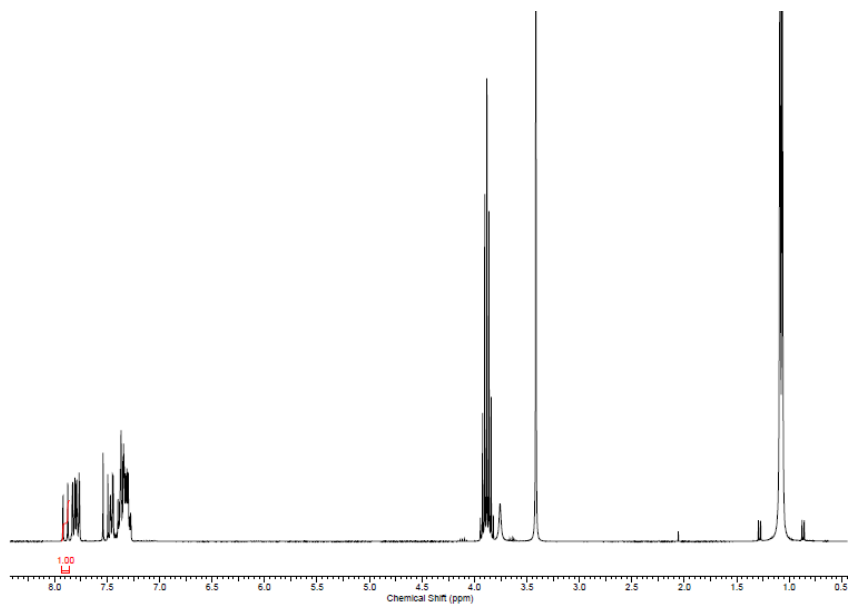
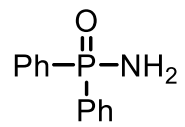
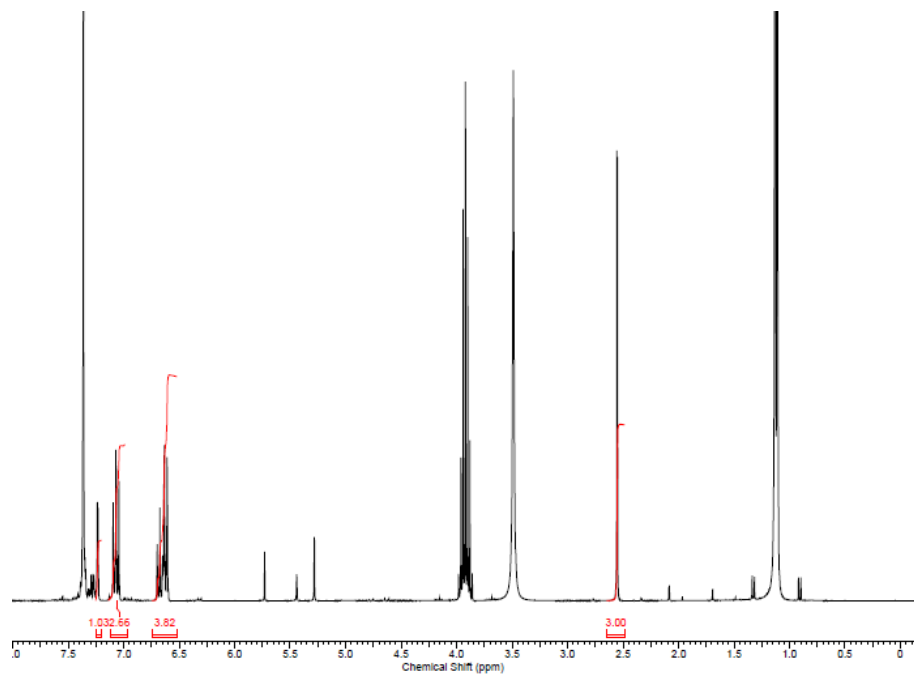
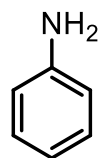
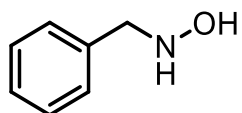
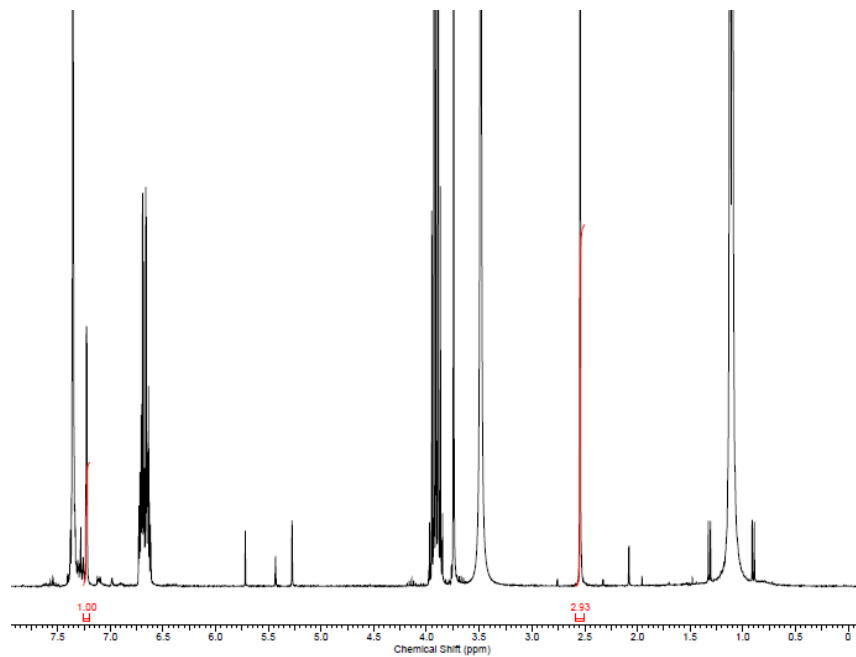
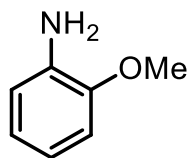


Figure 3.8 Evaluation of background with β,β -disubstituted nitroolefins for tripeptide catalysis





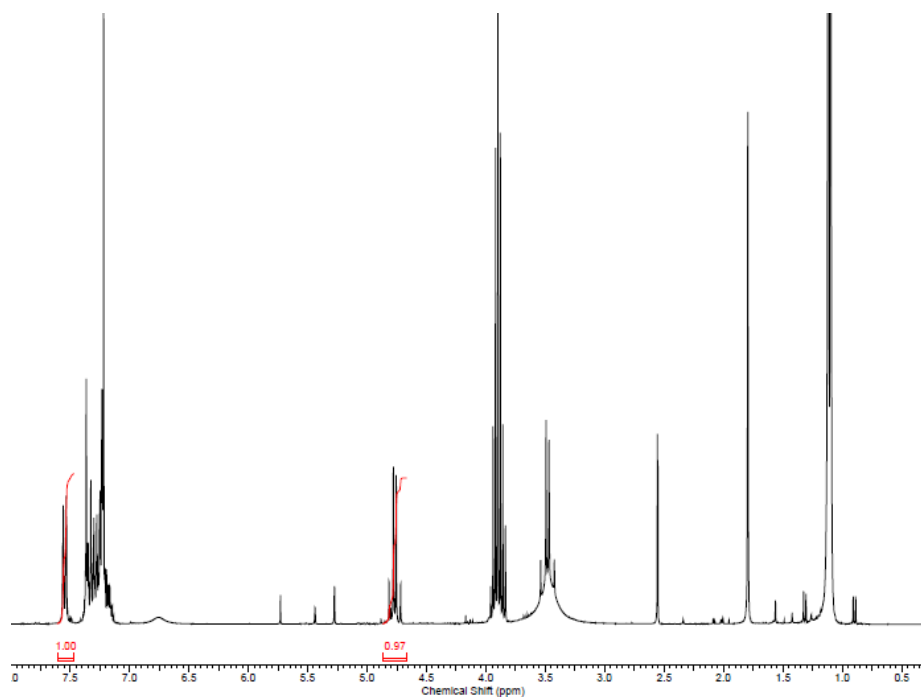
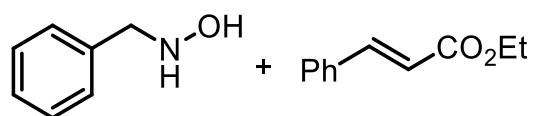
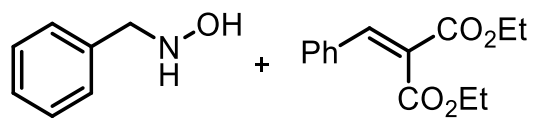
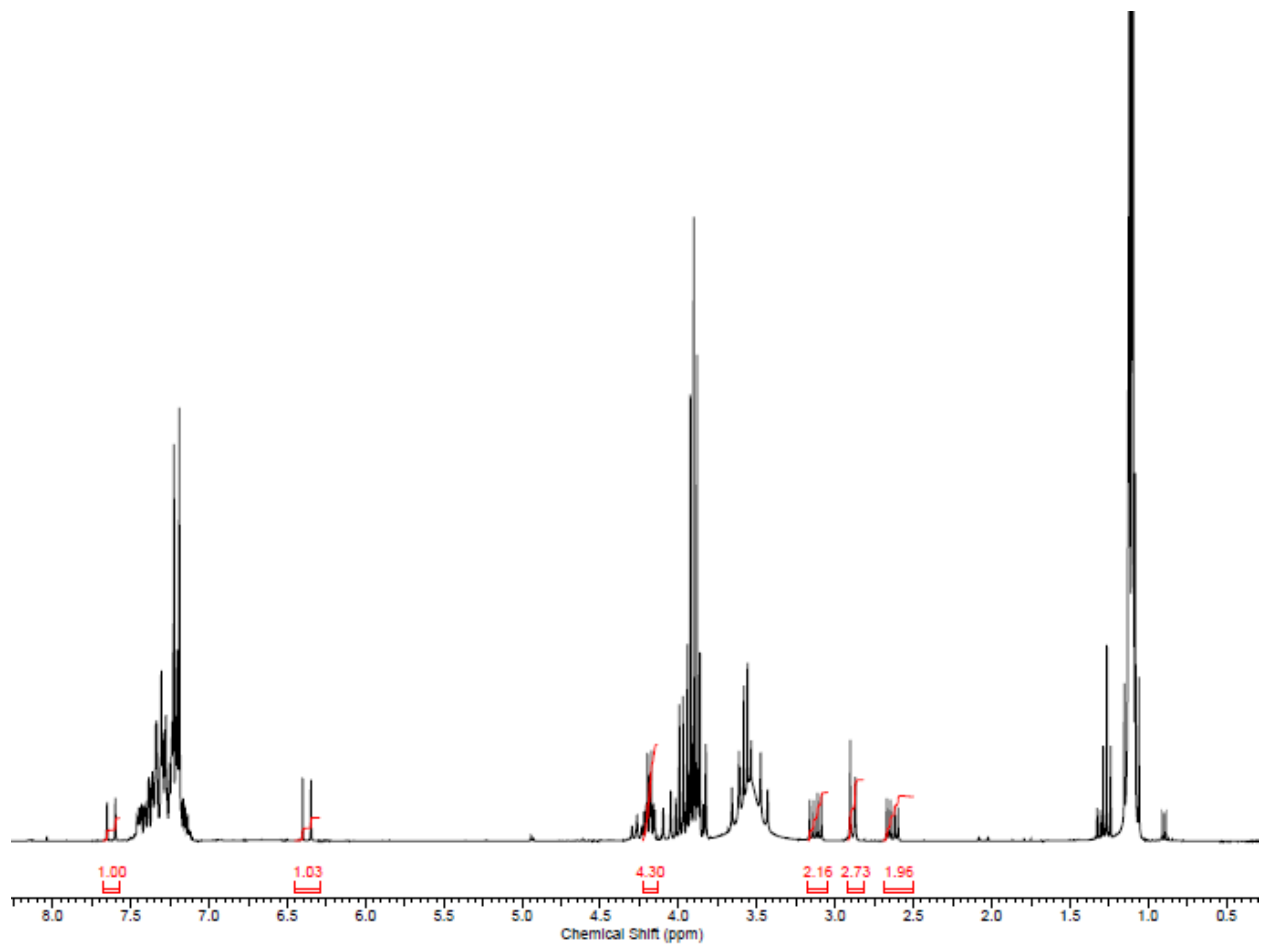
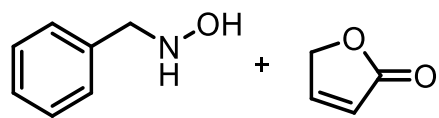
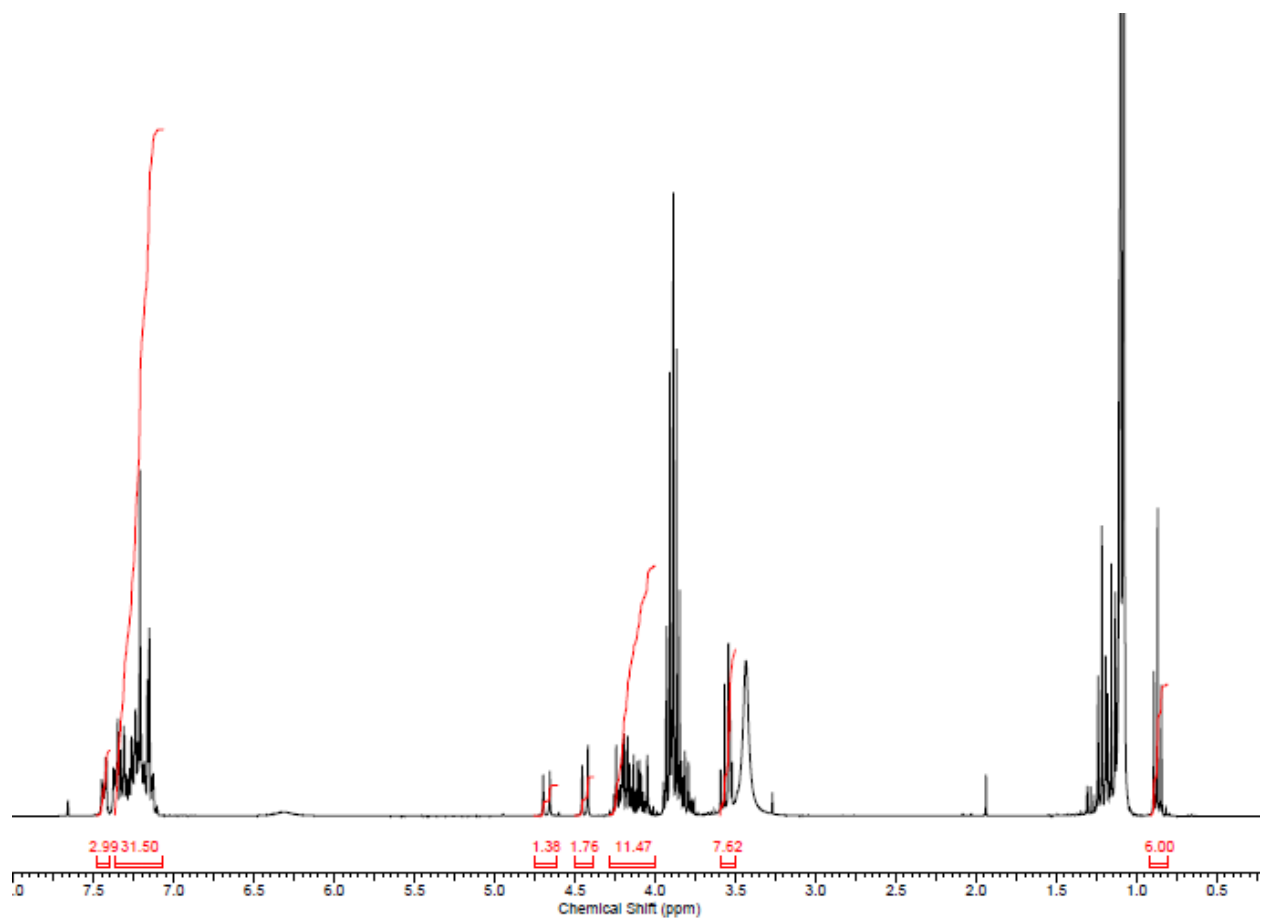
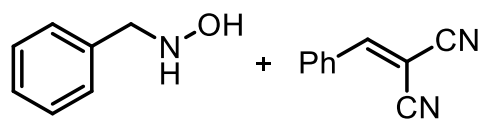
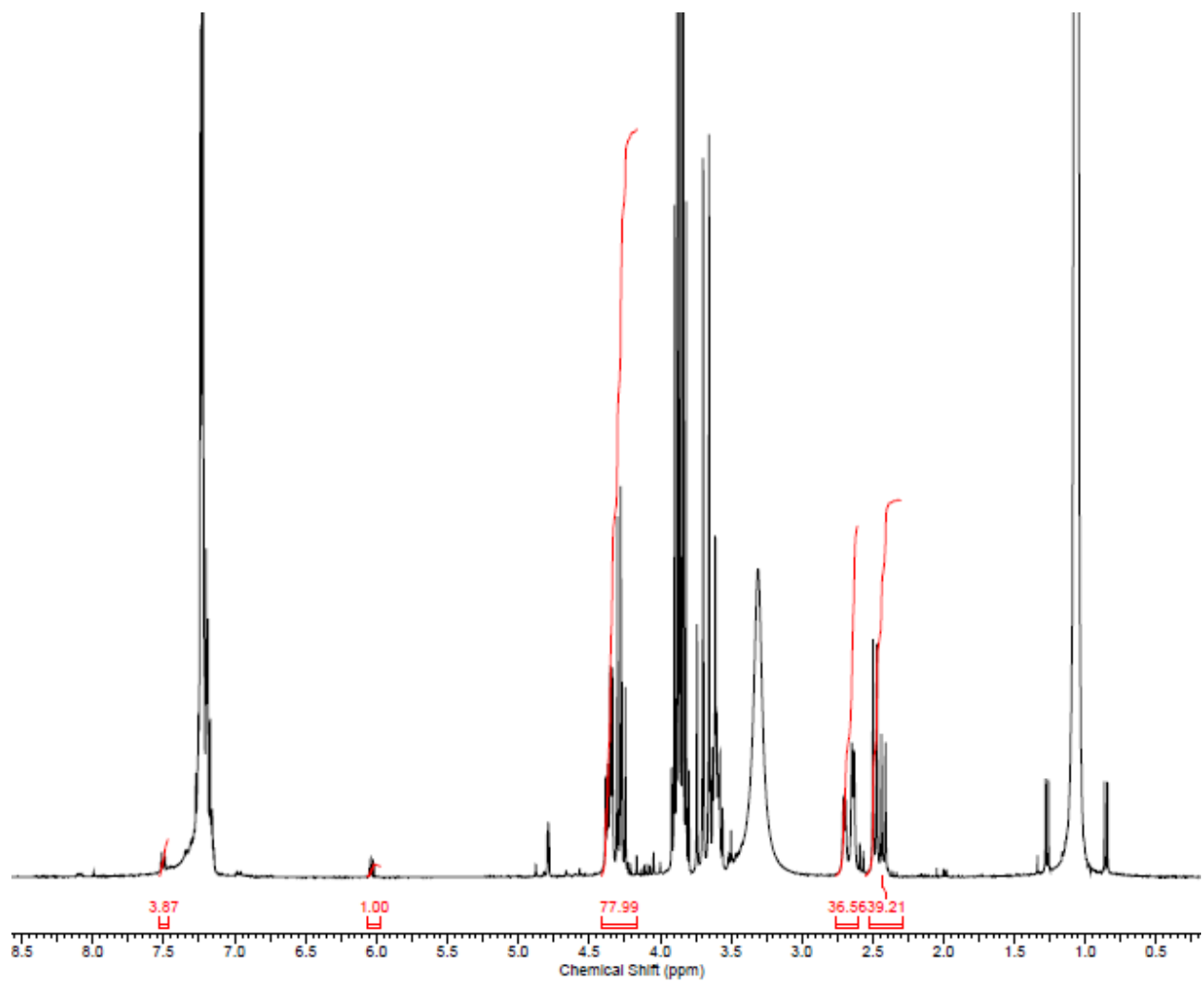


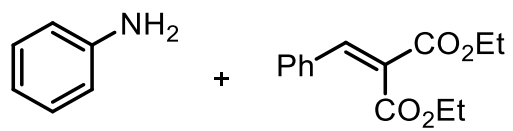
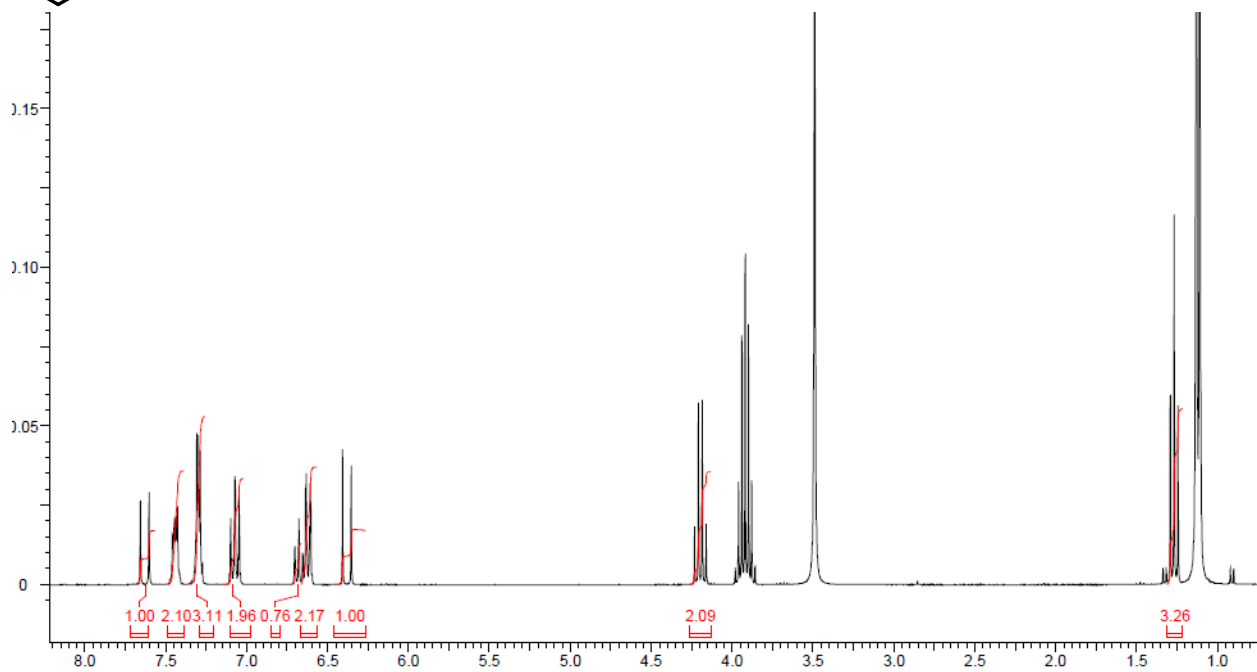
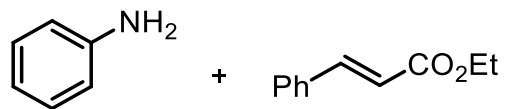
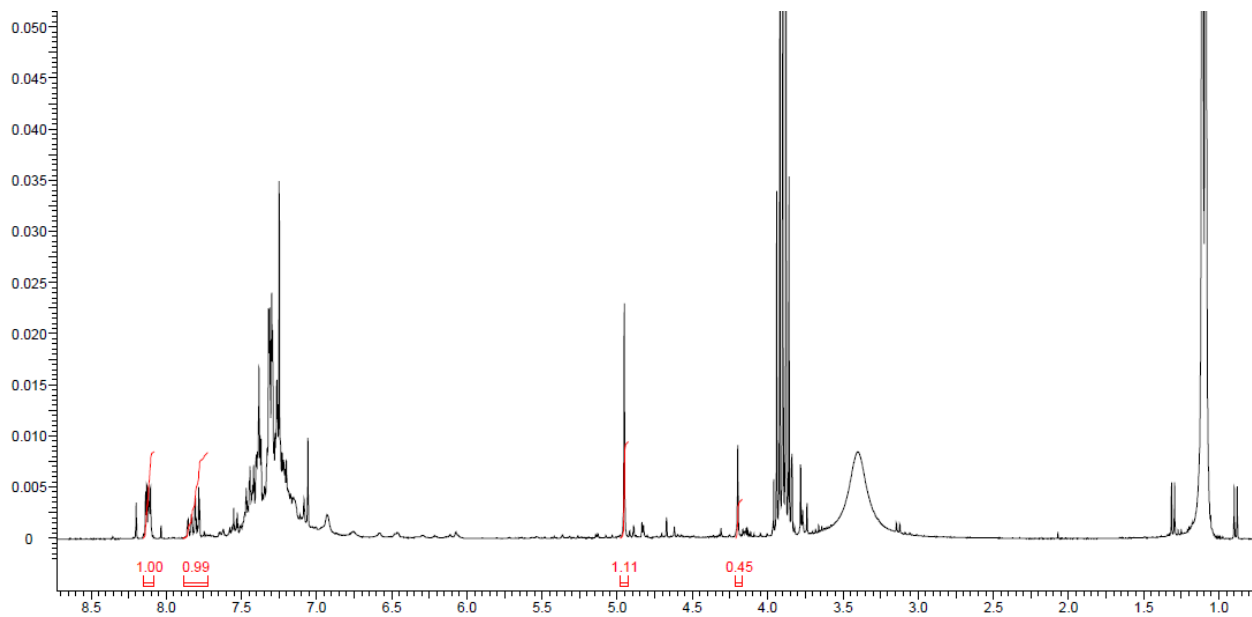
Figure 3.9 Evaluation of background reactivity between aniline and N-benzylhydroxylamine and various potential electrophiles for tripeptide catalysis

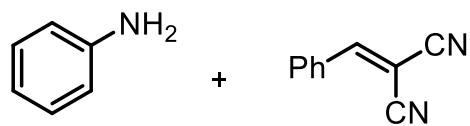
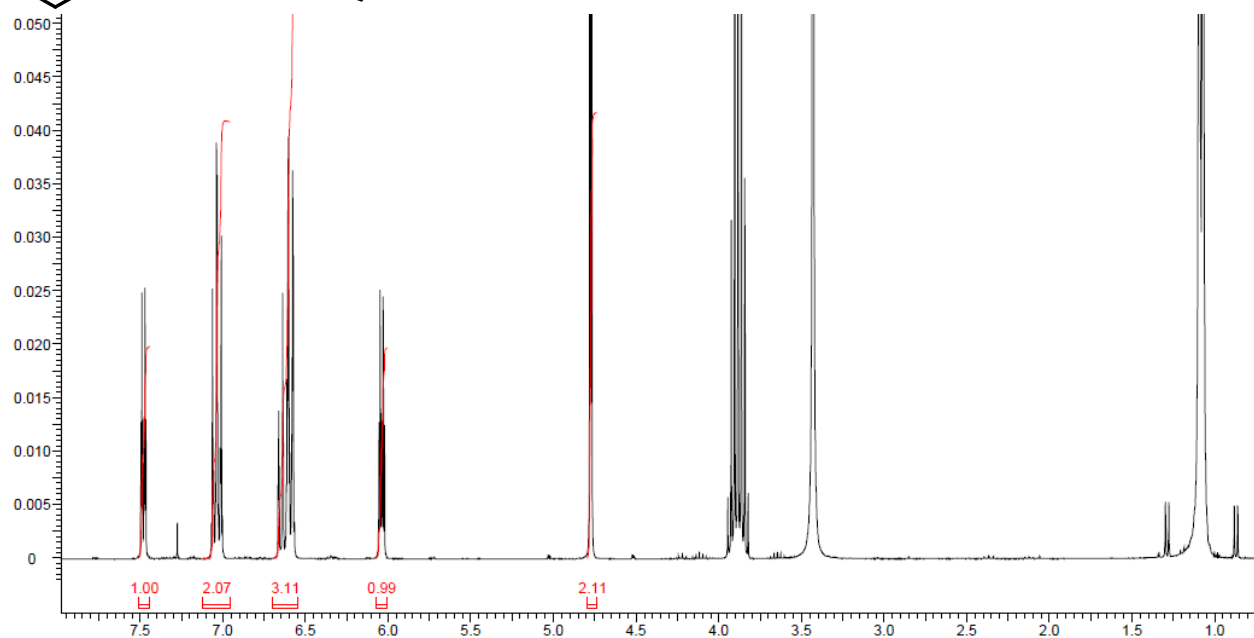
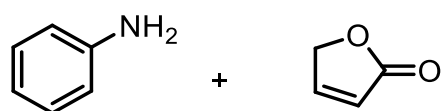
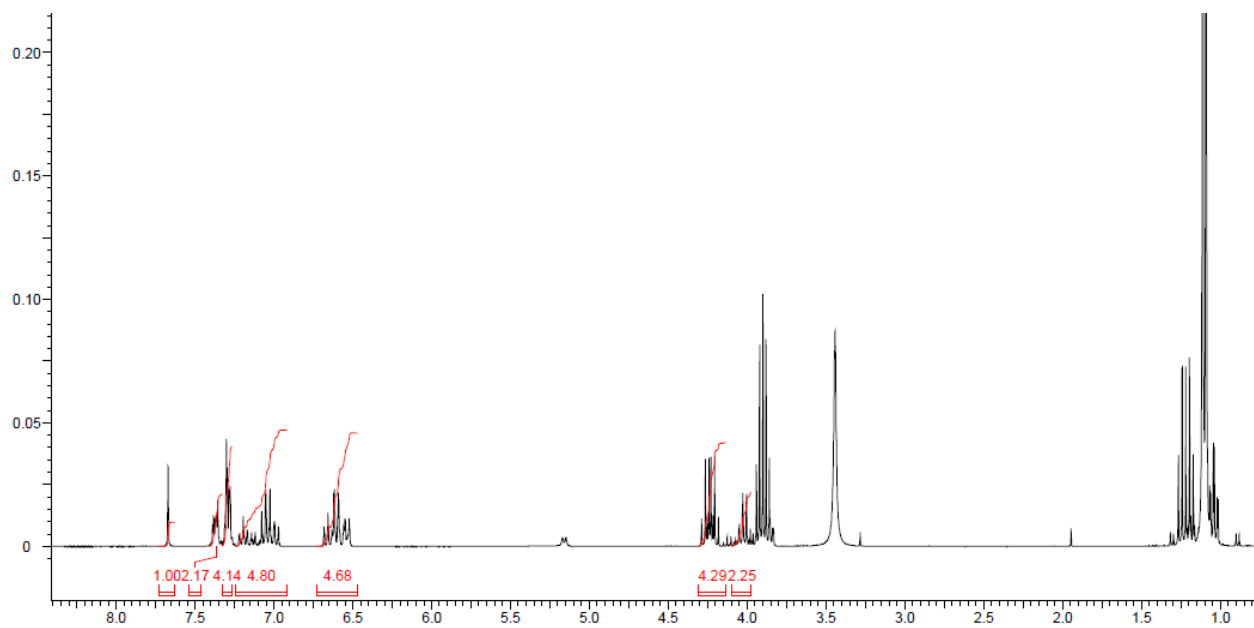












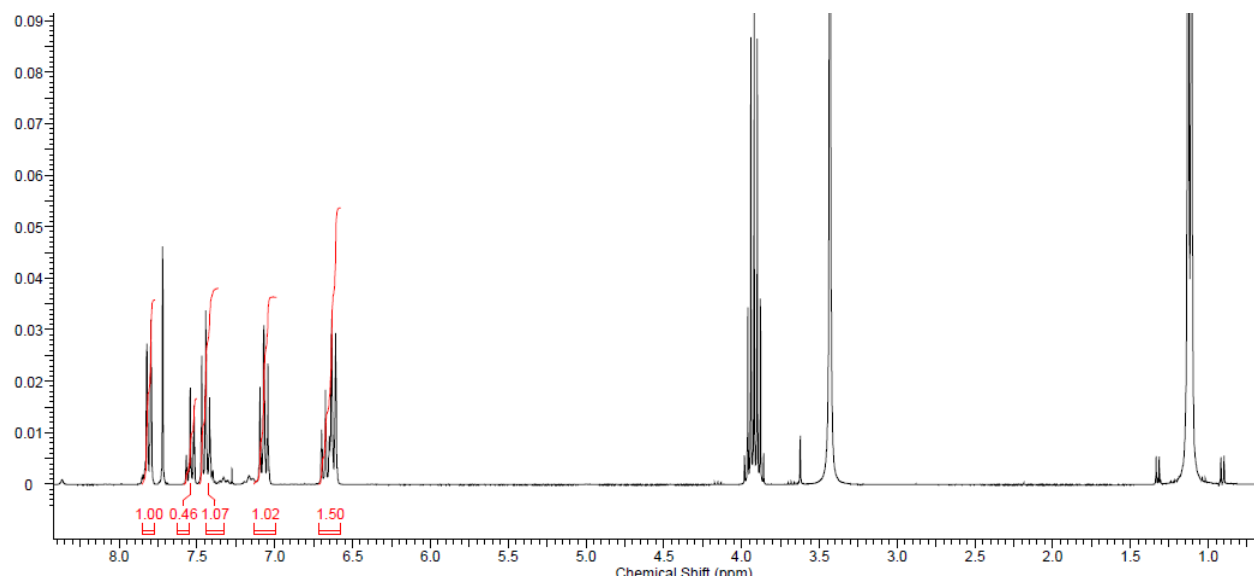


Figure 3.10 Investigations into aldehyde and small peptide dual-catalysis

